
Masters Theses

Student Theses and Dissertations

Fall 2016

Provenance and depositional environments of fluvial-lacustrine sandstones of lower Permian Lucaogou low-order cycle, Bogda mountains, NW China

Xiaowei Peng

Follow this and additional works at: https://scholarsmine.mst.edu/masters_theses



Part of the [Geology Commons](#), and the [Geophysics and Seismology Commons](#)

Department:

Recommended Citation

Peng, Xiaowei, "Provenance and depositional environments of fluvial-lacustrine sandstones of lower Permian Lucaogou low-order cycle, Bogda mountains, NW China" (2016). *Masters Theses*. 7615.
https://scholarsmine.mst.edu/masters_theses/7615

This thesis is brought to you by Scholars' Mine, a service of the Missouri S&T Library and Learning Resources. This work is protected by U. S. Copyright Law. Unauthorized use including reproduction for redistribution requires the permission of the copyright holder. For more information, please contact scholarsmine@mst.edu.

PROVENANCE AND DEPOSITIONAL ENVIRONMENTS OF FLUVIAL-
LACUSTRINE SANDSTONES OF LOWER PERMIAN LUCAOGOU LOW-ORDER
CYCLE, BOGDA MOUNTAINS, NW CHINA

by

XIAOWEI PENG

A THESIS

Presented to the Faculty of the Graduate School of the
MISSOURI UNIVERSITY OF SCIENCE AND TECHNOLOGY

In Partial Fulfillment of the Requirements for the Degree

MASTER OF SCIENCE IN GEOLOGY & GEOPHYSICS

2016

Approved by:

Wan Yang, Advisor
David J. Wronkiewicz
John P. Hogan

© 2016

Xiaowei Peng

All Rights Reserved

ABSTRACT

Compositional and textural maturity of sandstones may reflect provenance lithology and sediment transport distance, which are useful for paleogeographic reconstruction. 37 sandstones in six outcrop stratigraphic sections in Tarlong-Taodonggou and Zhaobishan areas in the greater Turpan-Junggar rift basin were studied to investigate the fluvial-lacustrine sandstone provenance in lower Permian Lucaogou (LCG) low-order cycle, Bogda Mountains, NW China. 400 points were counted in each thin section. All the samples are classified into lithic arenites, subarenites, wackes, and mudrocks. Three Petrofacies are defined. Petrofacies A is characterized by a high lithic content which is dominantly basaltic lithics with minor sedimentary lithics and felsic volcanic lithics with mean compositions of $Q_3F_{11}L_{86}$, $Qm_2F_{12}Lt_{86}$, $Qp_1Ls_7Lv_{92}$, and $Qm_{15}P_{84}K_1$ from four ternary classifications, respectively. Petrofacies B has a relatively high content of sedimentary lithics indicating a sedimentary source in the local rift shoulders with mean compositions of $Q_3F_5L_{92}$, $Qm_3F_8Lt_{89}$, $Qp_1Ls_{36}Lv_{63}$, and $Qm_{23}P_{71}K_6$. Petrofacies C has a higher content of felsic volcanic lithics with mean compositions of $Q_3F_8L_{89}$, $Qm_4F_9Lt_{87}$, $Qp_1Ls_{10}Lv_{89}$, and $Qm_{33}P_{63}K_4$. Tectonic setting is interpreted from ternary diagrams. All the samples fall in the recycled orogen and magmatic arc fields. Two sources, northern Tian Shan and rift shoulders, are differentiated on the basis of grain size and roundness. In Tarlong-Taodonggou area, similar trends of textural and compositional properties are present in N and NW Tarlong, and S Tarlong and Taodonggou indicating similar depositional history. SW Tarlong shows a unique trend due to the local sedimentary source. In Zhaobishan, the trend is highly variable, indicating episodic sediments influx from rift shoulders or a different catchment basin.

ACKNOWLEDGMENTS

I would thank my advisor, Dr. Wan Yang, for his patience, guidance, kindness and suggestions both in the field and lab.

I would thank my colleagues, Jaimeson Fredericks, Jing Duan and Mr. Li for their help and guidance in the field. I thank Yiran Lu, Zhixin Li, Xin Zhan, Xin Jiao, Bin Sun, Dongyu Zheng for their ideas, help, and suggestions.

I thank Dr. David J. Wronkiewicz and Dr. John P. Hogan for their advice and suggestions on the thesis.

Finally, I would thank my parents for their support and love for so many years. I couldn't have achieved these without them.

TABLE OF CONTENTS

	Page
ABSTRACT.....	iii
ACKNOWLEDGMENTS	iv
LIST OF ILLUSTRATIONS.....	vii
LIST OF TABLES.....	ix
SECTION	
1. INTRODUCTION.....	1
1.1. GEOLOGICAL BACKGROUND	1
1.2. STRATIGRAPHY.....	4
2. METHOD AND DATA	6
2.1. FIELD OBSERVATIONS	6
2.2. PETROGRAPHY.....	7
3. SANDSTONE PETROGRAPHY	11
3.1. FRAMEWORK GRAINS	11
3.1.1. Quartz (Q).....	11
3.1.1.1 Monocrystalline quartz (Qm).....	11
3.1.1.2 Polycrystalline quartz (Qp).....	14
3.1.2. Feldspar (F).....	14
3.1.2.1 Plagioclase (P).....	14
3.1.2.2 Potassium feldspar (K).....	14
3.1.3. Lithics (L).....	15
3.1.3.1 Volcanic lithics (Lv).....	15
3.1.3.2 Sedimentary lithics (Ls).....	16
3.1.4. Accessory Minerals.....	17
3.2. MATRIX AND CEMENTS.....	17
3.2.1. Matrix.....	17
3.2.2. Cements.....	18
3.3. SANDSTONE CLASSIFICATION.....	18
4. PETROFACIES.....	25

4.1. PETROFACIES A.....	26
4.2. PETROFACIES B.....	26
4.3. PETROFACIES C.....	27
4.4. PETROFACIES AND DEPOSITIONAL ENVIRONMENTS	30
5. PROVENANCE.....	32
5.1. TECTONIC SETTING.....	32
5.2. INTERPRETATION OF PROVENANCE.....	34
6. STRATIGRAPHIC TREND.....	38
6.1. TAODONGGOU.....	38
6.2. SOUTHWESTERN TARLONG.....	38
6.3. NORTHWESTERN TARLONG	39
6.4. SOUTHERN TARLONG.....	39
6.5. NORTHERN TARLONG	40
6.6. ZHAOBISHAN	40
6.7. CORRELATION.....	41
7. DISCUSSION	47
7.1. COMPLEXITY OF SOURCE	47
7.2. TECTONIC SETTING.....	48
7.3. COMPARISON BETWEEN TWO STUDY AREAS	49
8. CONCLUSIONS	50
APPENDICES	
A. N TARLONG SECTION	52
B. NW TARLONG SECTION.....	67
C. S TARLONG SECTION	88
D. SW TARLONG SECTION	101
E. TAODONGGOU SECTION	110
F. ZHAOBISHAN SECTION.....	120
G. GRAIN SIZE DISTRIBUTION OF ALL SANDSTONES	130
BIBLIOGRAPHY.....	144
VITA.....	148

LIST OF ILLUSTRATIONS

Figure	Page
1.1. Location of the study area.....	3
1.2. Chrono-, litho-, and cyclostratigraphy of upper Carboniferous-middle Permian strata in the Tarlong-Taodonggou area.....	5
2.1. Geologic map and satellite photo of the study areas.....	9
3.1. Photomicrograph of quartz and feldspars.	21
3.2. Photomicrograph of volcanic lithics and mud clasts.	22
3.3. Photomicrograph of sedimentary lithics and accessory minerals.	23
3.4. Photomicrograph of matix and cements.	24
4.1. QFL Ternary diagram showing all 37 samples from the LCG LC fall in litharenite field in the LCG LC, according to Folk's (1980) sandstone classification.	25
4.2. Roundness distribution of Petrofacies A.....	28
4.3. QpLvLs ternary diagram to differentiate Petrofacies B from the other two petrofacies.....	28
4.4. Roundness distribution of Petrofacies B.....	29
4.5. QmLvLvi ternary diagram showing relatively high Lvi content in Petrofaceis C compared with the other two petrofacies.....	29
4.6. Roundness distribution of Petrofacies C.....	30
5.1. QmFLt ternary diagram showing the Lucaogou sandstones fall in lithic recycled and undissected arc fields on the global tectono-sandstone composition scheme. Modified from Dickinson (1985).....	33
5.2. QpLvLs ternary diagram showing most of the Lucaogou sandstones are plotted in the arc orogen field suggesting a magmatic arc provenance. Modified from Dickinson (1985).	34
5.3. QmPK ternary diagram showing a high P/F ratio of Lucaogou sandstones. Modified from Dickinson (1985).....	35
6.1. Stratigraphic variation in depositional environments, grain size, sorting, and composition of the LCG sandstones in Taodonggou section.	42

6.2. Stratigraphic variation in depositional environments, grain size, sorting, and composition of the LCG sandstones in SW Tarlong section.	42
6.3. Stratigraphic variation in depositional environments, grain size, sorting, and composition of the LCG sandstones in NW Tarlong section.	43
6.4. Stratigraphic variation in depositional environments, grain size, sorting, and composition of the LCG sandstones in S Tarlong section.	44
6.5. Stratigraphic variation in depositional environments, grain size, sorting, and composition of the LCG sandstones in N Tarlong section.	45
6.6. Stratigraphic variation in grain size, sorting, and composition of the LCG sandstones in Zhaobishan section.	46

LIST OF TABLES

Table	Page
2.1. Grain types and modal parameters used in this study	10
3.1. Raw point-counting data and results of statistical grain size analysis of Taodonggou, S, SW, N Tarlong sections.....	12
3.2. Raw point-counting data and results of statistical grain size analysis of NW Tarlong and Zhaobishan sections	13
3.3. Classification of studied sandstones	20
4.1. Occurrence of petrofacies in relation to depositional environments	31

1. INTRODUCTION

The fluvial-lacustrine sandstones in Lucaogou low-order cycle (LCG LC) in Bogda Mountains, NW China, were deposited in a half graben in a rift basin setting (Yang et al., 2010). Half-grabens in rifts form due to block rotations along listric and planar-normal faults in zones of lithospheric attenuation (Wernicke and Burchfield, 1982). Fluvial sedimentation results from deposition in relatively low-gradient rivers that are oriented parallel to the basin axis. Lakes are developed in topographic depressions that commonly are elongate and parallel to the basin axis (Blair, 1987). Ancient fluvial-lacustrine sediments recorded tectonic, paleoclimate, and depositional conditions on the earth surface (Basu, 1976, Mack and Suttner, 1970). Provenance analysis of sandstone is an important and widely used means of tracing the origins of sedimentary basin fill and reconstructing the orogenic history of basin-bounding uplifts (Greene et al., 2005).

This study focuses on provenance lithology, transport distance and depositional environments during the deposition of sandstones in LCG LC. The well exposed LCG LC in the southern Bogda Mountains, NW China, offers an opportunity to study compositional and textural characteristics of fluvial-lacustrine sandstones. 400 points were counted on each of the 37 sandstone samples from six measured sections, five from Tarlong-Taodonggou area and one from Zhaobishan area. Compositional and textural characteristics are analyzed to determine provenance lithology, tectonic setting and transport distance. Provenance lithology is mainly determined by compositional properties; and transport distance is largely determined by textural properties. The results indicate a regional basaltic source and local rift shoulders including volcanic and sedimentary lithologies in all sections. A trend of increasing textural maturity from southern sections to northern sections is observed. If they share the same source, the northern Tian Shan source would be supported.

1.1. GEOLOGICAL BACKGROUND

This study focuses on the well exposed LCG LCs in Taodonggou-Tarlong area and Zhaobishan area in the southern foothill of the Bogda Mountains (Figure 1.1). The Tarlong-Taodonggou area is located ~15 km north of the town of Daheyang, a train depot

along the transcontinental railway. The Zhaobishan area is located ~90 km east of the Tarlong-Taodonggou area, ~ 15 km to the north of Shanshan railway station. During the early Permian time, this study area was in the southeastern Kazakhstan Plate, at the northwestern coast of Paleo-Tethys Sea at approximately 30°-40°N in the arid climate zone (Figure 1.1C). The LCG LC was deposited in the intracontinental greater Turpan-Junggar basin during the early Permian (Yang et al., 2010). The basin was developed on an Upper Carboniferous volcanic arc basement (Yang et al., 2010). The Bogda Mountains had not been uplifted by Early Triassic on the basis of provenance studies, the regional distribution of organic-rich lacustrine mudrock, and timing of unconformities (Carroll et al., 1992; Shao et al., 2001; Greene et al., 2005). Hence, the Turpan Basin was jointed with the Junggar Basin during the Permian; and the Permo-Triassic fluvial-lacustrine sedimentary rocks in Tarlong were deposited in the greater Turpan-Junggar Basin (Greene et al., 2001; Shao et al., 2001).

Northwestern China and adjacent areas of central Asia comprise a collage of disparate tectonic elements that amalgamated during the late Paleozoic (Burrett, 1974; Wang et al., 1990). However, the Permian tectonic evolution of the greater Turpan-Junggar Basin is poorly understood. Proposed models vary widely from extension, transtension, to foreland loading (Hsu, 1988; Peng and Zhang, 1989; Carroll et al., 1990; Allen et al., 1995). Yang et al. (2010) suggests the LCs formed during a rifting-drifting tectonic cycle. There are several lines of evidence supporting the extension rift origin of the Turpan-Junggar Basin. A N-S-oriented two-dimensional seismic profile across the Lunan Depression in central Junggar Basin, revealing half-graben structures with Permian syn-rift sediments (Peng and Zhang, 1989). The arrangement of depocenters in the basin and their proximity to normal faults, from geologic mapping and seismic profiles, suggest a series of half-graben in a rift basin (Yang et al., 2010). Half-grabens similar to those in the greater Turpan-Junggar basin in the latest Carboniferous to Early Triassic are present in the Quaternary Basin and Range Province of the western US (Yang et al., 2010). Bimodal magmatism as indicated by swarms of mafic-felsic dike in the Bogda Mountains has been interpreted as evidence for Permian extension (Allen et al., 1991).

The Bogda Mountains are a giant anticline and composed mostly of mid-Carboniferous volcanic arc rocks with scattered Permo-Quaternary sedimentary rocks exposed on both flanks (Xu et al., 2007). Permo-Triassic fluvial-lacustrine sediments are extensively exposed along the foothill of the Bogda Mountains (Liao et al., 1987; Carroll et al., 1995). The sedimentary rocks were deposited in the greater Turpan-Junggar rift basin on the uppermost Carboniferous volcanic-arc basement formed by collision between the Junggar and Northern Tian Shan plates according to the new dates (Yang et al., 2010). Lake expansion and contraction and source uplift to the south had occurred episodically in the region during the deposition of LCG LC (e.g., Shao et al., 2001; Wartes et al., 2002; Greene et al., 2005).

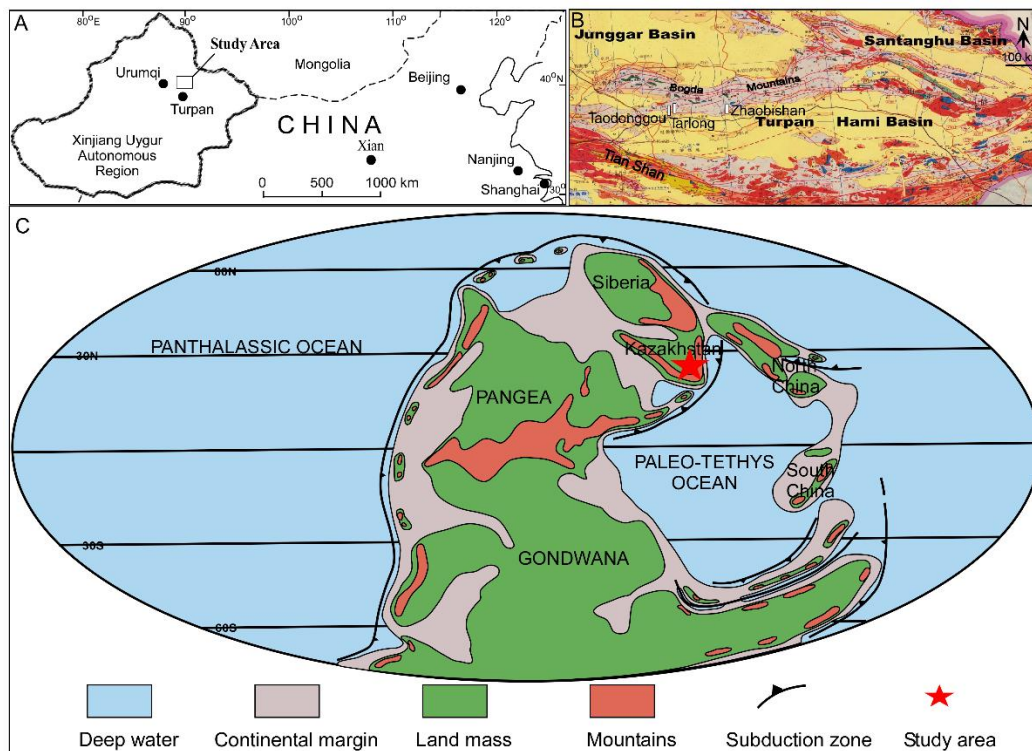


Figure 1.1. Location of the study area. A) Location of the study area in Xinjiang Uygur Autonomous Region, NW China. B) Geological map of eastern Xinjiang, showing locations of Tarlong-Taodonggou and Zhaobishan. Modified from XBGMR (1993). C) Global paleogeographic reconstruction for the early Permian. Modified from Scotese (1996). The location of the study area is marked with a red star.

1.2. STRATIGRAPHY

The Carboniferous–Triassic chronostratigraphy in the greater Turpan–Junggar basin is poorly constrained mainly by biostratigraphy of invertebrates (mainly ostracods and choncostracans), plants, spores and pollens, and vertebrates (Yang et al., 2010). The LCG LC is an informal cyclostratigraphic unit defined by Yang et al. (2010). The lower Daheyan, middle Daheyan, upper Daheyan, Lucaogou, and Hongyanchi LCs are constrained to a late Gzhelian–Artinskian age by an age of 281.42 Ma obtained from a volcanic ash in profundal shale in the uppermost Hongyanchi in SE Tarlong (Yang et al., 2010). In addition, biotite and sanidine from the ash-flow tuff underneath the Daheyan–Taoxigou unconformity in Taodonggou are dated as 301.61 and 300 Ma, respectively, which are used to determine the lower limit (Yang et al., 2010). The radiometric dates indicate the great uncertainty of previous biostratigraphy-based chronostratigraphy for the lower Permian. Thus, the age of the LCG LC was changed from Rodian to lower-middle Sakmarian and basal Artinskian (291–284 Ma; Figure 1.2). The LCG LC is overlain by Hongyanchi LC and underlain by upper Daheyan LC. The base of LCG LC is a sharp erosional surface mantled with a thin layer of well-washed and well sorted conglomerate, arenite, or pisolitic rudstone, interpreted as lag deposits on a graben-wide transgressive surface. The top of the LCG LC is a high-relief fluvial channel base in Taodonggou and NE Tarlong, and well-washed beach conglomerate and arenite in southern Tarlong, signifying a major regression (Yang et al., 2010). In Zhaobishan, the base of LCG LC is an unconformity in direct contact with upper Carboniferous basaltic basement and the top is a sharp conformable surface with sublittoral wackestone to mudrock deposits overlain by lacustrine shales of Hongyanchi LC. .

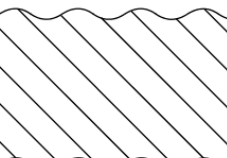
Period	Epoch	Lithostratigraphy	Cyclostratigraphy Low-Order Cycles (Yang et al., 2010)	Revised Cyclostratigraphy (Yang et al., 2010)		
				New dates	Stages	
Permian	Guadalupian	Quanzijie	Upper Quanzijie	281.42	Capitanian	
			Lower Quanzijie		265.8	Wordian
						268.0
	Cisuralian	Hongyanchi	Hongyanchi		270.6	Kungurian
		Lucaogou	Lucaogou		275.6	Artinskian
					284.4	Sakmarian
Carboniferous Pennsylvanian	Late	Daheyuan	Upper Daheyuan	294.6	Asselian	
			Middle Daheyuan	299.0	Gzhelian	
			Lower Daheyuan	301.26 ± 0.05 301.37 ± 0.07	303.4	
		Qiergusitao		305.50 ± 0.11 306.48 ± 0.32	307.2	Kasimovian

Figure 1.2. Chrono-, litho-, and cyclostratigraphy of upper Carboniferous-middle Permian strata in the Tarlong-Taodonggou area. Wavy lines are major unconformities; dashed lines disconformity; and hatched areas missing strata. Absolute ages at stage boundaries from Gradstein et al. (2004). Modified from Yang et al. (2010, 2013) and Obrist-Farner and Yang (2015).

2. METHOD AND DATA

Provenance and depositional conditions of sandstones in Lucaogou low-order cycle are the main concerns of the study. Fieldwork is essential for preliminary interpretation of structure, depositional environments, paleogeography, paleoclimate and tectonics based on cyclostratigraphy. Further composition and texture analysis was done through detailed petrographic work in lab.

2.1. FIELD OBSERVATIONS

Six stratigraphic sections of the Lucaogou low-order cycle were measured at a cm-dm scale in the Tarlong-Taodonggou area and Zhaobishan area by Dr. Yang and his colleagues in 2004, 2005, 2007, 2009, and 2014 (Figure 2.1). The author had visited the measured sections and collected some extra samples in 2015. First, lithology, sedimentary structures, texture, fossil content, boundary relationships, and stratal geometry of individual units were described. Depositional environments were interpreted based on lithofacies combined with stacking patterns and lateral changes. Second, three orders of sedimentary cycles were delineated by Yang et al. (2010) on the basis of repetitive depositional environment changes. A high-order cycle (HC) is the most basic cyclostratigraphic entity which is defined by a cycle of environment change associated with lake expansion and contraction or erosion and deposition of fluvial sedimentation. The stacking of one or more HCs will form a longer trend of depositional environment changes associated with larger scale transgression and regression, which can be defined as intermediate-order cycle (IC). An IC contains transgressive, condensed section, highstand, and regressive systems tracts (Yang et al., 2010). Low-order cycle (LC) is defined by repetitive stacking of ICs that show similar environments and climatic and/or tectonic conditions.

Thirty seven sandstones were collected from the LCG LCs. Five samples are from Taodonggou, four from SW Tarlong, six from S Tarlong, five from N Tarlong, eight from NW Tarlong, and nine from Zhaobishan, covering all parts of each section. Hand samples were cut to slabs, and then sent to Texas Petrographic Services for thin sectioning.

2.2. PETROGRAPHY

Microscopic petrographic study of thirty-seven sandstones was carried out to document framework grain compositions, size, roundness and angularity, grain contact, matrix composition, and cement types. 400 points were counted in each thin section, where altered grains were interpreted for their original grain types whenever possible, using the traditional point counting method. Another counting method is the Gazzi-Dickinson method (Gazzi, 1966, Dickinson, 1970). The two methods mainly differ in identifying the lithic grains. The traditional counting method would count a basaltic lithic grain containing feldspar laths as lithic. However, in the Gazzi-Dickinson method, basaltic lithics containing feldspar laths are counted as feldspar instead of basaltic lithic. In this study, the traditional method is applied due to the small size of the feldspar laths which are difficult to count. The small size of the feldspar laths will also largely reduce the size of the lithics, which will reduce the estimate of transport distance. All points were counted using the Nikon Labophot-pol polarizing binocular microscope. Thin sections were mounted on the stage using Nikon attachable graduated mechanical stage. The step size was one increment on the stage.

Quartz was divided into monocrystalline and polycrystalline varieties. Feldspars were divided into plagioclase and potassium feldspars. Volcanic and sedimentary lithics are recognized with no metamorphic lithics in the samples. Volcanic lithics were subdivided into basaltic and intermediate-felsic volcanic lithics. Sedimentary lithics including chert, mudrock, shale, and carbonate lithics were identified. Other accessory minerals including amphibole, biotite, chlorite, chalcedony, and zeolite were identified. Detailed subdivisions can be found in Table 2.1.

Grain shapes were described as equant, ellipse, elongate, very elongate, and wedge. Roundness and angularity were described as very angular, angular, subangular, subrounded, rounded, and well-rounded based on Powers' grain images for estimating roundness of sedimentary particles (Powers, 1953). Grain contacts were divided into floating, point, line, and concave and convex types.

The percentages of each component, framework work grains, matrix, and cement, among all counts were calculated. Sandstone classification is modified from Dott (1964).

A sandstone with 0-5% matrix is classified as arenite; 5-15% matrix subarenite; 15-50% matrix wacke; > 50% matrix mudrock.

Statistical analyses were carried out to determine mean grain size, sorting, and average roundness. Grain size is determined by

$$M_z = \frac{\phi_{16} + \phi_{50} + \phi_{84}}{3} \quad (2.1)$$

Where M_z is the graphic mean size of all the framework grains, ϕ_{16} , ϕ_{50} and ϕ_{84} are the 16th, 50th, and 84th percentile values of the cumulative curve (Folk and Ward, 1957).

Sorting is determined by the inclusive graphic standard deviation:

$$\sigma_i = \frac{\phi_{84} - \phi_{16}}{4} + \frac{\phi_{95} - \phi_5}{6.6} \quad (2.2)$$

Where σ_i is inclusive graphic standard deviation, ϕ_5 , ϕ_{16} , ϕ_{50} , ϕ_{84} , ϕ_{95} are the 5th, 16th, 50th, 84th and 95th percentile values of the cumulative curve (Folk and Ward, 1957).

The QFL ternary diagram (Folk, 1980) was plotted to determine petrofacies. Q includes monocrystalline quartz, polycrystalline quartz, and chalcedony; F plagioclase and potassium feldspars; L volcanic and sedimentary lithics. Other grains were not used in the plotting; and the QFL contents were normalized to 100%. Three ternary diagrams, QmFLt, QmLvLs, and QmPK (Dickinson 1985) were plotted using Tri-plot 4.1.2 software (Todd Thompson, 2009) to determine the tectonic setting of the sandstones. Compositional and textural properties are plotted along each measured section with interpreted depositional environments. Vertical and lateral changes of provenance and transport distance were interpreted from vertical and lateral trends in individual sections.

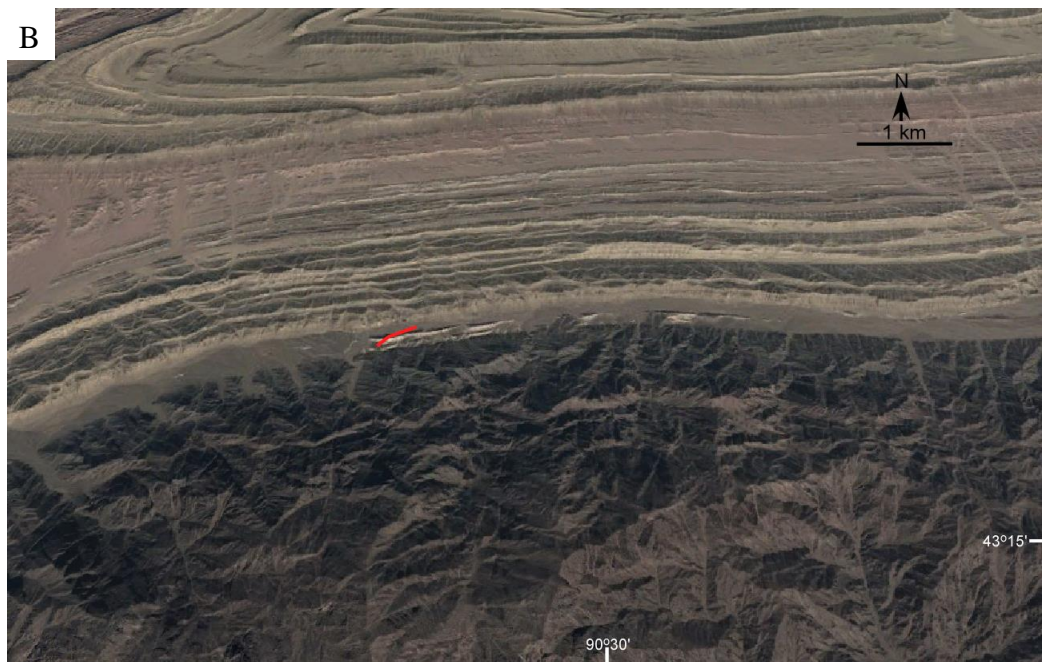
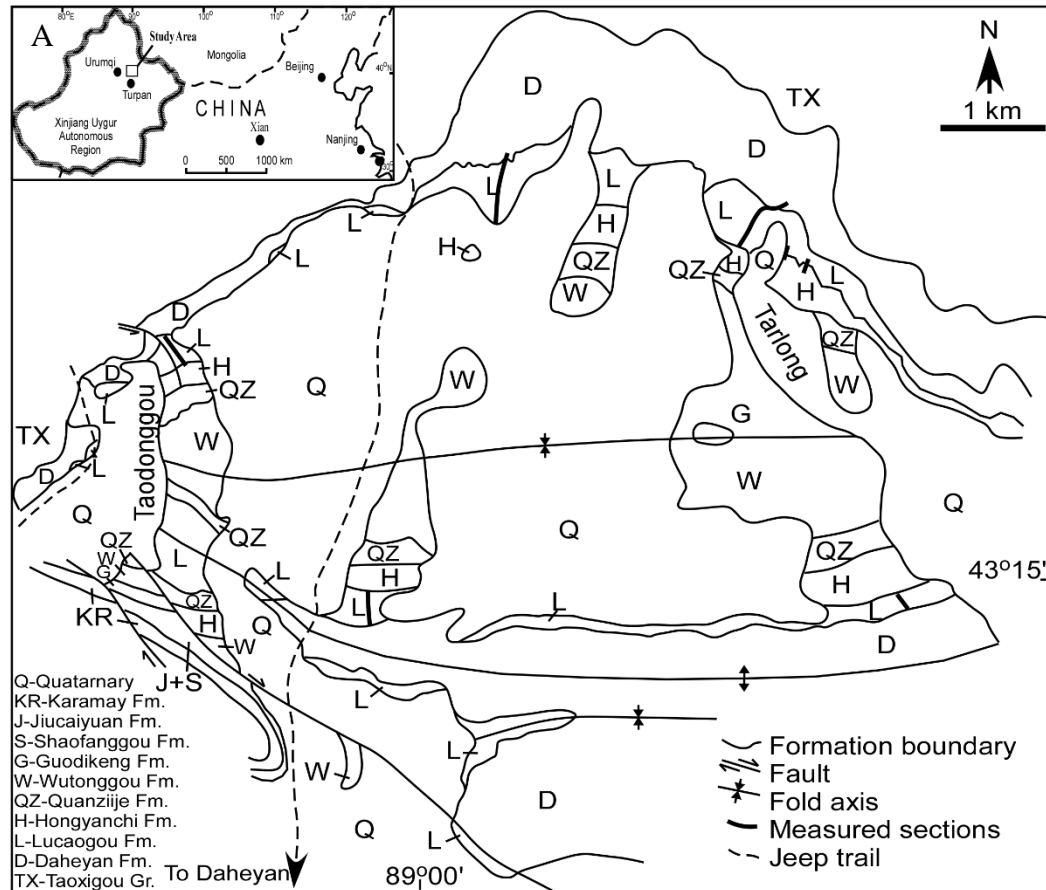


Figure 2.1. Geologic map and satellite photo of the study areas. (A) Tarlong-Taodonggou modified from Yang et al. (2010), (B) Zhaobishan area showing names and location (black and red lines) of measured sections. Satellite photo is from Google Earth.

Table 2.1. Grain types and modal parameters used in this study

Symbol	Definition
Qm	Monocrystalline quartz
Qp	Polycrystalline quartz
Qc	Chalcedony
K	Potassium feldspar
P	Plagioclase feldspar
Lvi	Intermediate volcanic lithic
Lvb	Basaltic lithic
Lvu	Undifferentiated volcanic lithic
Lv	Lvi+Lvb+Lvu
Lsm	Mudrock lithic and mud clasts
Lsc	Chert
Lss	Shale lithic and siltstone lithics
Lsca	Carbonate lithic
Ls	Lsm+Lsc+Lss+Lsca
Calculated parameters for sandstone classification (Folk, 1980)	
Q	Qm+Qp
F	K+P
L	Lv+Ls
Calculated parameters for Dickinson's ternary diagrams	
Q	Qm+Qp
Qp	Qp+Qc
F	K+P
L	Lv+Ls
Lt	L+Qp

3. SANDSTONE PETROGRAPHY

Sandstone petrography is a powerful tool for determining the origin of ancient terrigenous deposits and tectonic reconstructions of sedimentary basins (e.g., Blatt 1967; Dickinson, 1970; Pettijohn et al., 1972). Thirty seven sandstones range from coarse silt to coarse sand in size, are poorly sorted to moderately well sorted, and contain very angular to well-rounded framework grains. Intergranular components are pore-filling calcite, microcrystalline quartz, chalcedony, and calcitic mud. The raw point-counting and statistic data are shown in Table 3.1 and 3.2.

3.1. FRAMEWORK GRAINS

Framework grains are silicate detrital grains. Their function is to support the sandstone. Framework grains range in size from 1/16 to 2 mm. They are classified into three categories on the basis of their mineral composition: quartz, feldspar, and lithics, among which eight types were identified. Grain composition, size, sorting, roundness, and contact were examined.

3.1.1. Quartz (Q). Quartz is hard and chemically stable and, thus, can survive multiple recycling. As a result, it is the most abundant mineral with a 50%-60% occurrence in most sandstones in the geological history (Boggs, 2014). However, quartz content is low in Lucaogou sandstones, only 1.8% on average. This may be related to quartz-poor provenance lithology. Two types of quartz, monocrystalline and polycrystalline, are identified in the samples.

3.1.1.1 Monocrystalline quartz (Qm). Monocrystalline quartz makes up 85.14% of all quartz. Two types of mono-quartz grains are identified. Those from volcanic lithics show a euhedral to subhedral shape with embayed edges, straight extinction, and are clear and inclusion-free (Figure 3.1A). The other type is subrounded to rounded, and has straight or slightly undulose extinction, and possible internal fractures inside grain (Figure 3.1B). These features indicate that the grains had experienced transport and some compaction. Grain size Qm varies from coarse silt to coarse sand, and very fine sand on average. The roundness of Qm grains ranges from very angular to rounded and is mainly subrounded.

Table 3.1. Raw point-counting data and results of statistical grain size analysis of Taodonggou, S, SW, N Tarlong sections

Section	Sample No.	Qm	Qp	Qc	K	P	Lvi	Lvb	Lvu	Lsm	Lsc	Lss	Lsca	Cement	Matrix	Mz	σ_1	Sk1
Taodonggou	TD21	3	0	0	21	3	60	152	25	10	3	3	0	7	86	1.61	0.7	0.14
	TD27	3	0	0	3	0	6	39	45	0	0	3	0	10	272	3.34	0.73	0.66
	TD29	3	1	0	7	2	46	227	1	12	7	7	0	53	14	1.82	0.63	0.03
	TD35	4	0	0	16	2	39	143	5	7	6	12	0	97	46	2.3	0.57	-0.03
	TD37	22	3	0	7	3	4	66	24	11	2	22	0	133	51	3.41	0.62	-0.04
S Tarlong	TR1-13	3	1	0	15	0	9	154	13	10	3	4	0	148	14	2.34	0.77	-0.03
	S7-59	5	1	0	43	0	5	13	23	1	0	0	0	3	158	2.32	0.91	-0.15
	S7-65	2	0	0	18	0	14	147	63	4	2	1	7	76	61	3.07	0.77	-0.18
	S7-66	2	3	0	12	0	6	72	8	2	6	5	2	2	20	2.4	0.7	0.16
	S7-67	2	0	0	54	0	2	162	43	8	0	7	3	57	55	2.4	0.89	-0.07
	S7-73	7	1	0	34	5	16	41	90	16	1	0	0	79	67	3.83	0.73	-0.02
SW Tarlong	B09-1	7	0	0	22	0	5	153	0	3	1	6	0	117	38	2.47	1.02	-0.24
	B09-3	3	0	1	7	1	17	32	10	79	6	0	0	185	33	2.5	1.33	-0.21
	B09-4	6	0	0	15	5	11	51	10	93	5	29	0	141	18	1.54	0.89	0
	B09-7	5	0	0	6	1	21	70	91	13	0	1	1	38	177	4.05	0.66	-0.03
N Tarlong	TR30	0	0	0	8	0	69	278	2	0	4	0	0	0	35	1.61	0.61	0
	TR31	3	0	7	35	0	26	273	3	10	0	11	0	1	26	2.72	0.8	-0.15
	TR34-1	3	2	15	45	1	18	258	0	4	3	5	0	9	8	3.19	0.69	0.04
	TR34-3	4	1	25	47	0	21	225	1	2	1	9	2	44	0	2.72	0.73	-0.16
	TR40	6	0	0	11	0	12	152	31	6	0	16	0	142	23	1.8	1.001	-0.01

Table 3.2. Raw point-counting data and results of statistical grain size analysis of NW Tarlong and Zhaobishan sections

Section	Sample No.	Qm	Qp	Qc	K	P	Lvi	Lvb	Lvu	Lsm	Lsc	Lss	Lsca	Cement	Matrix	Mz	σ_1	Sk1
NW Tarlong	S7-42	2	0	0	10	0	5	55	32	0	0	0	1	1	198	1.24	1.74	0.12
	S7-44	1	0	0	15	1	33	197	6	0	0	3	0	52	88	0.07	1.27	0.22
	S7-47	8	7	0	59	0	36	184	10	0	0	24	0	54	0	2.9	0.6	0.07
	S7-48	16	0	0	68	0	9	201	22	1	0	31	0	35	7	2.7	0.55	0.03
	S7-52	1	0	0	26	0	1	57	23	2	0	9	0	133	144	2.54	0.7	-0.18
	S7-57	1	1	3	20	0	3	191	27	1	0	39	0	9	41	2.23	0.78	-0.19
	S8nw-2	2	1	8	46	5	23	228	32	1	0	10	0	34	14	1.96	0.59	0.01
	S8nw-16	0	1	0	3	0	6	273	31	18	1	2	1	54	0	1.35	0.89	0.1
Zhaobishan	SZ15-1	13	5	0	35	0	26	96	41	2	17	5	0	6	153	2.34	0.88	-0.28
	SZ15-2	2	2	0	35	0	15	128	34	14	0	6	1	43	108	2.41	0.54	0.04
	SZ15-3	0	1	2	19	0	16	60	30	8	6	47	2	170	24	2.01	0.75	0.03
	SZ15-4	2	0	0	14	0	6	98	22	2	9	17	5	171	43	2.12	0.87	-0.28
	SZ15-5	3	0	0	4	0	9	56	45	1	0	27	0	204	18	2.75	0.71	-0.2
	SZ14-45	0	0	11	2	0	5	86	159	4	1	21	0	24	46	2.11	1.2	-0.53
	SZ14-46	4	0	2	2	0	17	37	93	15	2	3	4	46	106	2.23	0.85	-0.03
	SZ14-48-1	12	0	0	24	2	17	92	39	6	0	3	1	44	57	2.68	0.63	-0.11
	SZ14-50	24	2	0	13	3	96	139	68	3	0	3	0	0	11	3.79	0.85	0.1

3.1.1.2 Polycrystalline quartz (Qp). Polycrystalline quartz only makes up 14.86% of all quartz. Most Qp grains are composed of interlocking subcrystals showing slight to high undulosity (Figure 3.1C). The properties of polycrystallinity and undulatory extinction can be used to distinguish quartz derived from different sources. Some authors (Folk, 1974; Basu et al., 1975) suggest that this property indicates plutonic or metamorphic sources. The size of Qp grains varies from coarse silt to coarse sand with an average fine sand size. Roundness varies from very angular to rounded, mainly subrounded.

3.1.2. Feldspar (F). Although feldspars are the most common minerals in igneous and metamorphic rocks, feldspars are less stable than quartz at conditions near the Earth's surface. Thus, feldspars make up only 10-15% of all framework grains in sandstones in the geologic record (Boggs, 2014). Feldspars account for 9.46% of all framework grains in Lucaogou sandstones, which is similar to that of world average. Feldspars have two types, plagioclase and potassium feldspars. Both types are observed in the samples. Twinning makes it easy to distinguish between feldspars and quartz. However, some potassium feldspars don't show twinning. Cleavage is another feature that can be used to identify feldspar. Feldspars have two cleavage planes that intersect at $\sim 90^\circ$. Plagioclase is the dominant feldspar in the samples while potassium feldspars are minor. The average P/F ratio is 0.93, which indicates a dominant volcanic source (Dickinson, 1985).

3.1.2.1 Plagioclase (P). Plagioclase feldspars form a complex solid solution series ranging in composition from albite through anorthite. They account for 92.85% of all feldspars. Plagioclase can be easily distinguished from potassium feldspar on the basis of optical properties such as albite twinning and zoning (Figure 3.1D, E). The grain size varies from coarse silt to very coarse sand with an average size of fine sand. Roundness varies from very angular to well-rounded, mainly subangular to subrounded. High plagioclase content, relatively angular shape, and compositional zoning support a nearby volcanic source.

3.1.2.2 Potassium feldspar (K). Potassium feldspars only account for 7.15% of all feldspars. Common species of potassium feldspar are orthoclase, microcline, and sanidine. But only orthoclase is observed in the studies samples. Orthoclase is identified by its platy shape, two sets of cleavages, and Carlsbad twinning (Figure 3.1F). Its size

varies from coarse silt to medium sand with an average of very fine sand. Roundness varies from very angular to rounded, mainly subrounded.

3.1.3. Lithics (L). Lithics are fragments of ancient source rocks and sediments that have not yet disintegrated to yield individual mineral grains. Lithics are the most dominant component in the studied samples, accounting for 88.74% of all framework grains. Volcanic lithics include basaltic and intermediate-felsic volcanic fragments; and sedimentary lithics including chert, mudrock, shale, and carbonate fragments. No metamorphic lithics were seen. The abundance of lithics indicates a low compositional maturity.

3.1.3.1 Volcanic lithics (Lv). Volcanic lithics in the sandstones are differentiated based on texture into felsitic, vitric, microlithic, and lathwork types. Felsitic grains are anhedral, microcrystalline mosaic composed of mainly quartz and feldspar. Vitric grains are glass or altered glass. Microlithic grains are subhedral to euhedral feldspars in pilotaxitic, felted, trachytic, or hyalopilitic groundmass of microlites, and represent mainly intermediate volcanic lithics (Figure 3.2D). Lathwork grains contain plagioclase laths in intergranular and intersertal textures representing mainly basaltic lithics (Dickinson, 1970; Figure 3.2A, B, C). The average percentage of basaltic grains is 88.4% of all grains; that of intermediate volcanic lithics ~10%; and felsic volcanic lithics 1~2%. Abundant lathwork grains with little microlithic and minor felsitic and vitric grains is typical of all the samples, indicating the dominance of a basaltic source and a distant secondary intermediate-felsic volcanic source. The size of volcanic lithics varies from very fine sand to granule. The roundness varies from very angular to rounded, mainly subangular to subrounded. A major portion of the volcanic lithics is partially or completely replaced by calcite, which makes it hard to interpret the exact type of volcanic lithics. These grains are not included in the calculation of basaltic and felsic volcanic lithics, but they are included in the calculation of volcanic lithics and lithics.

Basaltic lithics (Lvb) are the most abundant component in both lithic grains and framework grains. The Lvb can be identified by feldspar laths encased in brown or black groundmass (Figure 3.2A, B). The black groundmass is probably due to the abundance of Fe-bearing opaque minerals. The light color groundmass is the result of alteration into clay or calcite. Some of the Lvb show a preferred orientation of feldspar laths, referred as

trachyte and included in the Lvb on ternary diagrams. The size of the Lvb grains varies from coarse silt to fine pebble with an average size of fine sand. Roundness varies from very angular to well rounded, mainly subrounded.

Intermediate-felsic volcanic lithics (Lvi) are minor, accounting for 10% of all volcanic lithics. In some cases, they are hard to differentiate from chert grains. One difference between them is the relief of the feldspars and quartz can be differentiated in volcanic lithics under plane light based on Becker line, while chert shows a relative flat surface. The size of Lvi varies from coarse silt to fine pebble with an average size of fine sand. Roundness varies from very angular to well-rounded, mainly subrounded.

3.1.3.2 Sedimentary lithics (Ls). Sedimentary lithics account for 12.4% of all the lithics. Four main types of Ls, mudrock, shale, chert, and carbonate, are recognized in the samples.

Mudrock lithic (Lsm) is the most common Ls in the samples, and accounts for 35.5% of all Ls. It is characterized by clay matrix with scattered silt or sand grains (Figure 3.2E). Lsm are mainly rounded and well-rounded, indicating that the clasts were lithified or semi-consolidated during deposition. These grains can be interpreted as fragments of mudrocks or cohesive muddy sediments. Some of the mudrock clasts are subangular to subrounded with embayed edges, and may be rip-up mud clasts (Figure 3.2F).

Chert (Lsc) is the second most abundant Ls in the samples. It is characterized by relatively equant, uniform-sized grains in crenulate, sharp contacts (Figure 3.3A). Chert is not observed in NW Tarlong, but in other sections, and accounts for 9.3% of all Ls.

Shale lithics (Lss) are also present in the samples. It can be identified by clear laminations and deformation by adjacent hard grains (Figure 3.3B), indicating a shale origin. The shale lithics could have been derived from uplifted rift shoulders exposing shale, because shale would not have survived long-distance transport.

Some carbonate lithics (Lsca) are also seen in some samples, accounts for 6.9% of all Ls, and mostly occur as ooids (Figure 3.3C). The small amount of carbonate lithics suggests they are not formed in-situ. These lithics were derived from a provenance containing carbonate rocks.

In SW Tarlong, Ls grains account for 38.4% of all the lithics, while in other sections, the percentage is 10.0%. Most of the Ls in SW Tarlong are rounded to well-rounded mudrock lithics. The wide range of variation in abundance of Ls grains suggests a nearby local sedimentary source in SW Tarlong in addition to a regional dominant volcanic source. The small amount of Ls in other sections suggests a secondary sedimentary source. The size of the Ls varies from coarse silt to granule with an average fine sand size. Roundness varies from very angular to well-rounded, mainly (66.8%) subrounded to rounded.

3.1.4. Accessory Minerals. A wide variety of accessory minerals are present and account for less than 1% of all framework grains. Biotite, muscovite, chalcedony, chlorite, zeolites, magnetite, hematite, and amphibole (Figure 3.3D, E, F). Some of them are depositional, whereas others are formed through diagenesis. The size of the accessory minerals varies from very fine to medium sand. Roundness varies from angular to rounded.

3.2. MATRIX AND CEMENTS

Matrix and cements are dominantly calcitic. Grains in sandstones smaller than 0.03 mm, which fill interstitial spaces among framework grains, are referred to as matrix. Cements are minerals bounding the framework grains in most siliciclastic sedimentary rocks.

3.2.1. Matrix. Matrix originates in two principal ways. First, primary detrital matrix is transported and deposited with the sand-size framework grains. Second, matrix can also be produced by diagenesis: rock fragments are squashed and disaggregated; and feldspar is transformed into clay. In this study, the matrix is likely to be a diagenesis product. Two lines of evidence support the interpretation. First, no available source is known for the calcitic matrix. Most grains in the samples are terrestrial siliciclastic grains with scattered carbonate lithics. Second, replacement of volcanic grains by calcite is common in thin sections, which could be the first stage of alteration of volcanic grains into matrix.

Matrix in the samples is mainly calcitic mud of silt and clay size (Figure 3.4A). The calcitic composition is identified by HCL test on hand samples and staining with

Alizarin red S on thin sections. Some of the matrix is clay minerals which are hard to distinguish by routine petrographic microscope. Further identification using X-ray diffraction and electron microscopy would be needed. The percentage of matrix varies from 0% to 44.25% in all samples. Two mudrocks, described as muddy wackes in the field, are identified in Taodonggou and NW Tarlong with matrix percentages of 68.51% and 65.3%, respectively. The average matrix percentage in S Tarlong, Tadonggou, SW Tarlong, and Zhaobishan is 15% to 25%. In NW Tarlong, the matrix amount is 10.73%, and 4.6% in N Tarlong. This trend indicates a textural maturity decrease trend from south to north in the Tarlong-Taodonggou area.

3.2.2. Cements. Cements in the studied samples are mainly of two types, isopachous and pore-filling (blocky). Cement minerals are calcite, chalcedony, and microcrystalline quartz. Most samples experienced severe diagenesis. The amount of cements varies from 0 to nearly 50%. The average cements in S Tarlong, Taodonggou, SW Tarlong, N Tarlong, NW Tarlong and Zhaobishan are 15.36%, 15.00%, 29.75%, 9.80%, 11.68%, and 19.88%, respectively. Isopachous and blocky calcite cements are well developed in most samples; zeolite cement is well developed in NW Tarlong and rare in N Tarlong; and silica cement occurs in NW Tarlong, Taodonggou, and Zhaobishan. The formation of isopachous calcite cements (Figure 3.4B) could have been related to hydrothermal fluids; but more evidence is needed to support the interpretation. Poikilotopic calcite cements were observed in some samples.

In NW Tarlong, Zhaobishan and middle part of Taodonggou section, silica cements, such as microcrystalline quartz and chalcedony (Figure 3.4C, D), were present. This may indicate different pore water chemistry.

3.3. SANDSTONE CLASSIFICATION

There are more than 50 schemes of classifying sandstones, but the most commonly used ones incorporate both texture and mineralogy. In this study, the classification is from Dott (1964). This classification is better to portray the continuous nature of texture variation from mudrock to arenite and from stable to unstable grains. The classification is based on both the relative abundances of quartz (Q), feldspar (F), and rock fragments (R) and the abundance of matrix, modified from Dott (1964) (Boggs,

2014). Two parameters of relative abundance are used to subdivide terrigenous sandstones. The first parameter is the percentage of matrix in the mixture of framework grains and matrix, without considering cement and porosity. The second is the percentage among three types of framework grains, i.e., quartz, feldspar and rock fragments (lithics). Sandstones are divided into three groups: arenites, containing little or no matrix (<5%); subarenites, containing some matrix (5-15%); and wackes, containing perceptible matrix of 15-50%. Siliciclastic sedimentary rocks containing more than 50% matrix are called mudrock. The relative percentage of quartz, feldspar and rock fragments is used to subdivide arenites, subarenites and wackes. Other framework grains, such as micas and heavy minerals, are ignored. The arenites are subdivided into quartz arenite (more than 95% quartz grains), arkosic arenite/subarenite (more than 25% feldspar and more feldspar than rock fragments), subarkose arenite/subarenite (5–25% feldspar grains and more feldspar than rock fragments), lithic arenite/subarenite (more than 25% rock fragments and more rock fragments than feldspar), and sublitharenite/subarenite (5–25% rock fragments and more rock fragments than feldspar). The wackes are divided into quartz wacke (more than 95% quartz grains), lithic wacke (more than 5% rock fragments and more rock fragments than feldspar), and feldspathic (arkosic) wackes (more than 5% feldspar and more feldspar than rock fragments).

According to Folk (1959), the name of a rock must convey as much information as possible without being a complete description. Five properties including grain size, chemically precipitated cements, textural maturity, miscellaneous transport constituents, and clan designation, are proposed to define sandstone. Textual maturity is reflected by terms of arenite/subarenite and wacke in Dott's classification. Thus, the name could be in the following format: (Grain size) (chemically precipitated cements) (miscellaneous transported constituents) (clan designation). The grain size and clan designation should always be mentioned, while the other two aspects should be mentioned whenever observed. Due to severe diagenesis, the boundary of whether or not describing cements is set at 10% to differentiate degrees of cementation.

Overall, all the studied samples can be classified into four groups: eleven lithic arenites, fifteen lithic subarenites, nine lithic wackes, and two lithic mudrocks. More detailed classification of each sample is shown in Table 3.3.

Table 3.3. Classification of studied sandstones

Section	Sample No.	Classification
Taodonggou	TD21	Medium sand lithic wacke
	TD27	Very fine sand lithic mudrock
	TD29	Medium sand lithic arenite
	TD35	Fine sand calcitic lithic subarenite
	TD37	Very fine sand calcitic lithic subarenite
S Tarlong	TR1-13	Fine sand calcitic lithic arenite
	S7-59	Fine sand lithic wacke
	S7-65	Very fine sand calcitic lithic wacke
	S7-66	Fine sand lithic subarenite
	S7-67	Fine sand calcitic lithic subarenite
	S7-73	Fine sand calcitic lithic wacke
SW Tarlong	B09-1	Fine sand calcitic lithic subarenite
	B09-3	Fine sand calcitic lithic subarenite
	B09-4	Medium sand calcitic lithic arenite
	B09-7	Coarse silt lithic wacke
N Tarlong	TR30	Medium sand lithic subarenite
	TR31	Fine sand lithic subarenite
	TR34-1	Very fine sand lithic arenite
	TR34-3	Fine sand calcitic lithic arenite
	TR40	Medium sand calcitic lithic subarenite
NW Tarlong	S7-42	Medium sand lithic mudrock
	S7-44	Coarse sand calcitic lithic wacke
	S7-47	Fine sand calcitic lithic arenite
	S7-48	Fine sand lithic arenite
	S7-52	Fine sand calcitic lithic wacke
	S7-57	Fine sand lithic subarenite
	S8nw-2	Medium sand lithic arenite
	S8nw-16	Medium sand chalcedony lithic arenite
Zhaobishan	SZ15-1	Fine sand lithic wacke
	SZ15-2	Fine sand calcitic lithic wacke
	SZ15-3	Fine sand calcitic lithic subarenite
	SZ15-4	Fine sand calcitic lithic subarenite
	SZ15-5	Fine sand calcitic lithic arenite
	SZ14-45	Fine sand lithic subarenite
	SZ14-46	Fine sand calcitic lithic subarenite
	SZ14-48-1	Fine sand calcitic lithic subarenite
	SZ14-50	Very fine sand lithic arenite

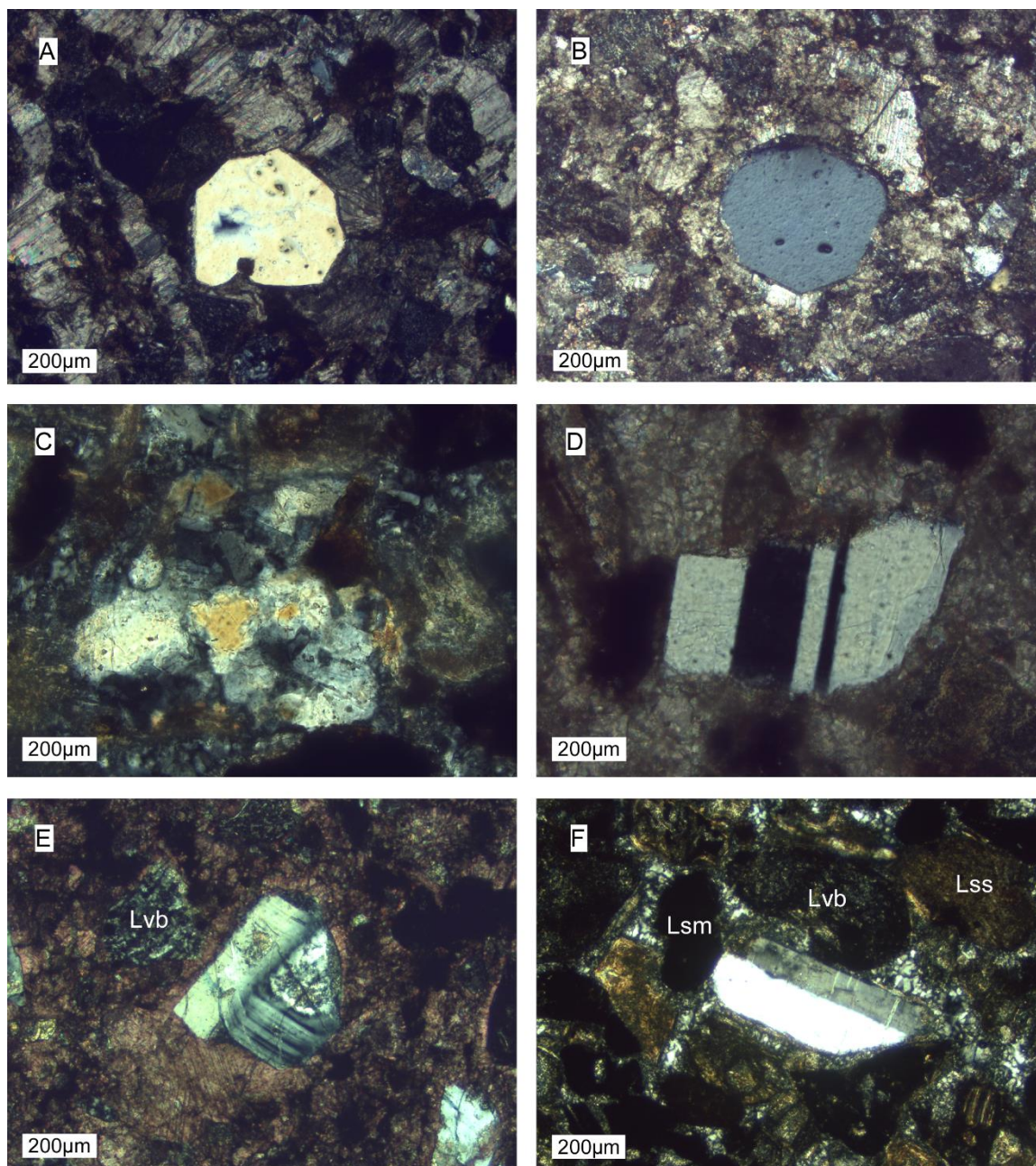


Figure 3.1. Photomicrograph of quartz and feldspars. A) Photomicrograph (XL) showing typical volcanic quartz indicated by a biprism shape and embayed edge. Adjacent grains are coated with isopachous calcite. Sample TR1-13 from S Tarlong. B) Photomicrograph (XL) showing a rounded monocrystalline quartz indicating long transport distance. Sample TR40 from N Tarlong. C) Photomicrograph (XL) showing a polycrystalline quartz or composite grain. Sample TD29 from Taodonggou. D) Photomicrograph (XL) showing a plagioclase with albite twinning. Sample TD35 from Taodonggou. E) Photomicrograph (XL) showing a subangular zoned plagioclase feldspar indicative of a volcanic origin. Sample B09-3 from SW Tarlong. F) Photomicrograph (XL) showing a rounded Carlsbad twinning potassium feldspar surrounded by rock fragments. Sample TD29 from Taodonggou. Lvb-basaltic lithic, Lsm-mudrock lithic, Lss-shale lithic.

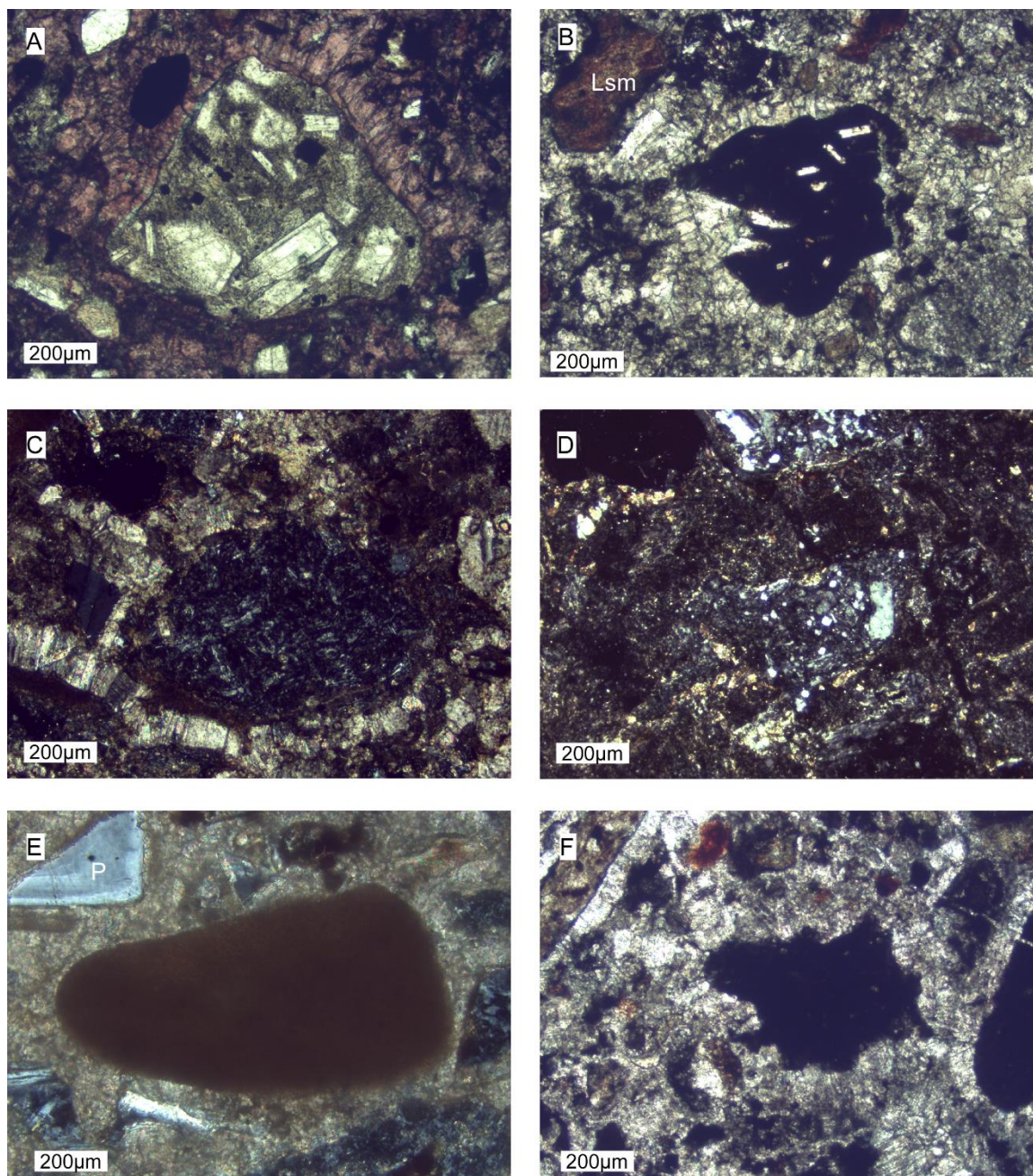


Figure 3.2. Photomicrograph of volcanic lithics and mud clasts. A) Photomicrograph (PL) showing a volcanic lithic. Feldspar laths are visible, and the groundmass is altered into clay. Sample B09-1 from SW Tarlong. B) Photomicrograph (XL) showing an angular basaltic lithic in a black groundmass. Sample B09-1 from SW Tarlong. C) Photomicrograph (XL) showing a lathwork grain indicating basaltic origin. Sample TR40 from N Tarlong. D) Photomicrograph (XL) showing a microlithic grain suggesting a felsic origin. Sample TR30 from N Tarlong. E) Photomicrograph (XL) showing a brown well-rounded mudrock indicating long transport distance. Sample S7-67 from S Tarlong. F) Photomicrograph (PL) showing a very angular mudclast indicating short transport. Sample b09-4 from SW Tarlong. Lsm-mudrock lithic, P-plagioclase.

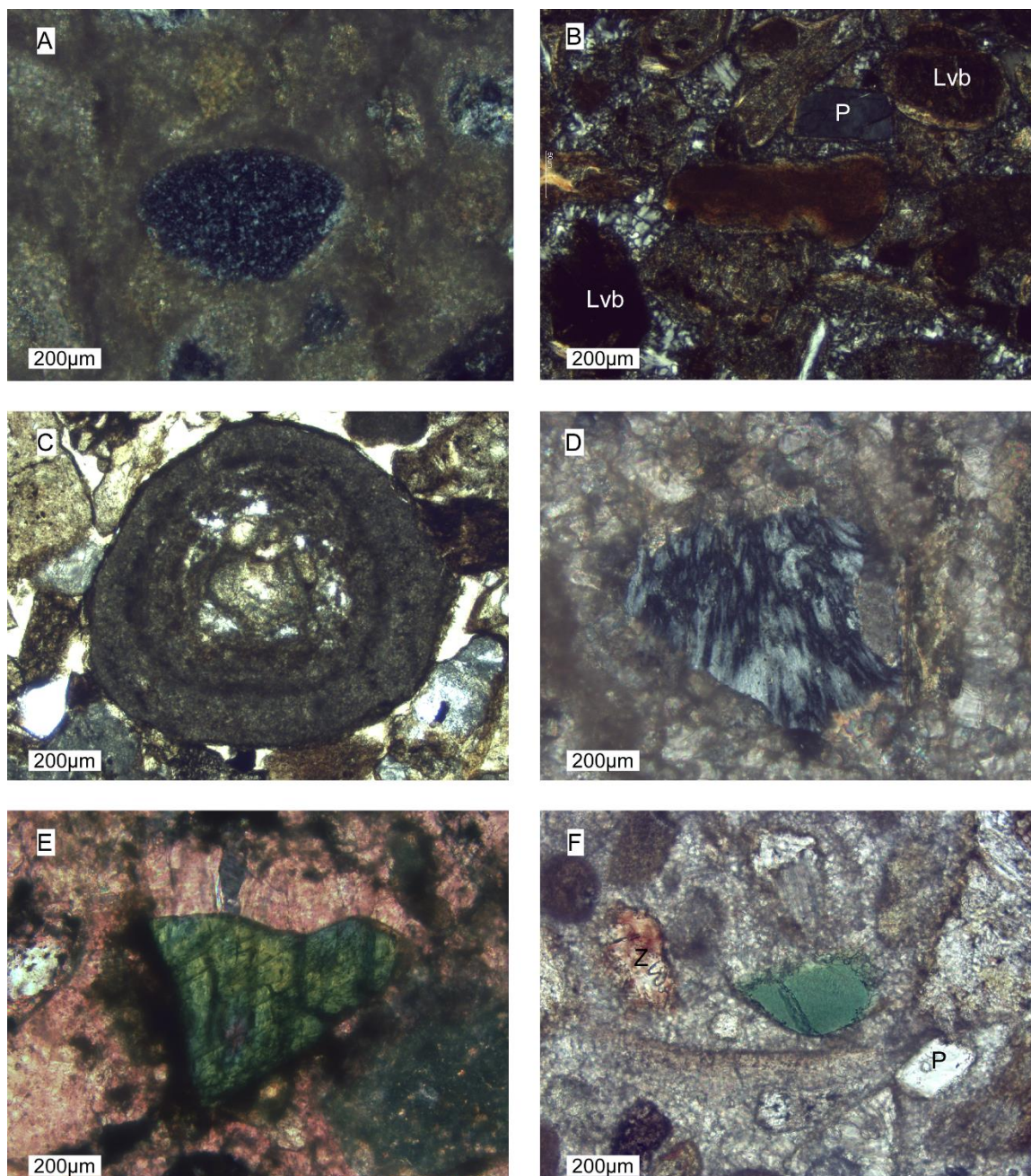


Figure 3.3. Photomicrograph of sedimentary lithics and accessory minerals. A) Photomicrograph (XL) showing a chert grain. Sample SZ15-1 from Zhaobishan. B) Photomicrograph (XL) showing a dark brown deformed rounded shale lithic in the middle. Sample TD29 from Taodonggou. C) Photomicrograph (PL) showing a carbonate fossil. Sample Snw8-16 from NW Tarlong. D) Photomicrograph (XL) showing a chalcedony grain. Sample SZ15-2 from Zhaobishan. E) Photomicrograph (XL) showing an amphibole characterized by pleochroism and two sets of cleavages. Sample B09-3 from SW Tarlong. F) Photomicrograph (XL) showing a chlorite characterized by its green color. The grain to the left could be a zeolite based on previous XRD result. Sample S7-65 from S Tarlong. P-plagioclase, Lvb-basaltic volcanic lithic, Z-zeolite.

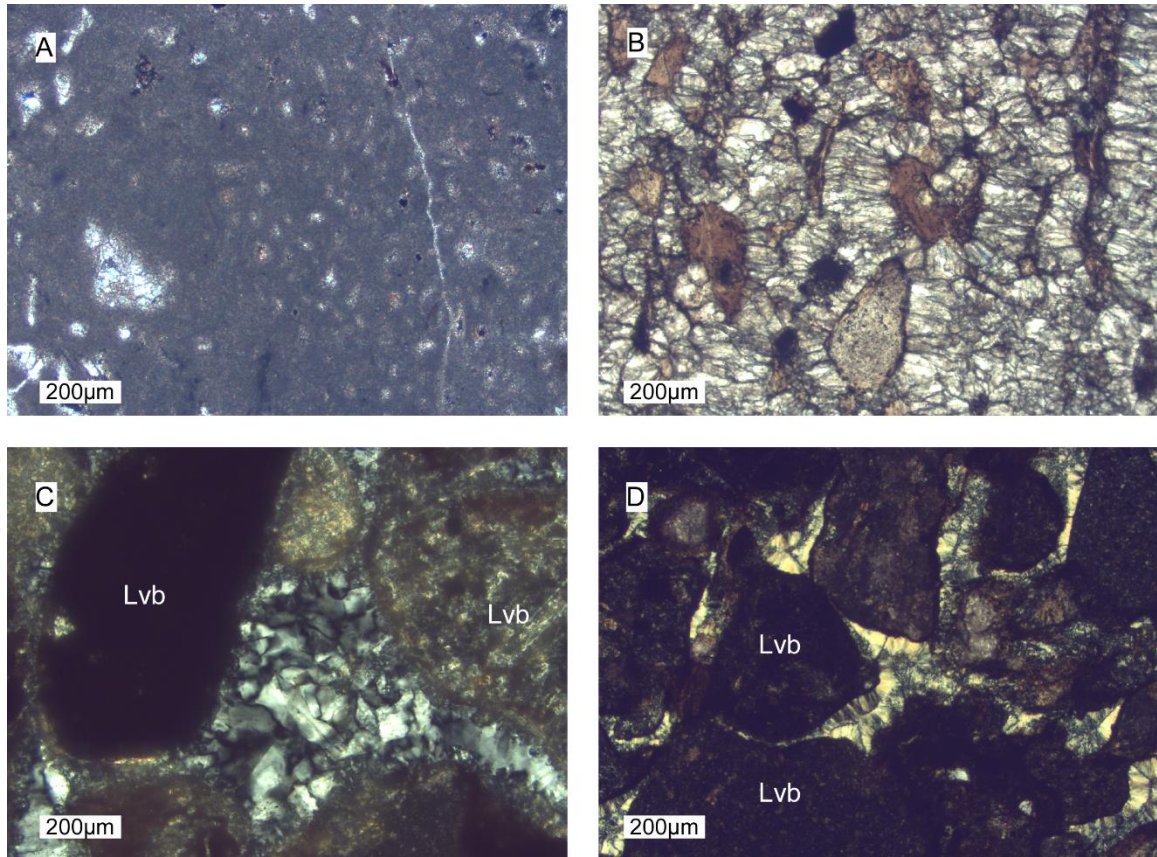


Figure 3.4. Photomicrograph of matrix and cements. A) Photomicrograph (XL) showing silt grains floating in calcitic mud tested by HCL acid from hand sample. Sample TD27 from Taodonggou. B) Photomicrograph (PL) showing abundant isopachous calcite growing inside and around grains. Sample SZ15-5 from Zahobishan. C) Photomicrograph (XL) showing a pore-filling silicate cement, probably microcrystalline quartz or zeolite. Sample TD29 from Taodonggou. D) Photomicrograph (XL) showing isopachous chalcedony cement around basaltic volcanic lithics. Sample S8nw-16 from NW Tarlong. Lvb-basaltic lithics.

4. PETROFACIES

A petrofacies (i.e., petrographic facies) is defined as facies distinguished primarily on the basis of appearance or composition, without respect to form, boundaries, or mutual relations (Bate and Jackson, 1984). Quantitative analysis by counting 400 points in each sample provides critical data to define petrofacies.

All the sandstones in this study cluster tightly on the QFL compositional ternary diagram of Folk (1980), with a mean composition of $Q_3F_9L_{88}$ (Figure 4.1). This clustering, essentially, defines one petrofacies for the entire LCG samples, signifying a first-order underlying control on the sandstone composition of LCG LC.

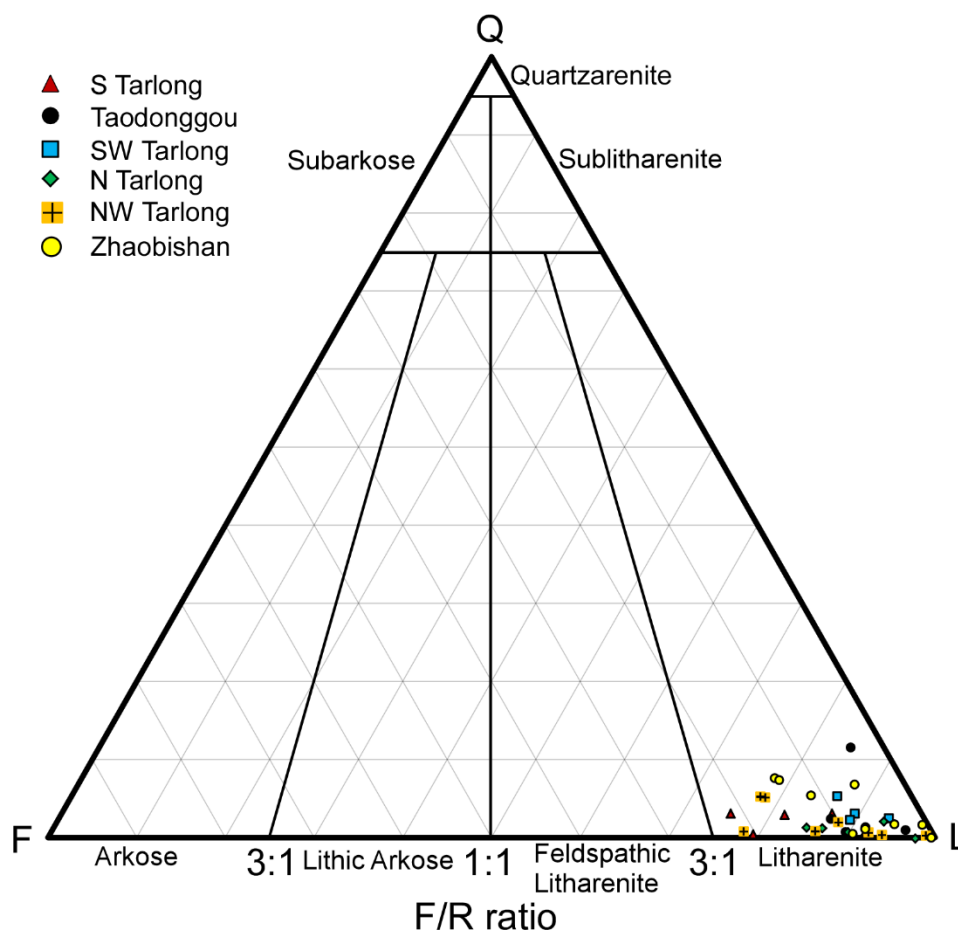


Figure 4.1. QFL Ternary diagram showing all 37 samples from the LCG LC fall in litharenite field in the LCG LC, according to Folk's (1980) sandstone classification.

With respect to the mean QFL composition of all the sandstones, average LCG sandstone is a litharenite according to Folk's (1980) classification. Mono- and polycrystalline quartz account for 85% and 15% of total quartz content, respectively. Plagioclase dominates the feldspars with a 96% and potassium feldspar is only 4%. Volcanic lithics account for 84% of the lithics where basaltic lithics (84%) dominate with minor intermediate volcanic lithics (16%). Basaltic lithics would have a low silica content (<52%), while intermediate-felsic would have higher silica content (>52%). Sedimentary lithics make up 16% of all the lithics with chert and mud clasts as the main types. Grain size varies from coarse silt to fine pebble. Roundness of the grains varies from very angular to well-rounded; and sorting from poorly to moderately well sorted.

However, a close examination of the apparently closely-related 37 sandstones differentiates three groups, that is, petrofacies. They have variable Lv/Ls and Lvb/Lvi ratios and are described as petrofacies A, B, and C in detail below.

4.1. PETROFACIES A

The mean compositions of Petrofacies A, as defined in three types of ternary diagrams, are $Q_3F_{11}L_{86}$, $Qm_2F_{12}Lt_{86}$, $Qp_1Ls_7Lv_{92}$, and $Qm_{15}K_1P_{84}$. This petrofacies encompass 22 samples in all sections. Volcanic lithics dominate in Petrofacies A, of 91.4% of all lithic grains, while sedimentary lithics of 7.2%. Of all the volcanic lithics, basaltic lithics account for 92.1% and intermediate-felsic lithics 7.9%. The average size is fine sand with a range from very fine to coarse sand. Roundness of the grains varies from subrounded to rounded (Figure 4.2); and sorting from poorly sorted to moderately well-sorted, and mainly moderately sorted. The skewness is mainly near symmetrical to coarse skewed. The amount of matrix varies from 0-39.5% with an average of 16.6%. The amount of cements varies from 0.33-35.5% with an average of 12.9%.

4.2. PETROFACIES B

Petrofacies B has mean compositions of $Q_3F_5L_{92}$, $Qm_3F_8Lt_{89}$, $Qp_1Ls_{36}Lv_{63}$, and $Qm_{23}K_6P_{71}$, which can be differentiated from QpLvLs ternary diagram (Figure 4.3). This petrofacies occurs in 8 samples from Taodonggou, SW Tarlong, N Tarlong, and Zhaobishan sections. It is characterized by a great percentage of sedimentary lithics

(36.5%). They are mainly mudrock and shale lithics. Volcanic lithics are still dominant in the samples (62.9%), where basaltic lithics are 87.1% and intermediate-felsic lithics 12.9%. The average size of the framework grains is fine sand, ranging from very fine to medium sand. Roundness is mainly subrounded to rounded (Figure 4.4); and sorting varies from poorly sorted to moderately well sorted. The skewness is coarse skewed to near symmetrical. The average amount of matrix is 11.6%, ranging from 8.3-21.5%. The average amount of cements is 27.1%, ranging from 0-42.8%. The relatively large amount of sedimentary lithics indicates a secondary sedimentary source.

4.3. PETROFACIES C

Petrofacies C has mean compositions of $Q_3F_8L_{89}$, $Qm_4F_9Lt_{87}$, $Qp_1Ls_{10}Lv_{89}$, and $Qm_{33}K_4P_{63}$, which can be differentiated from $QmLvLvi$ ternary diagram (Figure 4.5). Petrofacies C occurs in 7 samples in the upper part of the Taodonggou, SW Tarlong, S Tarlong sections and most parts of the Zhaobishan section. This petrofacies is characterized by a relatively high content (26.8%) of intermediate-felsic volcanic lithics of all volcanic lithics, while basaltic lithics only account for 73.2%. Volcanic lithics are dominant (89.3%), and sedimentary lithics account for 9.9% of all lithics. The average size of the framework grains is fine to very fine sand, ranging from coarse silt to fine sand. Roundness is mainly subrounded (Figure 4.6); and sorting is moderately-moderately well sorted. Near symmetrical is the main skewness. The average percentage of matrix is 20.9%, ranging from 2.8-44.3%. The average amount of cements is 15.6%, ranging from 0-42.5%. The relatively high content of intermediate-felsic volcanic lithics indicates a felsic volcanic source was exposed in the area. A slightly higher quartz content in Petrofacies C would also suggest intermediate-felsic source due to the presence of quartz in intermediate-felsic volcanic source rocks.

All three petrofacies show a very low compositional maturity. Texturally, Petrofacies B has the least amount of matrix (11.6%), which can be classified into subarenite, whereas the other two petrofacies are wackes. Roundness is almost identical among all petrofacies due to the large amount of lithics. Petrofacies C is slightly better sorted than the other facies. The smallest grain size is also observed in Petrofacies C.

Overall, all the petrofacies are immature to submature based on the amount of matrix and textural properties on the basis of Folk's textural maturity classification (Folk, 1951).

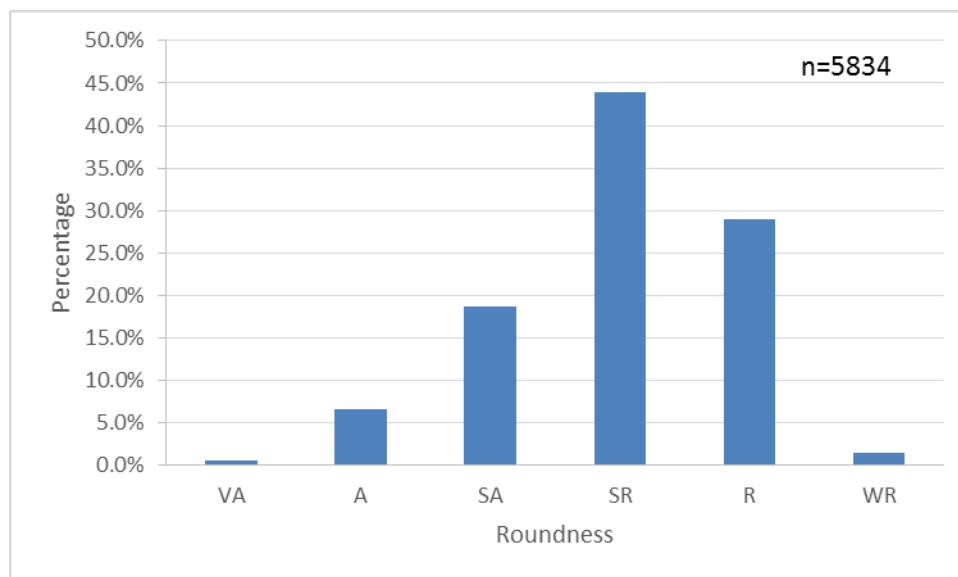


Figure 4.2. Roundness distribution of Petrofacies A

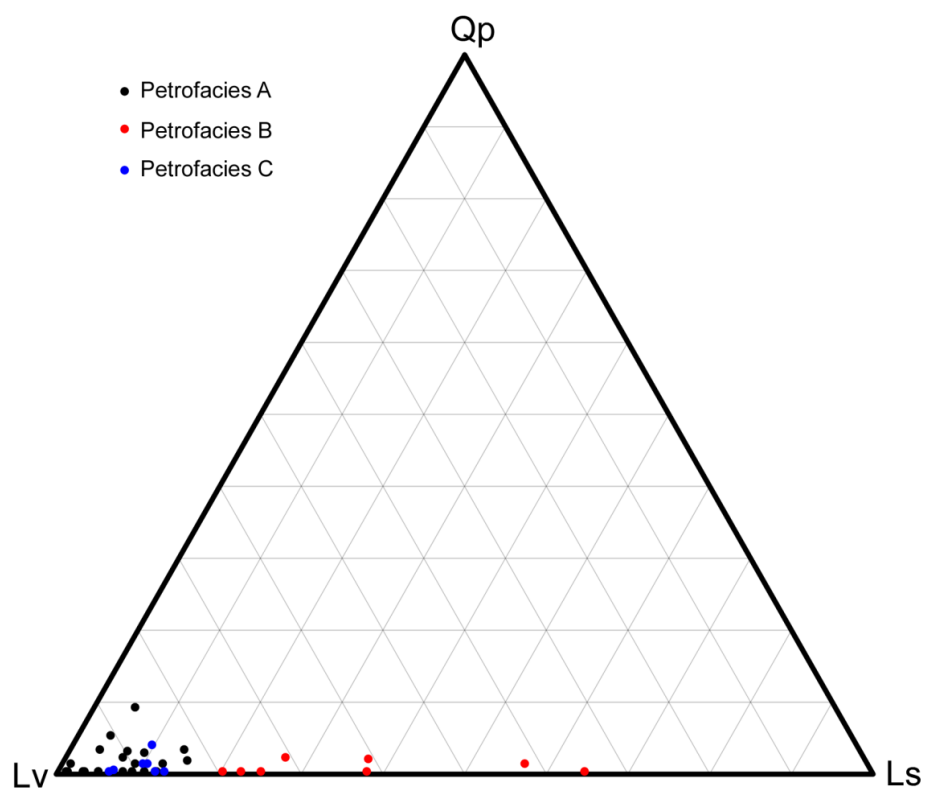


Figure 4.3. QpLvLs ternary diagram to differentiate Petrofacies B from the other two petrofacies.

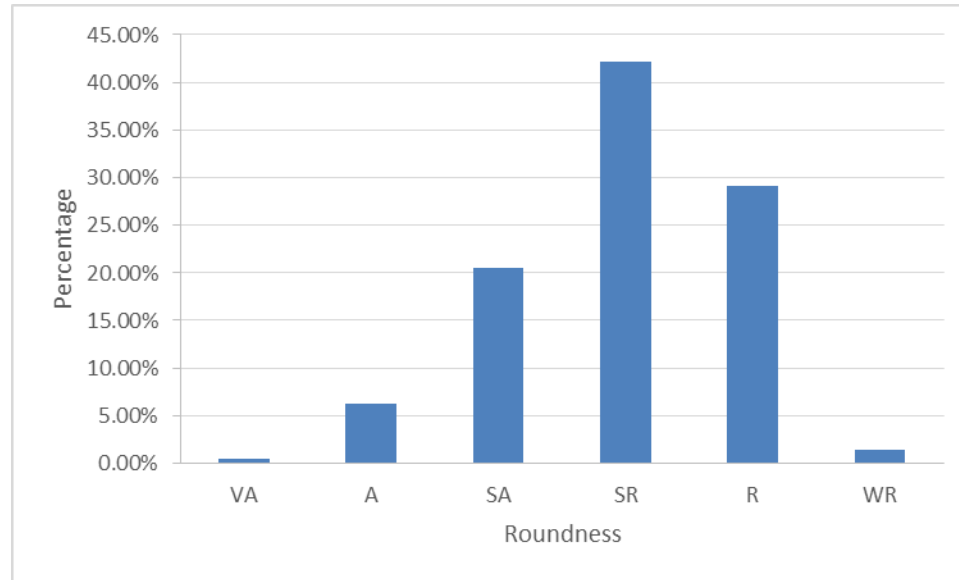


Figure 4.4. Roundness distribution of Petrofacies B

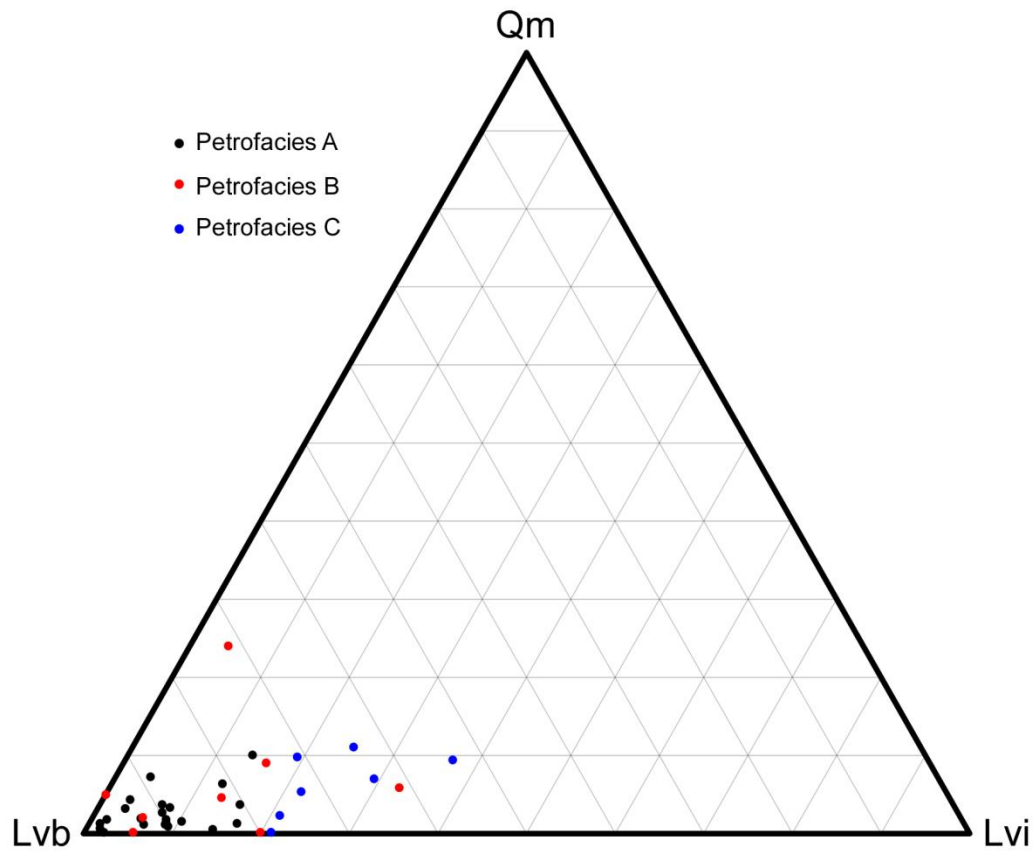


Figure 4.5. QmLvbLvi ternary diagram showing relatively high Lvi content in Petrofacies C compared with the other two petrofacies

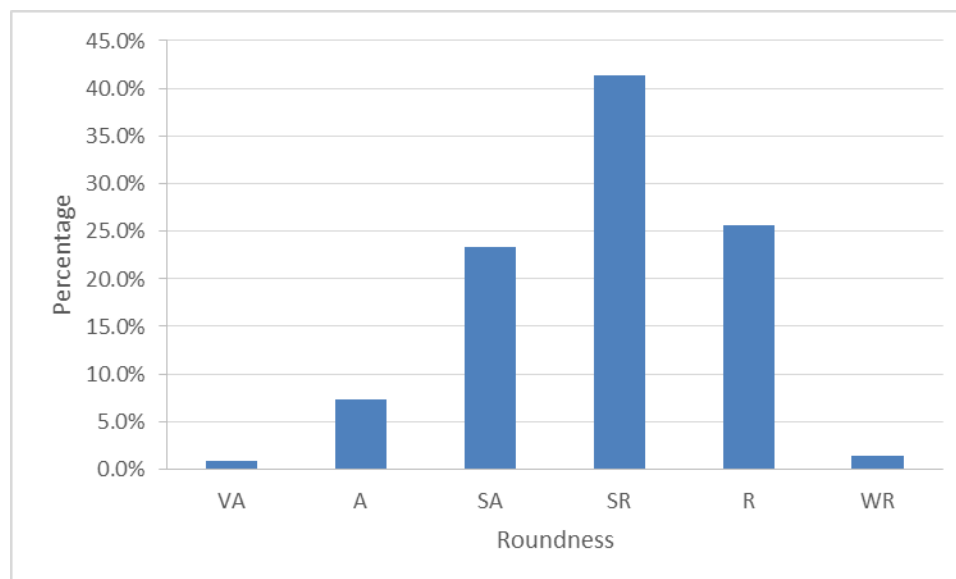


Figure 4.6. Roundness distribution of Petrofacies C

4.4. PETROFACIES AND DEPOSITIONAL ENVIRONMENTS

Fluvial, lake plain, littoral, and delta are the depositional environments for the sandstones in this study. The interpretation of depositional environments was done in the field based on sedimentary texture and structures, stacking pattern, and stratal geometry by Dr. Wan Yang (see Yang et al., 2010 for interpretation criteria; Appendix). Of all the samples, three are fluvial, one lake plain, twenty-five littoral, and eight deltaic. The distribution of sandstones with respect to Petrofacies and depositional environments is shown in Table 4.1.

Petrofacies A occurs in all the depositional environments. Fluvial sandstones are only observed in Petrofaices A. The abundant basaltic lithics with minor sedimentary and felsic lithics would indicate low source lithology diversity. Petrofacies B occurs in eight delta-front and littoral facies. It is characterized by a relatively large amount of sedimentary lithics and mostly subrounded to rounded. The relative roundness of all the sedimentary lithics would indicate high total energy or softness of the lithic grains. These two environments are of relatively high energy. Petrofacies C occurs in seven samples from lake plain, delta, and littoral facies. No clear link between Petrofacies C and depositional environments is present.

Overall, the link between petrofacies and depositional environments are not clear. Petrofacies are distinguished by compositional differences, which are largely determined by provenance lithology. However, the composition of sandstones in different depositional environments are largely affected by both provenance lithology, transport distance, and diagenesis. As a result, the direct relationship between petrofacies and depositional environments is not well defined.

Table 4.1. Occurrence of petrofacies in relation to depositional environments

	Fluvial	Lake plain	Delta	Littoral
<i>Petrofacies A</i>	3	0	5	14
<i>Petrofacies B</i>	0	0	2	6
<i>Petrofacies C</i>	0	1	1	5

5. PROVENANCE

The use of quantitative detrital modes, calculated from point-counting data, to infer sandstone provenance is well established (Dickinson and Suczek, 1979). The tectonic setting of the provenance apparently exerts primary control on sandstone compositions, though relief, climate, transport mechanism, depositional environment, and diagenesis all can be important secondary factors (Dickinson, 1985). Provenance refers specifically to the composition, location, and dimensions of source rocks, and relief, climate, and tectonic setting of the source area. Point-counting data are plotted on various ternary diagrams from Dickinson (1985) to speculate provenance conditions.

5.1. TECTONIC SETTING

Fourteen of the 37 samples fall in the undissected arc field, and the rest 23 samples in the lithic recycled field on the QmFLt plot (Figure 5.1). Half of the samples from Petrofacies A fall in the undissected field, while the other half in the lithic recycled area. Most samples of Petrofacies B, except one sample from the lower part of the Taodonggou section, fall in the lithic recycled area. Two samples of Petrofacies C fall in the undissected arc field, and the rest five samples in the lithic recycled field.

Undissected arc is inferred from volcanoclastic debris shedding from volcanogenic highlands along active island arcs and on some continental margins where arc volcanic chains have undergone only limited erosion. This would indicate that a nearly continuous volcanic cover was present during the deposition of the samples in the undissected arc field. The lithic recycled field is defined as subduction complexes of sediments and lavas (Dickinson, 1985). This field indicates that tectonically uplifted subduction complexes composed of old rocks form a structural high along the trench-slope break between the trench axis and the volcanic chain within an arc-trench system. The distribution on the QmFLt plot indicates that most of the samples have a lithic recycled orogen provenance and some undissected arc provenance.

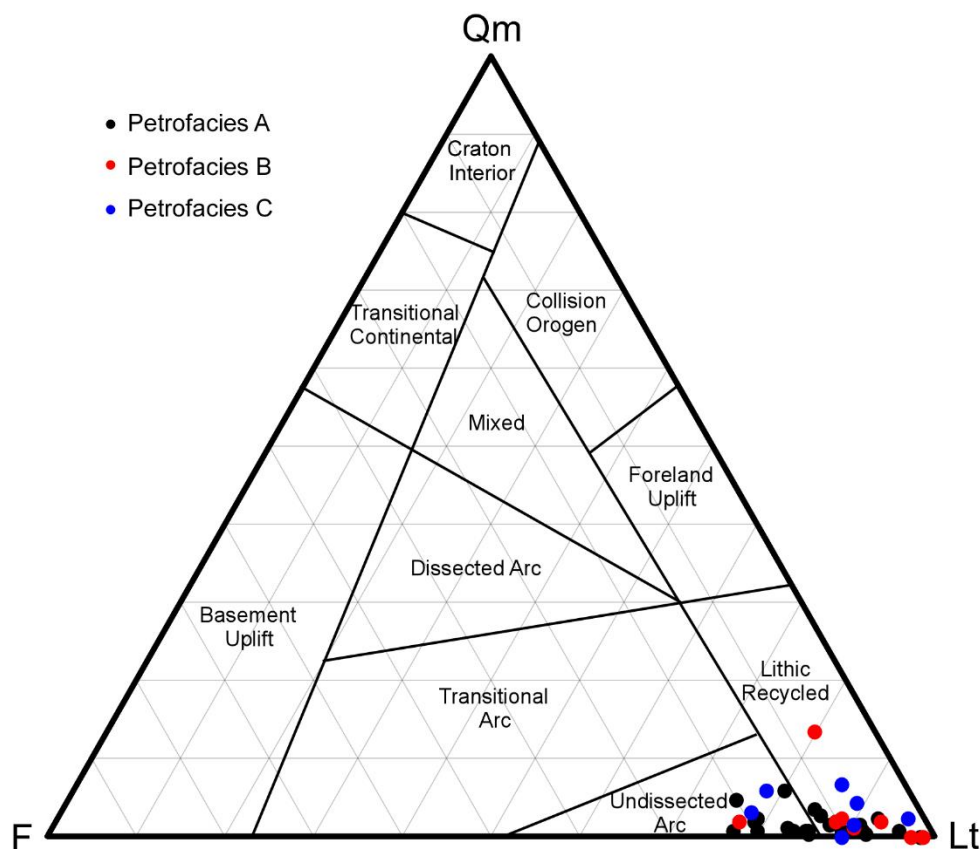


Figure 5.1. QmFLt ternary diagram showing the Lucaogou sandstones fall in lithic recycled and undissected arc fields on the global tectono-sandstone composition scheme. Modified from Dickinson (1985).

The other ternary plot used to determine provenance is the QpLvLs ternary diagram, showing the relative proportions of lithics of different origins. This diagram shows a slightly different story from the QmFLt plot. Most samples, except Sample B09-4 of Petrofacies B from SW Tarlong, are plotted in the magmatic arc field (Figure 5.2). This indicates a predominant magmatic arc provenance, which is in conflict with the magmatic arc and lithic recycled provenances interpreted from the QmFLt diagram. Sample B09-4 and B09-3 are characterized by a very high sedimentary lithic content, more than 50% of all lithics. This suggests the presence of a local sedimentary source. According to the ternary diagram, sample B09-4 is classified as mixed orogenic provenance.

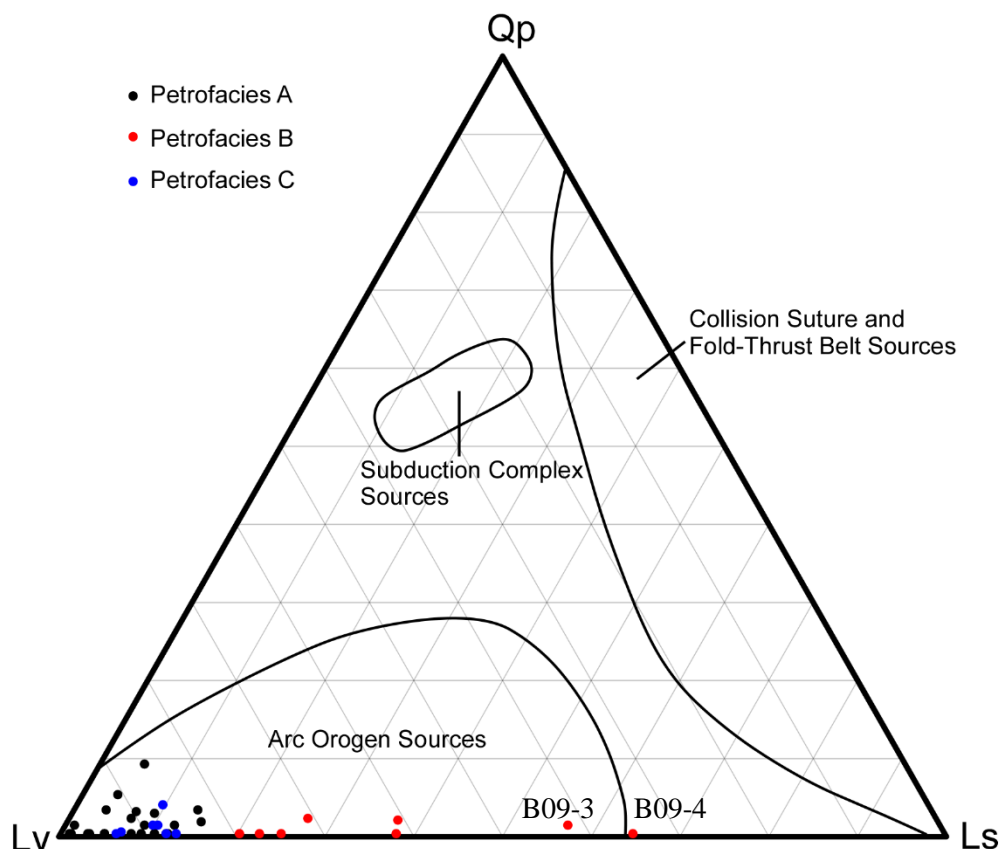


Figure 5.2. QpLvLs ternary diagram showing most of the Lucaogou sandstones are plotted in the arc orogen field suggesting a magmatic arc provenance. Modified from Dickinson (1985).

QmKP ternary diagram is used to compare the abundance of monocrystalline quartz with both potassium feldspars and plagioclase, using common monomineralic grains. This diagram shows concentration of monocrystalline quartz and plagioclase with minor potassium feldspar (Figure 5.3). For all the samples, the average P/F ratio is 95%. From Petrofacies A to B and B to C, average Qm content shows an increasing trend. Based on Dickinson (1985), this trend indicates an increase in plutonic source in a magmatic arc provenance. However, the trend is poorly defined, indicating a mixed provenance or the increasing influence of other non-provenance factors.

5.2. INTERPRETATION OF PROVENANCE

Magmatic arc is the provenance interpreted from two ternary diagrams. However, the location of the magmatic arc still needs to be determined.

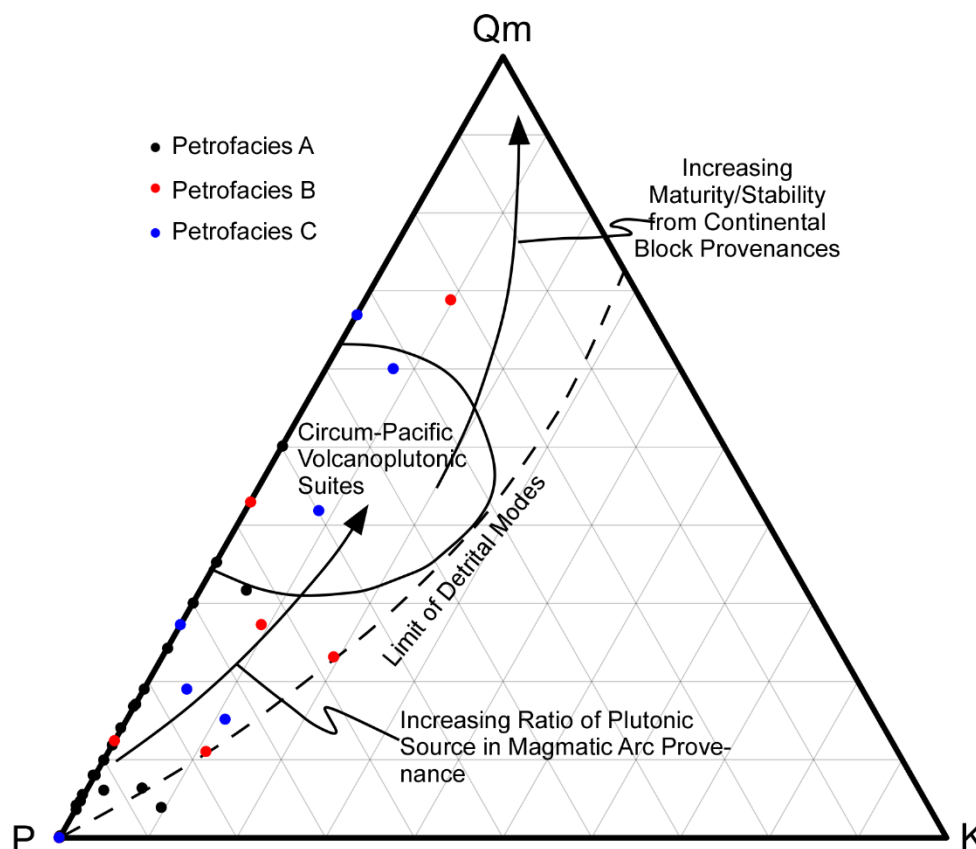


Figure 5.3. QmPK ternary diagram showing a high P/F ratio of Lucaogou sandstones. Modified from Dickinson (1985).

The young arc signature combined with tectonic studies from previous workers (Shao et al., 2001; Greene et al., 2001) suggests that the late Carboniferous northern Tian Shan volcanic arc to the south is the primary provenance of the Tarlong-Taodonggou sandstones. However, basaltic lithics from different sources are difficult to differentiate. In the study area, thick basalt basement is observed in the field, which could also be a possible source. Regional versus local volcanic sources can be distinguished based on textural attributes. Some of the volcanic lithics are rounded, suggesting a long transport distance, which will support the distant Tian Shan origin. However, some of the volcanic lithics and zoned plagioclase are angular to subangular and indicate a close source. The surrounding rift shoulders could have exposed underlying upper Carboniferous oceanic arc basement basalts (Carroll et al., 1990; Graham et al., 1993; Yang et al., 2013).

Some samples are characterized by a relatively high intermediate-felsic volcanic lithic content, which is defined as Petrofacies C. In addition, most of the Lvi are

subangular to subrounded, which suggests a short transport distance. This can be interpreted as exposure of felsic volcanic rocks in the rift shoulders.

A small quartz content (<10%) in all the samples indicates the absence of or limited source for quartz. Therefore, other possible sources should be considered. Angular subhedral quartz with embayment on the edge suggests a volcanic source with a short transport distance. This could come from rift shoulder exposure of felsic volcanic lithics or contemporary volcanic ash deposits. Some rounded quartz are also present in the samples. This type of quartz could have been recycled from sedimentary rocks exposed in the local rift shoulder or could be the first-cycle quartz transported from long distance. Yang et al. (2013) reported turbidites and shallow marine sandstones intercalated with basement basalts, which can be the possible source of quartz. It is difficult to tell the two origins apart solely based on petrographic data. Other techniques should be applied to interpret the exact provenance of the quartz grains.

Petrofacies B is characterized by a high percentage of sedimentary lithics, where most of them are mudrock lithics and mud clasts. Mud clasts are angular to subangular, indicating a short transport distance. Their source could be intrabasinal mudrocks or semi-consolidated muddy sediments. Rounded mudrock lithics indicate a relatively long transport distance. Nevertheless, the low resistance of mudrock to physical transport suggests that the source would still be in the local area. This characteristic suggests a secondary sedimentary source.

Overall, basaltic, intermediate-felsic volcanic and sedimentary lithics were all possibly exposed in the rift shoulders during the deposition of LCG LC. The diverse lithology of the rift shoulders makes the trace of sediment sources more complicated.

Textural attributes are closely linked with transport distance. In Taodongou-Tarlong area, the highest textural maturity is observed in N Tarlong section, which would indicate the longest transport distance. While the other sections show a decreasing trend of maturity from south to north. If all the sections are receiving sediments from the same source, this would support the northern Tian Shan source area to the south. In Zhaobishan area, the samples are dominantly subarenite, subrounded to rounded, fine to very fine sand-sized, and moderately sorted. These characteristics indicate that the sandstones are texturally mature, which, in turn, suggests a long transport distance. In addition,

Petrofacies C is more developed, while Petrofacies A is less observed in Zhaobishan. Both compositional and textural differences from those in Tarlong and Taodonggou suggest that Zhaobishan and Tarlong-Taodonggou areas were in different catchment systems.

6. STRATIGRAPHIC TREND

Systematic trends of compositional and textural characteristics of sandstones would provide clues on long-term changes in environmental conditions and elements of catchment basins (Obrist-Farner, 2015). Petrofacies A occurs in all sections; Petrofacies B in middle and upper parts of the Taodonggou, middle part of the SW Tarlong, lower part of N Tarlong, and middle part of Zhaobishan sections (Figure 6.1-6.6); and Petrofacies C mostly in Zhaobishan (Figure 6.6). Vertical trend of depositional environments, grain size and sorting, grain composition, and petrofacies are compared within and between sections to identify the differences and similarities between them.

6.1. TAODONGGOU

In Taodonggou, the section started from Petrofacies B, then switched to Petrofacies A in the middle part, and finally back to Petrofacies B. The amount of matrix is the least in the middle part, while the upper and lower parts have more matrix. Grain size shows two upsection fining trends. Sorting gets slightly better upsection. Roundness shows no trend through the section. Quartz content increases upsection. Sedimentary lithics are most concentrated in the middle part. Volcanic lithics show the opposite trend. Overall, compositional maturity inferred from quartz content increases upsection, while textural maturity is the highest in the middle part (Figure 6.1).

All the samples are from littoral environment. Thus, the two upsection grain size decreases suggest episodic expansion and contraction of the catchment basin, resulting in a longer transport distance with minor influence from depositional environment. The decrease in matrix content in the middle part indicates a decrease in suspension load. The upward increase in quartz content indicates an increasing compositional maturity. High Ls content in the middle section suggest a sedimentary source from the rift shoulder.

6.2. SOUTHWESTERN TARLONG

In SW Tarlong, the samples are in the middle-upper part of the section. The section starts with Petrofacies A; the middle two samples show Petrofacies B with a high Ls content; the uppermost sample belongs to Petrofacies C. The matrix content is the

lowest in the middle part. Grain size in the middle is the coarsest, while the upper and lower parts are finer. Sorting is the worst in the middle part. The highest quartz content and sedimentary lithics occur also in the middle part. Basaltic lithics decrease in the middle part (Figure 6.2).

The low matrix content in the middle part indicates a low suspension load. Coarse grain size in the middle is caused by the local sedimentary source. The high amount of quartz content in the middle is caused by the increasing amount of felsic volcanic lithics. The high L_s/L_v ratio in Petrofacies B suggests a local sedimentary source in the middle part.

6.3. NORTHWESTERN TARLONG

In NW Tarlong, a simple trend composed only Petrofacies A is observed. Two upsection decrease trends of matrix are observed. Grain size shows a general upsection increase trend from fine to medium sand. Sorting gets better upsection in the lower part from poorly sorted to moderately well sorted, and then maintains the moderately sorting to upper section. Quartz content is high in the lower part with an exception of S7-44, then a decrease trend upsection. Basaltic lithics are dominant in the section with minor sedimentary lithics (Figure 6.3).

Two upward-decreasing trends of matrix indicate decrease of suspension load. The upward-coarsening trend indicates the contraction of catchment basin, resulting in a shorter transport distance. The relatively high quartz content in the lower part is caused by a local felsic source, which is supported by the small decrease trend of the L_{vb}/L_v in the lower part.

6.4. SOUTHERN TARLONG

In S Tarlong, only the uppermost part shows Petrofacies B, the rest of the section shows Petrofacies A. The amount of matrix is the highest in the middle part. Grain size is very fine sand in the middle part, while fine in the lower and upper parts. Sorting is the best in the middle section, being moderately well sorted, while less well sorted in the other parts, being moderately sorted. Roundness also is the best, as rounded, in the

middle section. Quartz content varies between 1-3%. Ls shows a relatively low content in the middle section (Figure 6.4).

The high matrix content in the middle section indicates a high suspension load. The smallest grain size in the middle indicates expansion of catchment basin followed by a contraction, resulting in a longer transport distance in the middle section. The variations in quartz content indicate slight difference in compositional maturity difference, which could have been caused by a slightly variation of source rock type between mafic and felsic.

6.5. NORTHERN TARLONG

The N Tarlong section starts with Petrofacies B, and then changes to Petrofacies A upsection. The amount of matrix is the lowest in the middle part. Grain size decreases in the middle part to very fine sand from upper and lower medium sand. Sorting gets slightly worse upsection from moderately well sorted to moderately sorted. Roundness is subrounded through the section. Quartz content increases upsection from 0-2%. Sedimentary lithics increase upsection with an exception of TR30 of Petrofacies B in the lowermost section (Figure 6.5).

The low matrix content in the middle part indicates a low suspension load in the middle part. Fine grain size in middle section indicates expansion of catchment basin followed by a contraction, resulting in the longest transport distance in the middle LCG LC. Increasing quartz content indicates increasing compositional maturity. The relatively high content of Ls indicates the existence of a local sedimentary source.

6.6. ZHAOBISHAN

In Zhaobishan, the lower part varies between Petrofacies C and B; the middle part is dominantly Petrofacies B; and the upper part varies between Petrofacies C and A. Petrofacies A is the least common in all sections. Two upward-decreasing trends of matrix are observed. Grain size shows a general fining-upward trend from fine to very fine sand. Slightly worse sorting is observed in the middle part. High quartz content occurs in the lower and upper parts. Ls/L ratio is high in the middle part. Lvb/Lv varies greatly from 95% to 60%, but overall shows an upsection decrease trend (Figure 6.6).

The trend of matrix indicates episodic decrease of suspension load. Upsection fining grain size trend indicates expansion of catchment basin, resulting in a longer transport distance. The high quartz content in upper and lower sections suggests a local felsic source, which is supported by the low Lvb/Lv percentage.

6.7. CORRELATION

In Taodonggou-Tarlong area, a general upward-coarsening trend is observed in N Tarlong and NW Tarlong, and a general upward-fining trend is observed in S Tarlong, Taodonggou, and SW Tarlong. In addition, a similar compositional trend and the dominance of Petrofacies A in N and NW Tarlong indicate a similar depositional history. S Tarlong and Taodonggou are also similar in grain composition trend, suggesting a similar depositional history. SW Tarlong has the unique trend showing high sedimentary lithics in the middle, indicating a local sedimentary source. The increase in average grain size from Taodonggou, S and SW Tarlong to N and NW Tarlong indicates progressively shorter transport distance. Decrease in average matrix amount from Taodonggou, S Tarlong, SW Tarlong to N and NW Tarlong indicates a progressively longer transport distance for the source area. This is apparently in conflict with the interpretation from grain size trend. Possible reasons could be the different depositional environments and complex source lithology. Sandstones from different depositional environments experienced different total energy which will affect the amount of matrix and grain size. In addition, different types of grains have varying resistance to weathering and transport. Thus, the grain size may not be solely determined by transport distance.

In Zhaobishan, which is ~90 km from Tarlong-Taodonggou area, a unique trend is observed. This indicates a different catchment system. Thus, it is very hard to correlate the Zhaobishan section with the other sections. Attempt has not been made in this study.

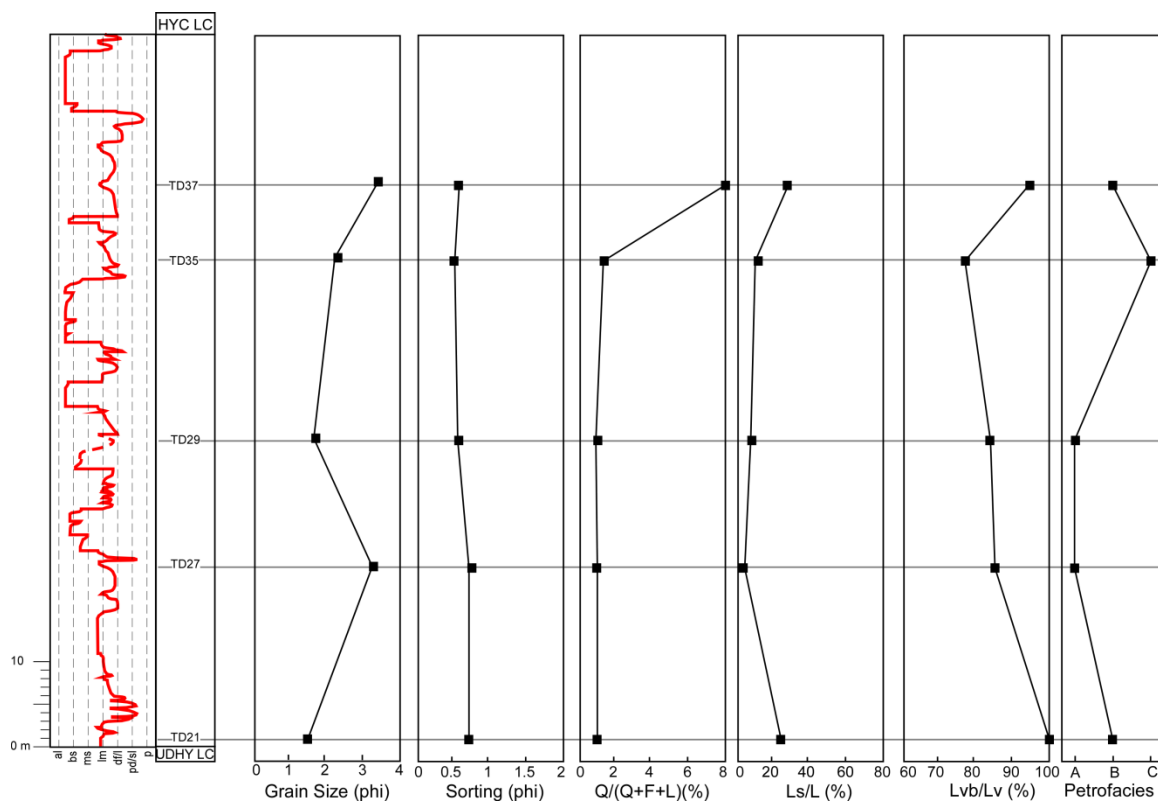


Figure 6.1. Stratigraphic variation in depositional environments, grain size, sorting, and composition of the LCG sandstones in Taodonggou section.

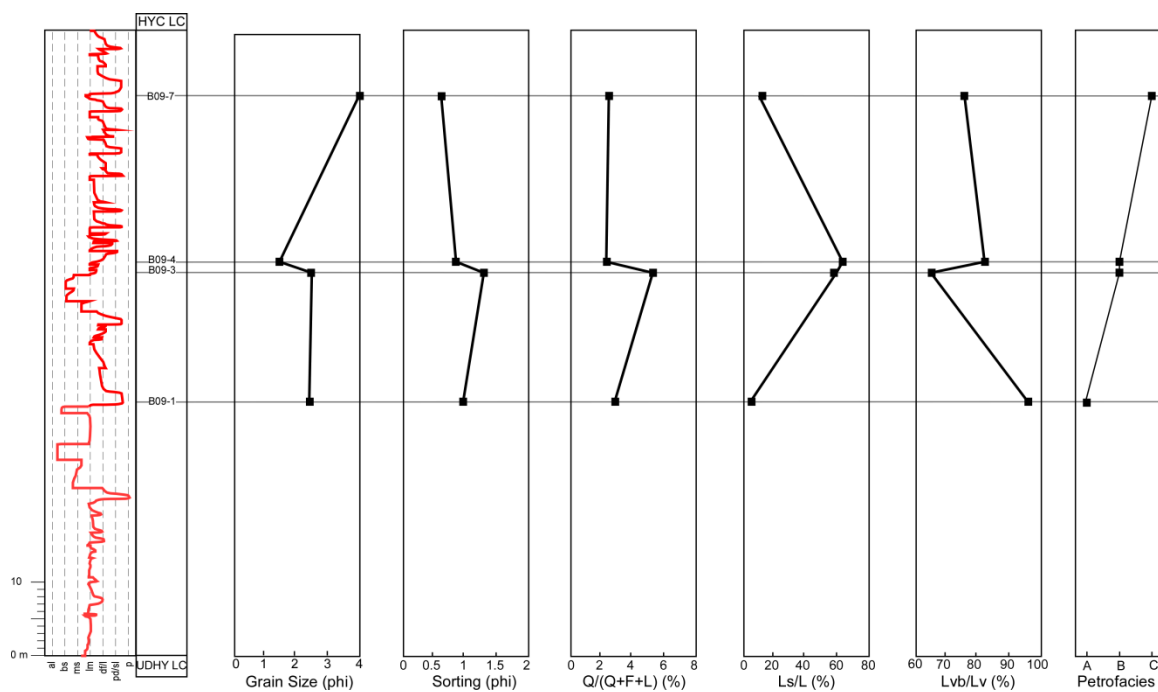


Figure 6.2. Stratigraphic variation in depositional environments, grain size, sorting, and composition of the LCG sandstones in SW Tarlong section.

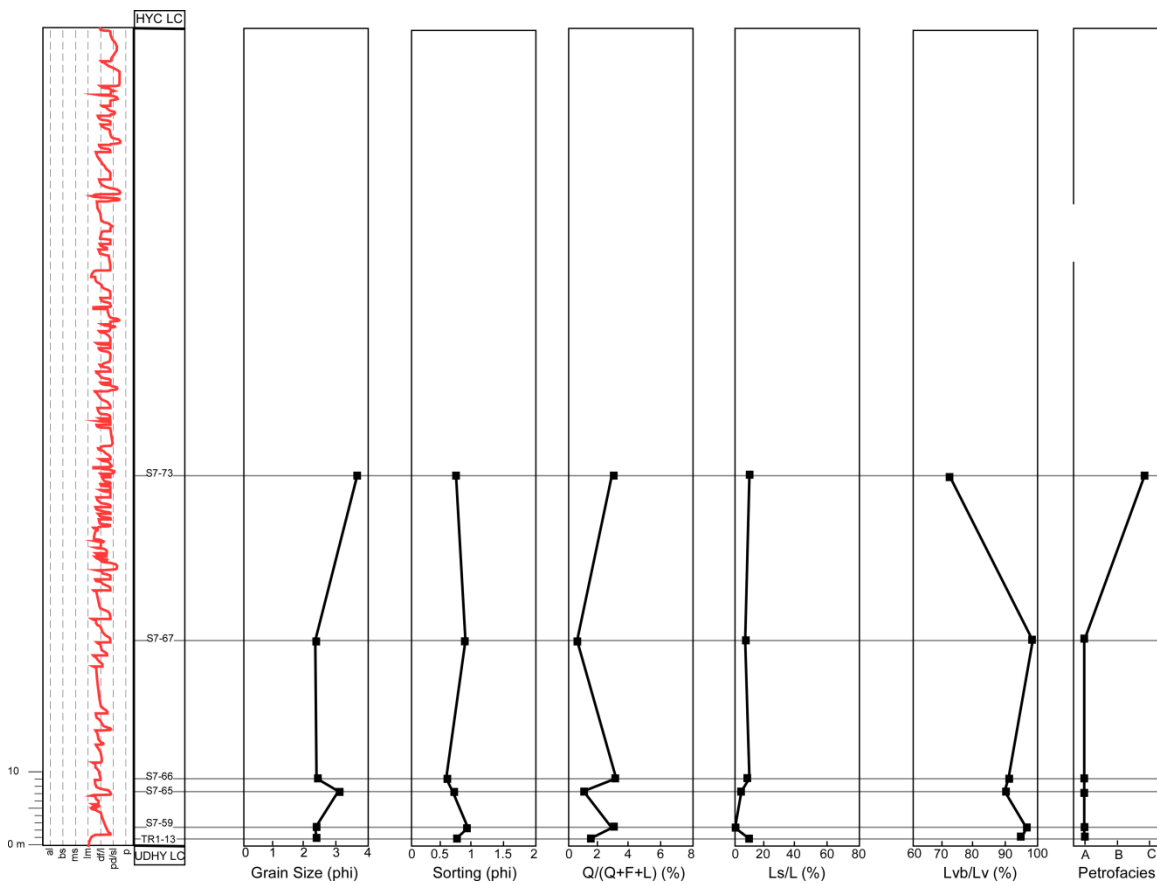


Figure 6.4. Stratigraphic variation in depositional environments, grain size, sorting, and composition of the LCG sandstones in S Tarlong section.

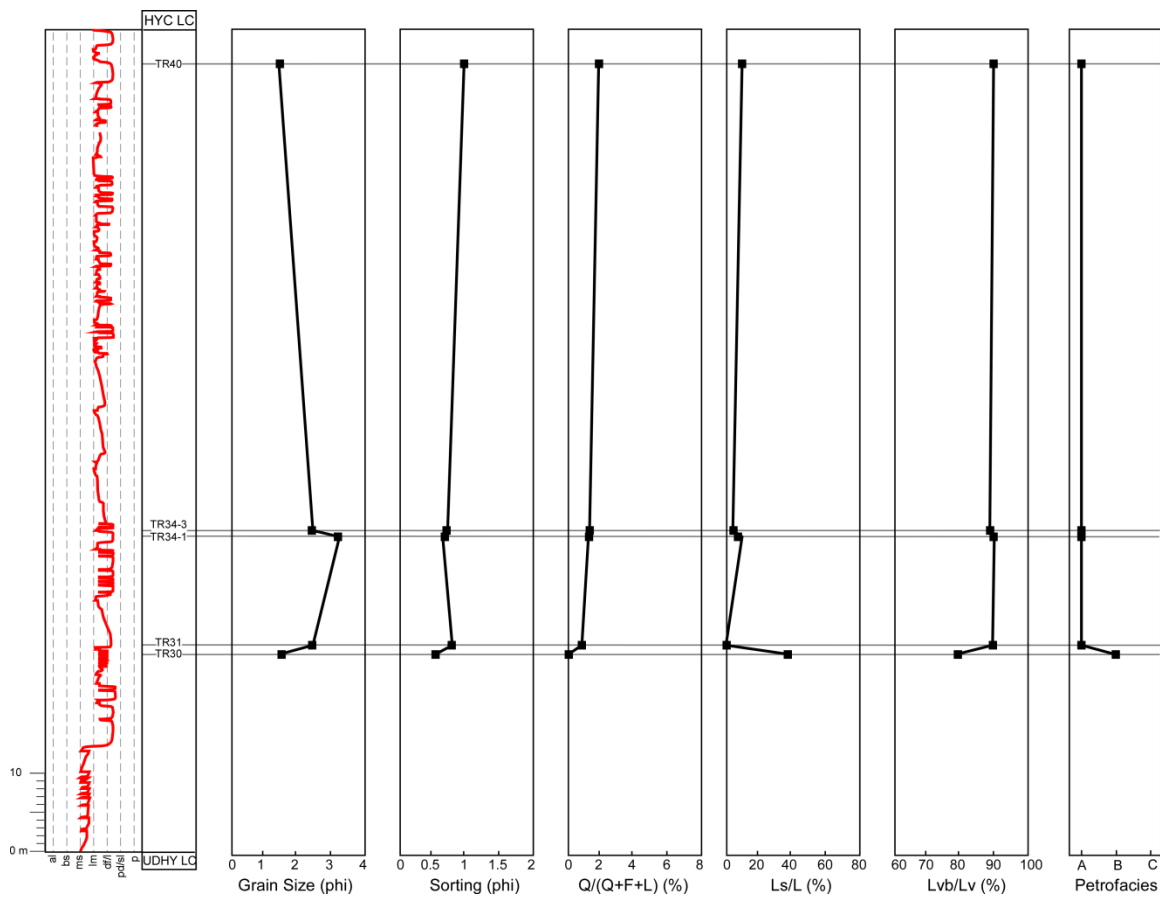


Figure 6.5. Stratigraphic variation in depositional environments, grain size, sorting, and composition of the LCG sandstones in N Tarlong section.

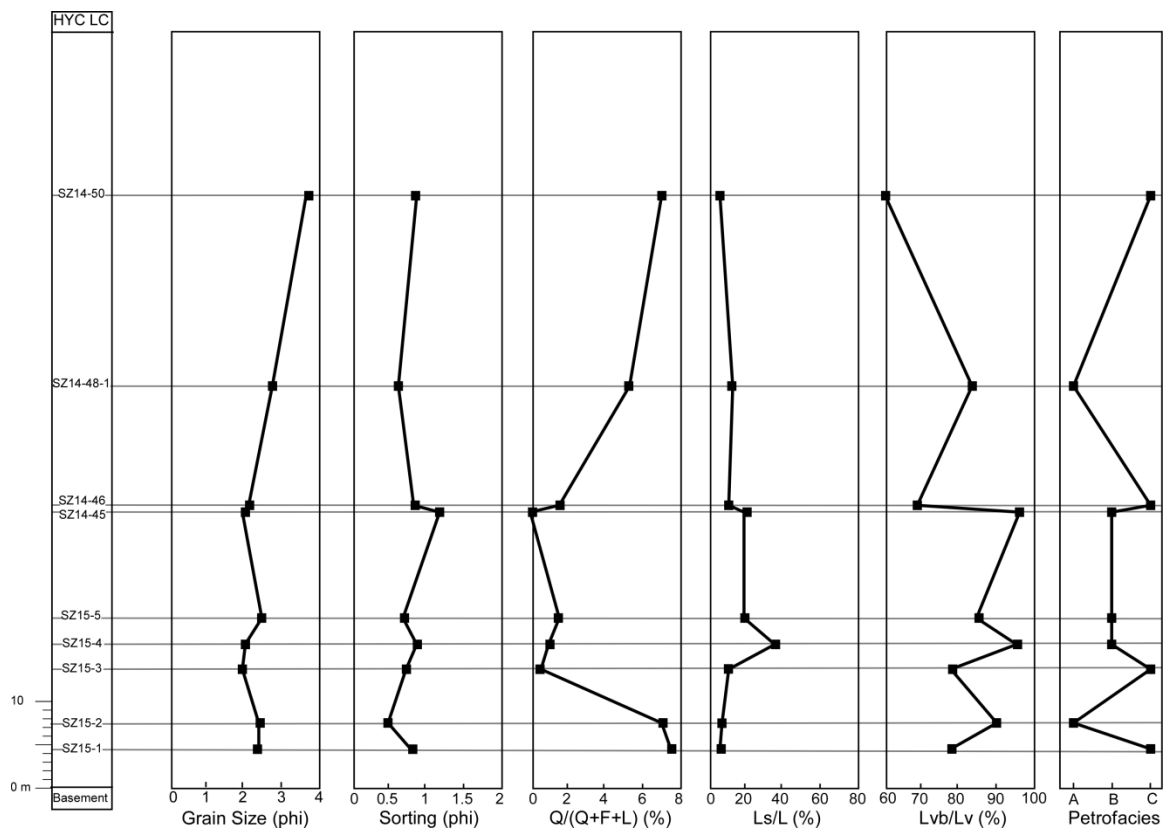


Figure 6.6. Stratigraphic variation in grain size, sorting, and composition of the LCG sandstones in Zhaobishan section.

7. DISCUSSION

7.1. COMPLEXITY OF SOURCE

Provenance information is important to understand basin-filling history and paleogeography, and can be inferred from petrographic data of sandstones. However, multiple factors, provenance lithology, transport distance, depositional environments, paleoclimate, and diagenesis, control the compositional and textural attributes and make it hard to disentangle the effects of individual factors.

Textural properties are applied to differentiate same type of framework grains from different sources. For the basaltic grains, it is widely distributed in the study area, which makes it hard to tell the exact source areas only based on compositional properties. Differences in grain size and roundness would be a good indicator to determine transport distance in order to differentiate sources from different areas. Of all the basaltic lithics, 30% are rounded-well rounded, and 70% are angular to subrounded. If all the grains are divided by the limit ($\Phi=3$) between fine and medium sand, 23% of the grains are finer and 77% are coarser. This trend is consistent with the roundness trend. Both characteristics indicate ~25% of all the basaltic lithics are from distal source, while 75% of them from a close source. The distant source could be northern Tian Shan based on previous studies (Shao et al., 2001; Yang et al., 2010). Deep-sourced basalts are not uncommon in a rift setting (Condie, 1997). Thus, the close source could be the exposure of upper Carboniferous oceanic arc basement in rift shoulders, resulting in a short transport distance (Obrist-Farner, 2015). Angular and zoned plagioclase would conform with a local source from nearby volcanic fields.

Abundant sedimentary lithics in Petrofacies B are angular mud clasts in some cases and occur commonly in the middle part of the SW Tarlong section. The angularity of the grains supports a short transport distance. The source could be intrabasinal rip-up clasts. The existence of the mud clasts is unique in SW Tarlong; and their absence in other sections would indicate a local sedimentary source. Other types of sedimentary lithics including mudrock lithics, chert, and shale lithics are also observed. These grains show a more rounded shape, indicating a longer transport distance. Finally, these grains are widely present in all the sections, suggesting a regional or background distribution

trend. This source could also from the exposed sedimentary rocks in the uplifted rift shoulders.

Petrofacies C is characterized by a relatively high felsic volcanic content but still dominated by basaltic lithics, and is especially well developed in the Zhaobishan section. Two possible sources are possible, one is the central Tian Shan containing felsic volcanic lithics; the other local rift shoulder. Grain size and roundness trend would suggest both sources contributed to the framework grains. 30% of all the intermediate-felsic grains are smaller than fine sand size and rounded to well-rounded, indicating a long transport distance. The other 70% suggest a shorter transport distance from local uplifted rift shoulder.

Petrofacies A is dominant in sections in Tarlong-Taodonggou area. However, Petrofacies B and C are better developed with minor Petrofacies A in Zhaobishan. This suggests a different depositional history in the two areas. The Tarlong-Taodonggou area is more controlled by sources from northern Tian Shan and local uplifted rift shoulders. But in Zhaobishan, the source from northern Tian Shan is not dominant, changes in local sources occurred more frequently.

Overall, the sediments sources are controlled by distant northern Tian Shan and local uplifted rift shoulders with complex rock types. The regional source would only account for 30%, whereas the local sources for 70% for all the framework grains. A local sedimentary source was available for SW Tarlong in mid-upper LCG LC. The frequent petrofacies changes in Zhaobishan suggest episodic introduction of local sedimentary and felsic volcanic sources.

7.2. TECTONIC SETTING

Rift basins are not included in tectonic classification of sandstones by Dickinson (1985; see also Dickinson and Suczek, 1979; Dickinson et al., 1983) because of the diverse lithology exposed in rift shoulders that generate contrasting results of tectonic settings (Ingersoll, 1990). The classification is based mainly on grain composition and ignores texture. Lithic recycled orogen and undissected arc are the two contrasting provenances interpreted from the ternary diagram. From the QmFLt ternary diagram, mixed recycled orogen and magmatic arc are indicated. But in QpLvLs and QmPK

diagrams, only magmatic arc provenance is significant. The diversity of lithologies exposed in the rift shoulders would explain the different inferences. The coexistence of sedimentary and volcanic rocks in the rift shoulders in the study areas would make the composition of the sandstones more complicated, resulting in a signal of mixed provenance.

7.3. COMPARISON BETWEEN TWO STUDY AREAS

Samples from two separate areas ~ 90 km apart may provide clues to regional paleogeography. LCG sandstones were deposited in the greater Turpan-Junggar basin during the early Permian. Relatively similar framework grain compositions suggest similar provenance lithology, or even same source. In Tarlong-Taodonggou area, Petrofacies A is dominant in all sections except for the local rip-up mud clasts in the SW Tarlong. This is an indication of relatively stable and persistent source areas. This feature suggests a similar depositional condition in the Tarlong-Taodonggou area. However, in the Zhaobishan area, Petrofacies B and C dominate, which are characterized by a relatively high sedimentary and felsic volcanic lithic content. Yang et al. (2010) argued that the Permian greater Turpan-Junggar Basin was a rift basin composed of many grabens and half-grabens. Thus, the difference may indicate that these two areas are in two different grabens. The volcanic source from Tian Shan area supplied sediments to both half grabens, but local exposed lithology in rift shoulders varies greatly. Correlations between different grabens are extremely difficult in lacustrine environment due to the high frequency of facies change both vertically and laterally.

8. CONCLUSIONS

Field and petrographic study of fluvial-lacustrine sandstones of Lucaogou low-order cycle in Tarlong-Taodonggou and Zhaobishan areas in the southern foothill of the Bogda Mountains, NW China, documented compositional and textural maturities of 37 sandstones. Both vertical and lateral compositional changes indicate changes in provenance lithology and transport distance. The diverse grain types, especially abundant rock fragments, indicate complex sediment sources. Quartz, feldspar, rock fragments, and accessory minerals are subdivided into detailed subcategories. Textural attributes include grain size, roundness, and sorting. All these properties provide information on transport distance.

Three petrofacies were defined based on the Ls/Lv and Lvb/Lvi percentages. They are related to provenance lithology, transport distance, and depositional environments.

Tectonic interpretation was made using ternary diagrams of grain composition. Both recycled orogen and magmatic arc provenances were interpreted. The two provenances suggest complexity of the lithology in low rift shoulders and regional northern Tian Shan suture zone. The rounded and angular volcanic lithics indicate two sources with different transport distances. One source is the Tian Shan area and the other local uplifted rift shoulders. For sedimentary lithics, angular intrabasinal rip-up mud clasts and more rounded sedimentary lithics coexist. Rift shoulders were also interpreted as the source for the rounded sedimentary lithics. The distant volcanic source and local rift shoulders both contributed to the sediments in the study area.

Vertical and lateral stratigraphic trends are delineated on the basis of depositional environments, grain size, sorting, and compositional change. Provenance lithology change, catchment basin evolution, and transport distance were compared vertically within each section and laterally between different sections. A similar trend was observed between different sections, indicating similar depositional history. Increasing textural maturity from south to north in the Tarlong-Taodonggou area suggests a longer transport

distance in the north. The highly variable trend in Zhaobishan indicates episodic sediment influx from rift shoulders and/or a different catchment system from that of Taodonggou and Tarlong.

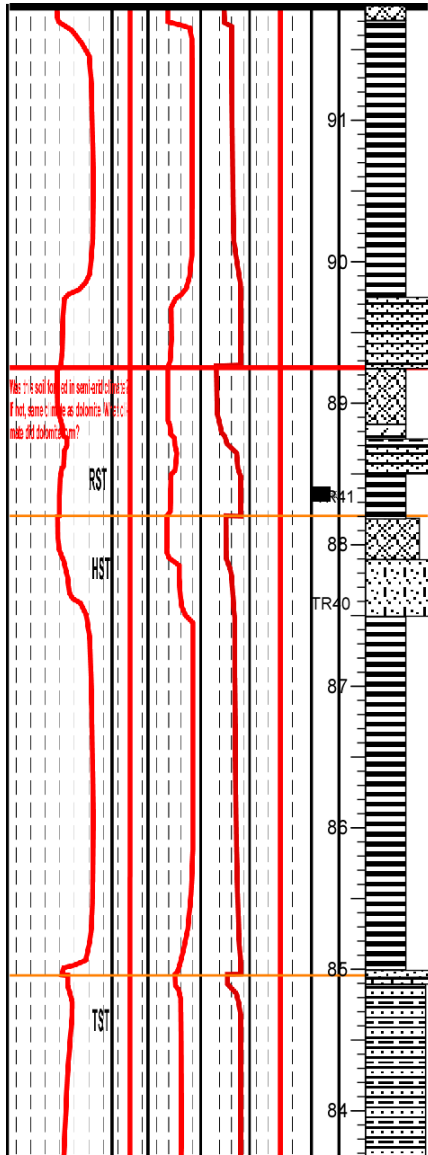
APPENDIX A

N TARLONG SECTION

(Measured by Dr. Wan Yang and Colleagues in 2004, 2005, 2007, 2009, 2014. Further inquiries should be directed Dr. Wan Yang at Missouri University of Science and Technology)

Legend

LITHOLOGY	SEDIMENTARY TEXTURE AND STRUCTURE
Normal graded conglomerate or sandstone	Soil slickensides
Reverse graded conglomerate or sandstone	Illuviated muddy sediments
Clast-supported conglomerate	Root mold, silicified/calcified stumps or branches
Matrix-supported conglomerate	Calcareous claystone and sandstone nodules, commonly root mottled
Sandstone	Rhizoconcretion or calcitic nodules
Well-bedded sandstone	Limonitic clayey soil pisoid
Well-laminated sandstone	Mud cracks
Cross-bedded sandstone	Petrified wood
Conglomeratic sandstone	Mud chips, rip-up clasts
Calcareous sandstone	Pisoids
Muddy sandstone	Ooids and superficial ooids
Interbedded sandstone and shale/siltstone	Invertebrate bone fossils
Shale	Trace fossils
Silty shale	Plants and plant debris
Calcareous shale or mudstone	Plant remains and fragments, carbonaceous laminae
Dolostone	Fish or fish scale fossils
Shale, dolomitic.	Shell fragments
Mudstone	Burrows, mottling structure
Conglomeratic mudstone	Planar, tabular, and/or trough x-bedding
Calcrete or altered palustrine limestone	Erosional surface
Paleosol	Internal erosional surface
Limestone with shale partings	Ripple and climbing ripple laminations
Limestone	Hummocky cross stratification (HCS)
Arenaceous limestone	Contorted bedding
Argillaceous limestone	Cryptalgal lamination
Oolitic packstone/grainstone	Symmetrical ripple marks
Pyroclastic breccia	Vesicles filled with calcite or other minerals
Extrusive igneous rocks	Normal graded bedding
Modern salt accumulation	Reverse graded bedding
Intrusive igneous rocks	Algal coated pisoid and oncoid
Pillow basalt	Microfaults
Mafic porphyry	Dissolution cavities/vugs
Felsic porphyry	Extensive brecciation structure
Breccia	LA - Lithic arenite
Tuffaceous sandstone	LSA - Lithic subarenite
Tuffaceous shale	LW - Lithic wacke
Oolitic sandstone	CRL - Climbing ripple laminations
Gypsiferous sandstone	High-order cycle boundary
Bedded halite	Low-order cycle boundary
Bedded gypsum	Lst xx Cycle number
Gypsum and shale interlaminite	tr xx Sample
	s7-xx
	TDxx
	sz14-xx



Mudstone, blackish gray, blocky.

Shale, black, fissile, abundant fish scales.

3.7.4 Sandstone, greenish gray, well laminated thin beds.

Mudstone, gray, blocky with angular, <1 cm peds.

Shale, black, fissile, dolomitic. Lower contact gradational.
Wackestone, blackish gray, with dolomitic shale partings (mm). Altered.
Sandstone, gray, well bedded and laminated.

3.7.3 Shale, black, fissile, extremely rich in plant remains, few ostracod or chonchostracod(?).

Mudstone, blackish gray, silty, blocky.

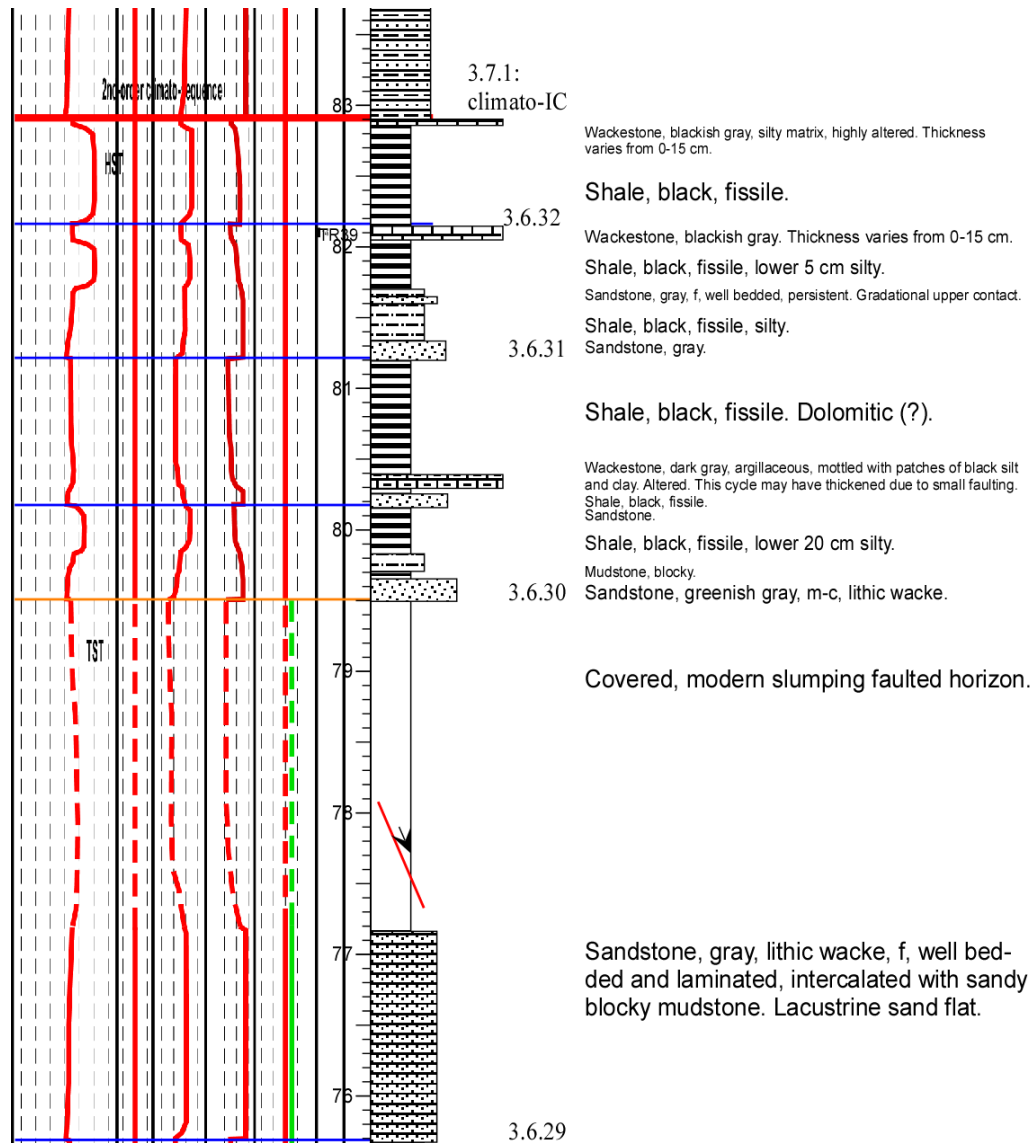
Sandstone (or arenaceous limestone), yellowish gray, dense, f-m, very calcareous, well rounded, mottled.

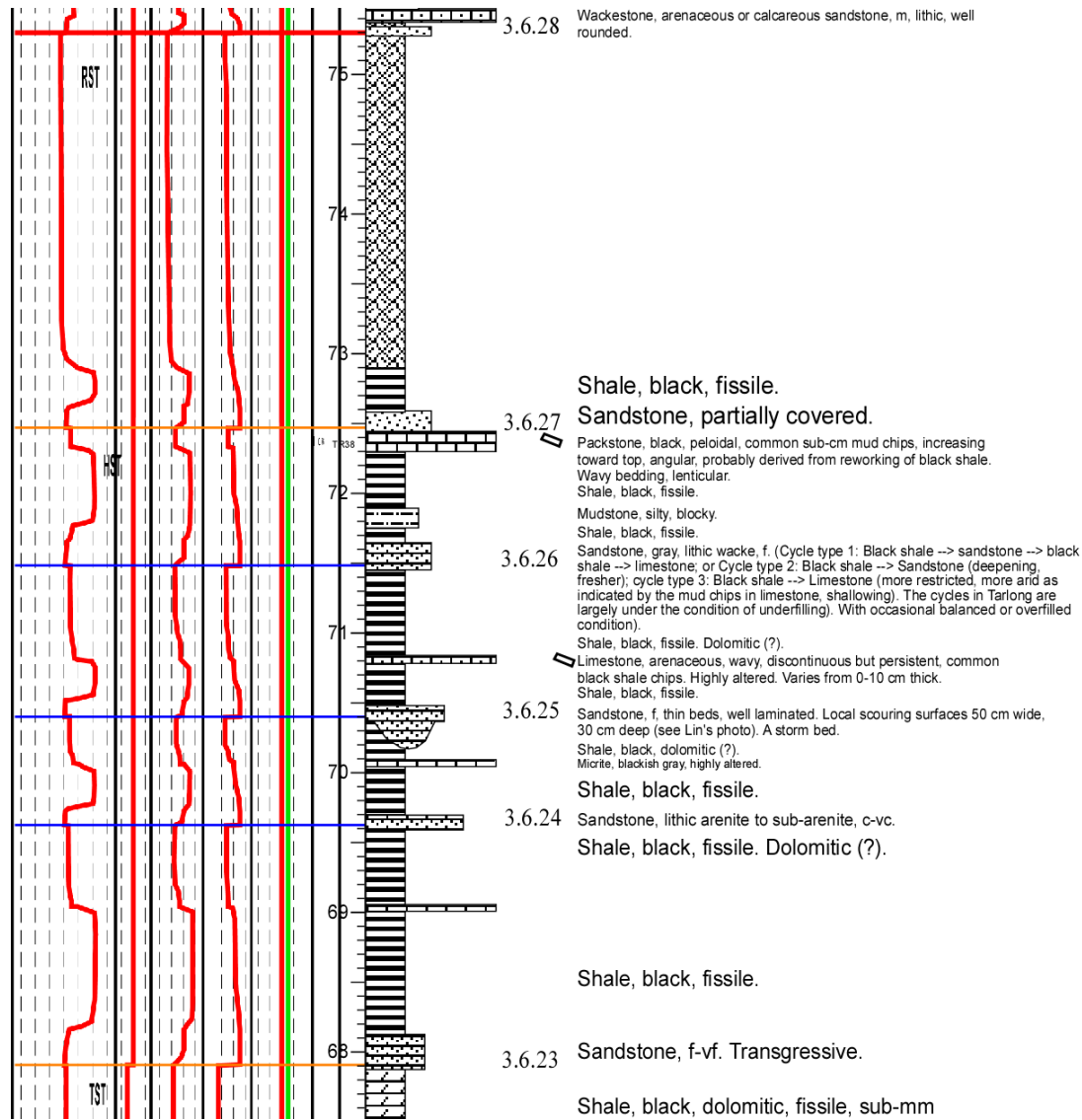
Shale, black, fissile. Silty toward the top.

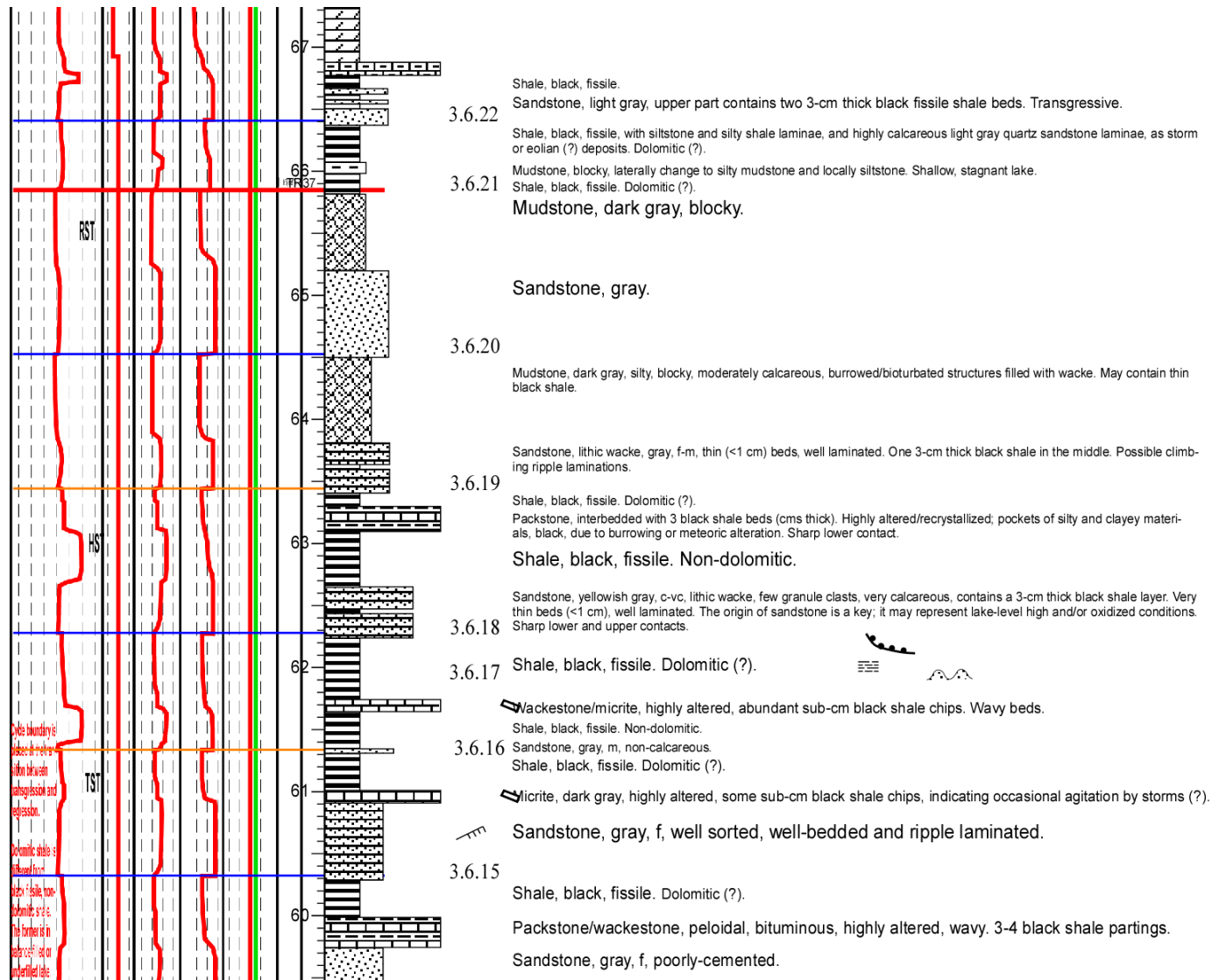
3.7.2 Sandstone, gray.

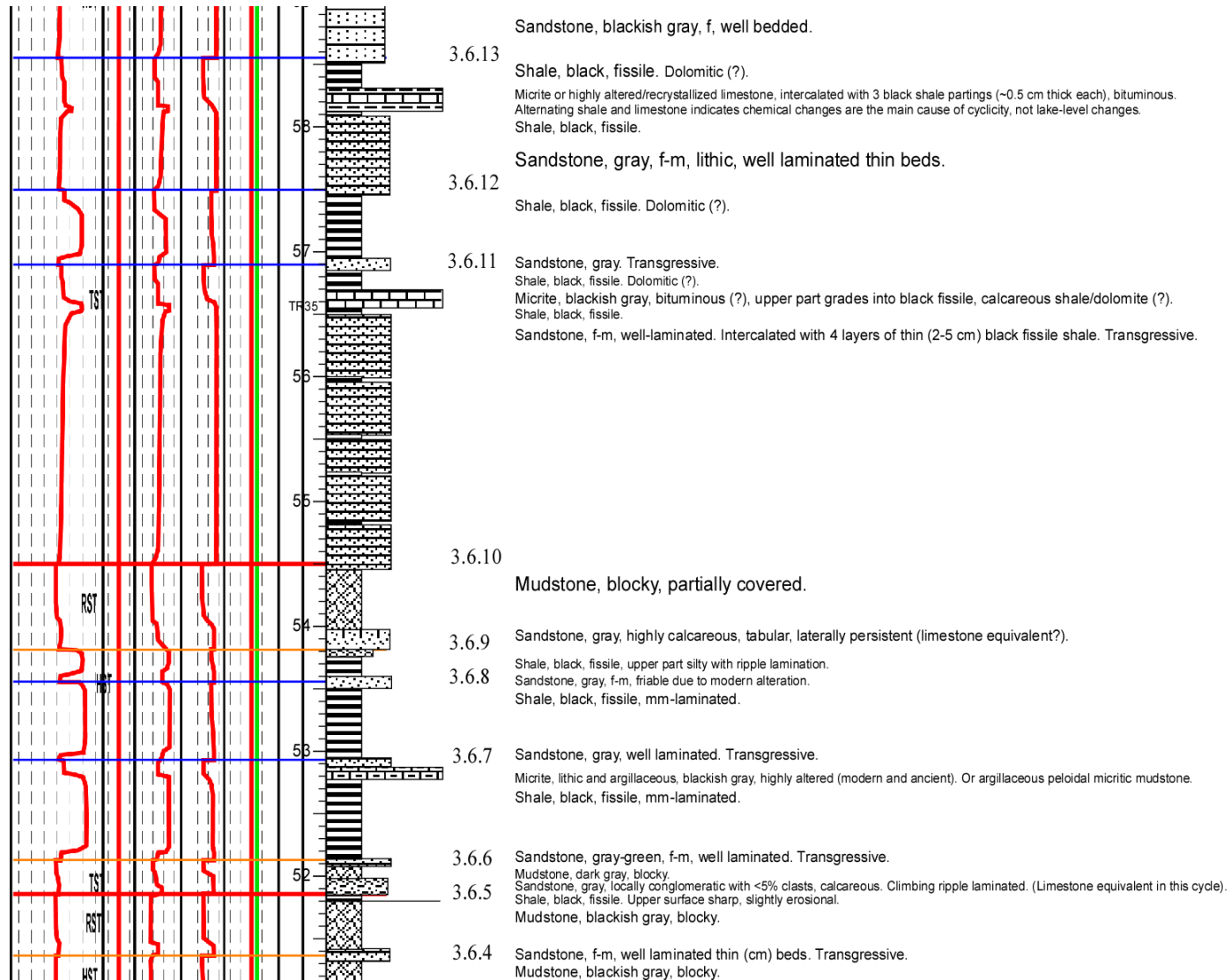
Wackestone, dark gray, peloidal, arenaceous with medium sand grains.

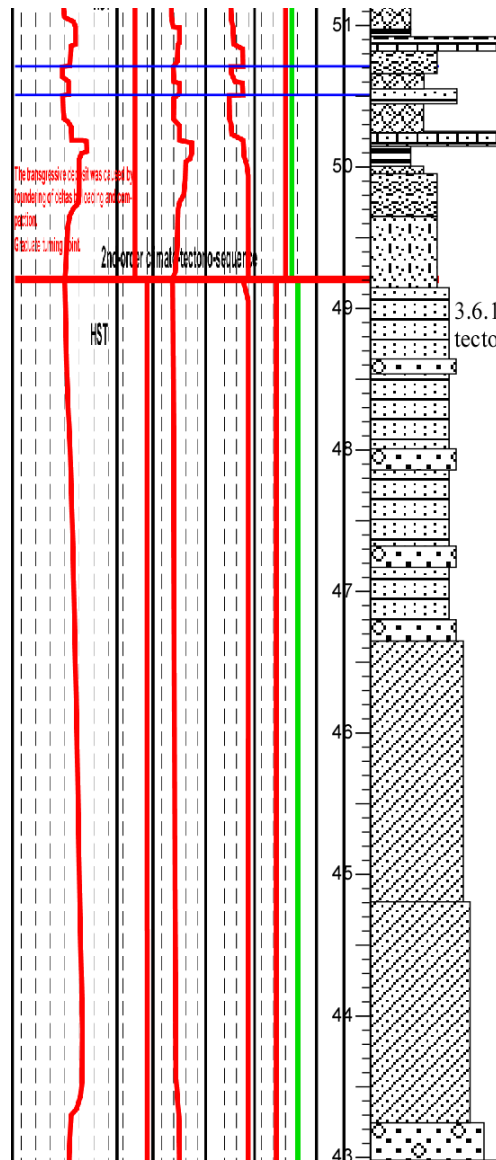
Sandstone and shale interbeds, partially covered.











Shale, black, fissile, mm-laminated.
 Micrite with shale partings, or argillaceous wackestone, black, several thin (~3 cm) beds. Sub-mm laminated. Shale partings, black, fissile. Continuous and persistent. Wavy base and sharp top. See field notes for different cycle classification scheme (a siliciclastics-carbonate couplet vs. subaerial-subaqueous couplet).
 Sandstone, brownish gray, f, climbing ripple laminated.

3.6.3
 3.6.2
 Mudstone, silty, and siltstone, blocky.
 Sandstone, m-c, well bedded, thin (~1 cm) beds, persistent

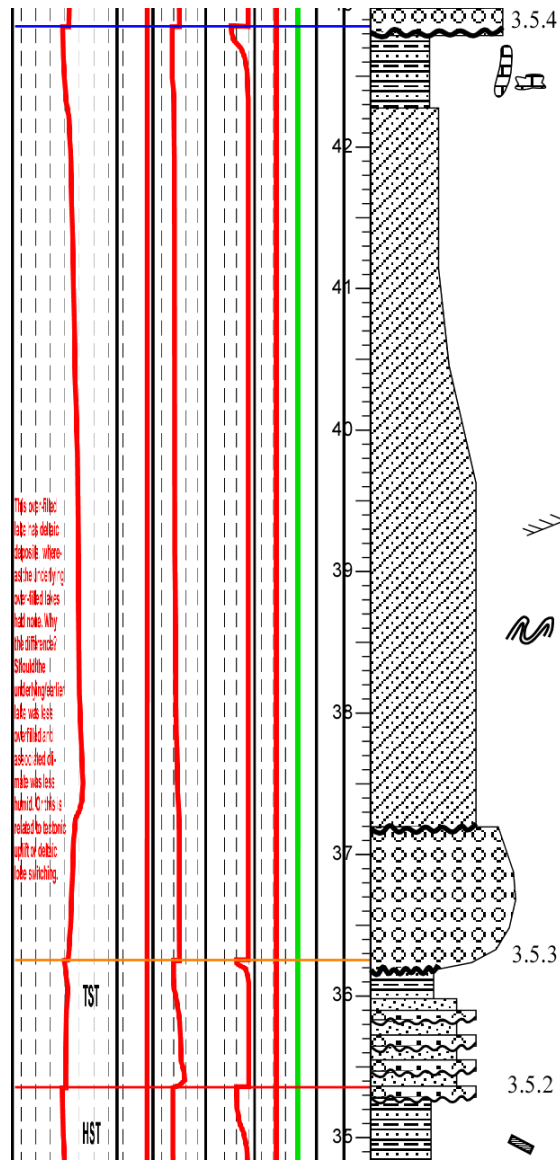
Shale, silty, and siltstone, blocky, angular peds ~1 cm in size. No evidence of bioturbation. Sharp upper surface. Balanced fill, fluctuating profundal (?)
 Packstone to wackestone, arenaceous/lithic, dark gray, single bed, wavy base and top. Lenticular, discontinuous, but persistent.
 Shale, black, mm-laminated, fissile to blocky. Shallow lacustrine deposit.
 Shale, silty, black, blocky, dense, angular peds 1-2 cm in size, moderately calcareous. Gleyed paleosol.
 Sandstone, whitish gray, f, lithic with some quartz grains, calcareous, lower part tabular x-bedded, upper part climbing ripple laminated. Lower contact sharp. Lake shore sand flat deposit.

★
 Sandstone, greenish gray. Several fining-upward units from basal conglomeratic sandstone (with 5% clasts) to m sandstone. Well bedded and laminated thin (<5 cm) beds. Uppermost 50 cm is very calcareous, f sandstone, increased quartz content, blocky with carbonaceous partings. Delta plain or flood plain.

3.6.1: climato-tectono-IC

Conglomeratic sandstone, and sandstone, greenish gray. Lithic wacke to subarenite, m-c, moderately to poorly sorted, calcareous, clasts rounded. Large low-angle tabular x-bedded. Overall fining upward from c-vc to m. Coarse-grained meandering stream or delta front deposit.

Conglomerate and conglomeratic sandstone (with 30% clasts), clast-supported. Clasts of volcanic, sedimentary, and soil nodules, up to 10 cm in diameter, parallel to bedding. Basal surface erosional with a channel form, contorted; upper surface gradational. Base of a distributary channel. Beginning of another deltaic pro-



This one filled
 late was debris
 deposit where
 and the underlying
 coarse-filled laves
 that make. Why
 the difference?
 Should the
 underlying inter
 late was less
 coarse-filled or
 coarse-bed of
 coarse was less
 humid. Or this is
 related to debris
 split or debris
 beds switching.

3.5.4

gradational episode.

Sandstone, siltstone, and silty shale interbeds, greenish gray to brownish gray. Sandstone f-vf, moderately to poorly sorted. Thin (cms), well bedded. Mud cracked surface found in rubbles. Laterally persistent. Common irregular to tabular, subvertical cm-10 cm calcitic soil nodules although beddings are largely preserved, indicating slight to moderate pedogenesis. Upper delta plain deposits. Complete a fining-upward succession.

Sandstone, greenish gray, lithic, some quartz and feldspar, m-c-vc, conglomeratic (<5%, <1 cm clast size), large low-angle tabular x-beds of multiple directions; low-angle contacts between sets of x-beds. Locally distorted beddings. Overall fining upward from c-vc to f. Basal erosional contact with a 20-cm relief (see Lin's photo), upper contact sharp. Middle part of a CMB.

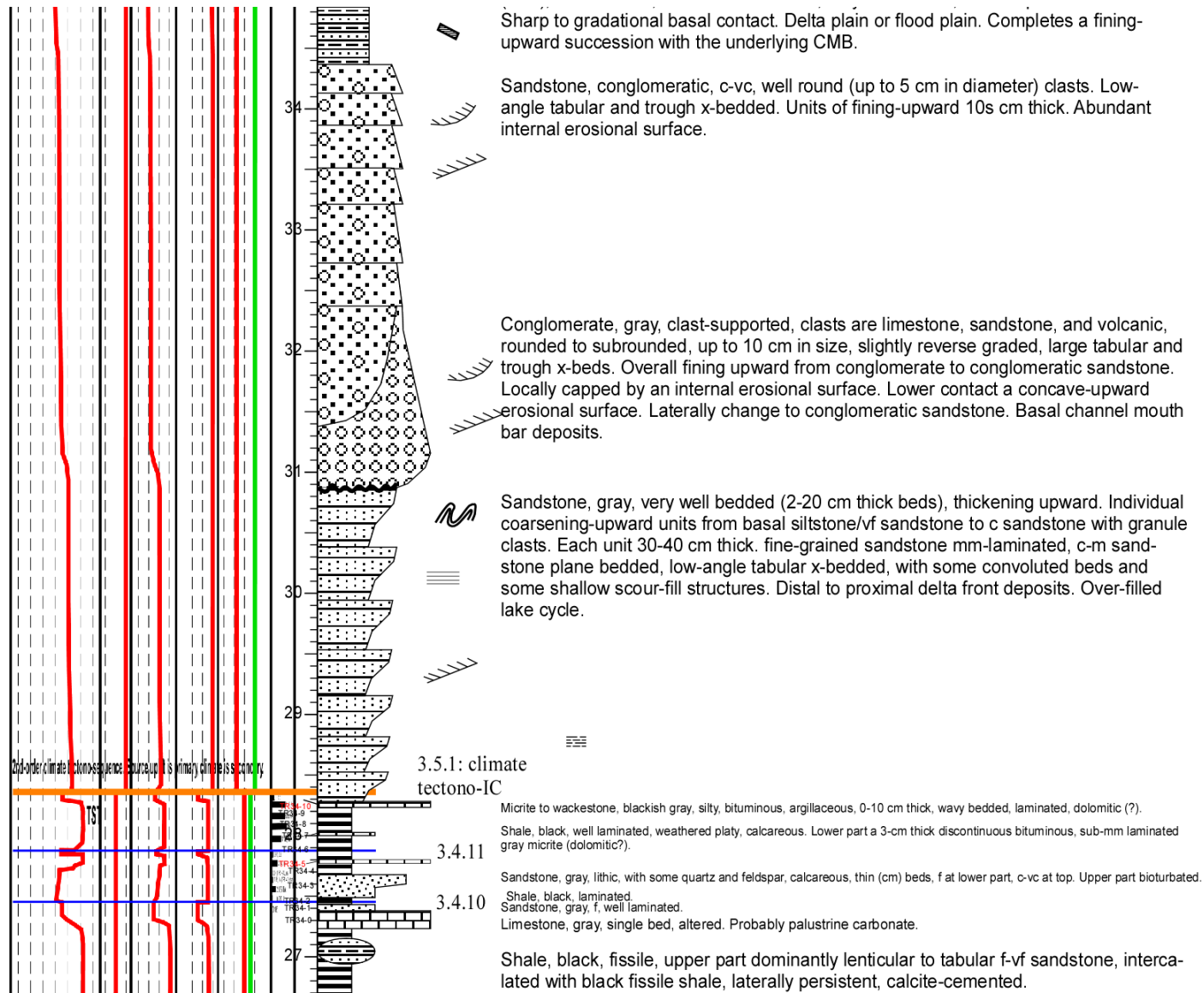
3.5.3

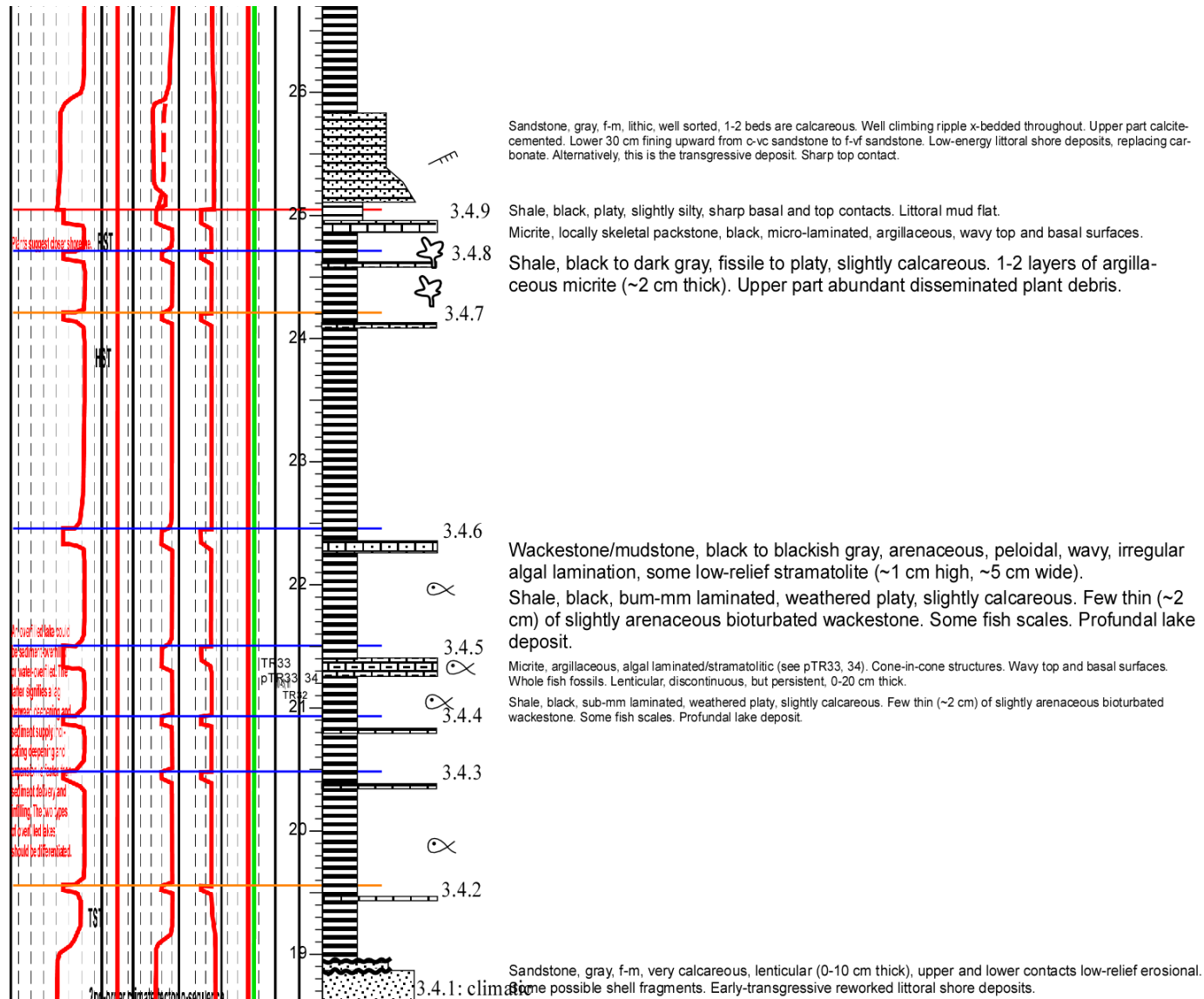
Sandstone, siltstone, silty shale, thin and well bedded, thick laminated, upper part eroded. Completes a fining-upward succession with the underlying CMB.

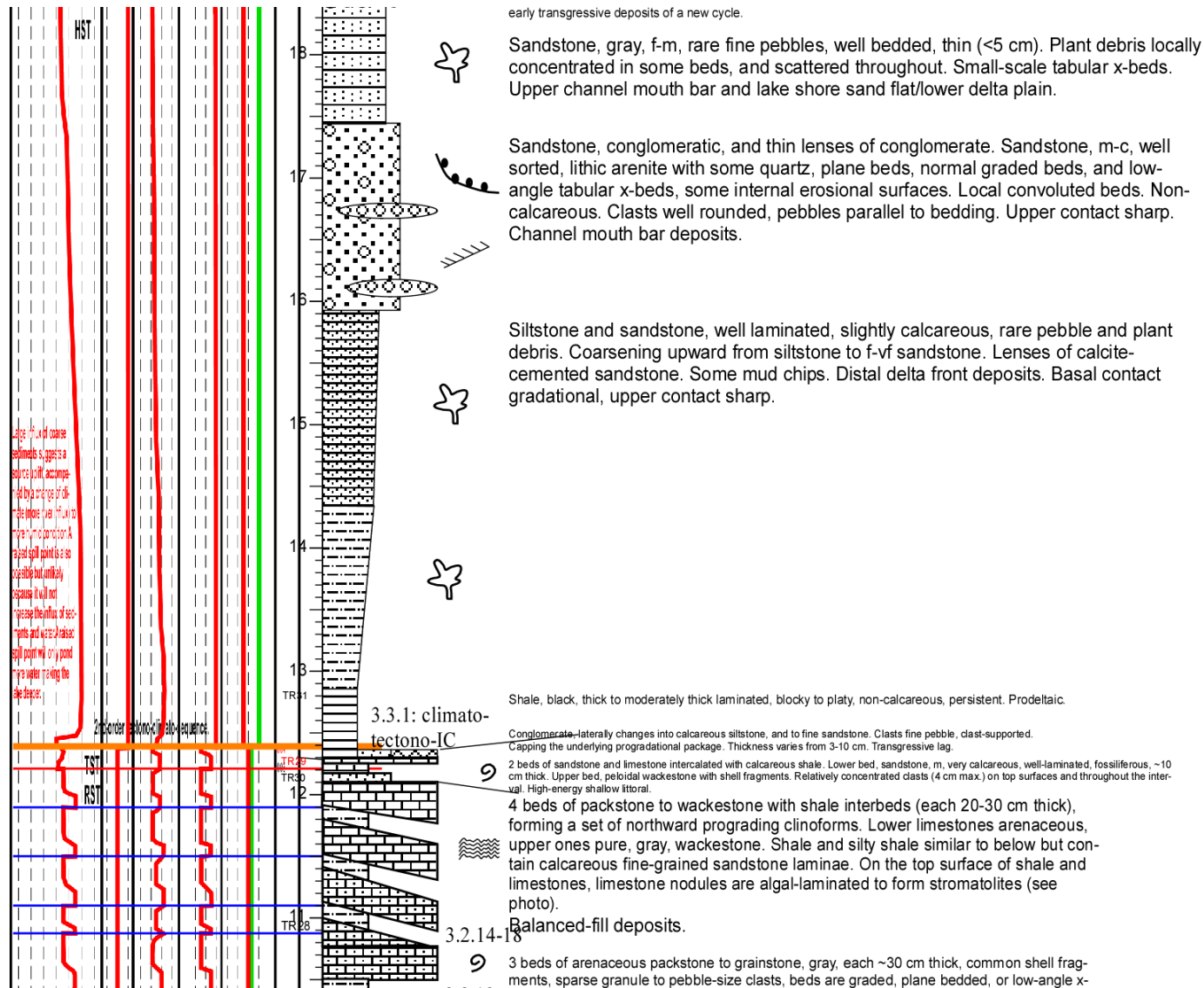
Sandstone and conglomeratic sandstone, greenish gray. Each unit is 10s cm thick, composed of a basal conglomeratic sandstone with a basal scour surface, overlain by f-m sandstone; individual units are normal graded. Off center of CMB (another episode/cycle of deltaic progradation).

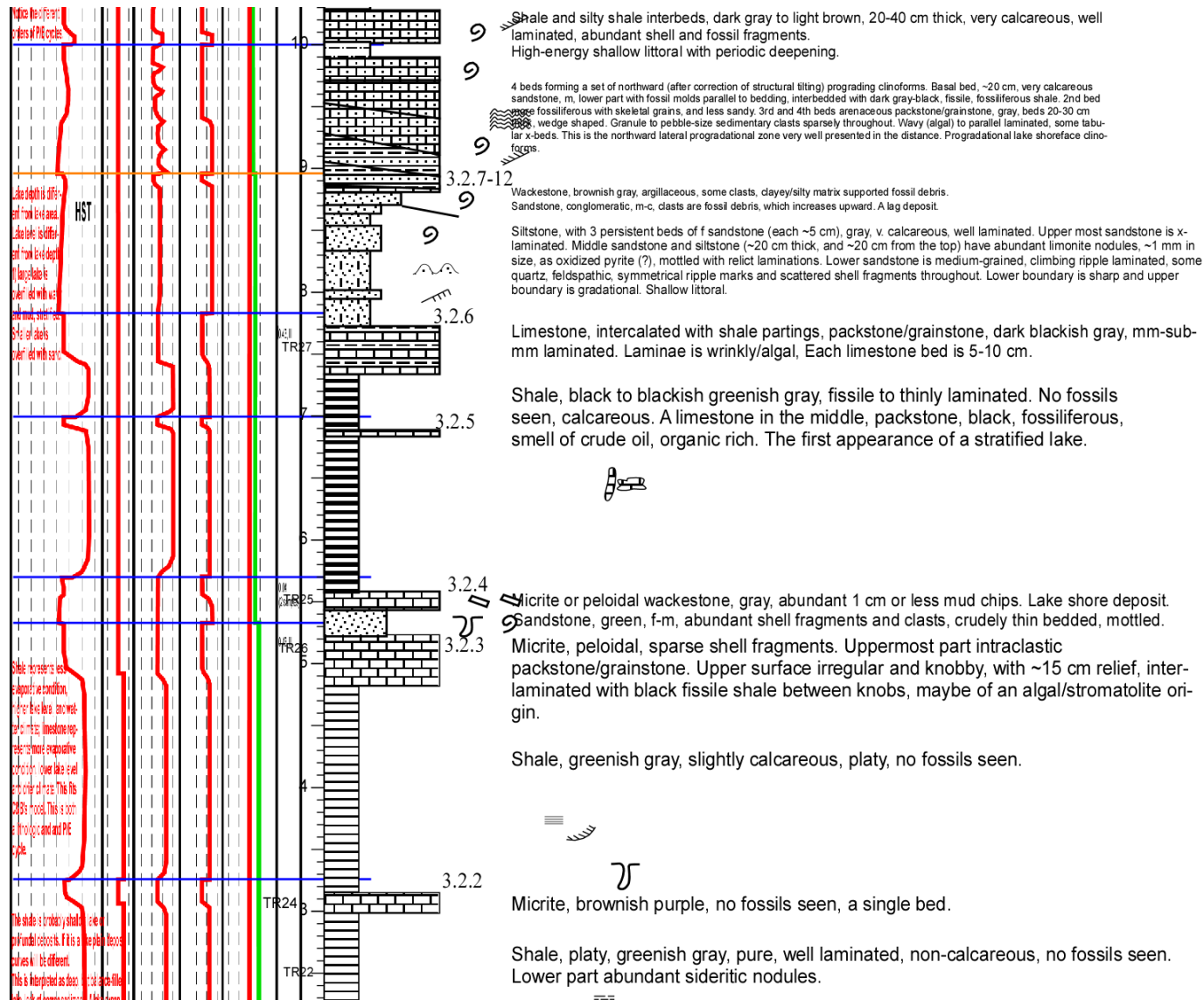
3.5.2

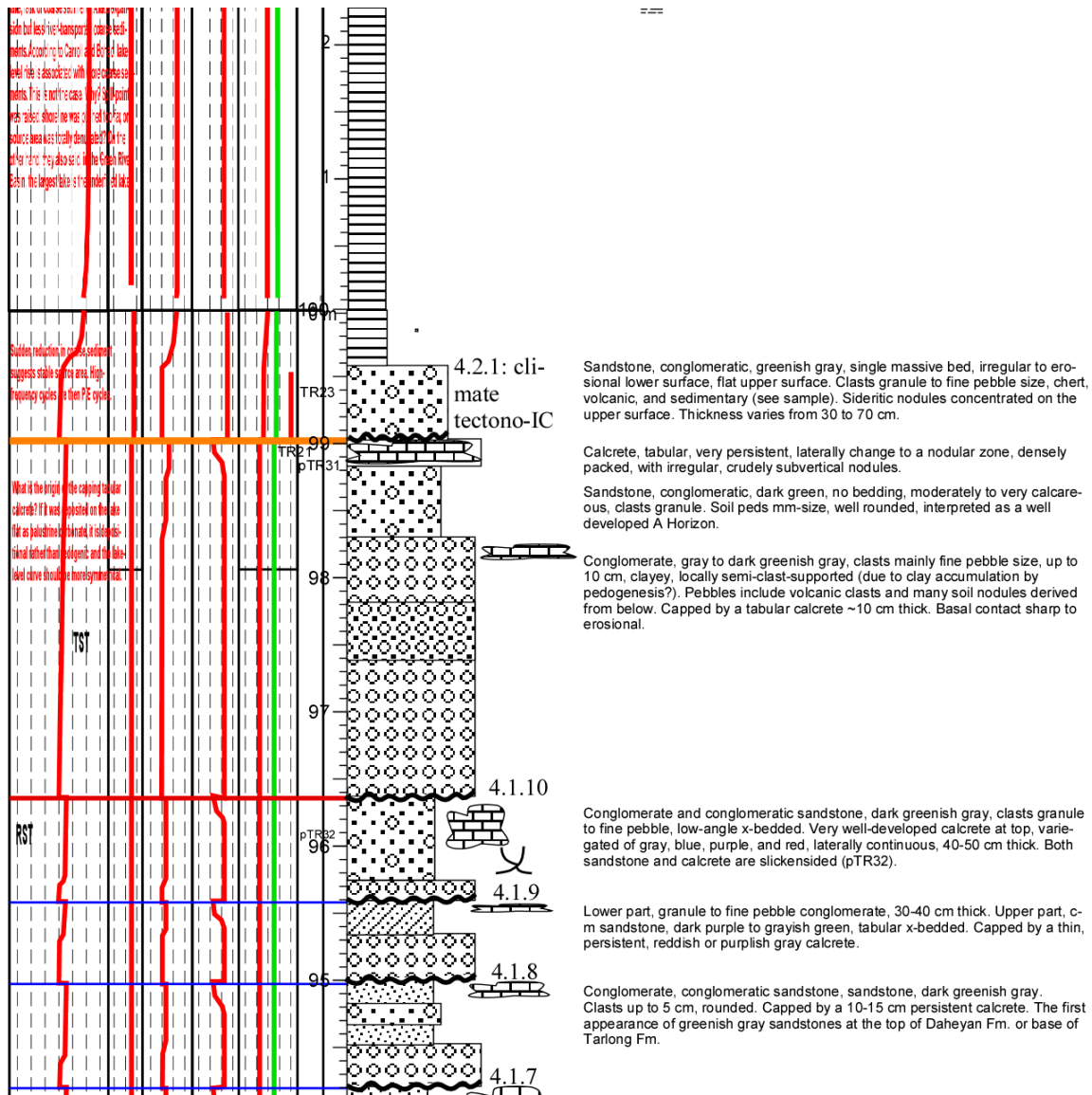
Sandstone, siltstone, silty shale, greenish gray. Sandstone is fine-grained. Thin (cms), well bedded, and thick laminated; very calcareous, mud chips common.

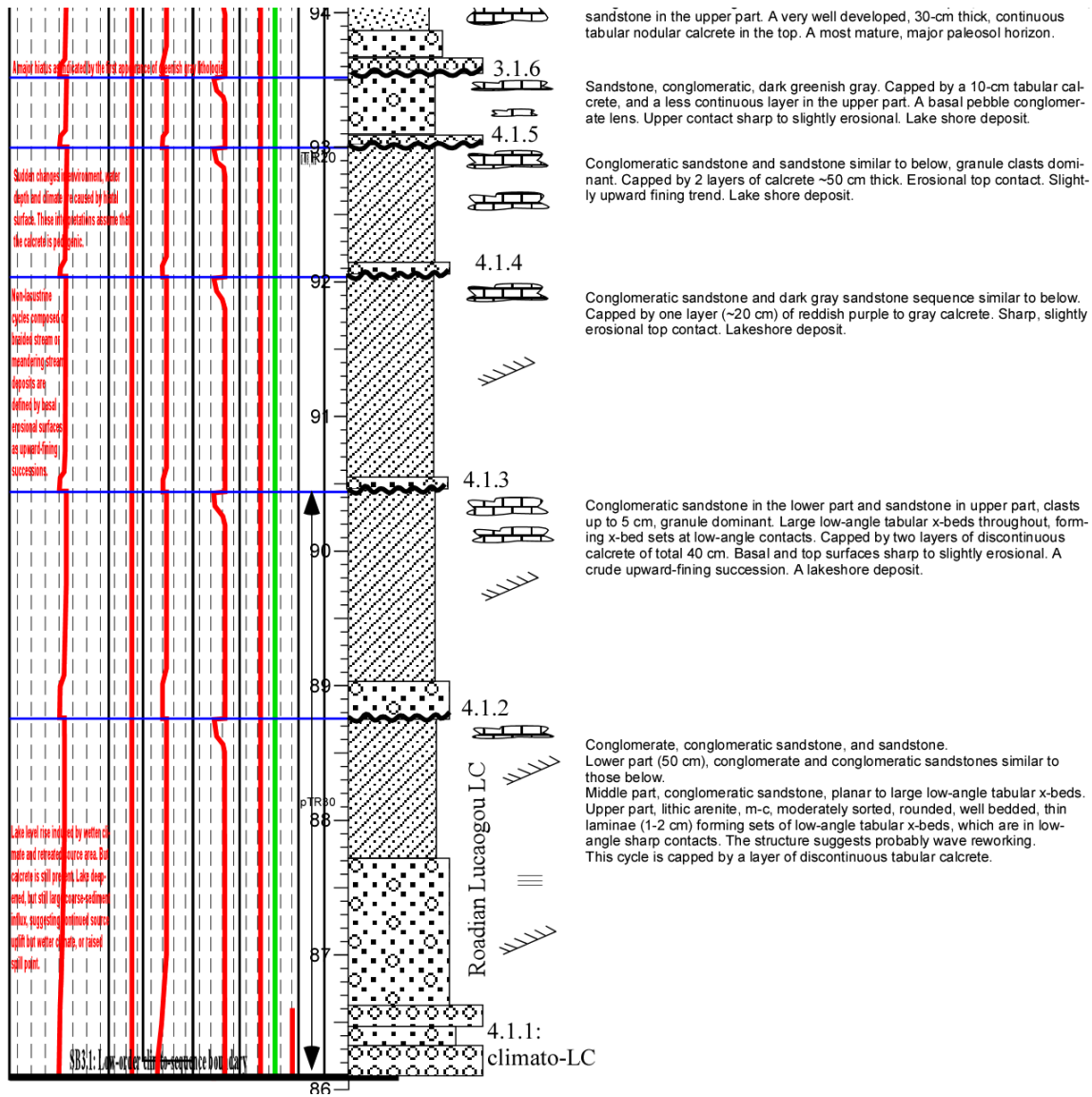




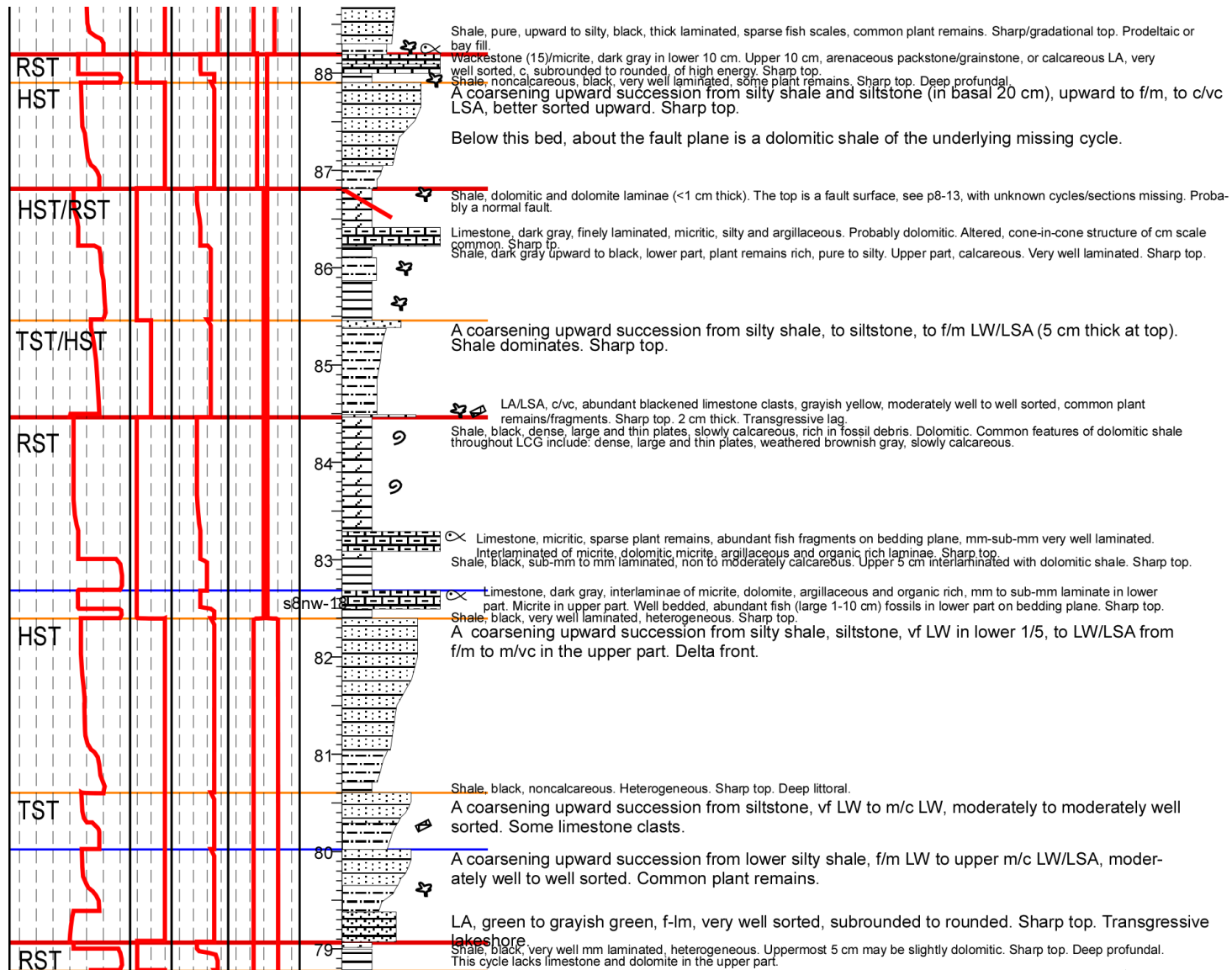


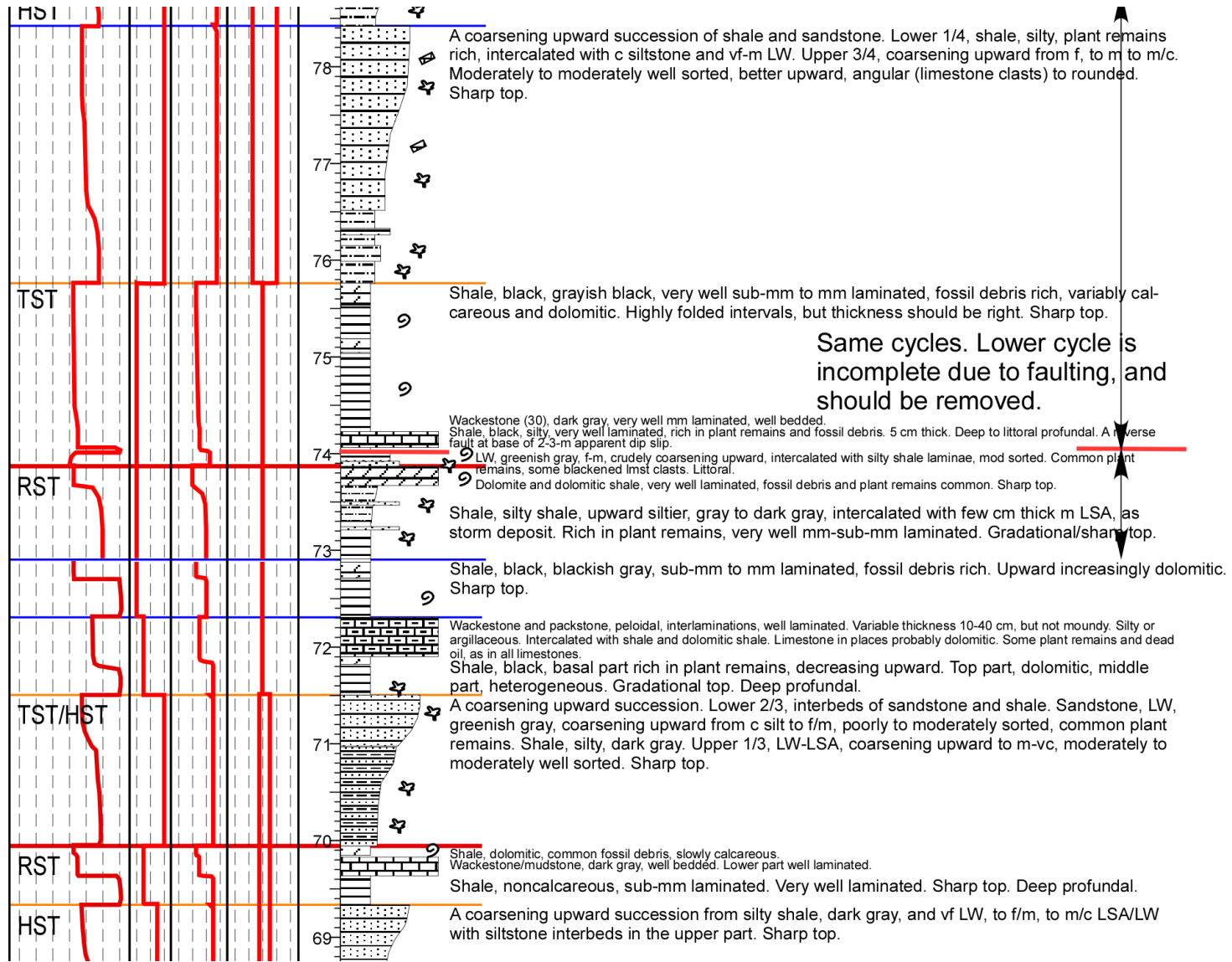


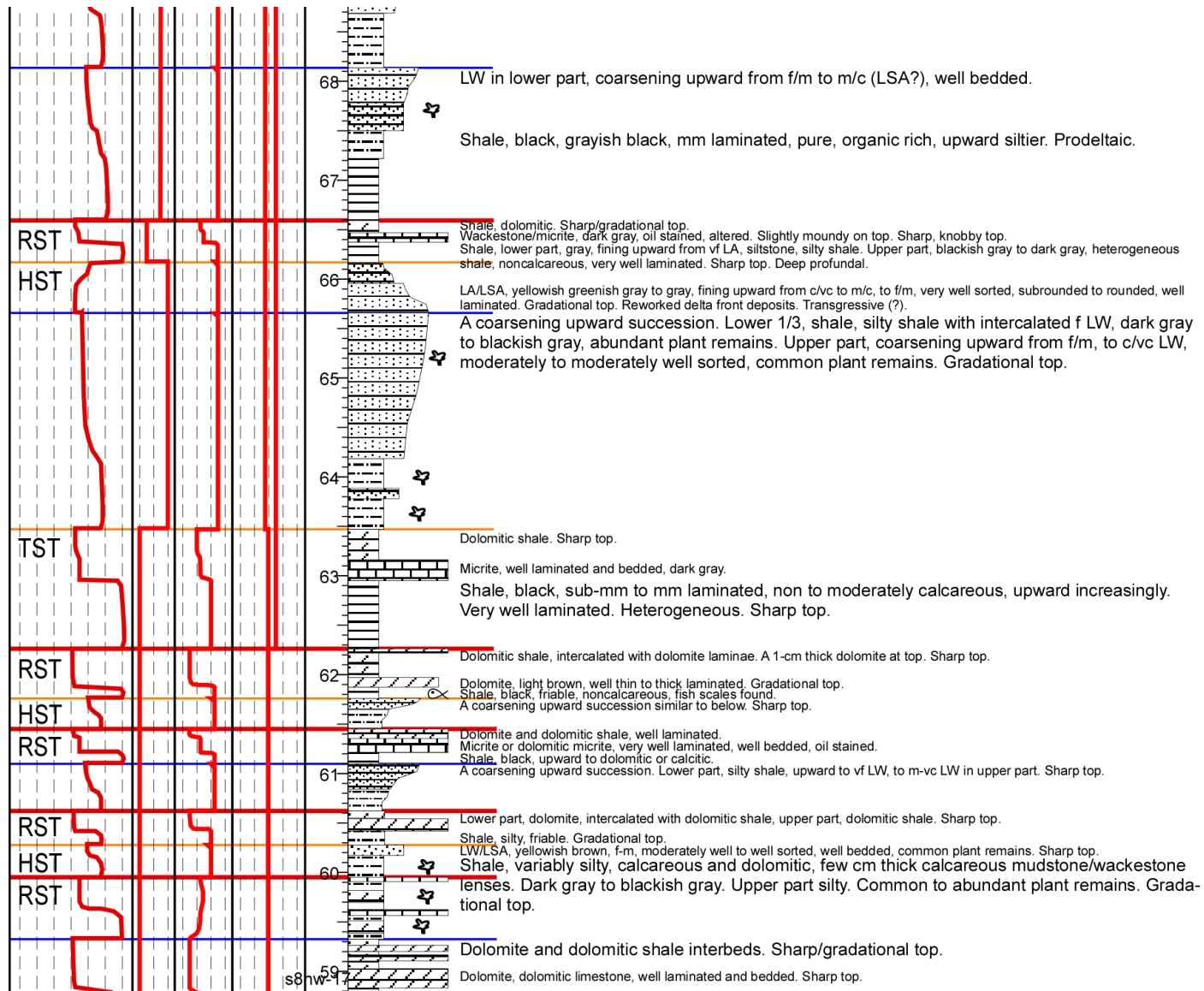


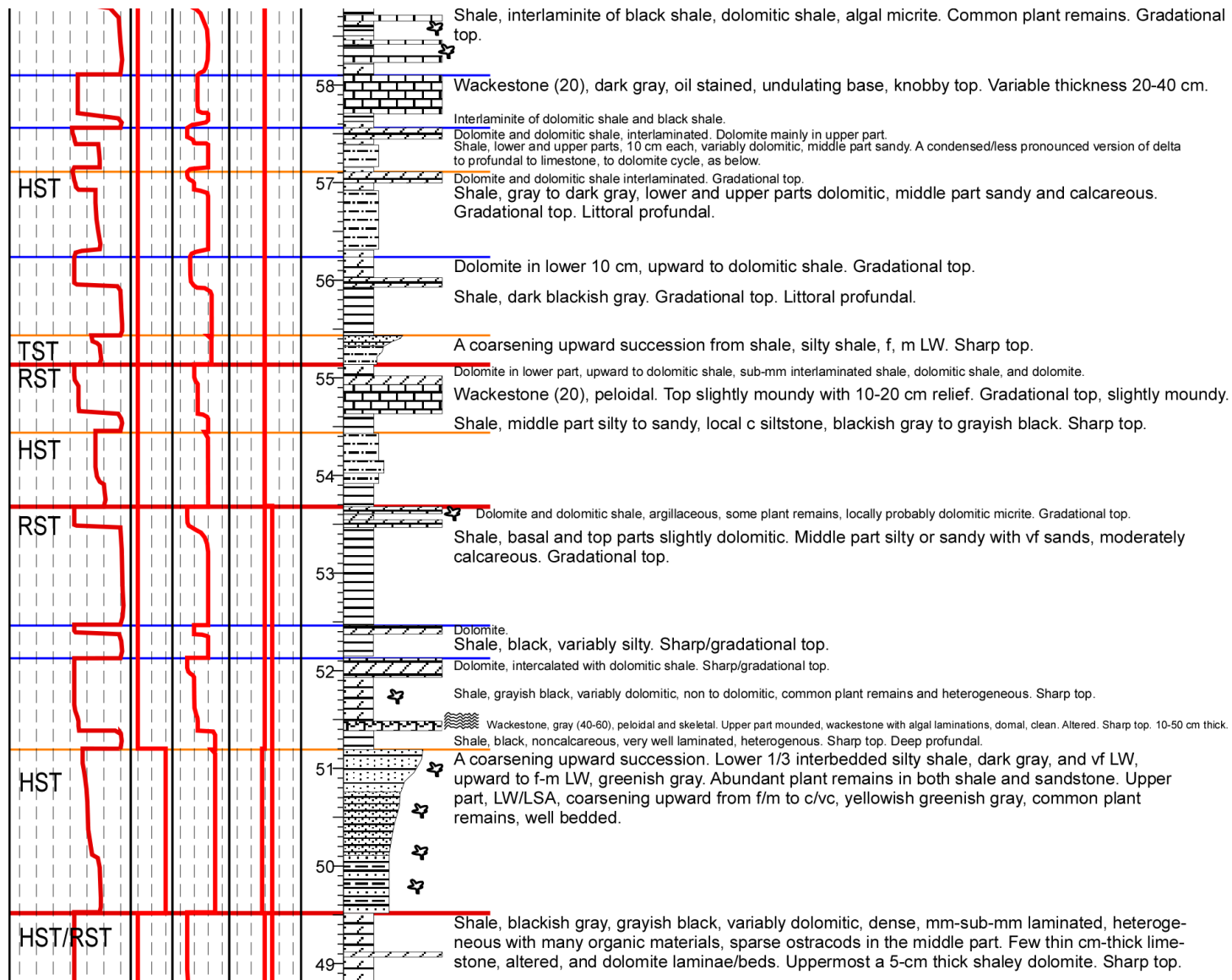


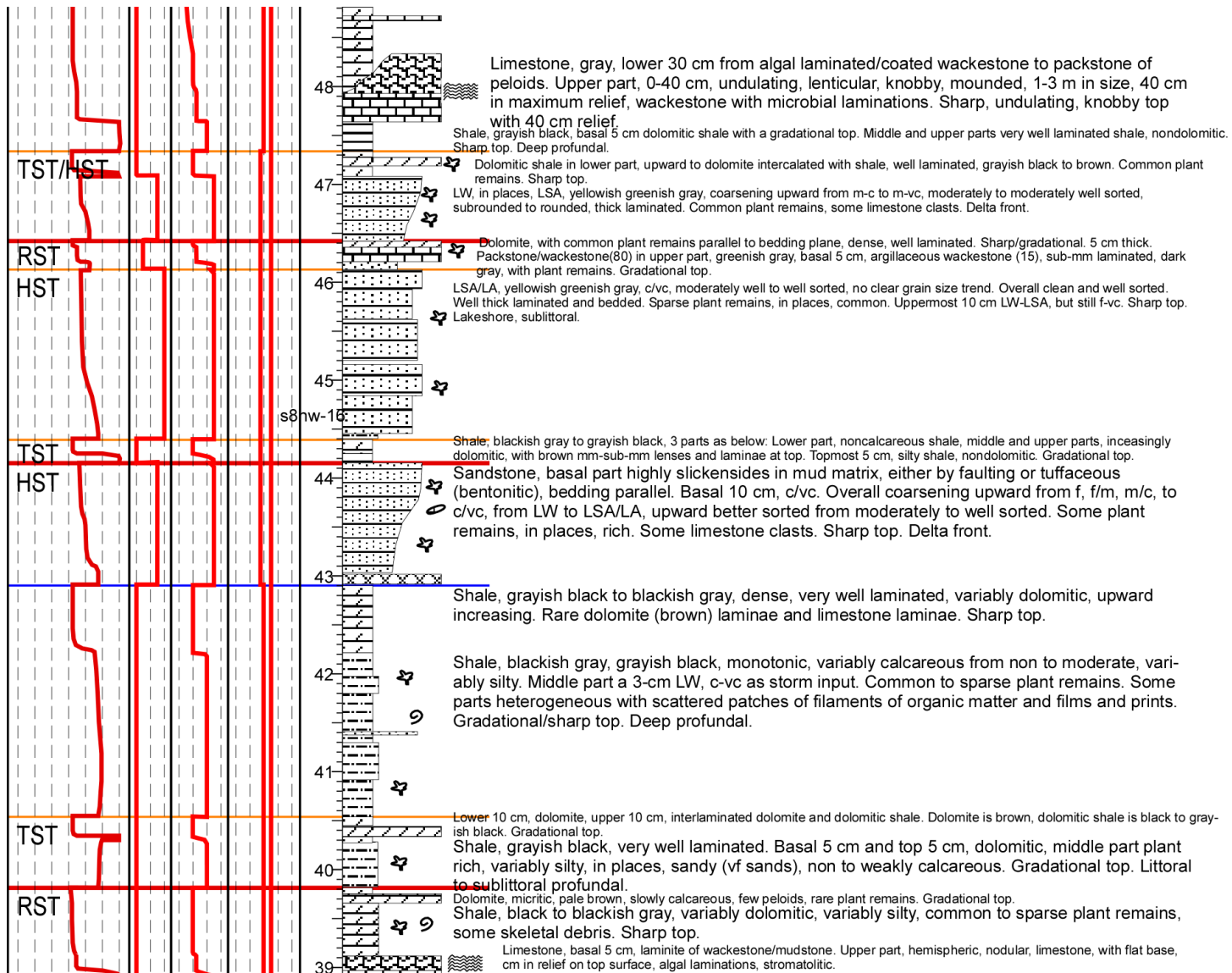
APPENDIX B
NW TARLONG SECTION

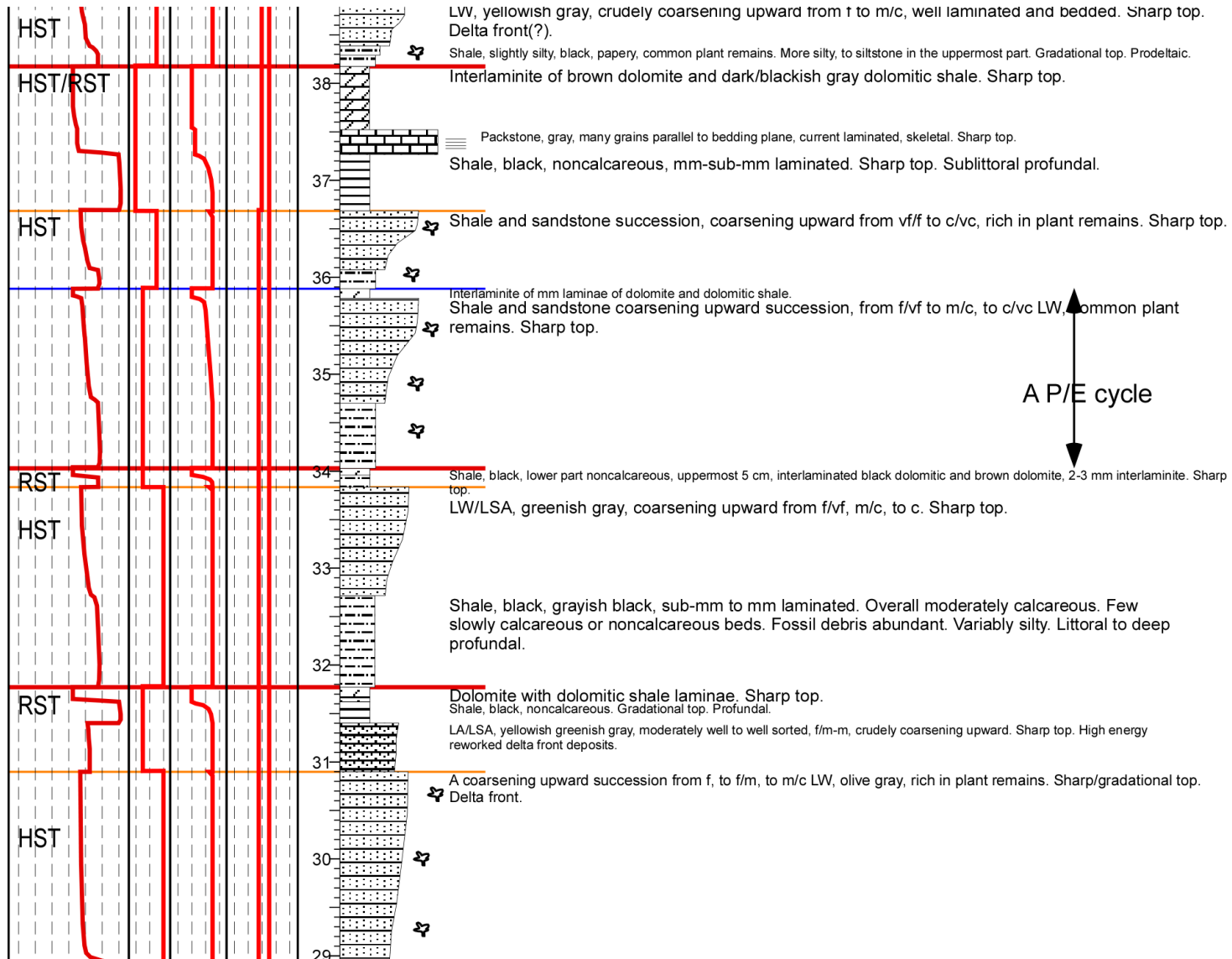


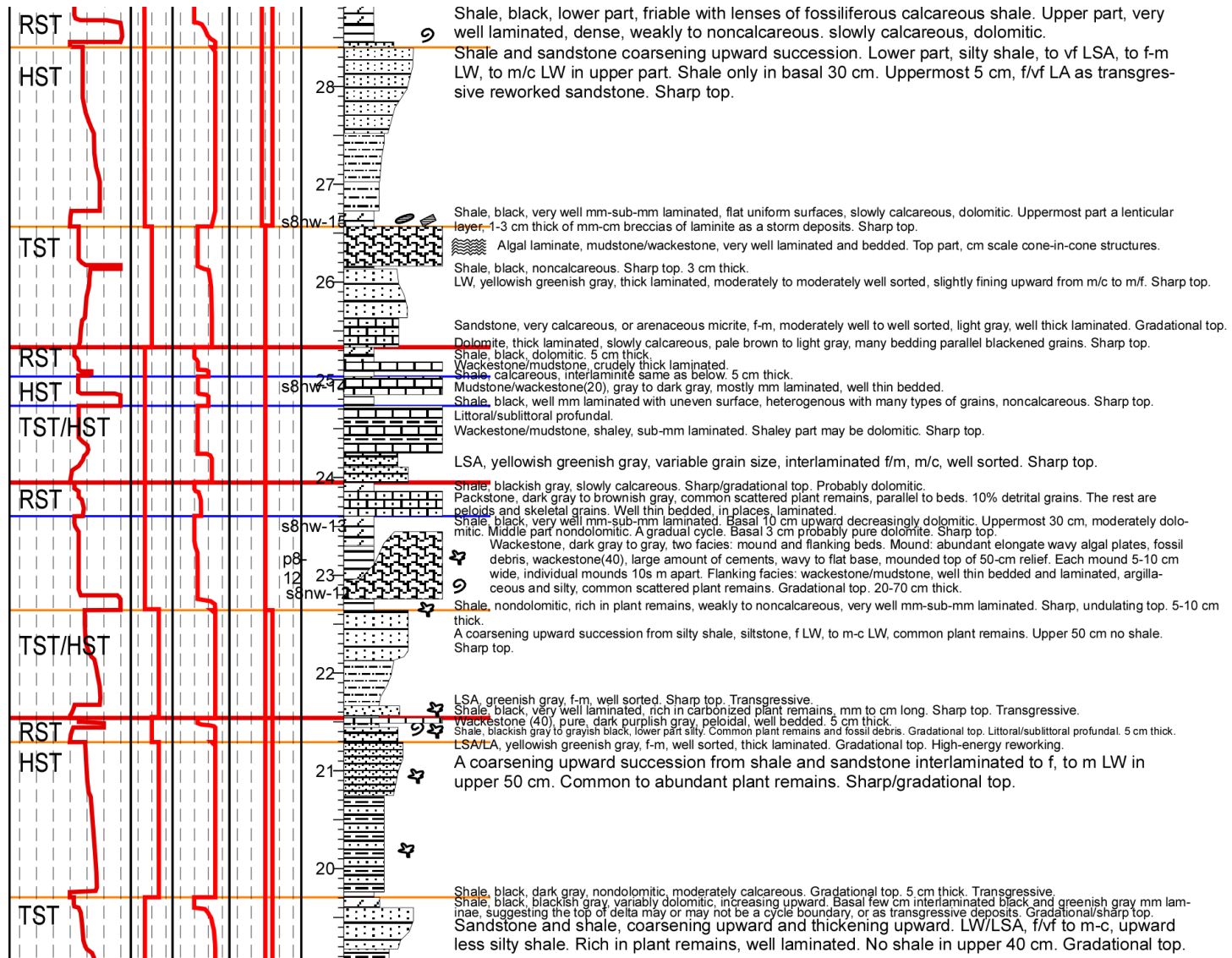


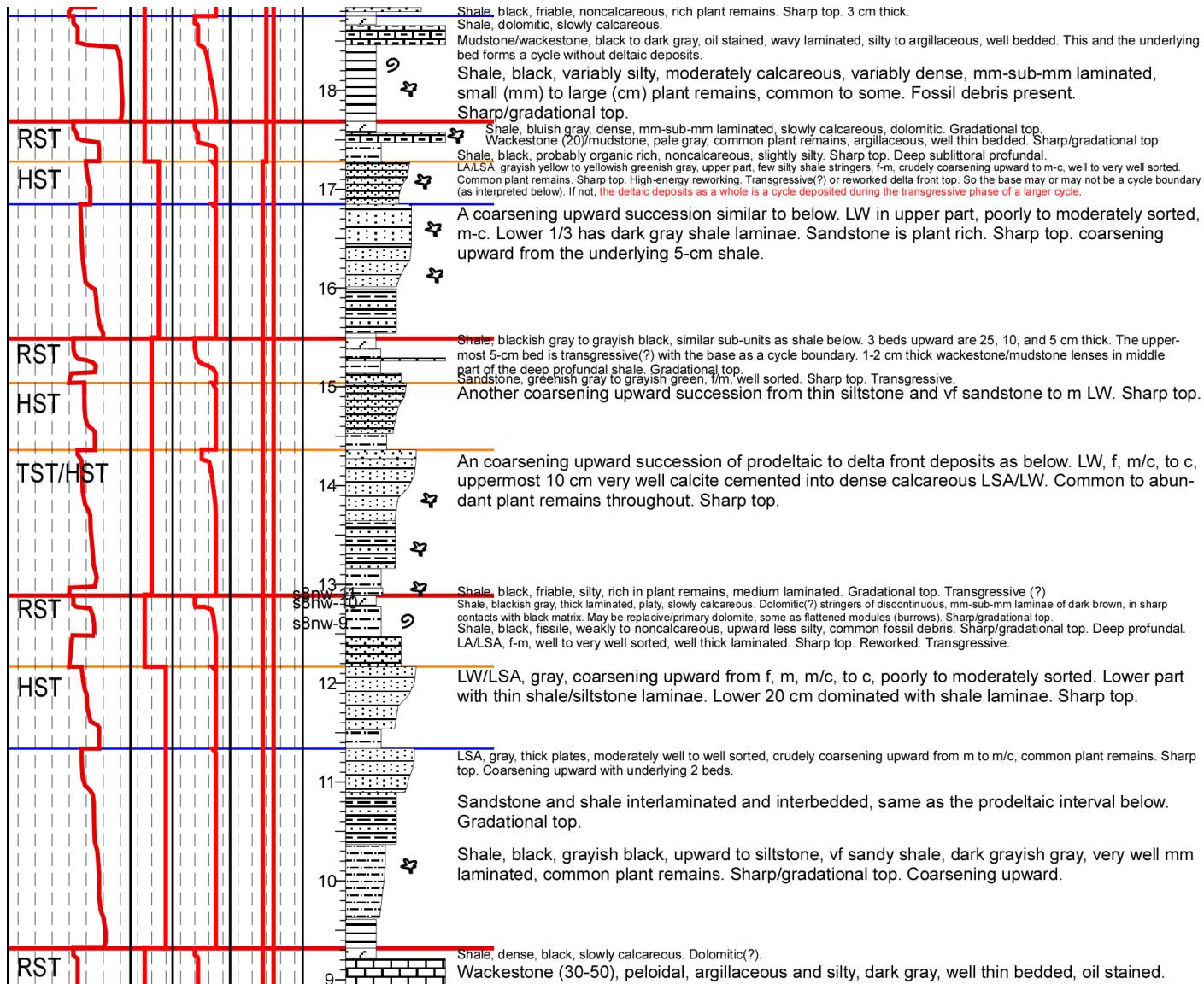


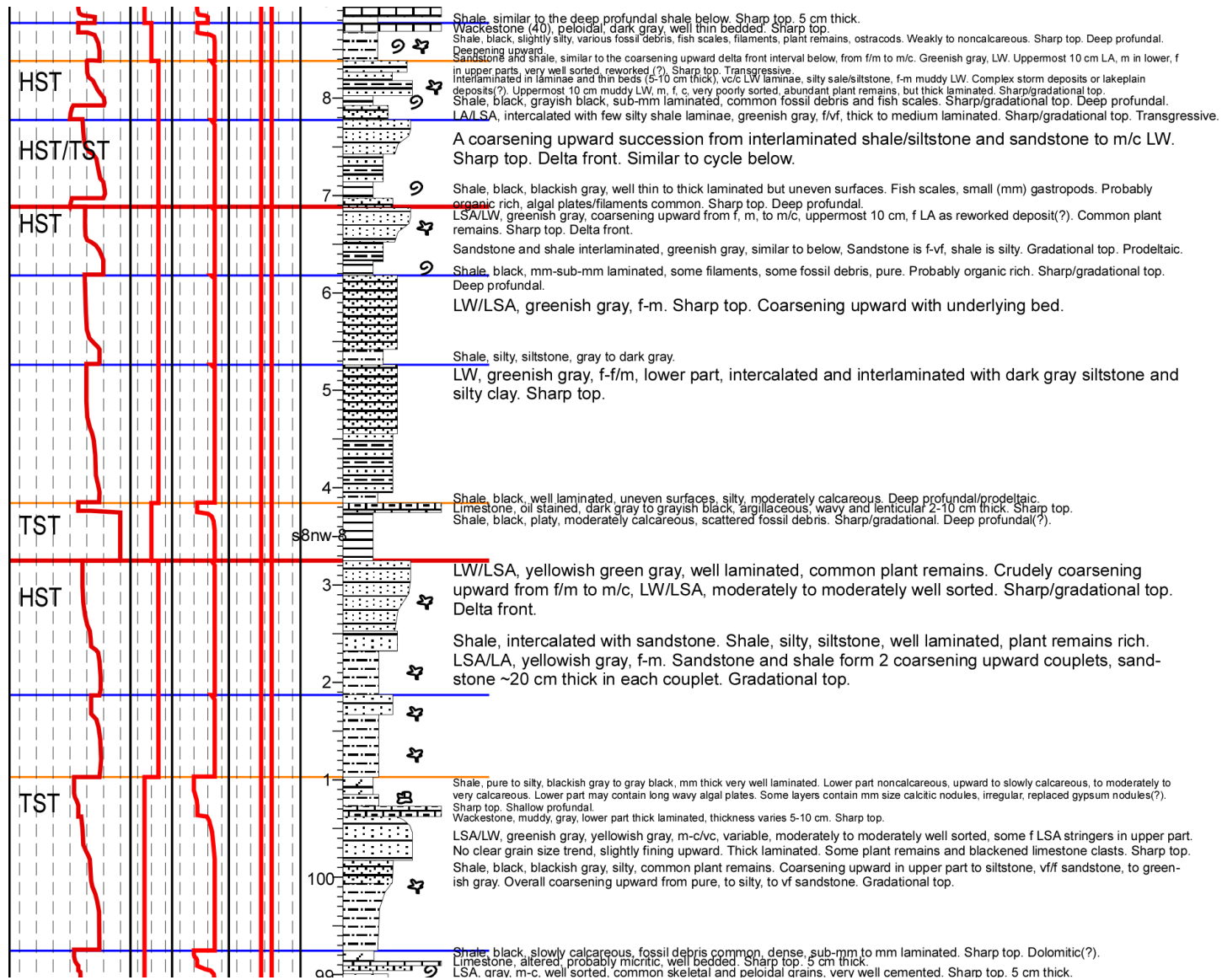


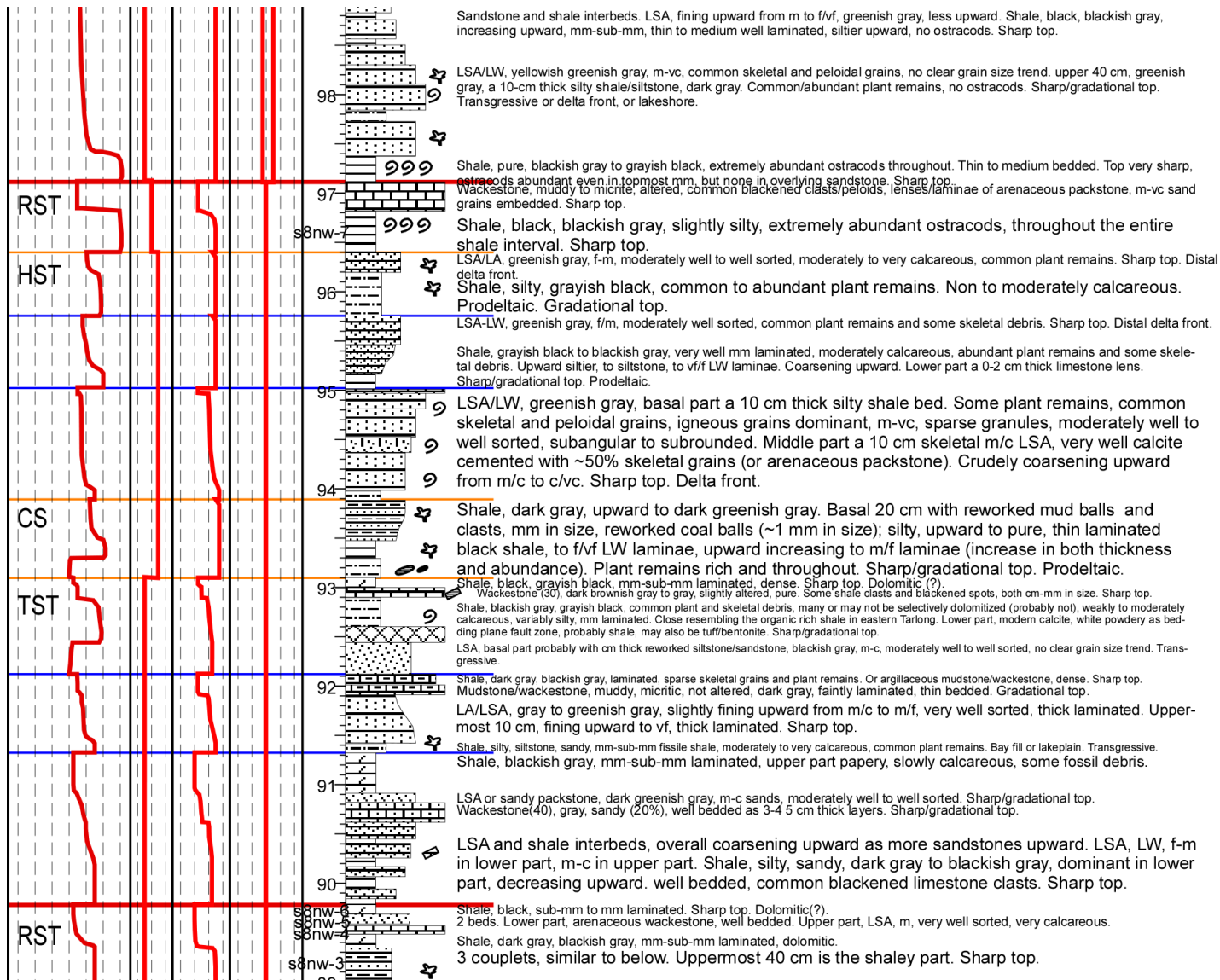


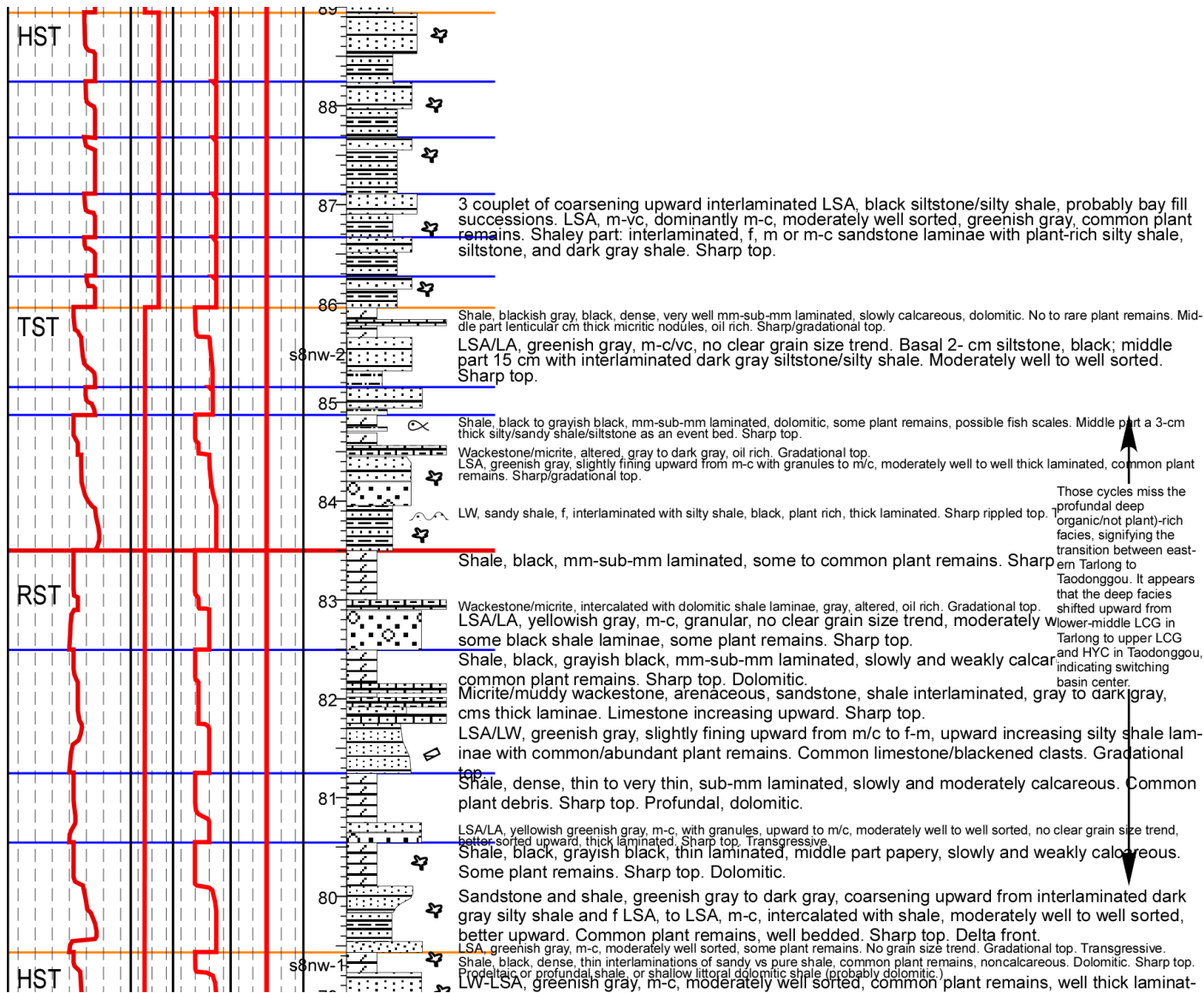


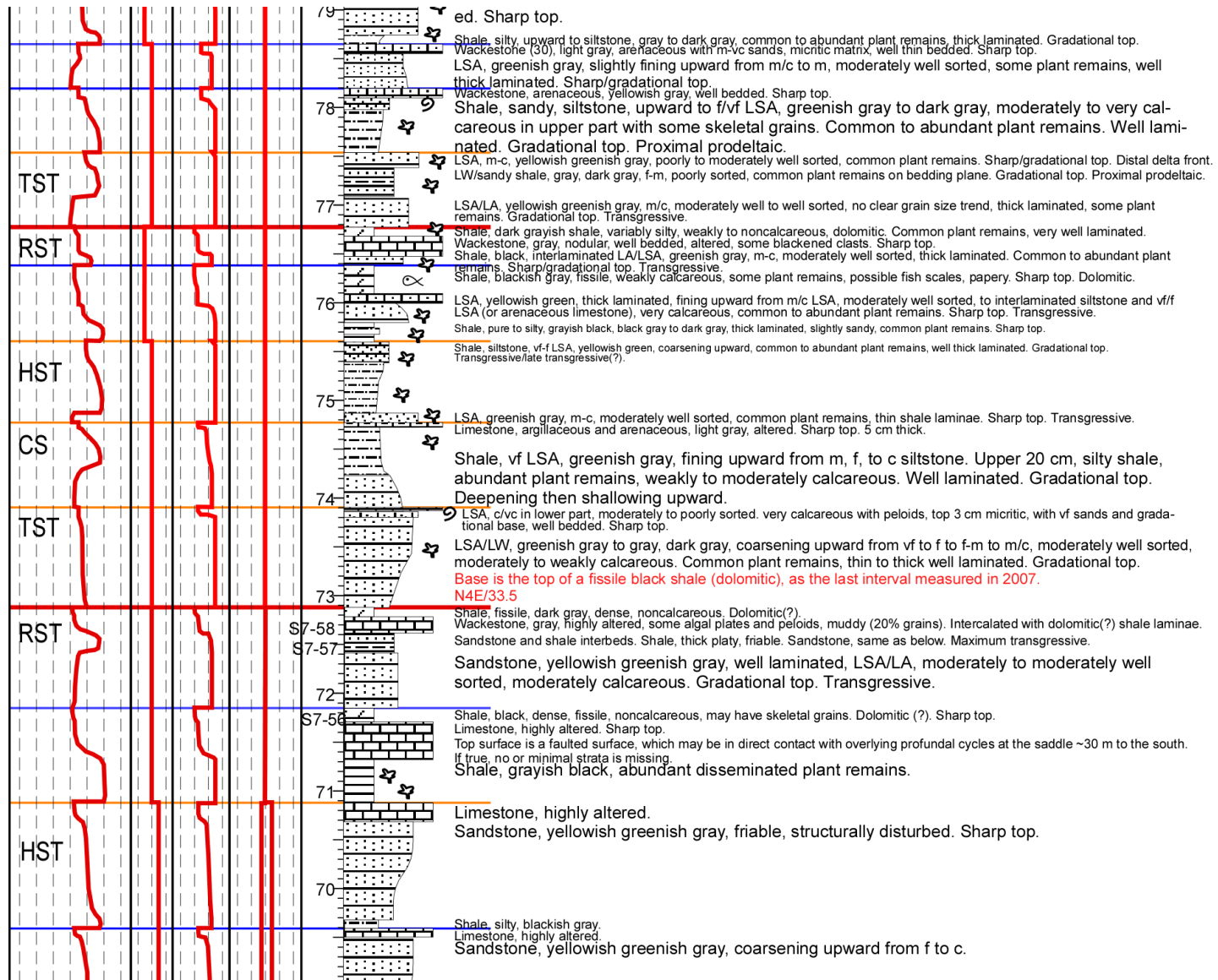


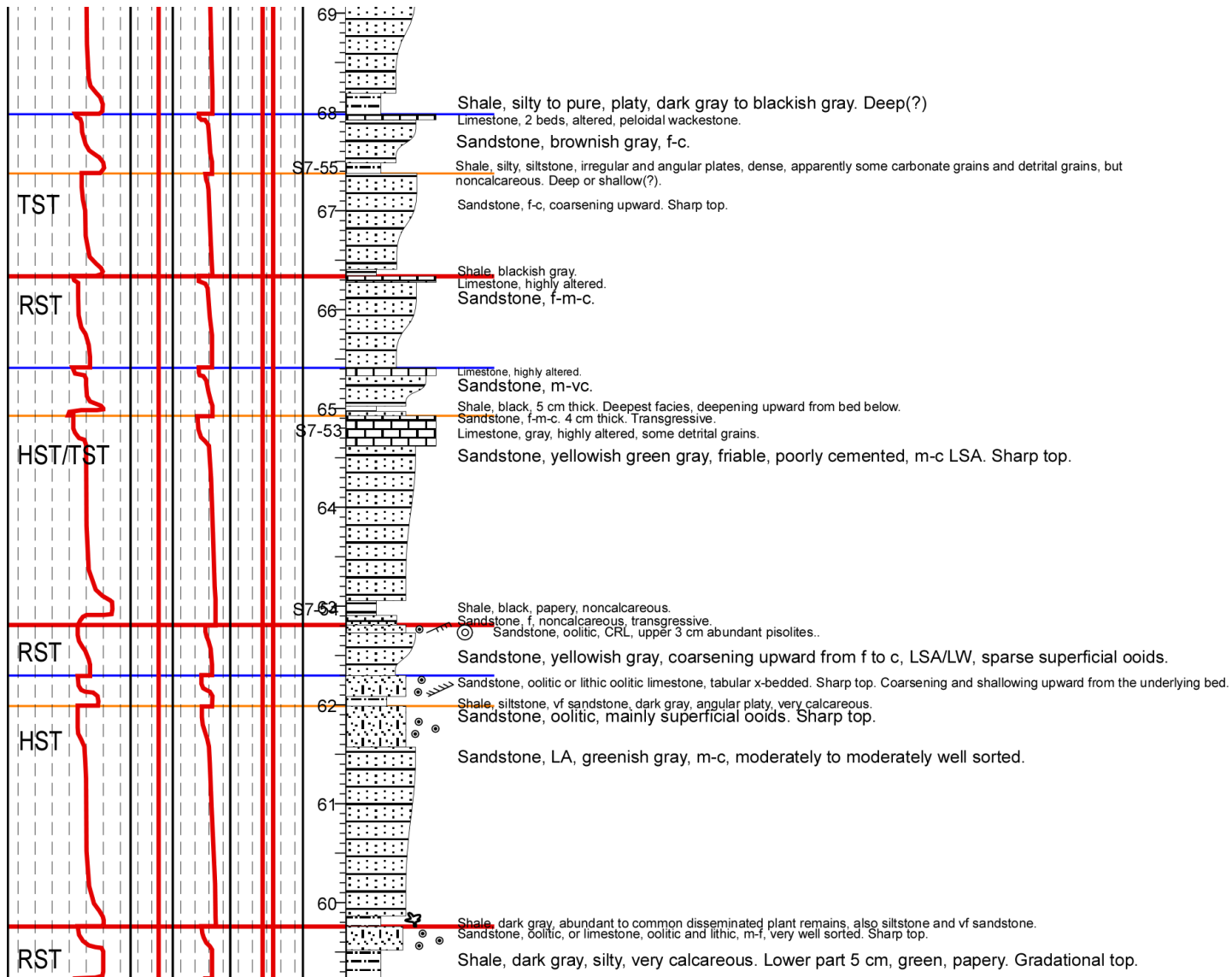


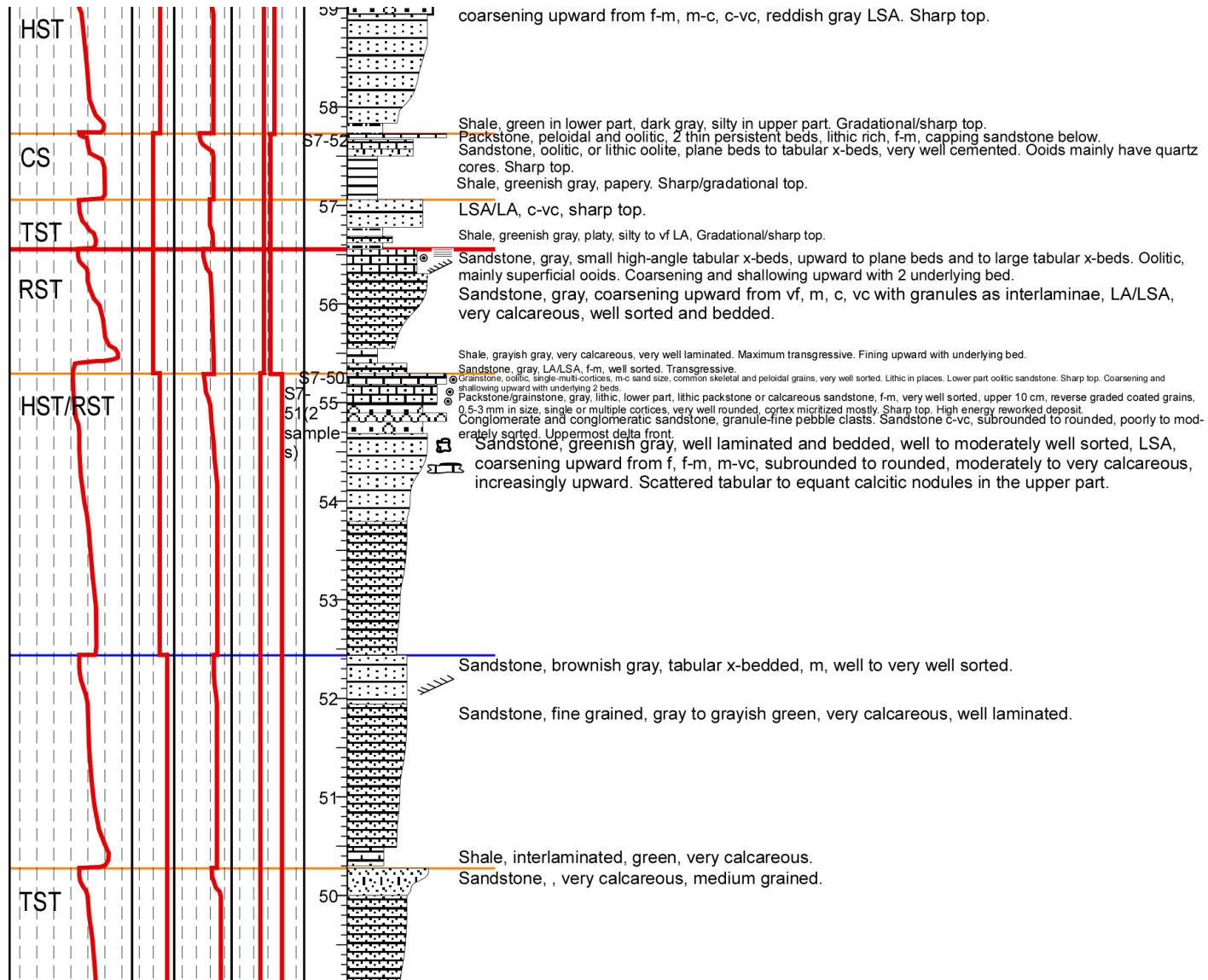


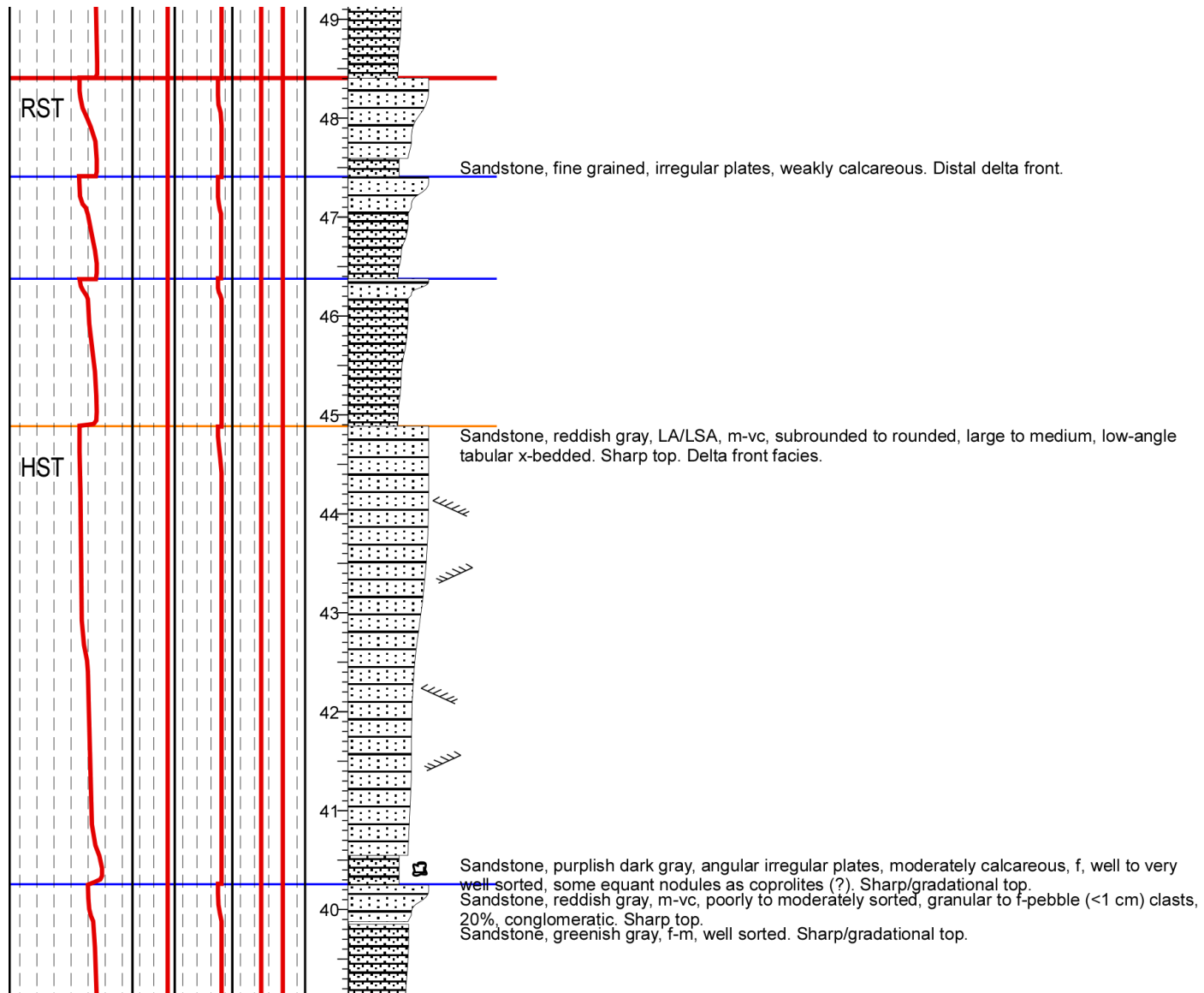


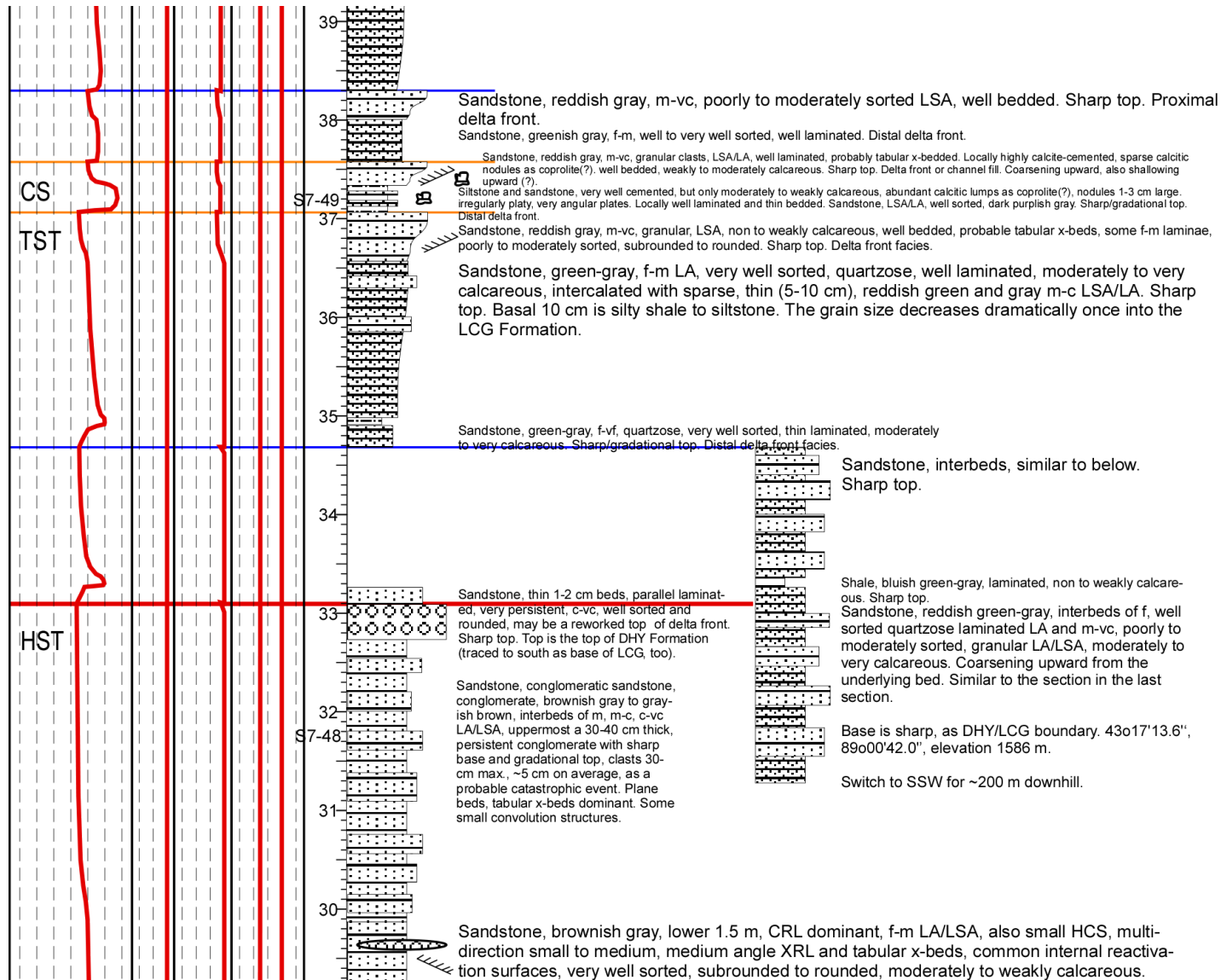


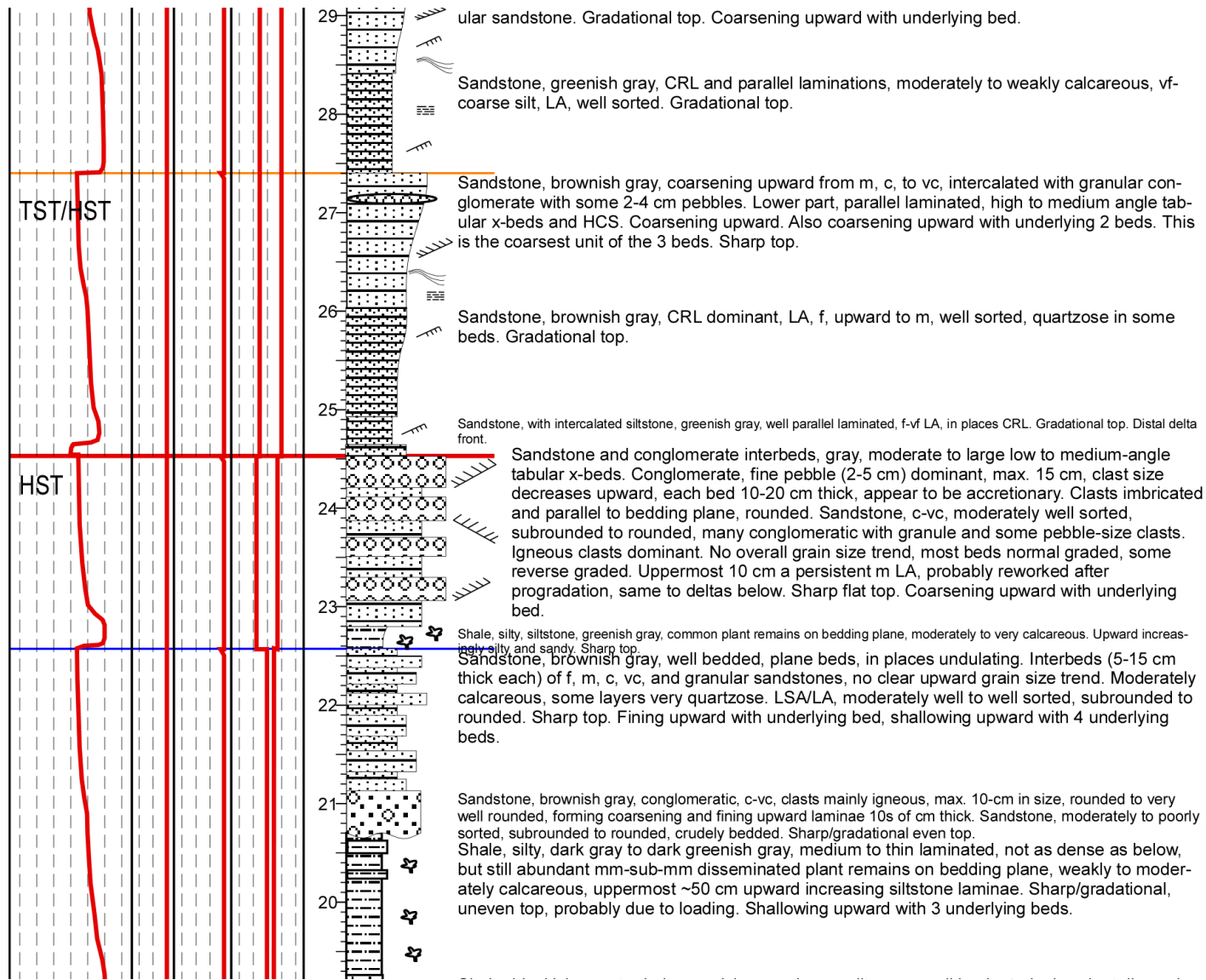


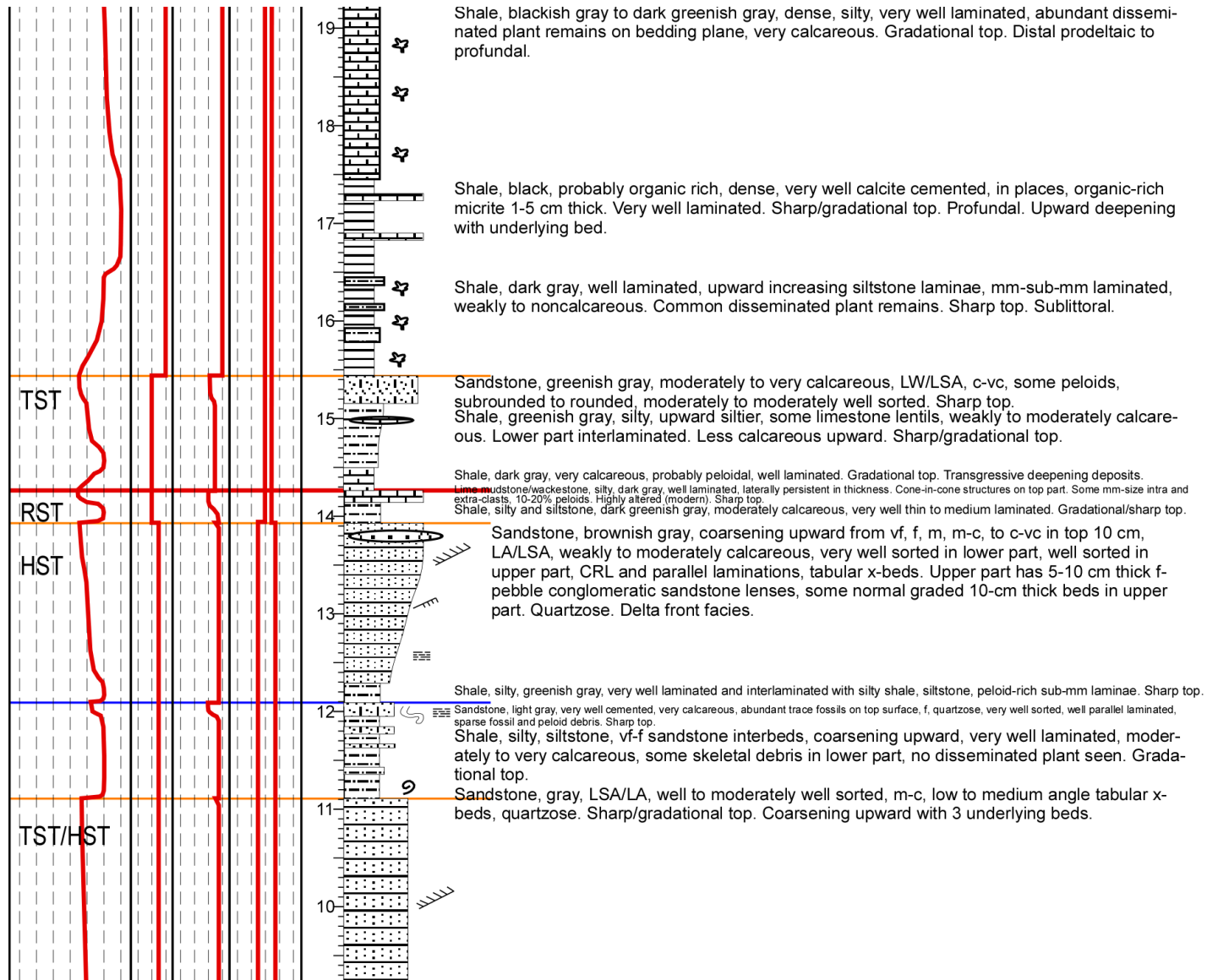


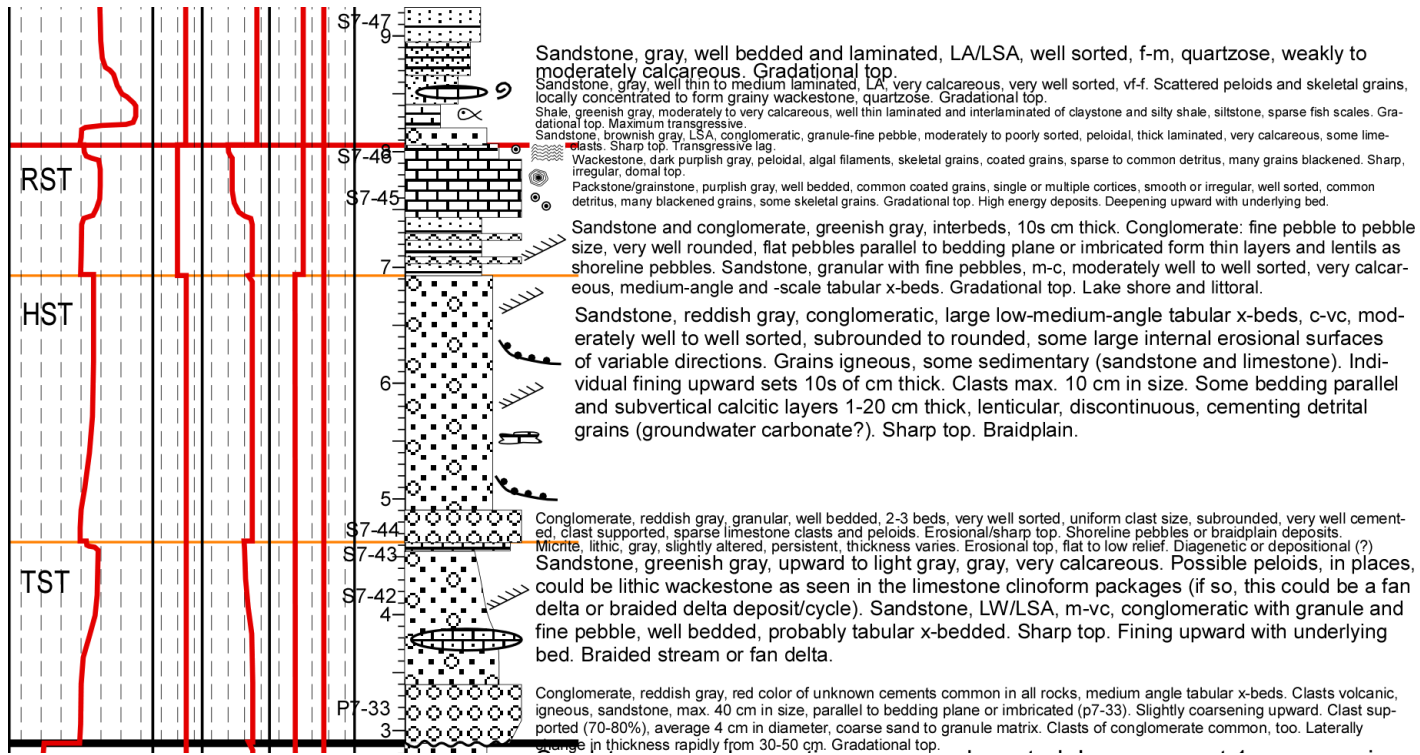




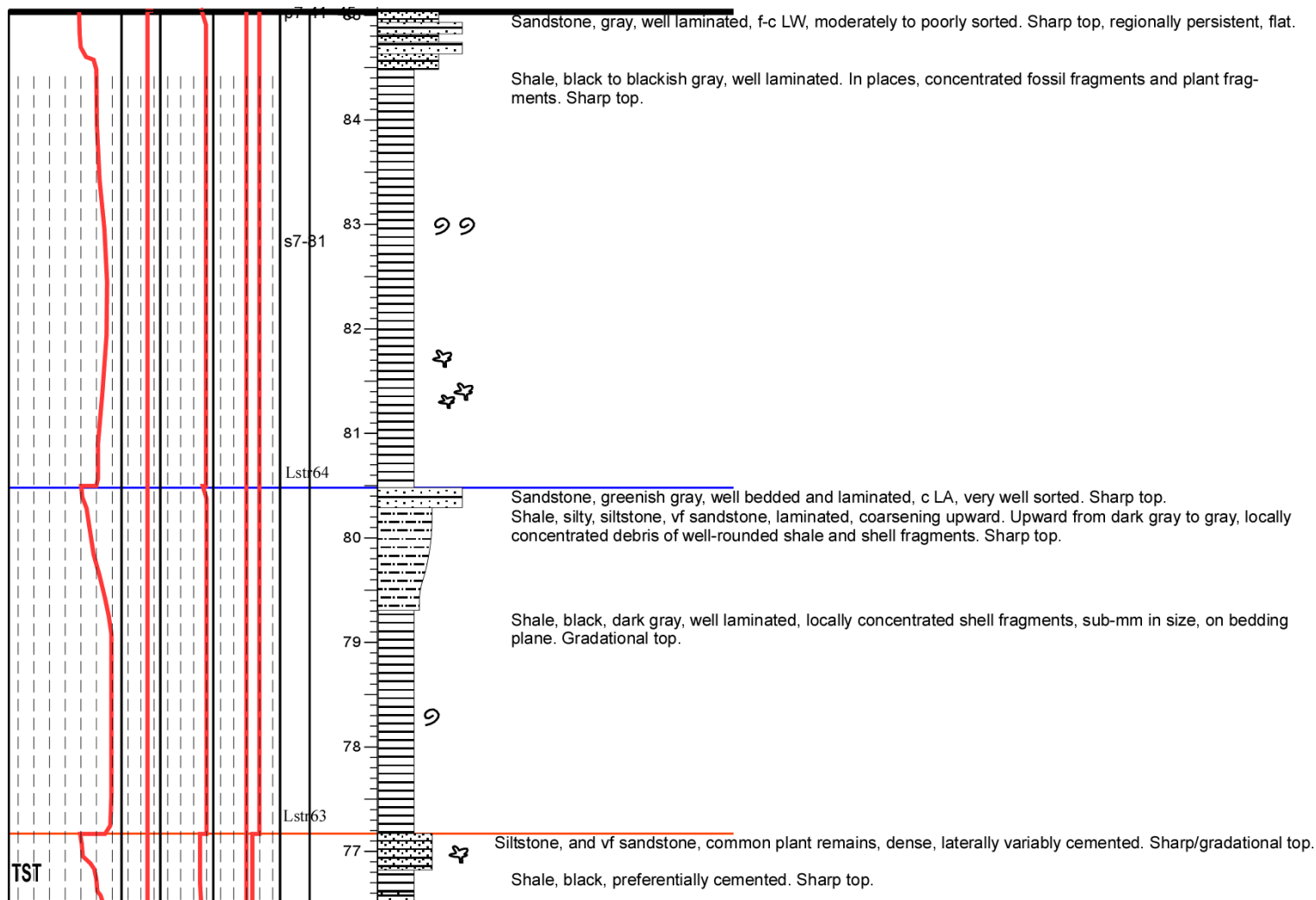


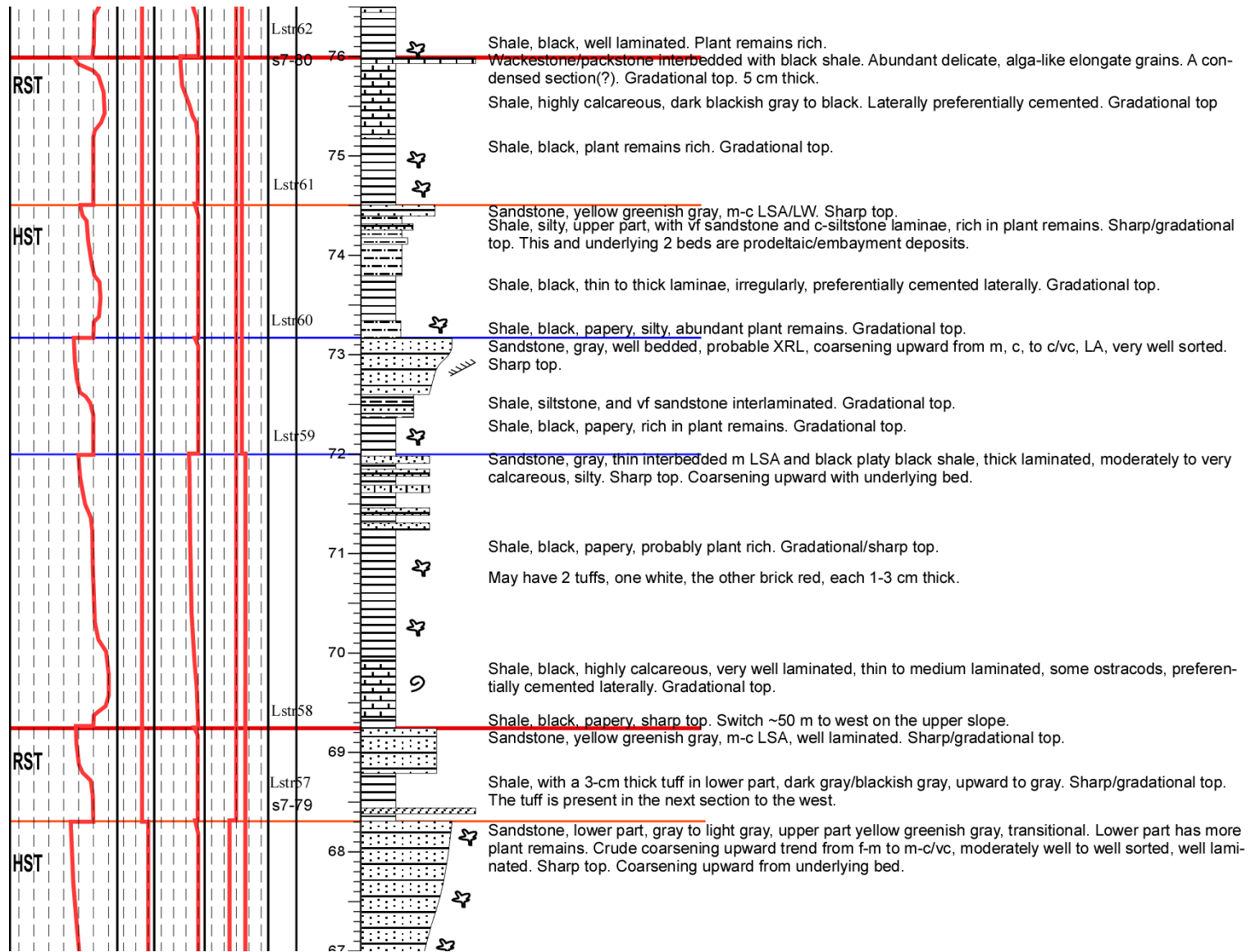


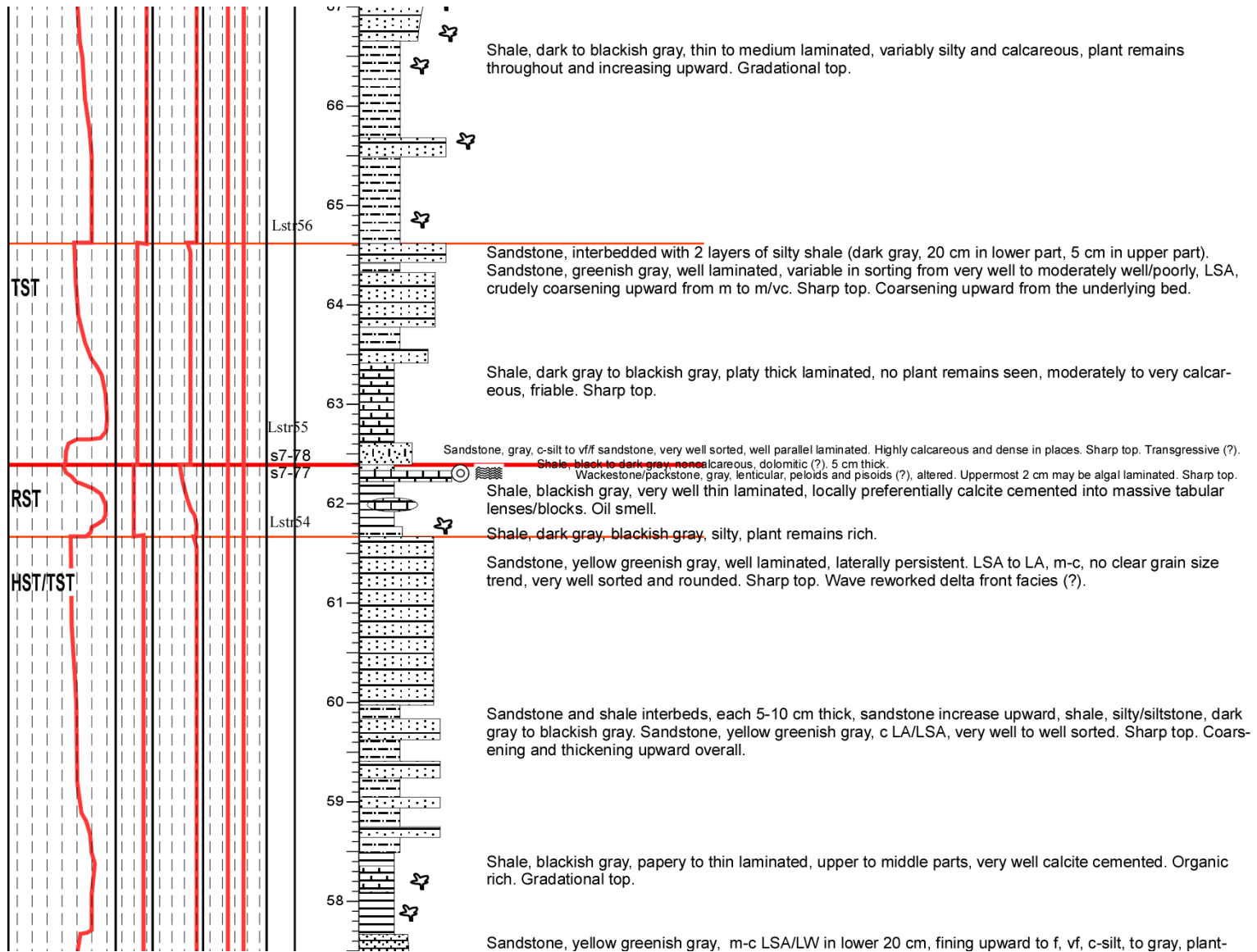


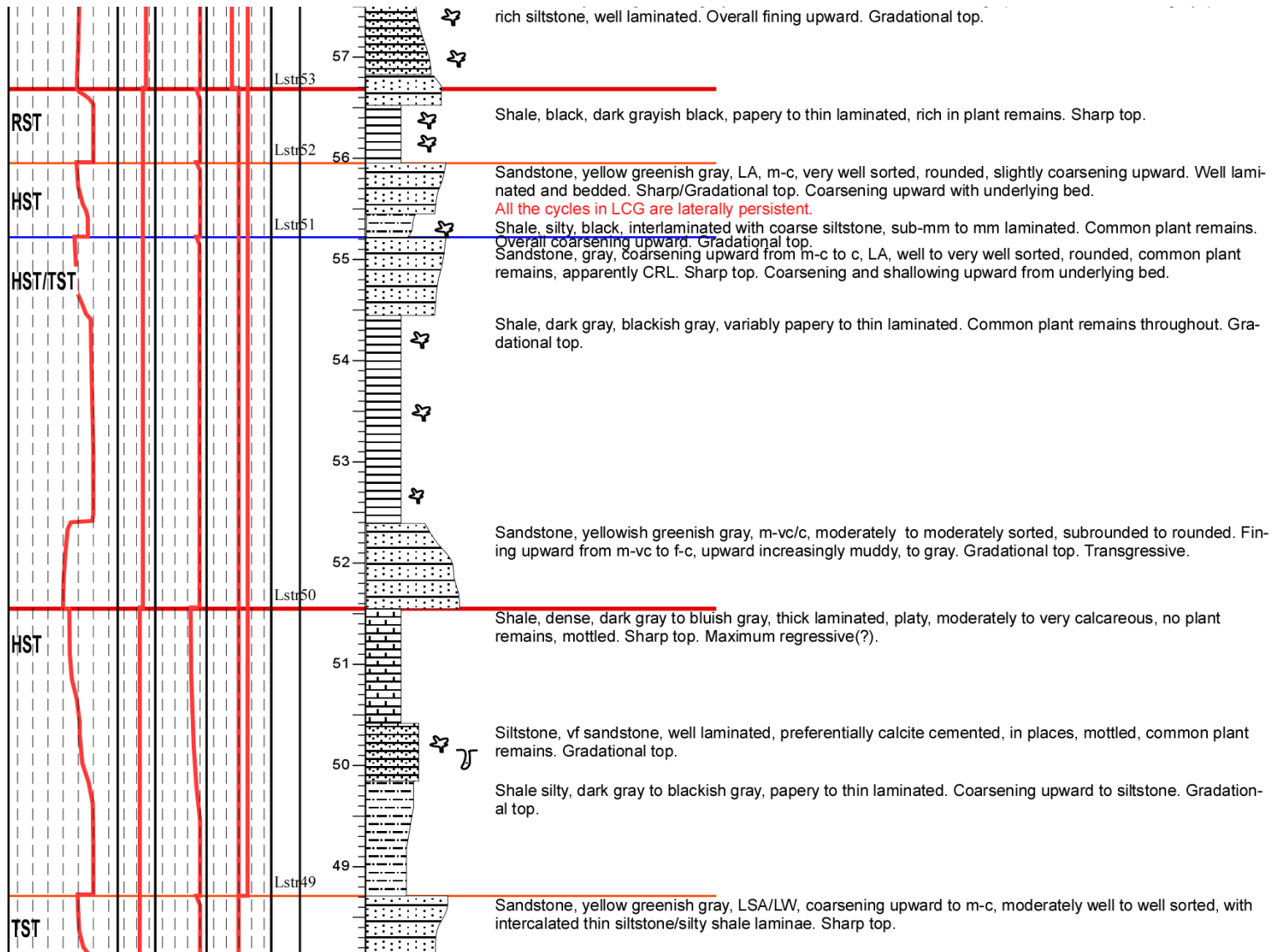


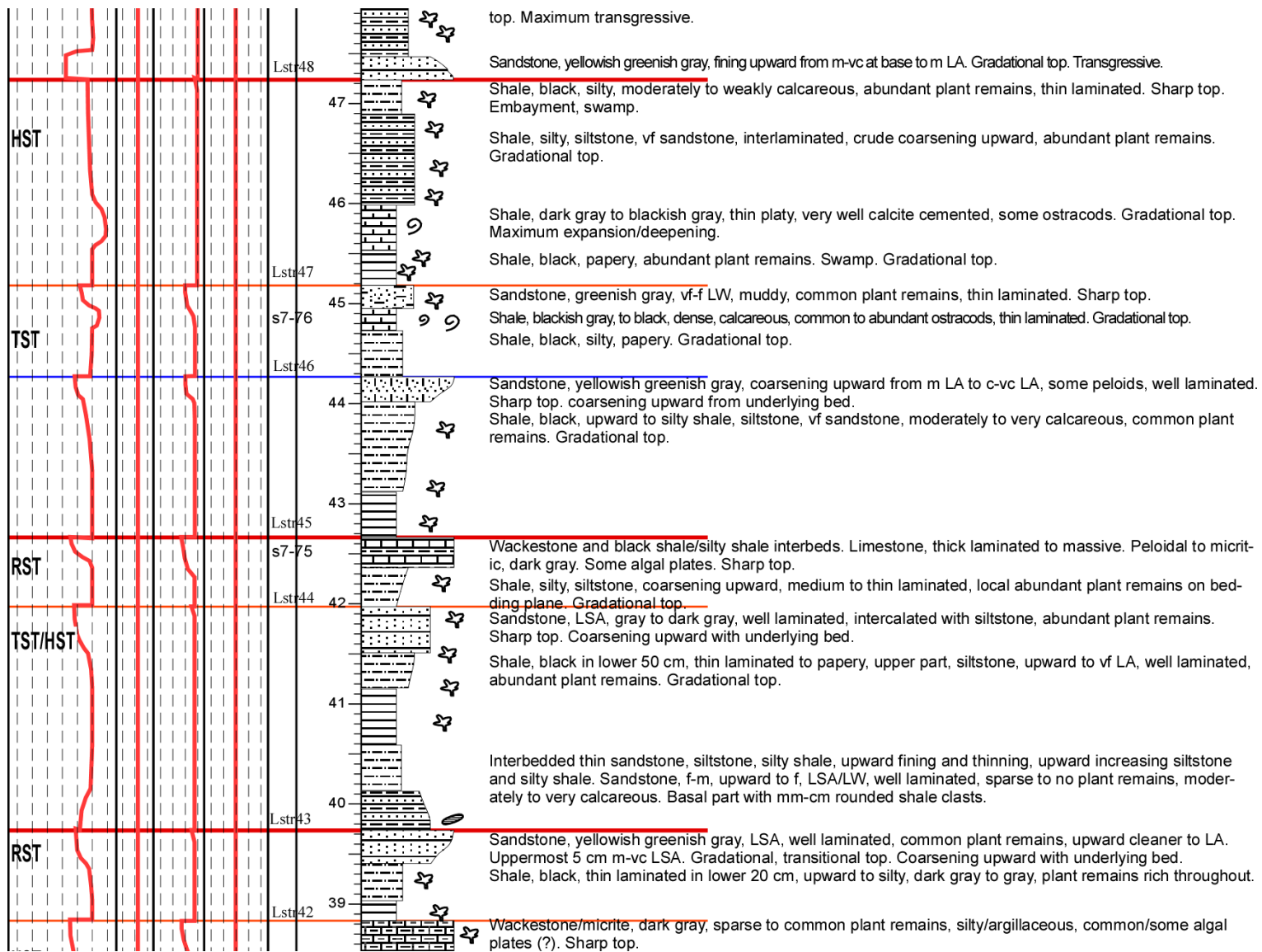
APPENDIX C
S TARLONG SECTION

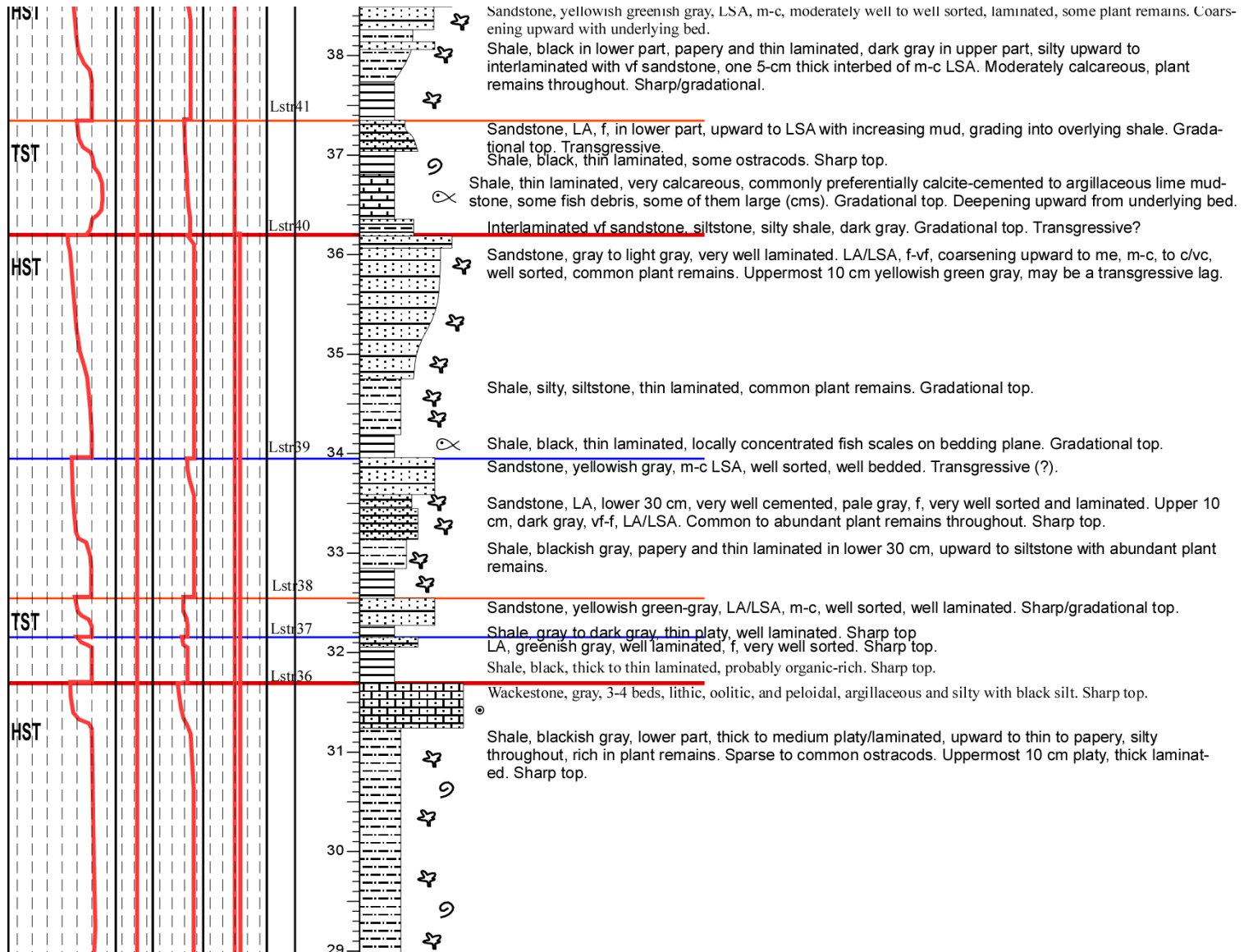


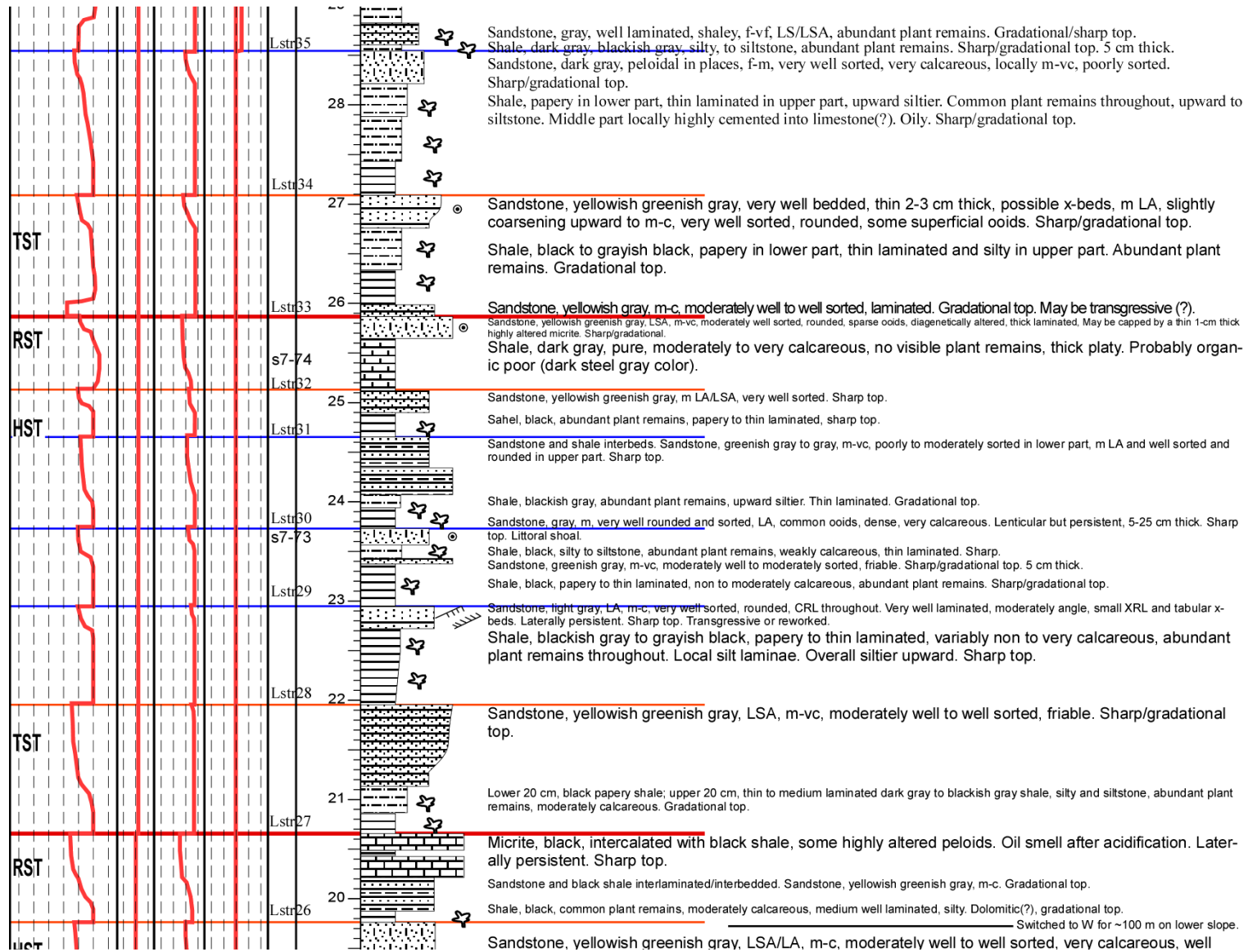


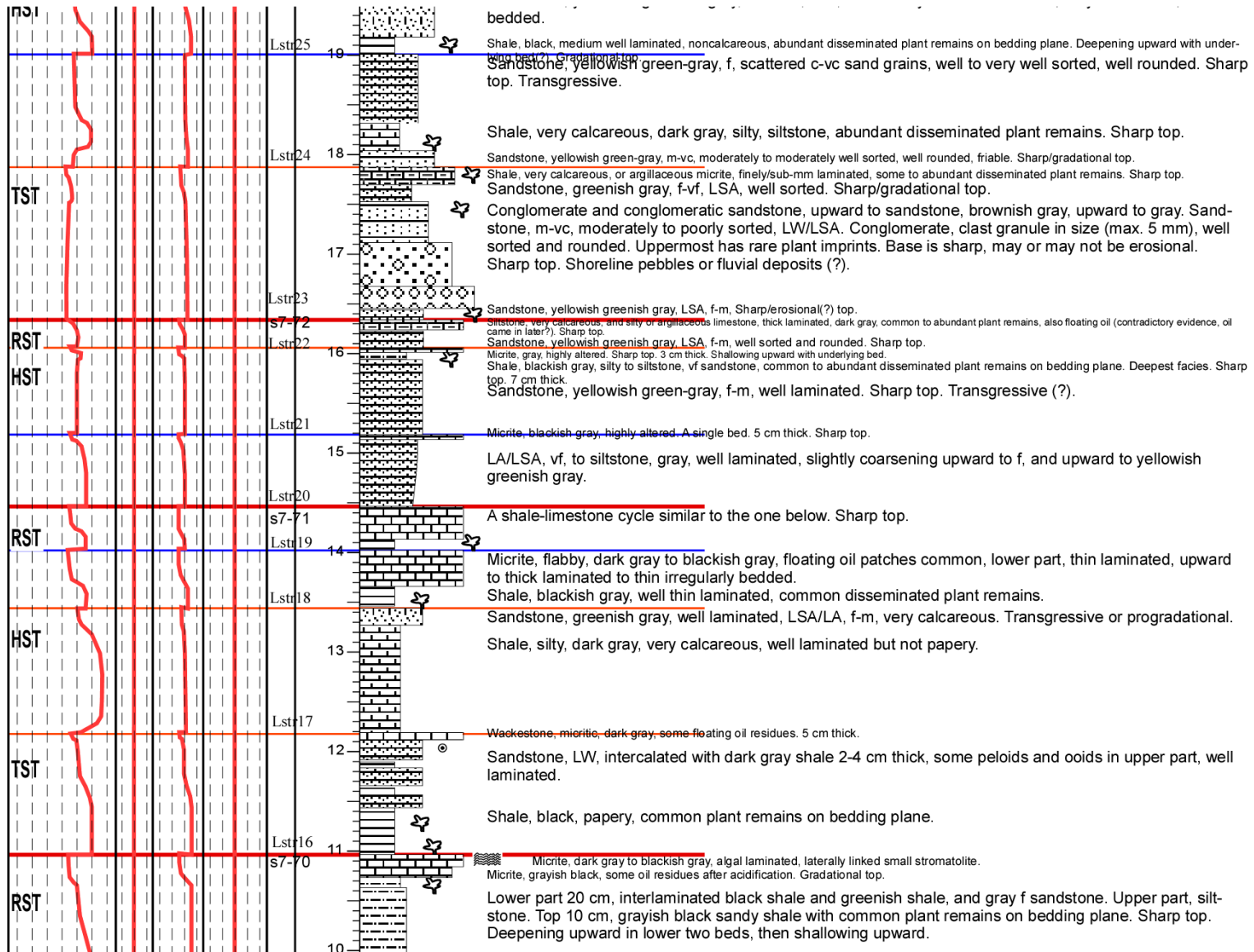


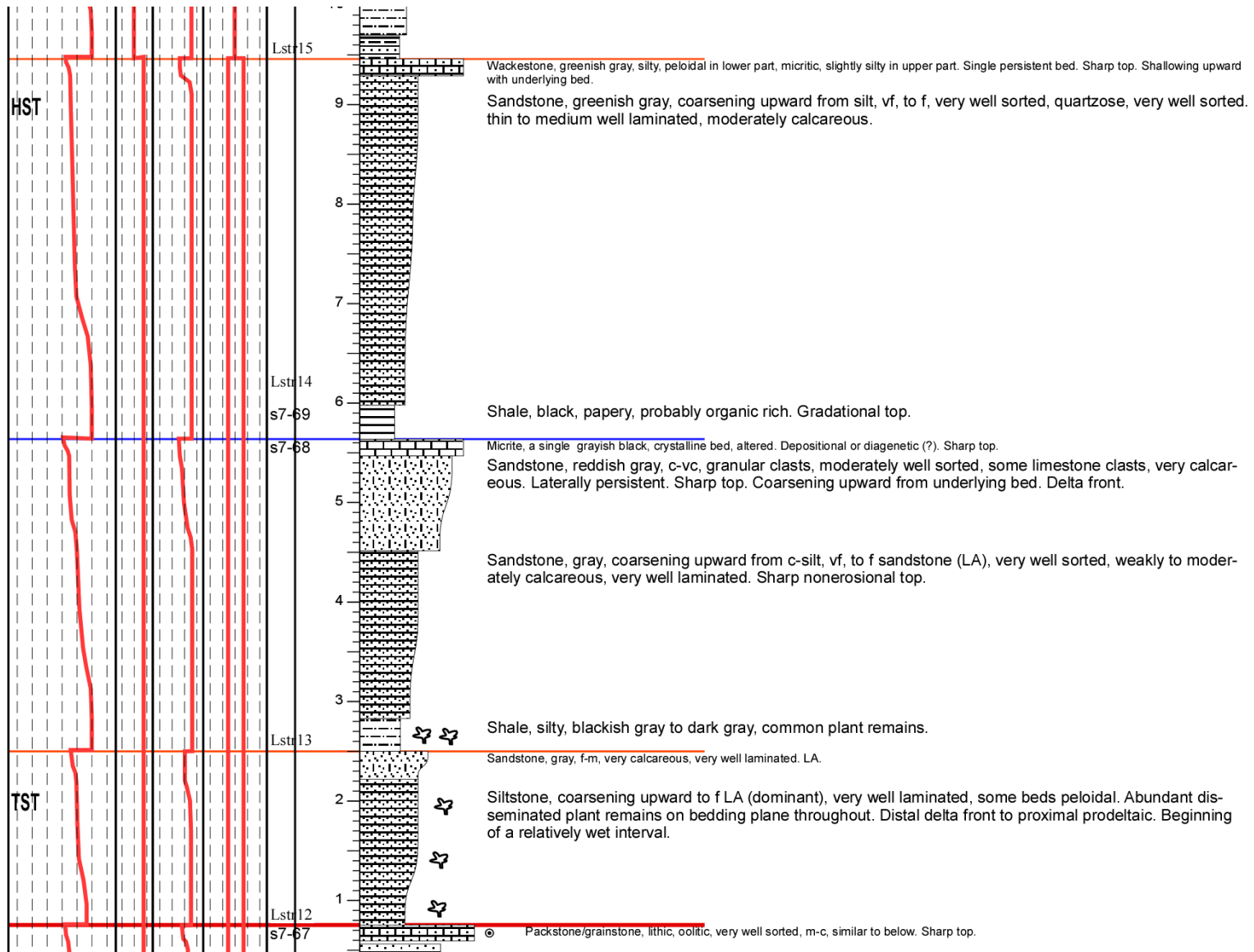


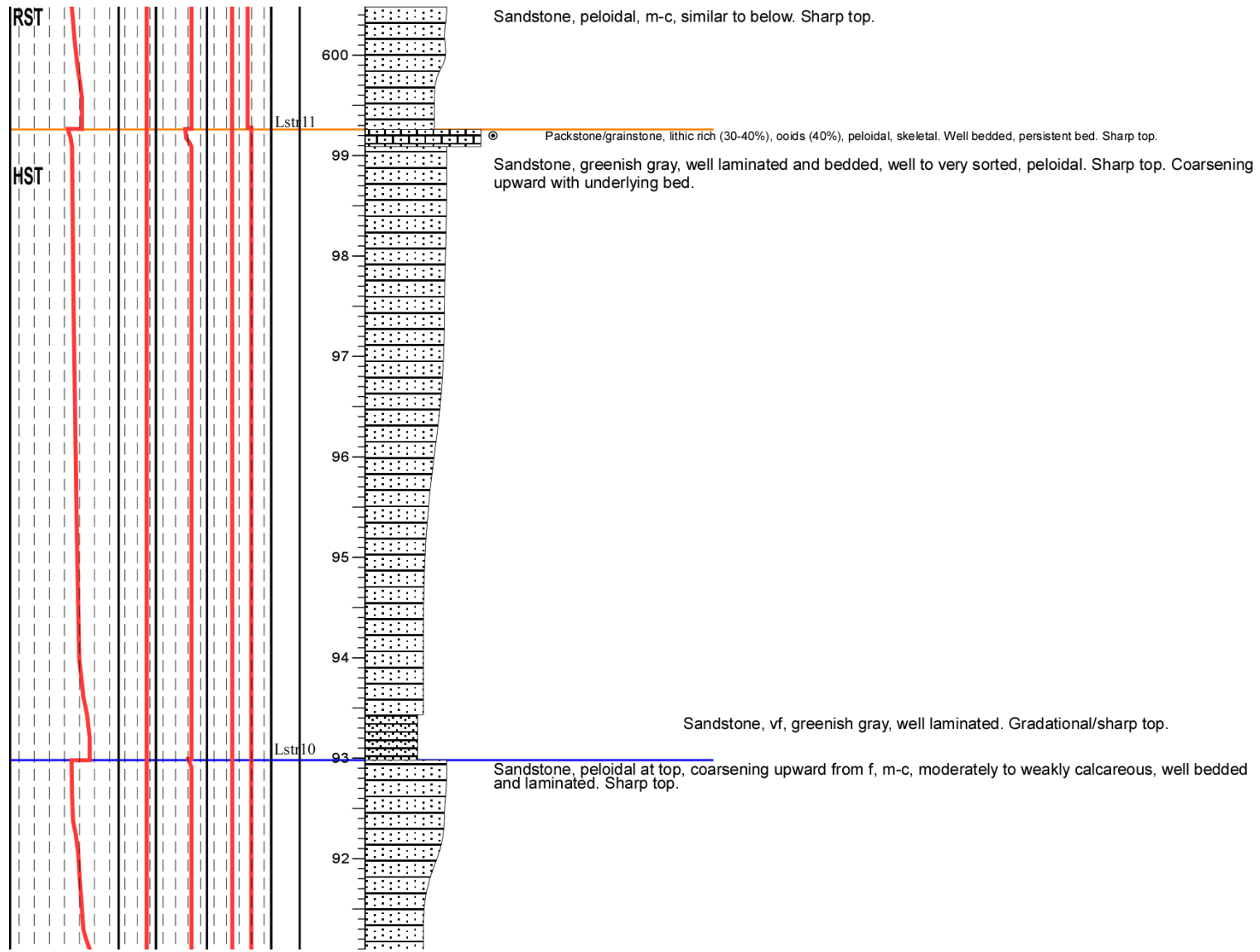


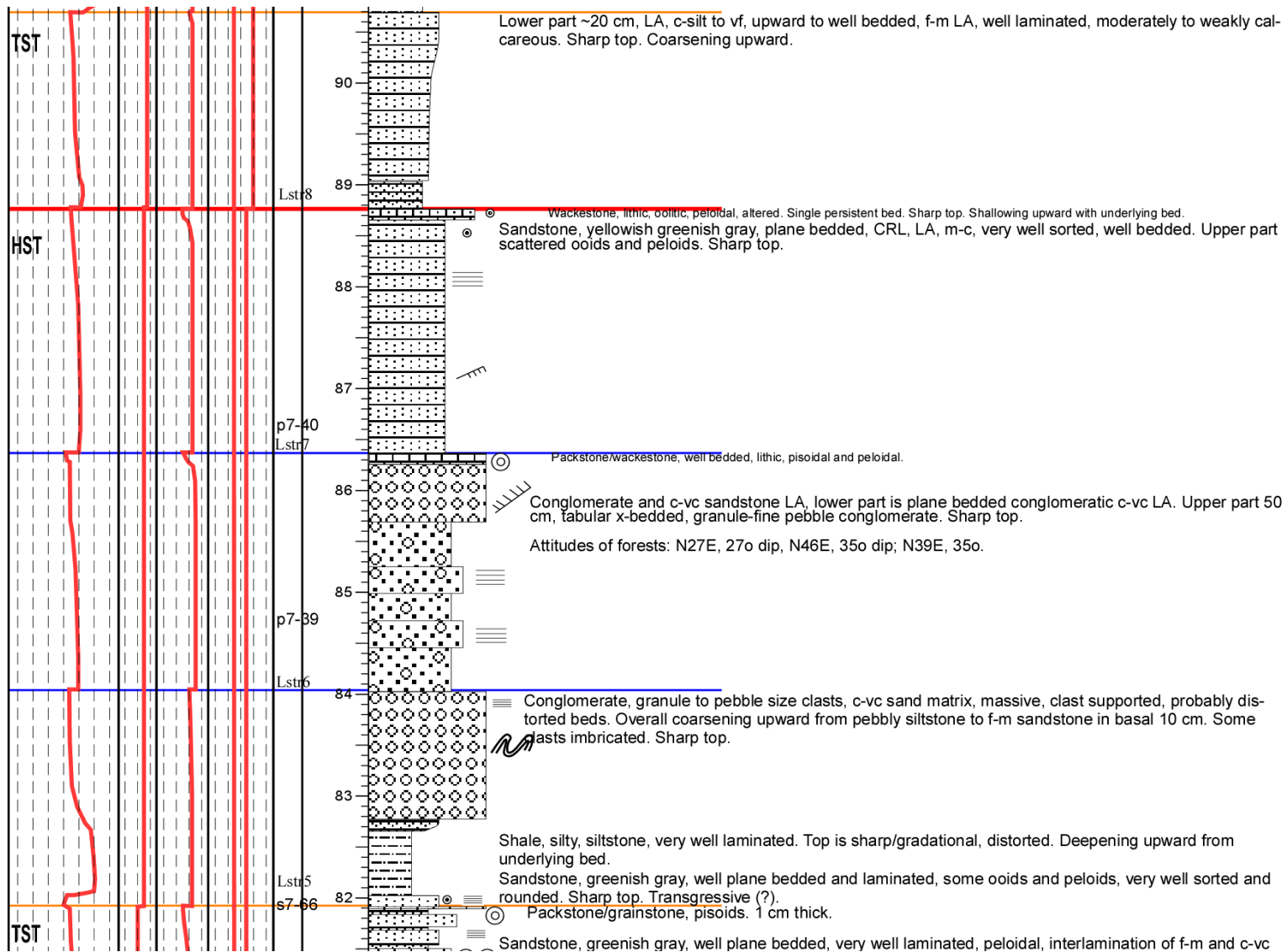


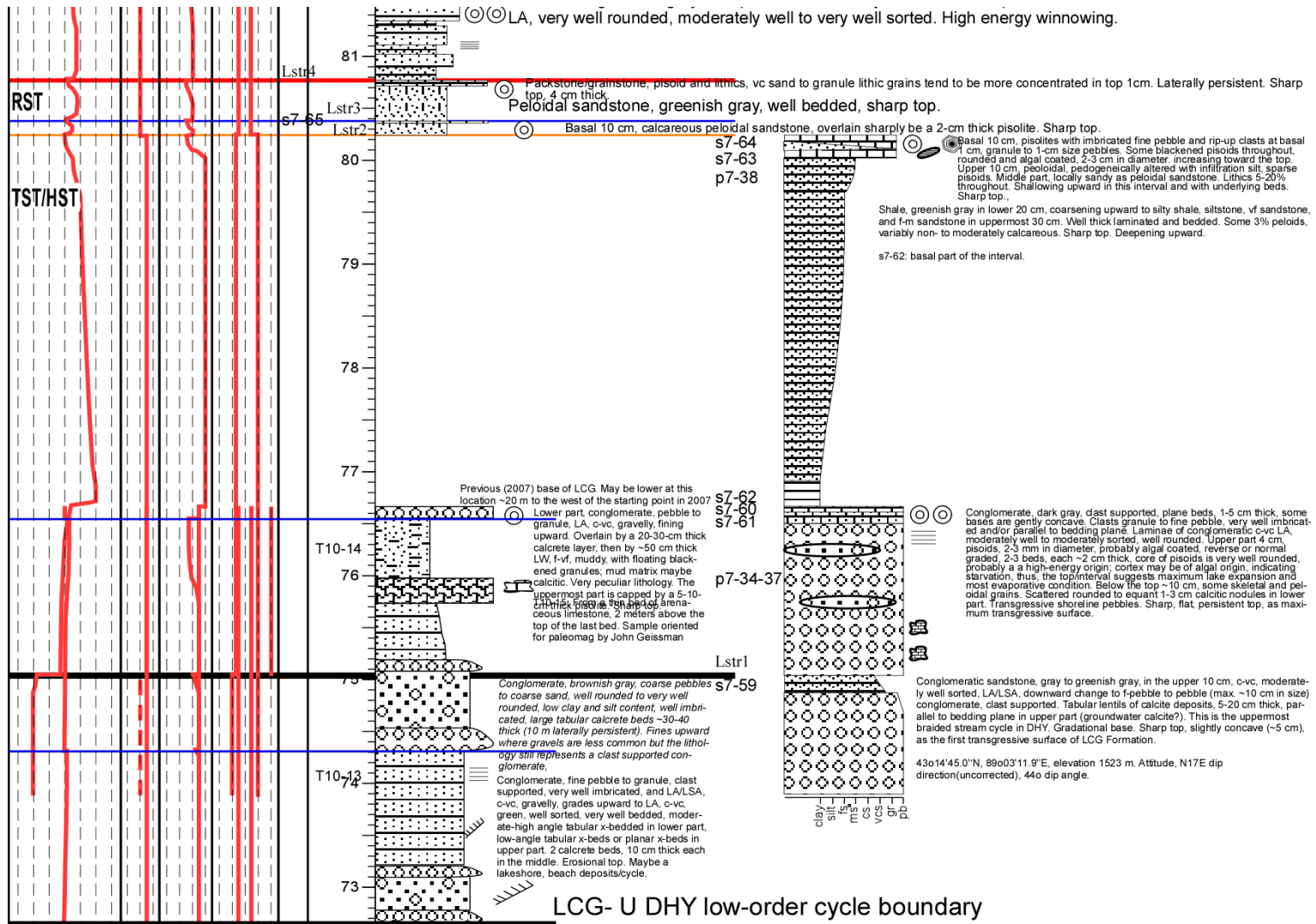




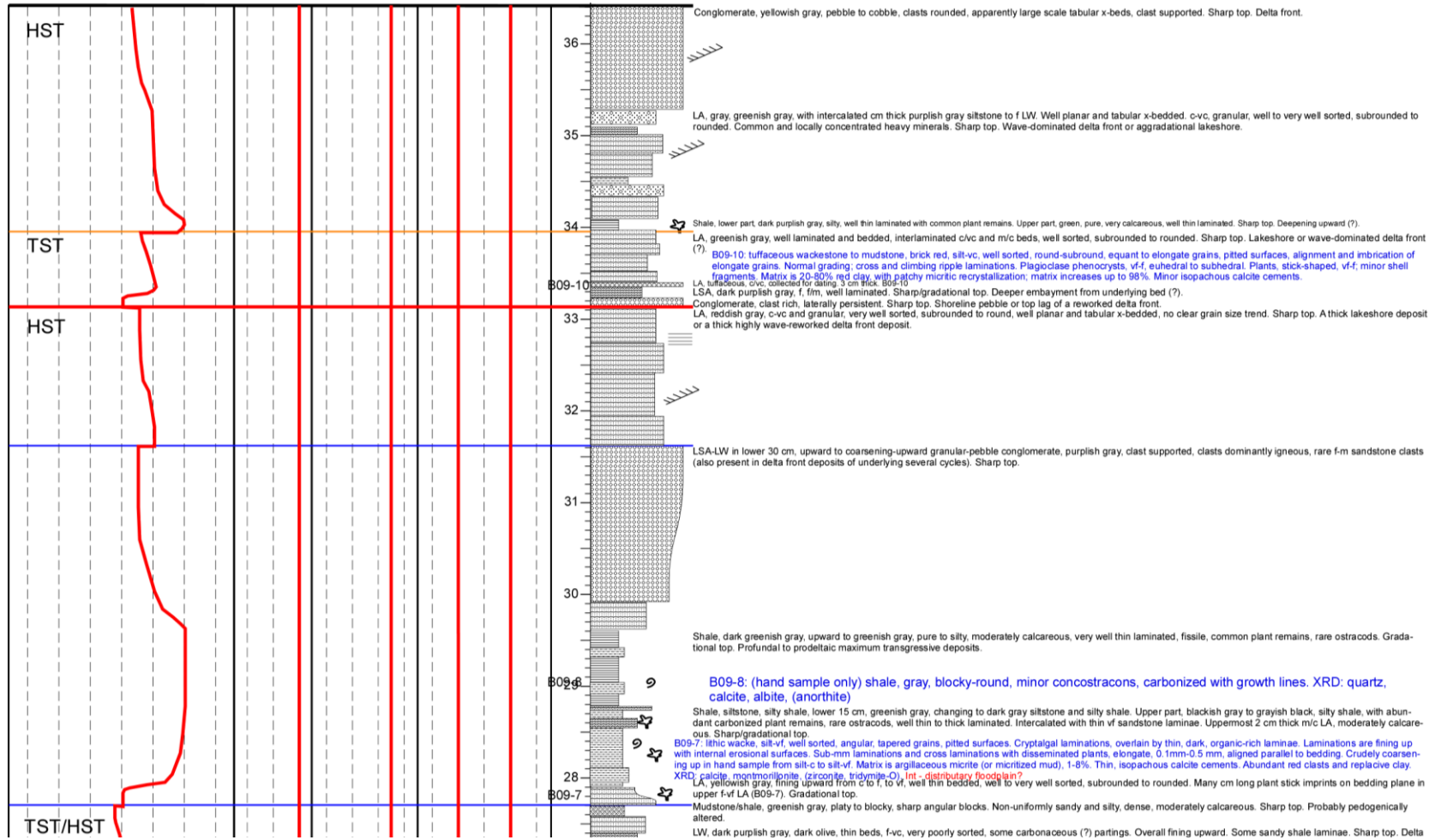


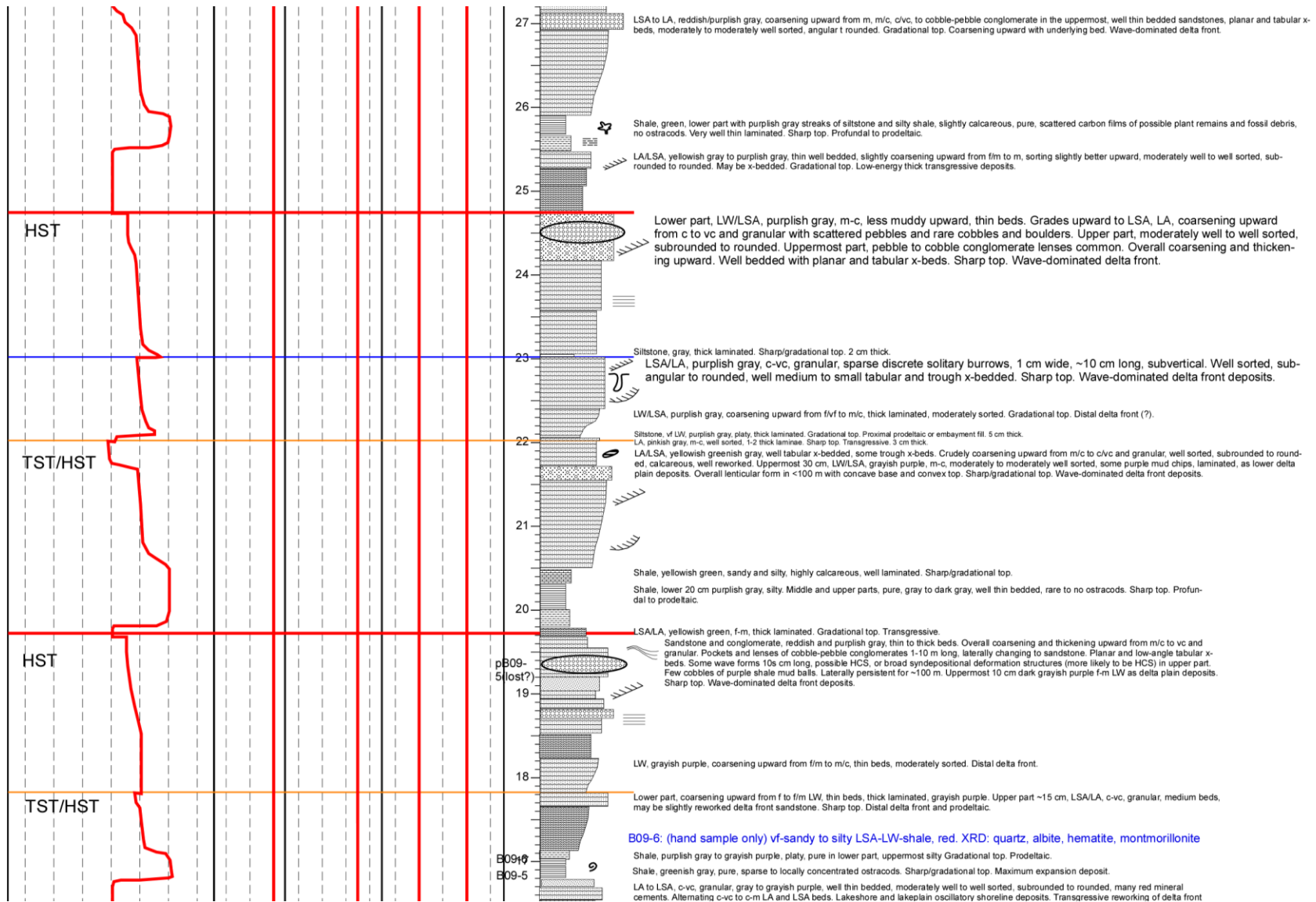


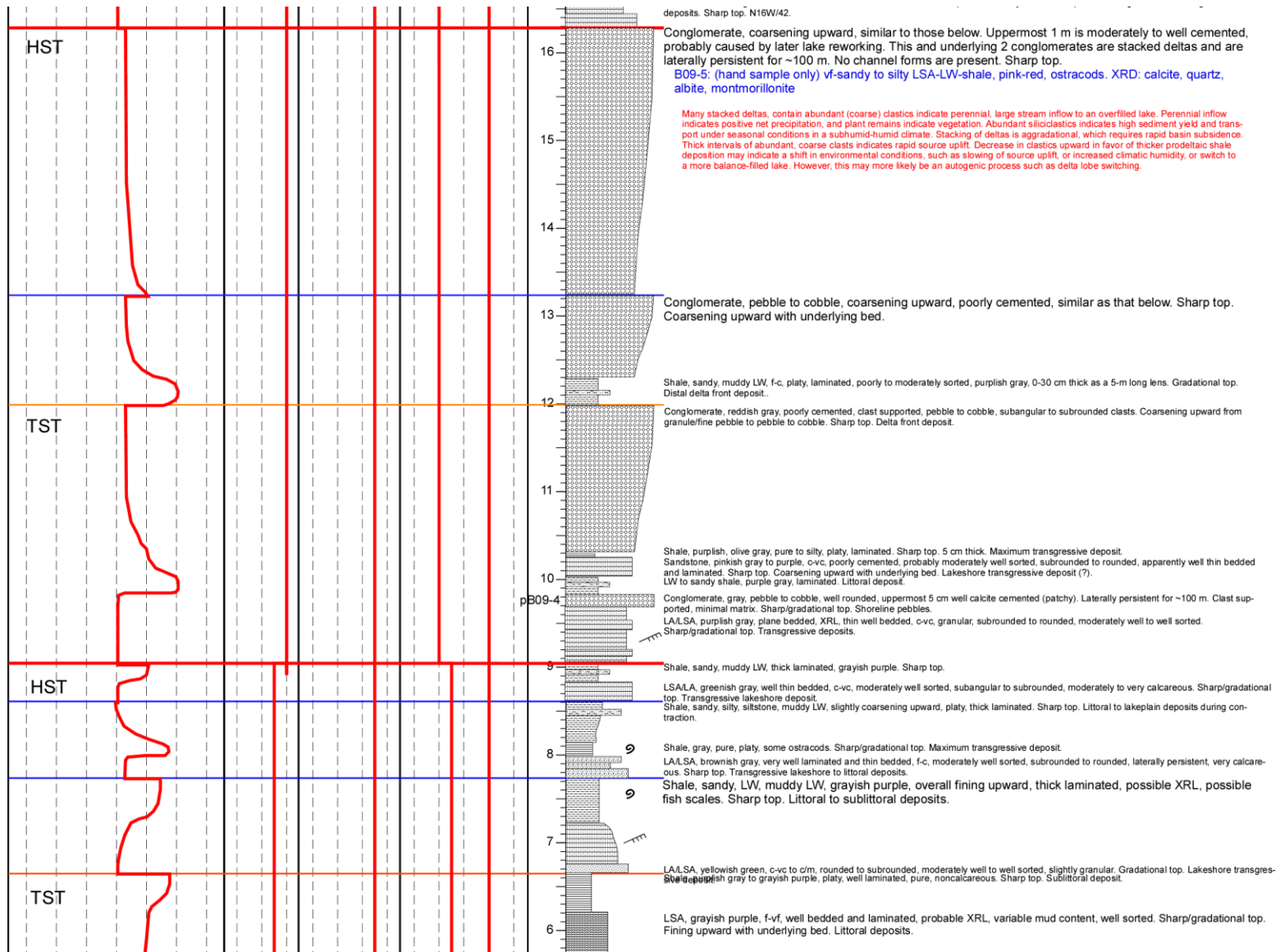


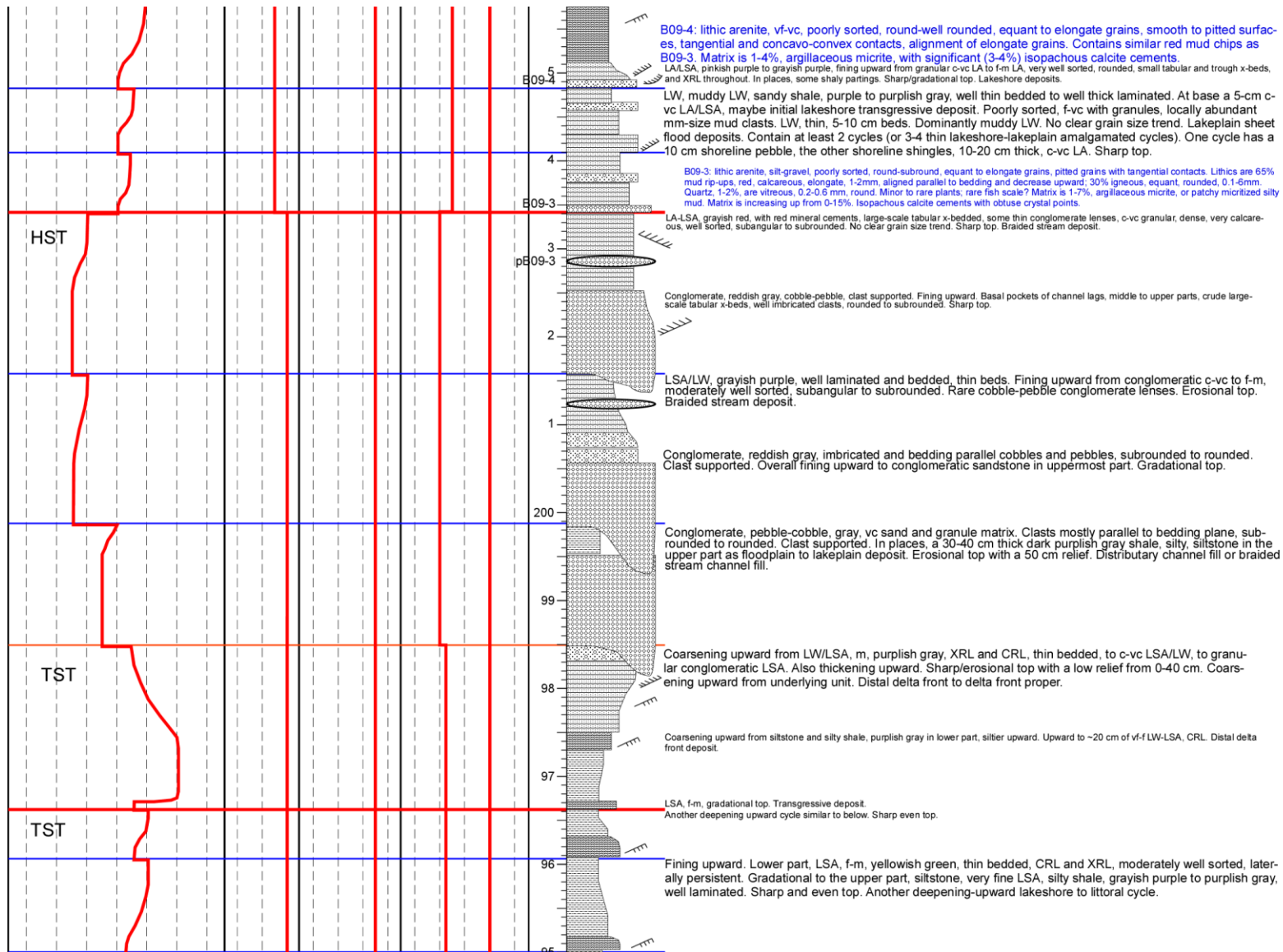


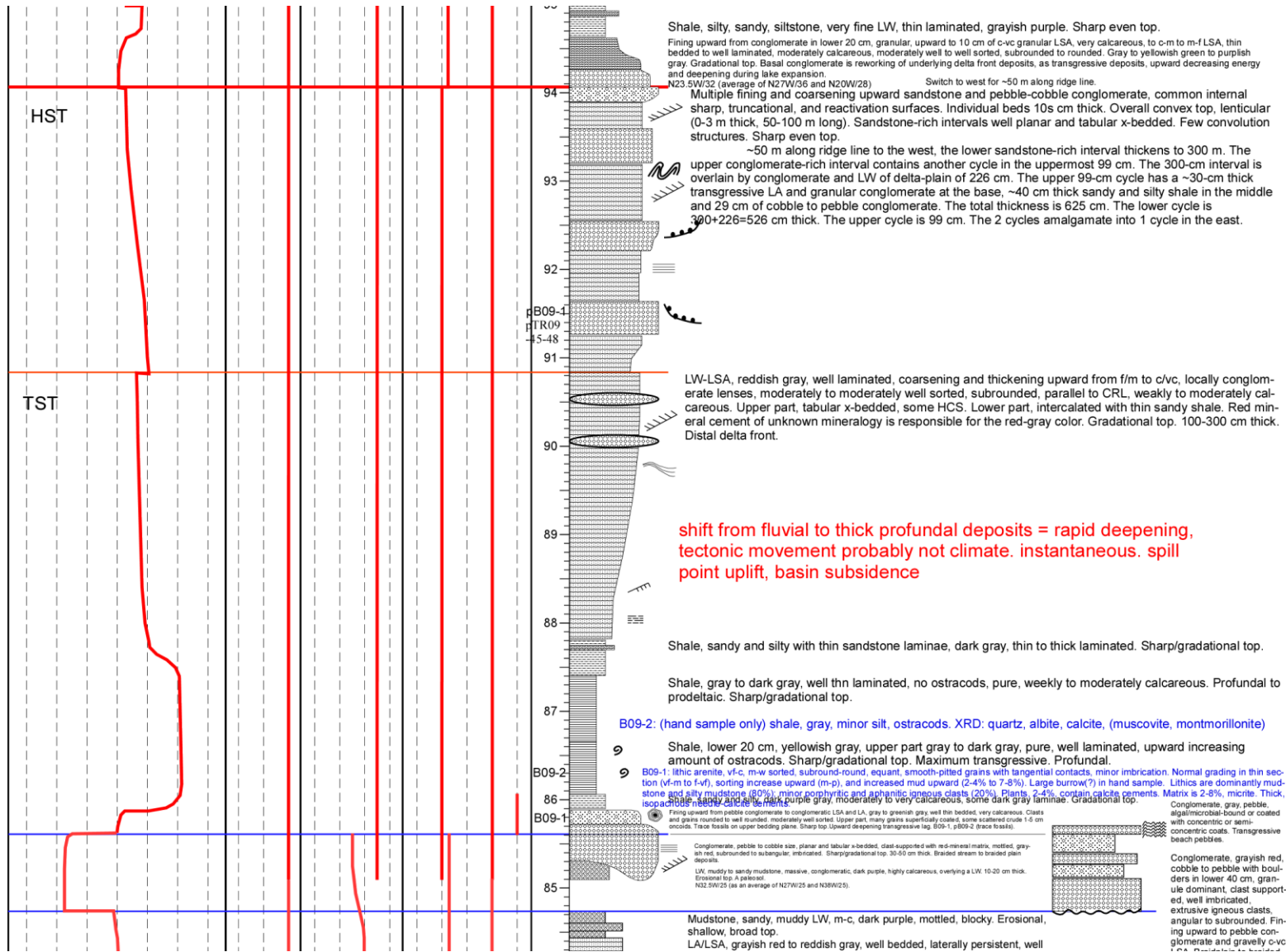
APPENDIX D
SW TARLONG SECTION





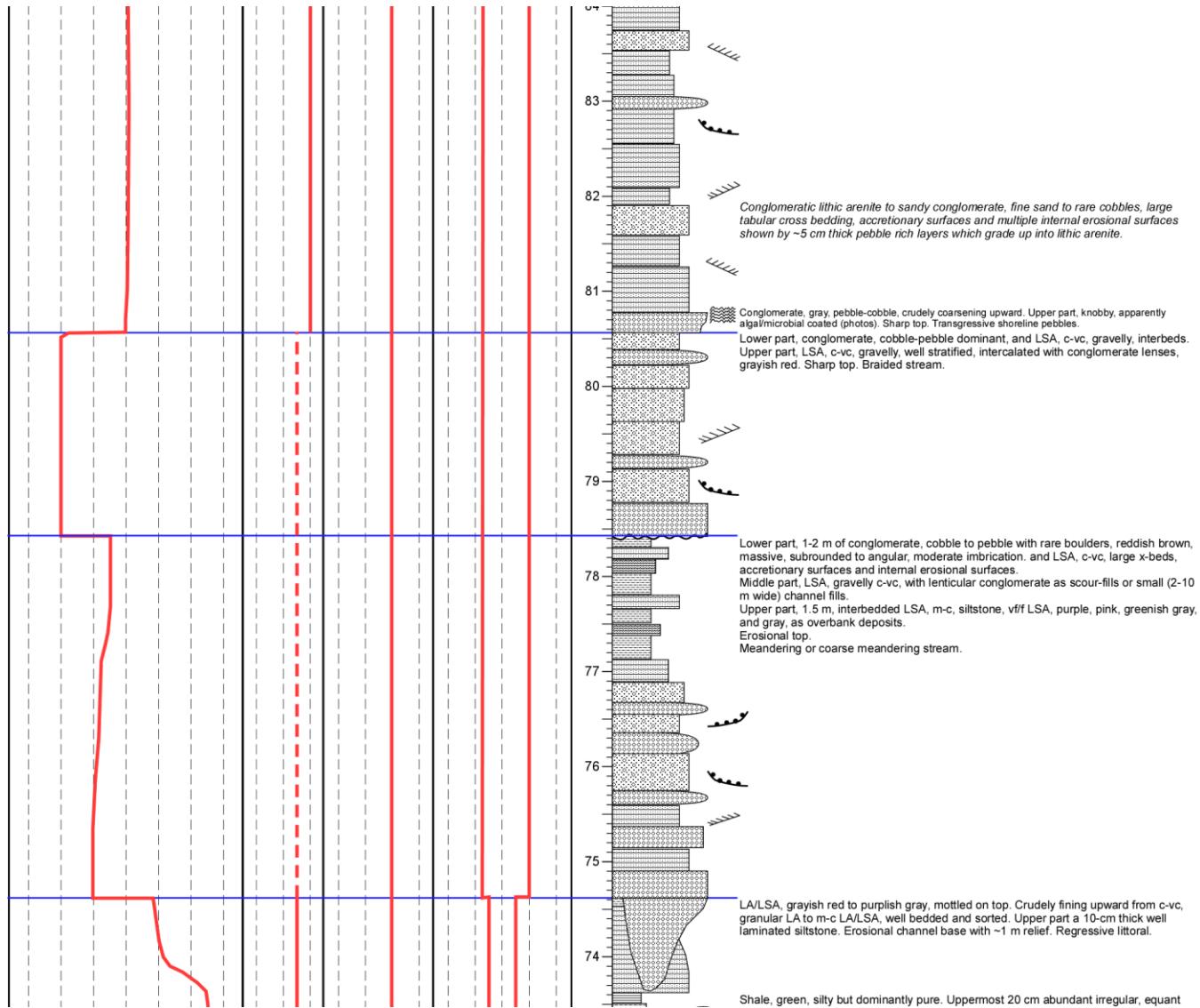


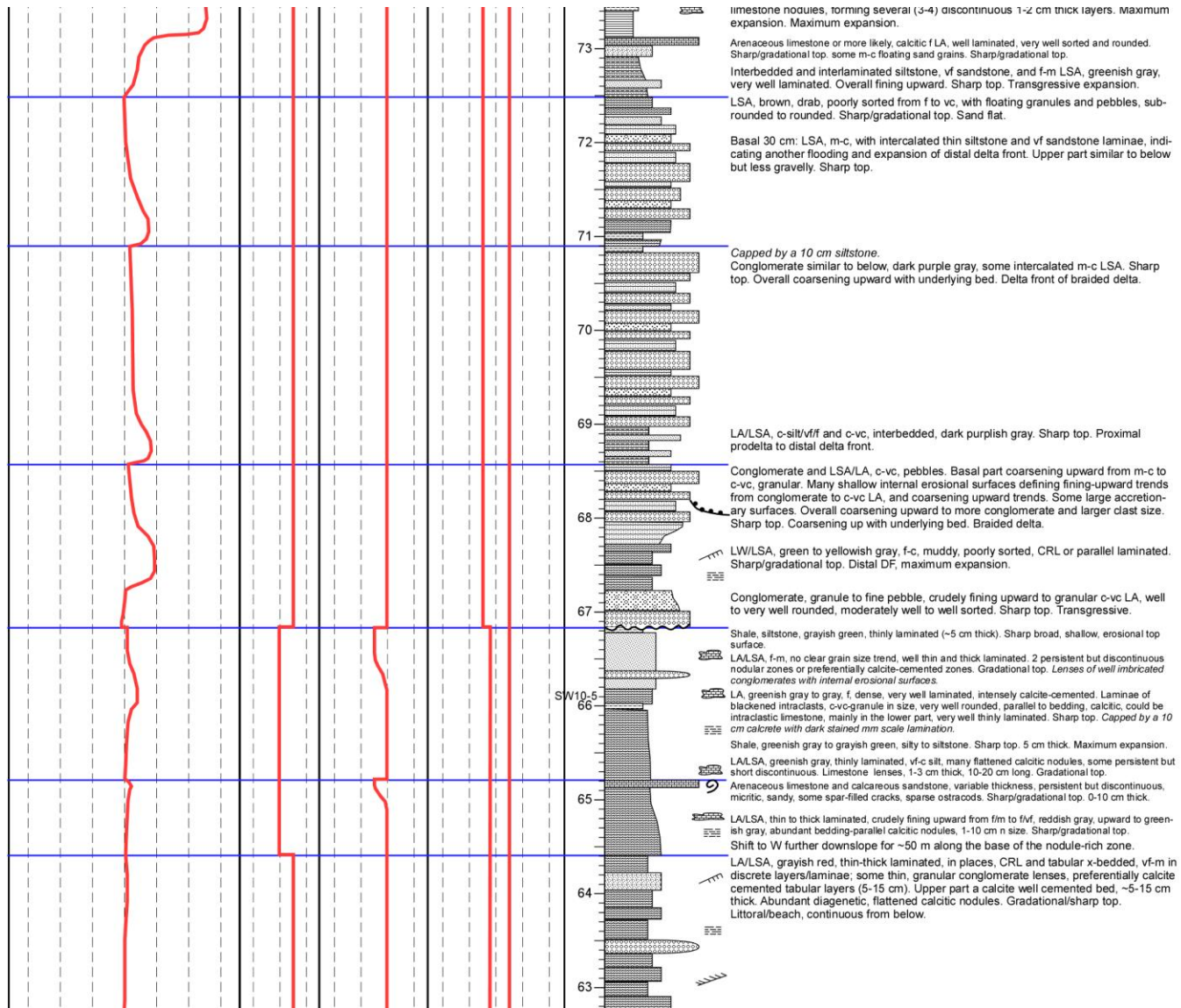


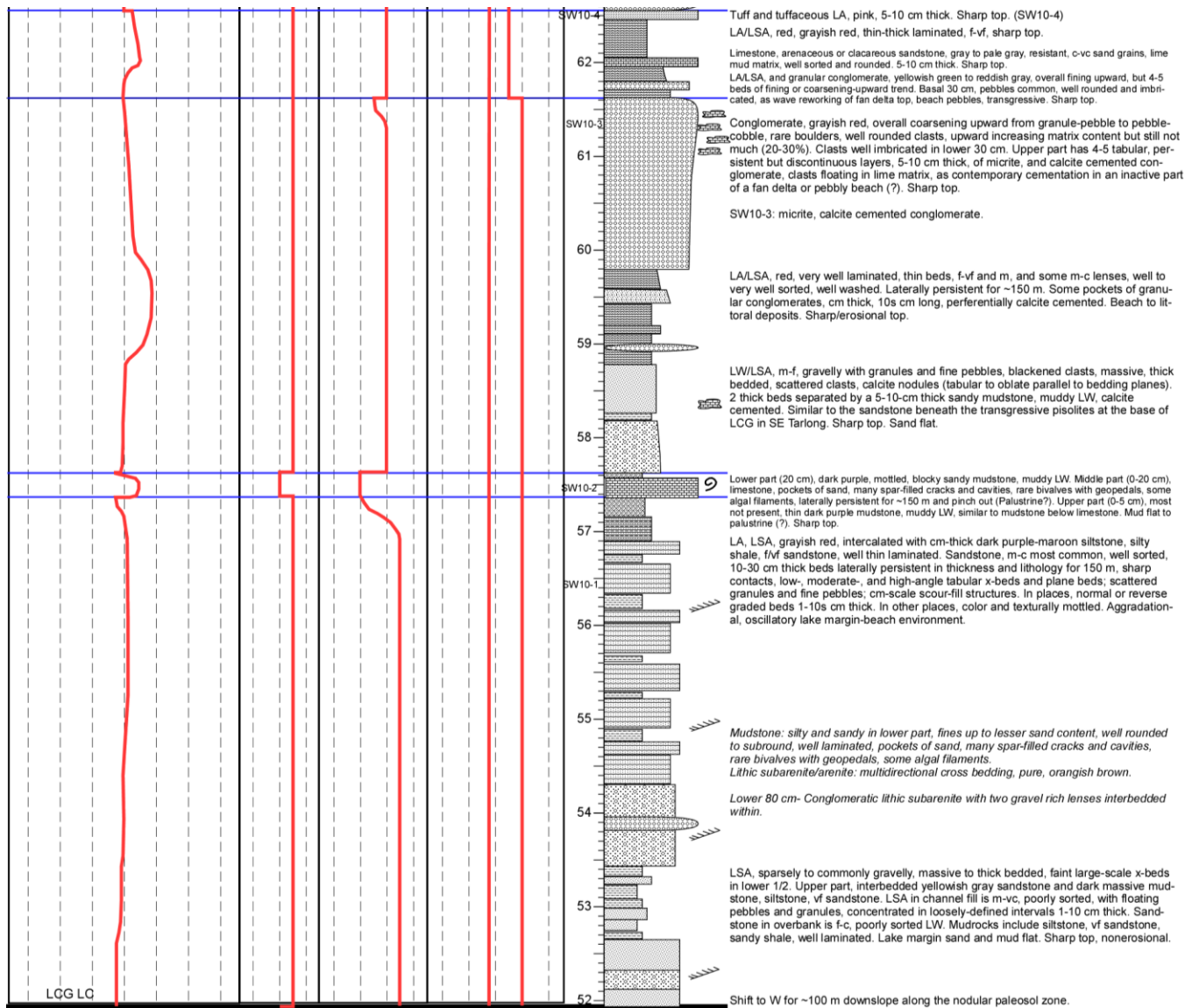


shift from fluvial to thick profundal deposits = rapid deepening, tectonic movement probably not climate. instantaneous. spill point uplift, basin subsidence

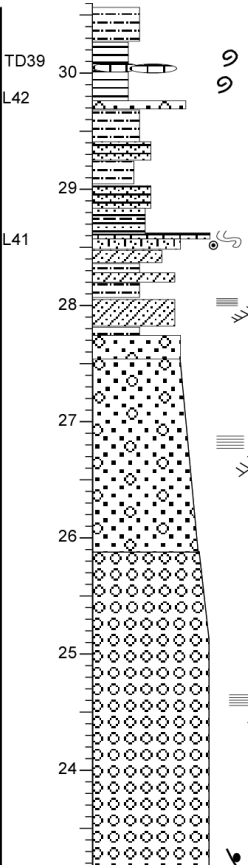
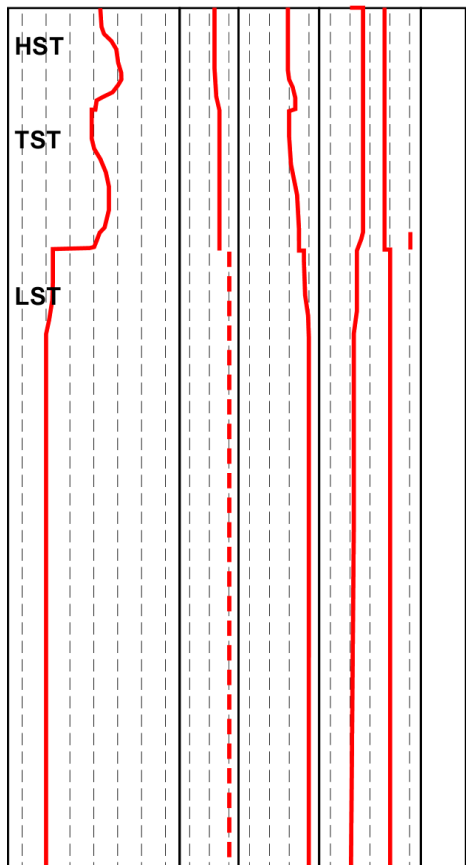
shifted down section for ~33 m).







APPENDIX E
TAODONGGOU SECTION



Shale, silty shale, well laminated, non or weakly calcareous. Lake plain mud flat, laterally change to interbedded c-m sandstone and shale, well bedded, persistent.

Shale, greenish gray, pure, basal 5 cm purple, non-calcareous to weakly calcareous, some ostracods. A lenticular/nodular micrite at top, green to gray, finely laminated, micritic, some microfossils (TD39).

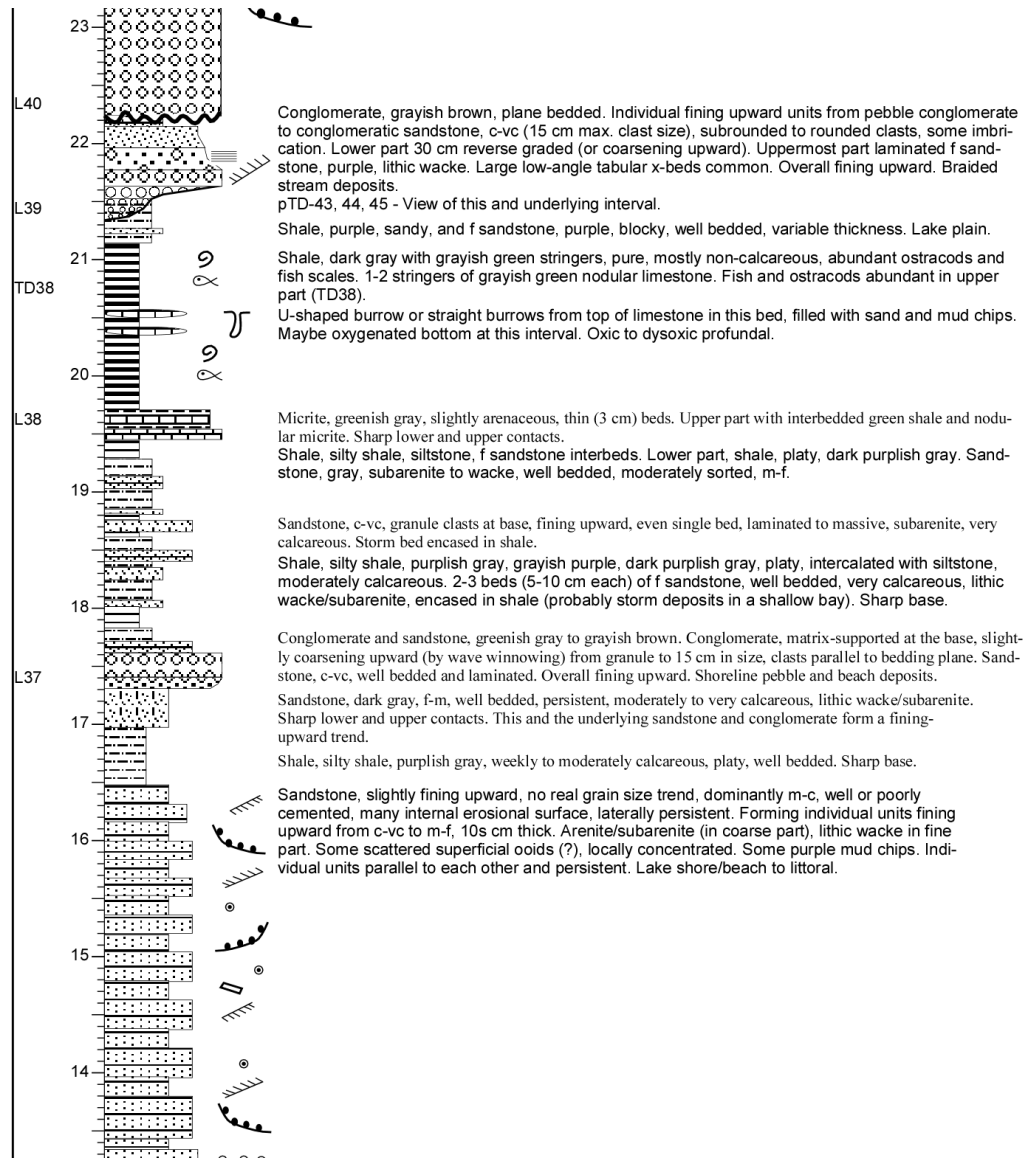
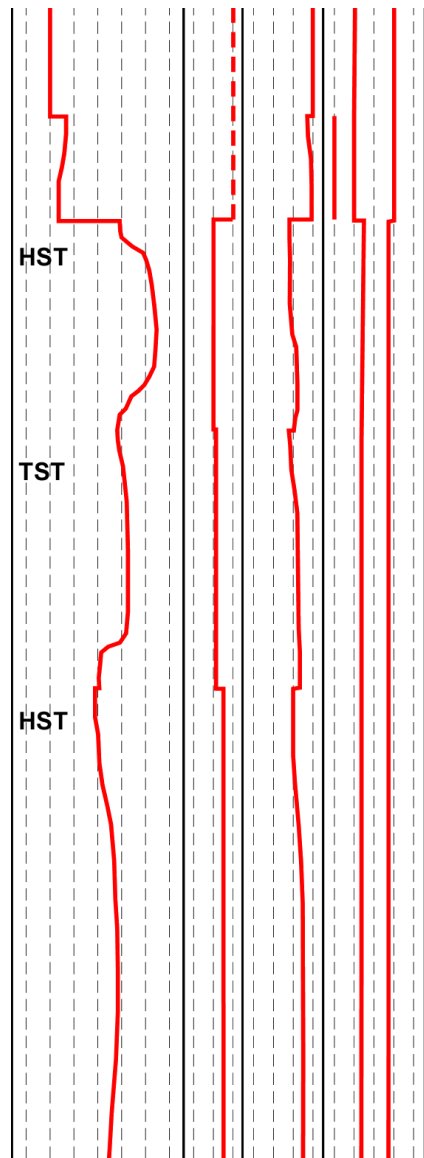
Sandstone, grayish brown, c-vc, well sorted, some pebbles. A single bed. Shoreline pebbles and sandstone.

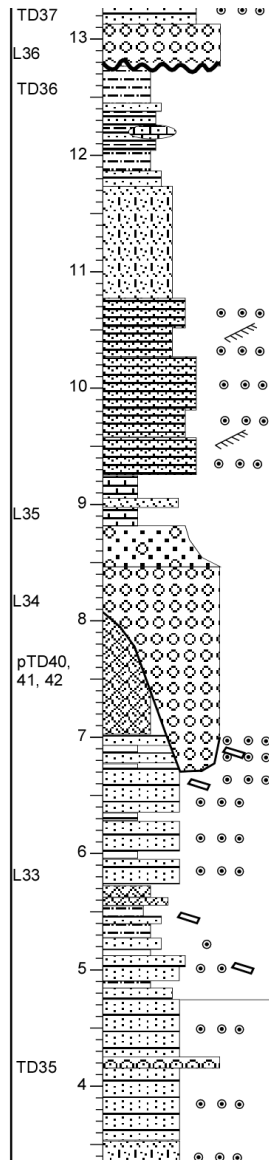
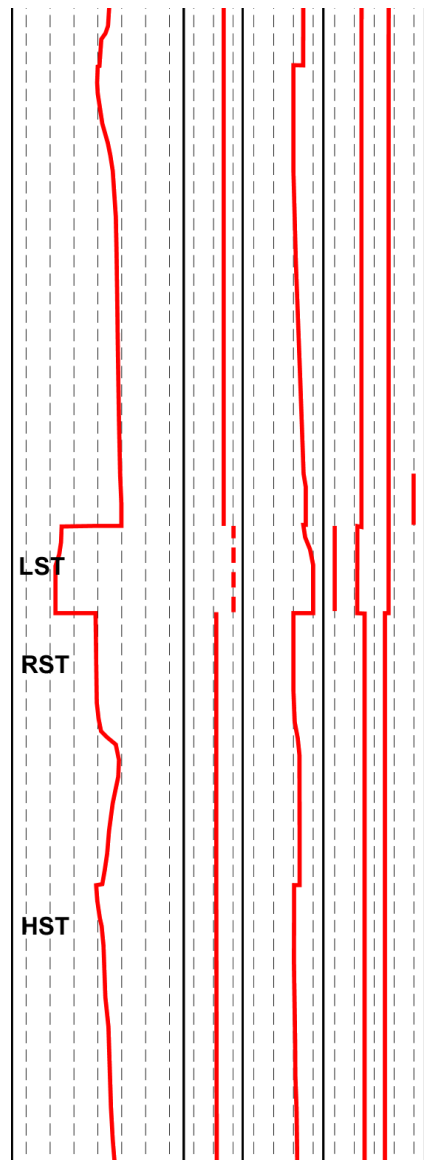
Sandstone, silty shale, siltstone, grayish purple, well bedded. Sandstone, f, subarenite to lithic wacke. Lake plain.

Sandstone, brownish gray, c-vc, with granule clasts, single persistent bed, very calcareous, well cemented and laminated. Uppermost ~5 cm calcitic, maybe arenaceous limestone. Some bedding plane trace fossils. Scattered superficial ooids. Sharp upper contact. Lake shore and lake plain.

Sandstone, siltstone, sandy shale interbeds, purple. Sandstone dominant, f-m, well bedded, planar, tabular x-beds, local x-lamination. Overall fining upward. Sharp conformable lower contact, sharp upper contact. Upper braided stream deposits.

Conglomerate and intercalated conglomeratic sandstone, grayish brown, Sandstone, c-vc. Mostly poorly cemented, clasts 30 cm (max.), clast composition variable. Sandstone is x-bedded. Overall fining upward. Lower braided stream.





Conglomerate, grayish brown, granule to fine pebble clasts, rounded, crude fining or coarsening upward trends, poorly cemented, volcanic, shale, and marine limestone clasts. Upper surface sharp to gradational. Shoreline pebbles (?).

Sandstone, silty shale, siltstone interbeds, purplish gray to dark blackish gray, platy, moderately calcareous. Sandstone f-vf. Sparse bedding parallel calcareous sandstone or arenaceous limestone nodules. Well bedded. Upper contact sharp, slightly erosional. Shallow littoral. Overall this and underlying 2 units are shallowing upward.

Sandstone, gray to yellowish brown, lithic wacke, f-m, very calcareous, poorly to moderately sorted, well bedded, laterally persistent. Littoral.

Sandstone, gray to yellowish gray, common superficial ooids, well sorted and bedded, very calcareous, m-vc, arenite to subarenite, well laminated and x-laminated. Laterally persistent. Sharp upper contact.

Shale, purplish gray in lower part, grades upward into greenish gray in upper part, very calcareous, middle part a bed of c-m sandstone, gray, very calcareous. Sharp lower and upper boundaries. Lake plain, initial expansion.

Conglomerate and conglomeratic sandstone, fining upward from pebble (10-15 cm) to granule clasts, well rounded, imbricated, including conglomerate, mudstone, and abundant marine limestone (with crinoids, spicules, forams) clasts. Laterally wave-reworked into calcite-coated grains. Sandstone, c-vc, well rounded, moderately sorted. This unit thins to SW and thickens to ~1.5 m to NE. Lower contact erosional with 1 m relief, cutting into oolitic sandstone.

Mudstone, dark purple, blocky, peds 5 mm. Lake plain. **No nodules, not that dry.**

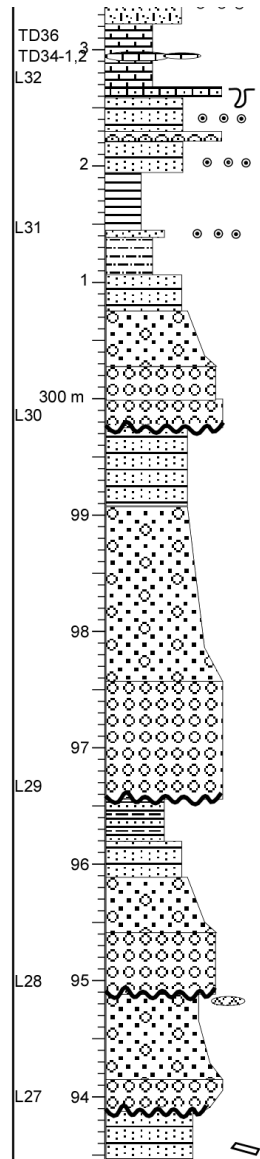
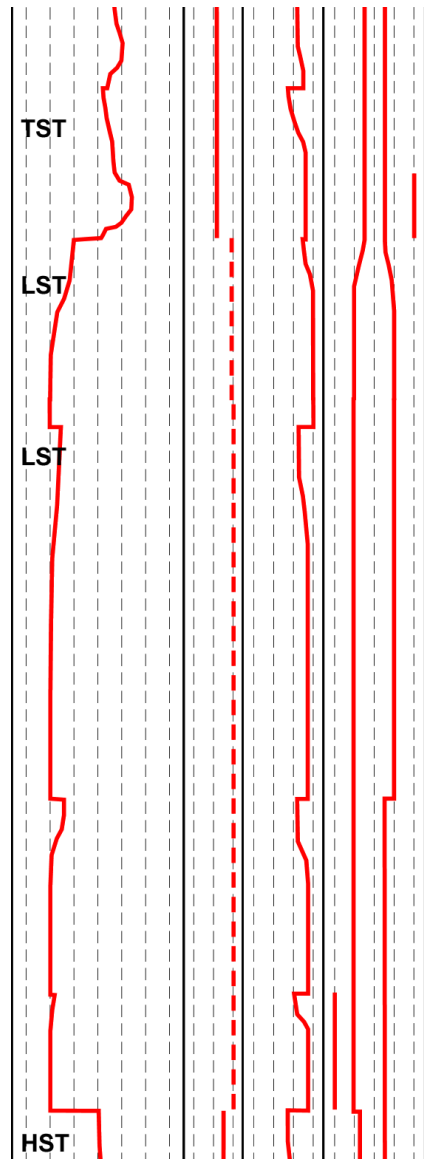
Sandstone, intercalated with shale, grayish brown, m-c, well sorted, very well laminated, parallel to x-laminations, well bedded, persistent. Abundant superficial ooids, some contain mud chips, some x-laminated. Very calcareous. Lake shore/beach, shallow littoral. (50 m to the west, much more gravels, granule to pebble, forming 10s cm thick, coarsening upward units, interbedded with oolitic sandstone. Lateral facies changes). Lower 100 cm has less shale than the upper 30 cm. Sharp upper contact.

Lower part, sandstone, siltstone, intercalated with silty shale, purplish gray, lithic subarenite to wacke, very calcareous, platy, common mud chips, well bedded. Sandstone common, small to moderately amount of superficial ooids, f-m-c, moderately to poorly sorted. Beach, lake shore. Upper part, increased siltstone and silty shale, sandstone has no ooids, less platy, blocky with peds 1-0.5 cm in size, still bedded. Lake plain. Shallowing upward from lake shore to subaerial lake plain.

Sandstone, similar to below, yellowish to purplish gray, contains superficial ooids, very calcareous, well sorted and bedded.

Sandstone, gray to grayish brown, very calcareous, c-m, well sorted and bedded, many superficial ooids. The uppermost part is oolitic grainstone.

Sandstone, gray to brownish yellow, m-c, well sorted and bedded, very calcareous, lithic arenite to



subarenite.

Shale, dark gray with purple tint, silty, platy, very calcareous. A 5-10 cm lenticular limestone (TD34-1, 34-2) in middle, micritic, finely laminated, scattered particles of possible microfossils.

Limestone, gray, 2 thin beds, pockets of sand with 20% quartz, micritic. Secondary calcite growth. In places, brecciated and bioturbated. Palustrine limestone.

Sandstone, yellowish brown, m-c, lithic arenite, well sorted and rounded. Some beds contains >50% ooids and can be arenaceous oolitic grainstone. Well bedded. Lake shore, shallow littoral. Sharp lower and upper contacts.

Shale, brownish gray, greenish gray to brown. A 3-cm f sandstone at base with some superficial ooids. Lake shore, lake plain.

Conglomerate, sandstone, siltstone. Upper contact sharp.

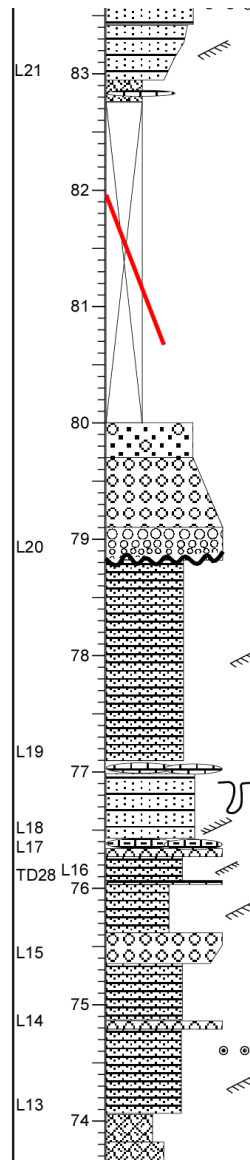
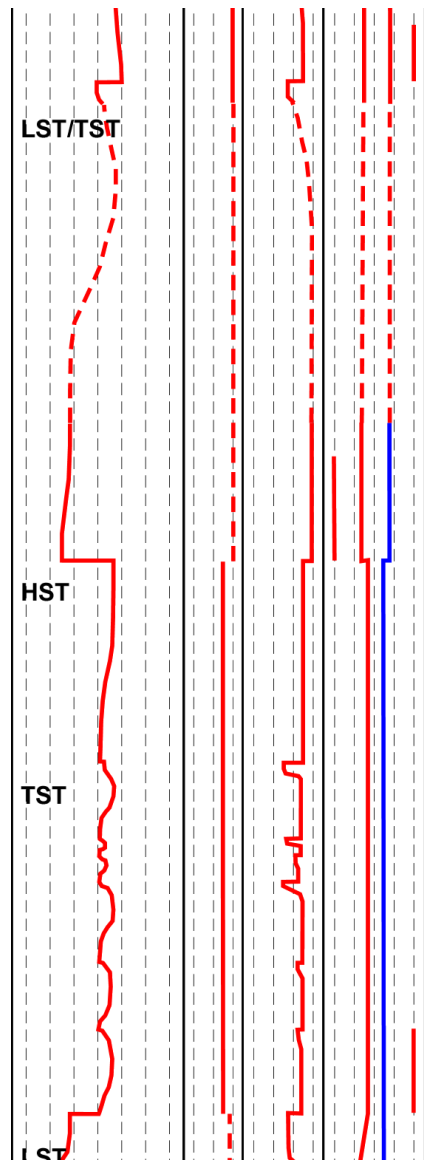
Where are TD32, 33???

Conglomerate, grayish red to brown.

Conglomerate and sandstone, grayish red to purple. Conglomerate, lower 50 cm granule to pebble clasts, grade upward into conglomeratic sandstone and m-c sandstone. Uppermost part f sandstone and shale interbeds. Braided stream deposits, less coarser than below. Sharp, probably erosional top and base.

Conglomerate, grayish brown, pebble clasts (1-15 cm), lower 20 cm coarsening upward, upper part fining upward. Conglomeratic sandstone, c-vc, uppermost some mudstone lentils/stringers. Braided stream.

Sandstone, brownish gray, lithic wacke, c-vc, some mud chips of underlying shale. Lake plain sand flat. Sharp base, erosional top.



Sandstone, grayish brown, lithic subarenite, slightly coarsening upward from f-m to c, rare granules, moderately to very calcareous, well sorted, moderately rounded. X-laminated, well bedded. Sharp lower and upper contacts. Littoral or lake shore sand flat.

Mudstone, purple red, blocky to platy, very calcareous. A layer of lenticular brecciated micritic nodular limestone, ~3 cm thick. The lower boundary may correlate with that of the 80-cm calcareous sandstone bed (between 27407 and 27487 cm), if so, there is a 870 cm overlap. This surface has the same elevation as that of the upper surface of the underlying covered interval. 117/43.

Covered, across a small fault. Amount of missing strata uncertain, probably less than 10 m, still within Luocaogou Fm.

Conglomerate, dark gray, lower 30 cm reverse graded. Overall fining upward. Clasts, 1-30 cm (5 cm most common), subangular to rounded. Clast supported, some limestone clasts, conglomeratic sandstone clasts, volcanic clasts still dominant. Upper contact covered. Braided stream deposits.

Sandstone, dark brown, subarenite, m-c, well sorted and rounded, few granules, moderately to very calcareous, well bedded, possible x-lamination. Upper contact sharp to erosional, lower boundary uncertain. Littoral to lake shore.

Sandstone, grayish brown, lithic arenite, c-vc, thin-medium bedded, mottled, possibly x-bedded. Uppermost part ~10 cm nodular limestone, greenish gray.

Grainstone, greenish gray, arenaceous, probably abundant skeletal grains. Nodular, lenticular. Lower part fine pebble to pebble conglomerate, imbricated, well rounded, up to 15 cm, as shoreline pebbles.

Sandstone, brown, m-c, well rounded, moderately sorted, ripple x-laminated, well bedded.

Limestone, green gray, micritic. 3 cm thick. TD28.

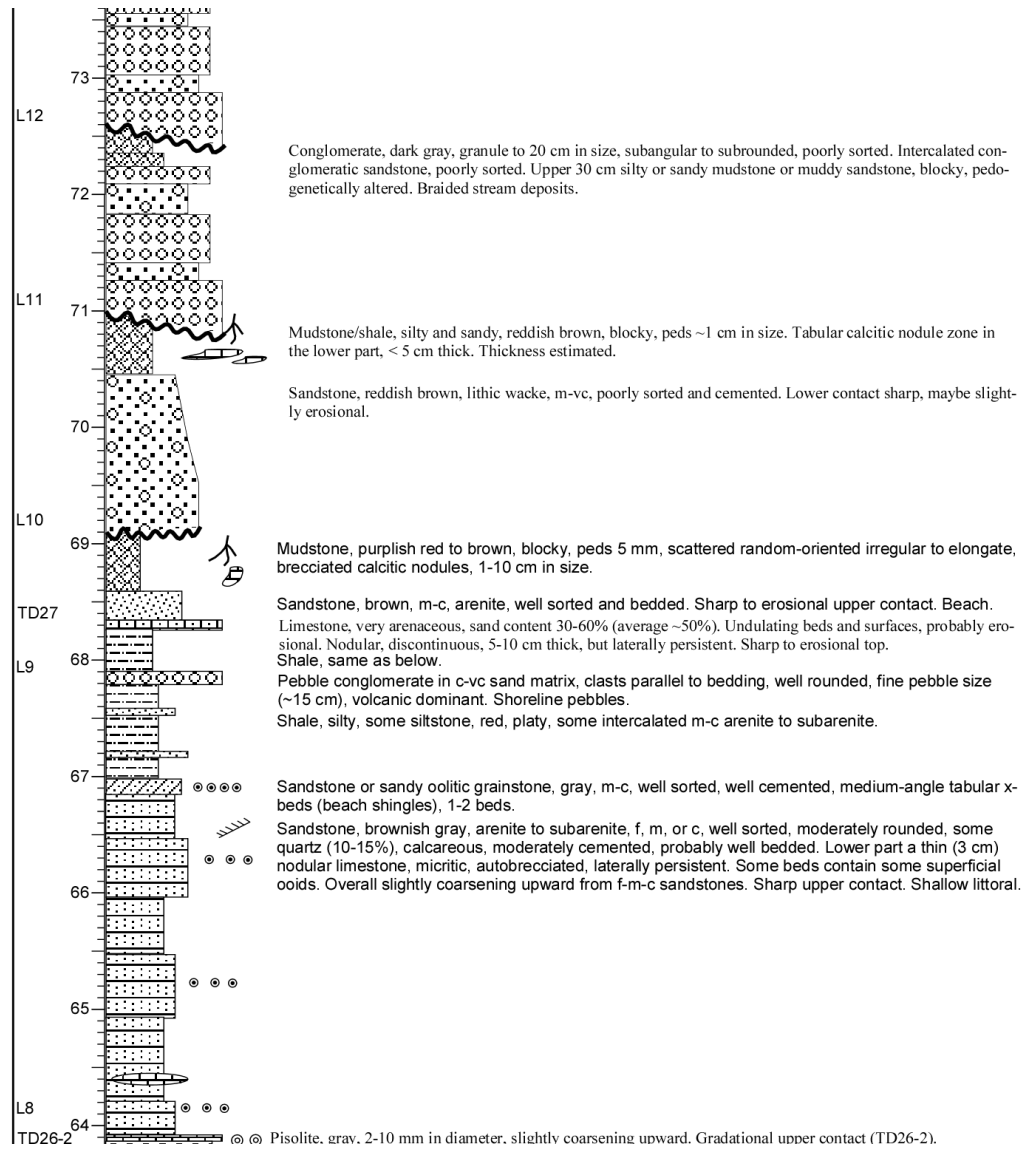
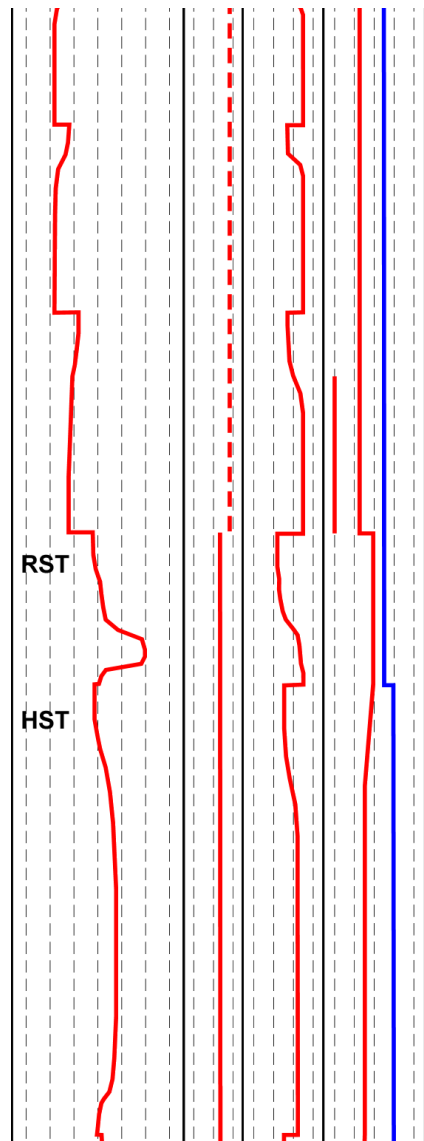
Sandstone, brown, f-m, x-laminated, well bedded. Thin bed.

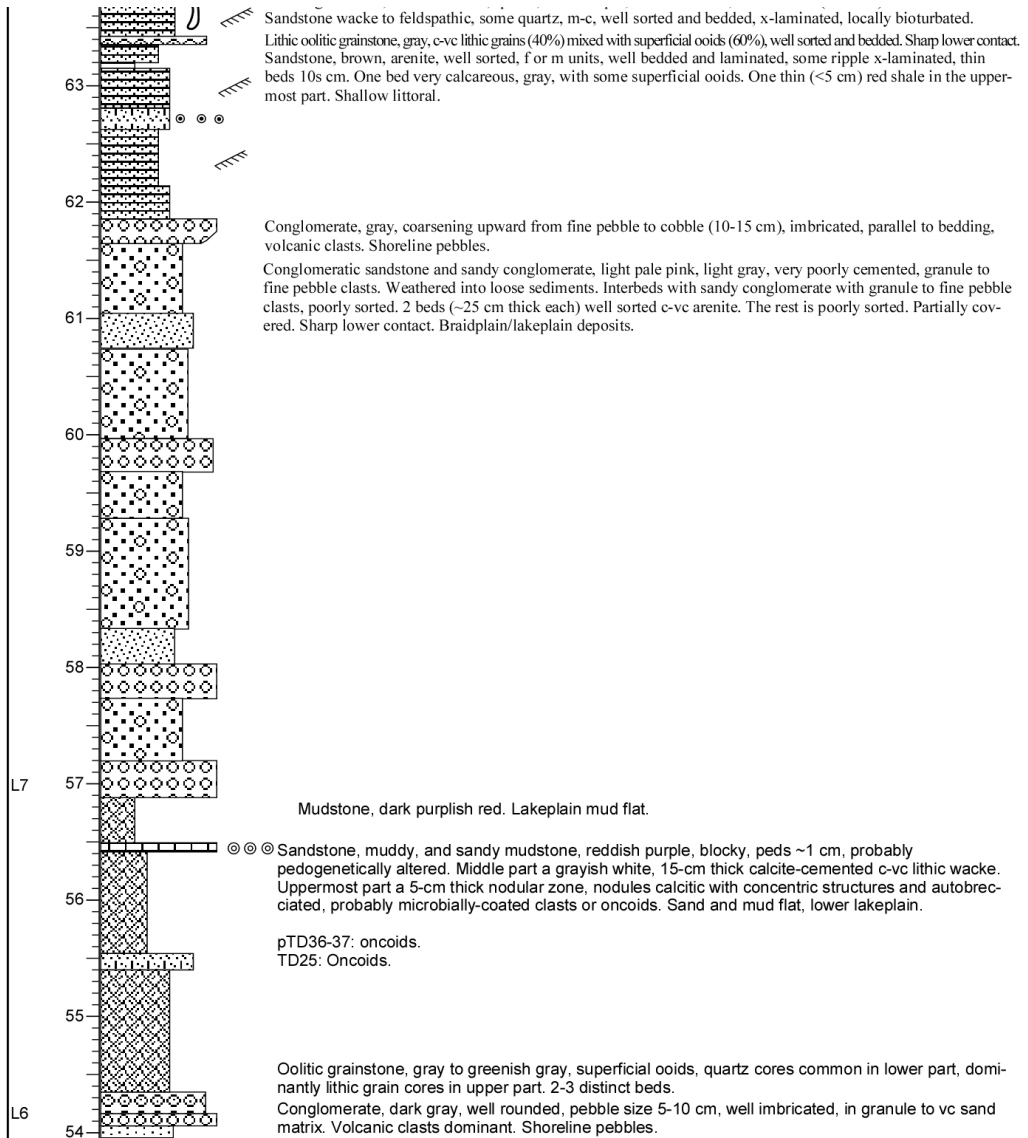
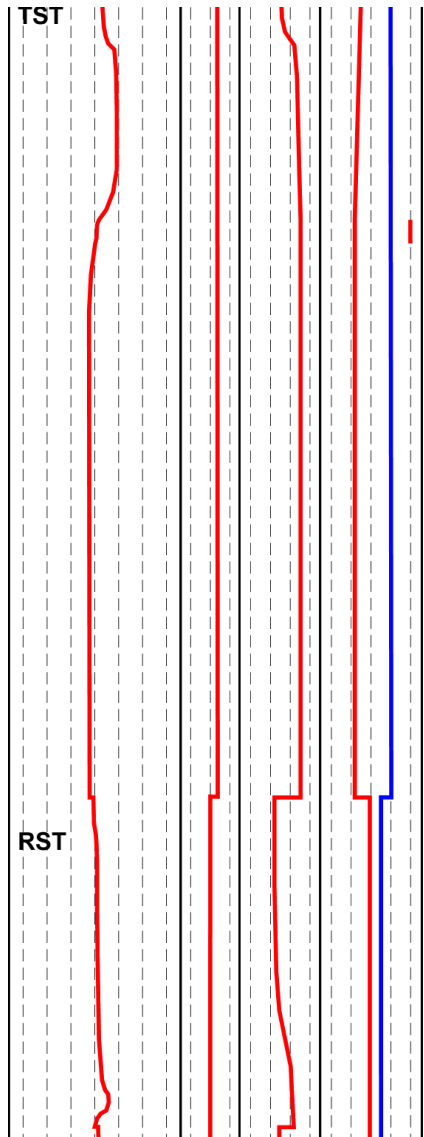
Pebble conglomerate, clasts imbricated, 5-20 cm in size, parallel to bedding plane. Slightly coarsening upward. Shoreline pebbles.

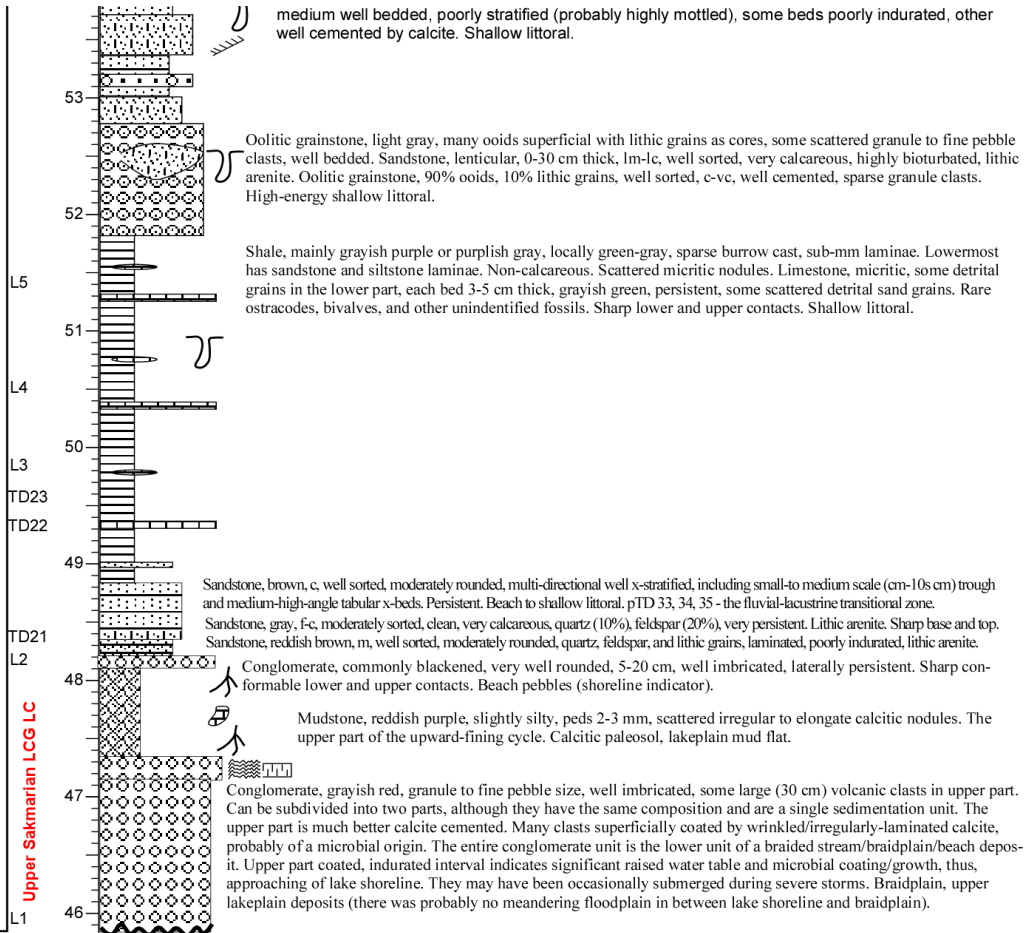
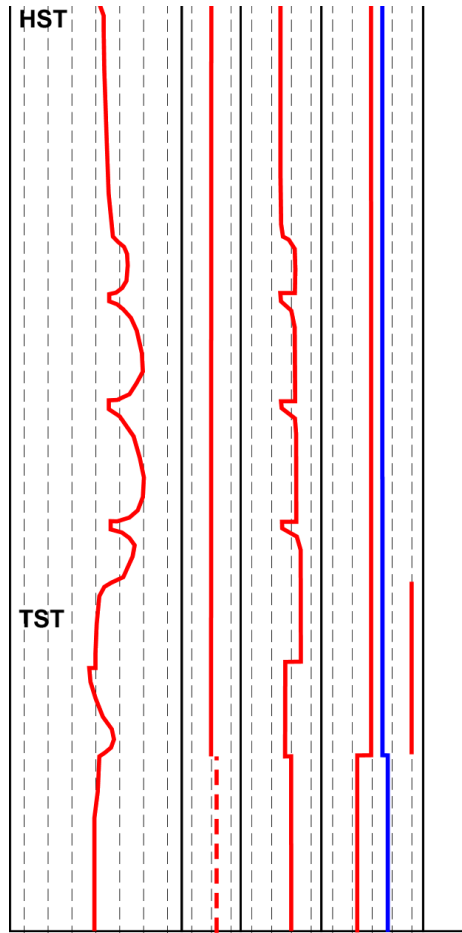
Sandstone grayish brown, containing some granular clasts, poorly cemented, well bedded. Base a thin conglomerate.

Sandstone, brownish gray, arenite, m-c, calcareous, well sorted and bedded, x-laminated, some superficial ooids. Thin (~10 cm) beds. Uppermost part contains scattered, well-rounded volcanic clasts of fine pebble size (shoreline pebbles, suggesting oscillating shorelines).

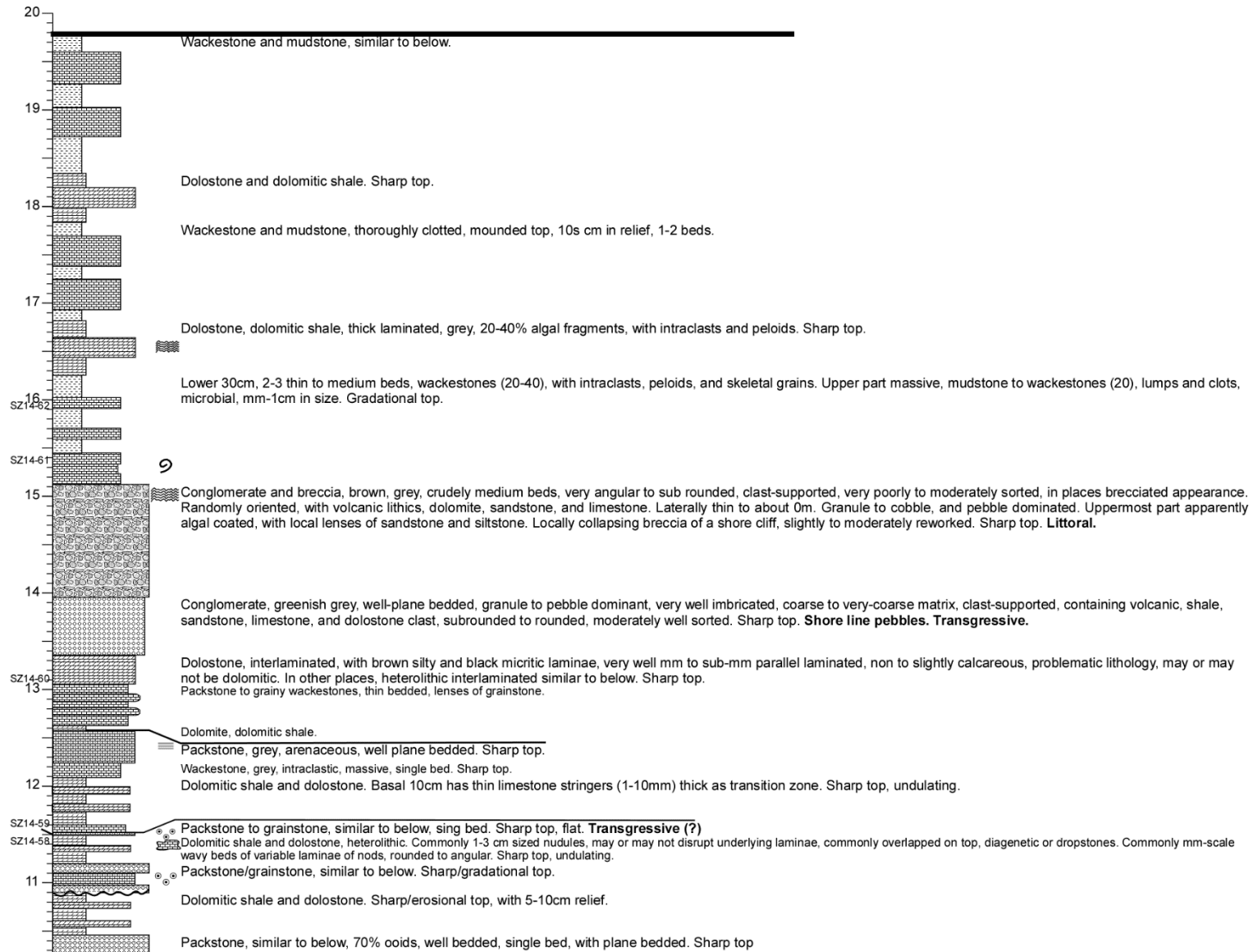
Same as below. Uppermost part 40 cm pedogenically altered. The two cycles were measured together of roughly equal thickness. Not differentiated.

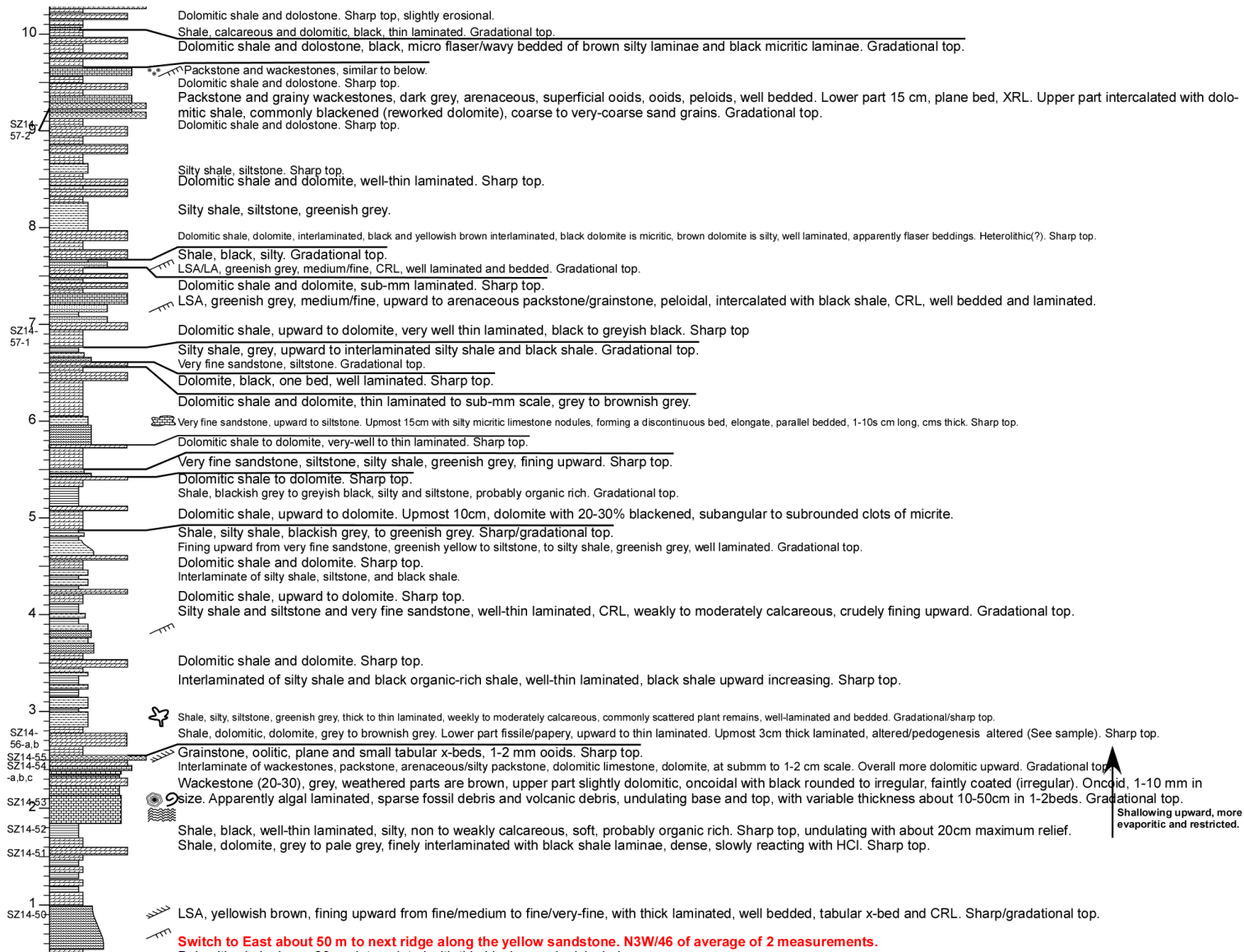


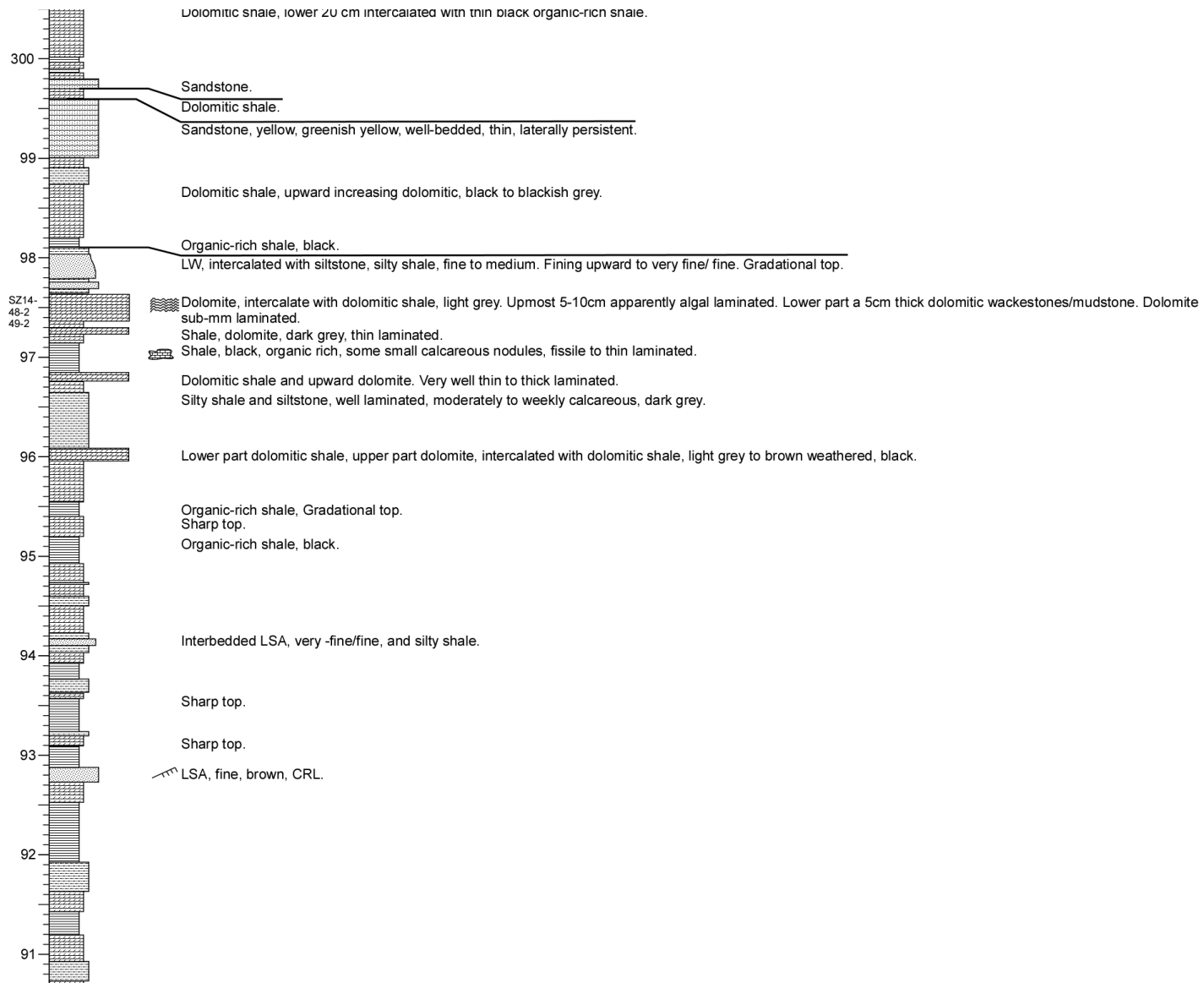




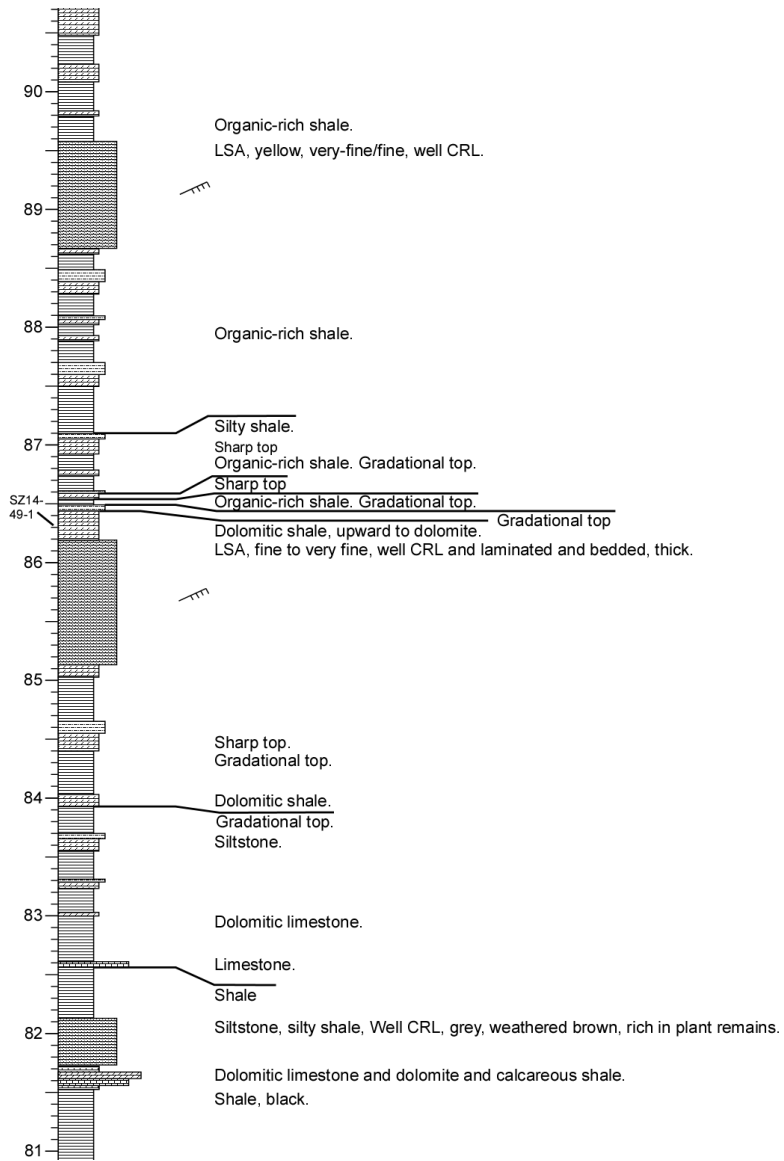
APPENDIX F
ZHAOBISHAN SECTION



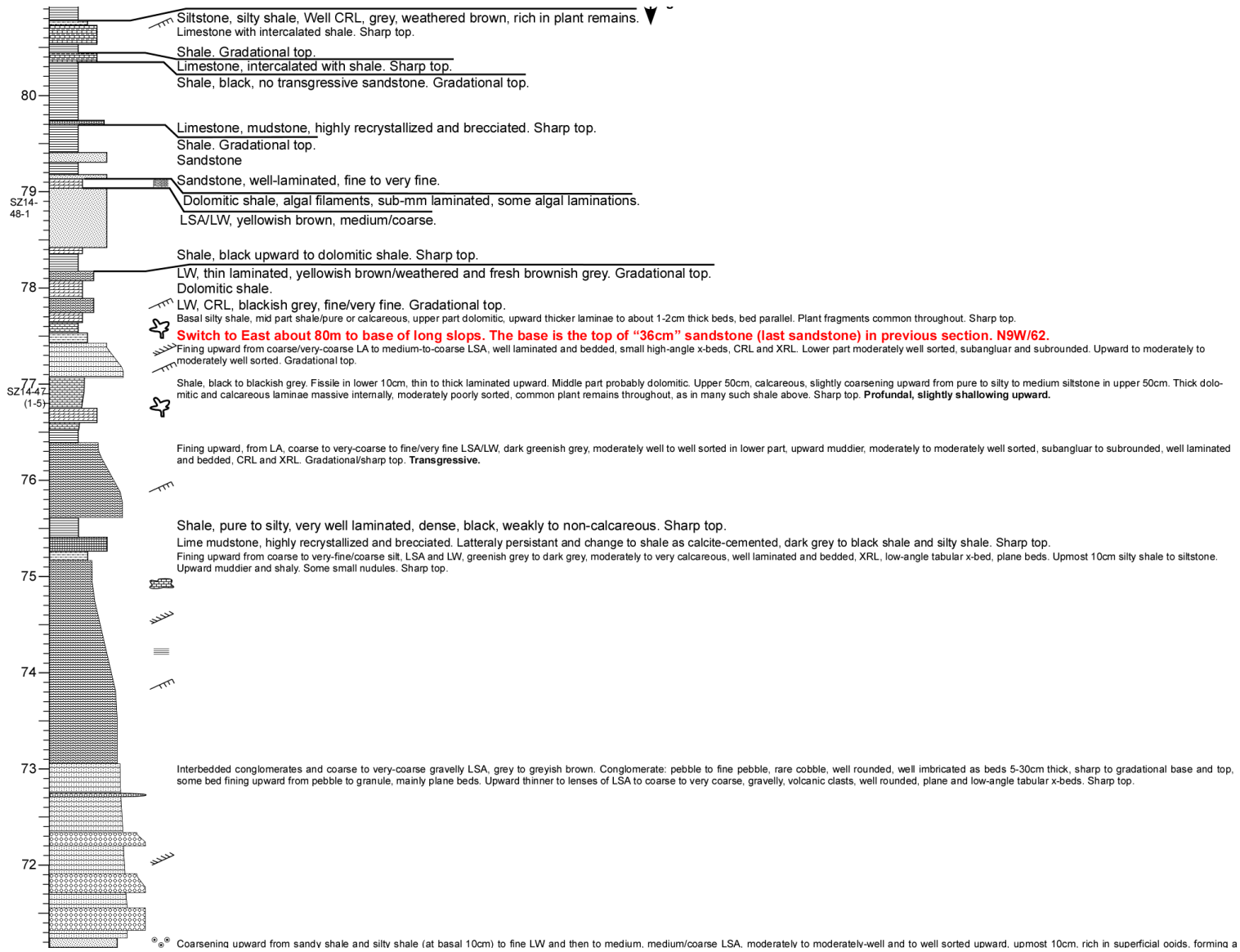


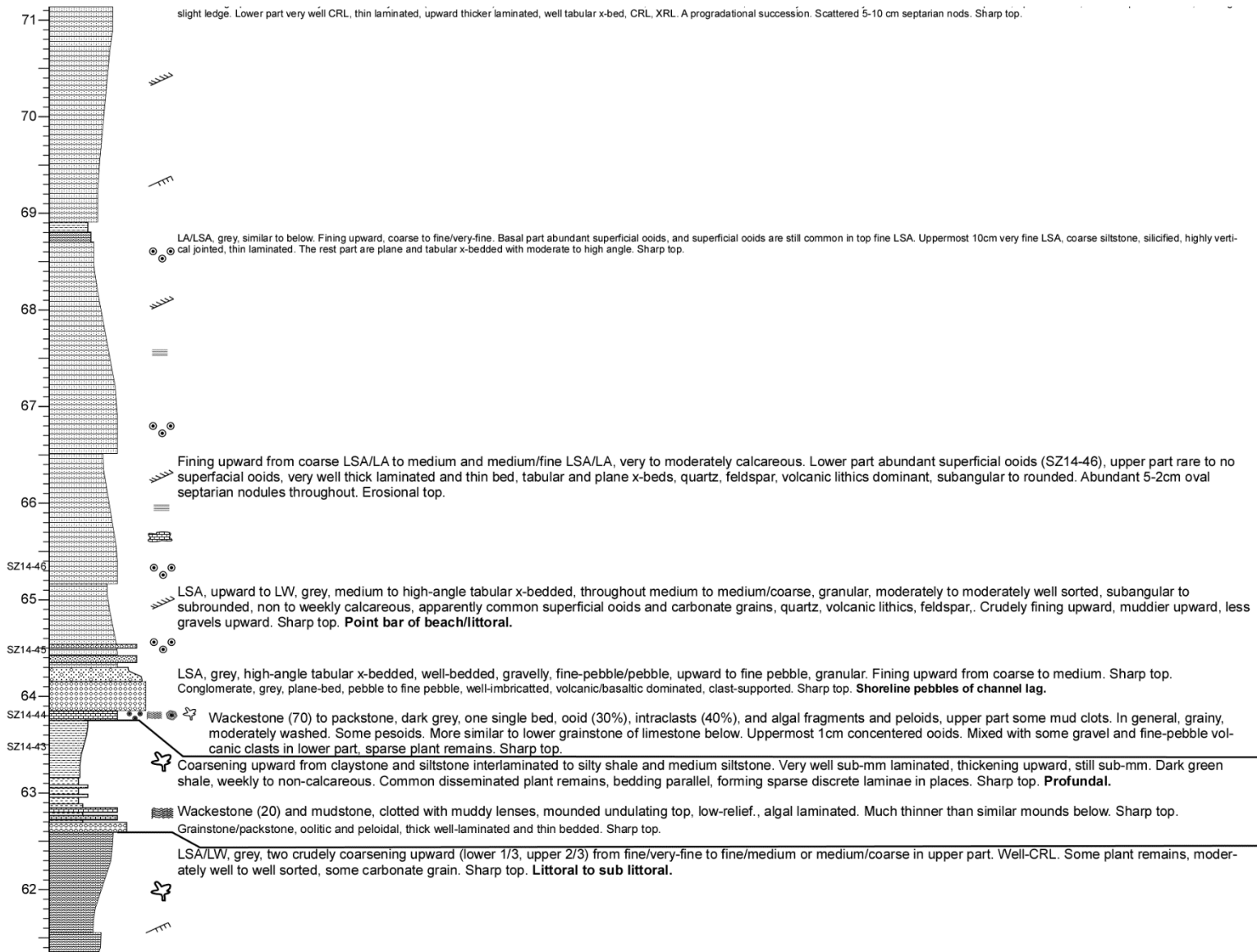


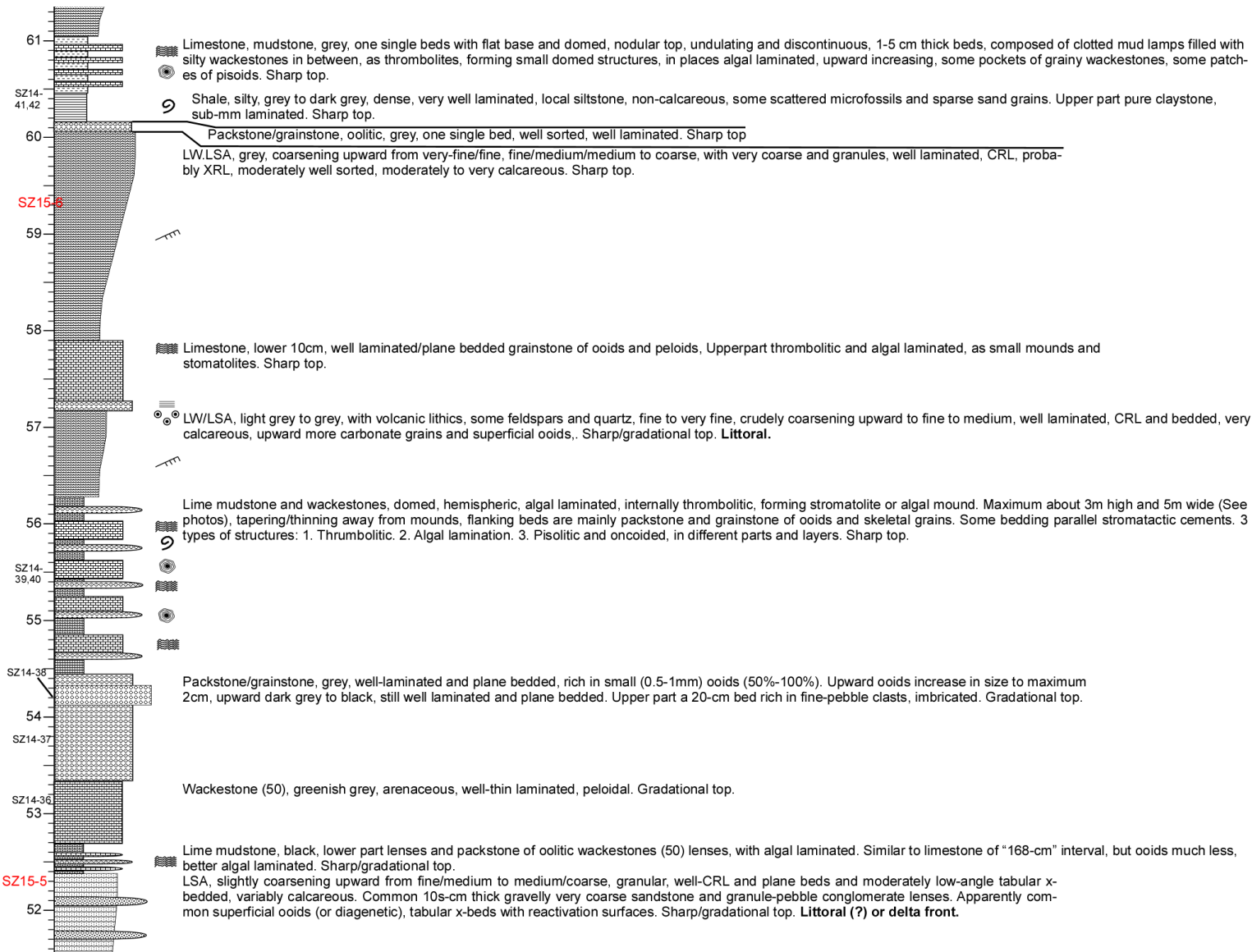
See photos

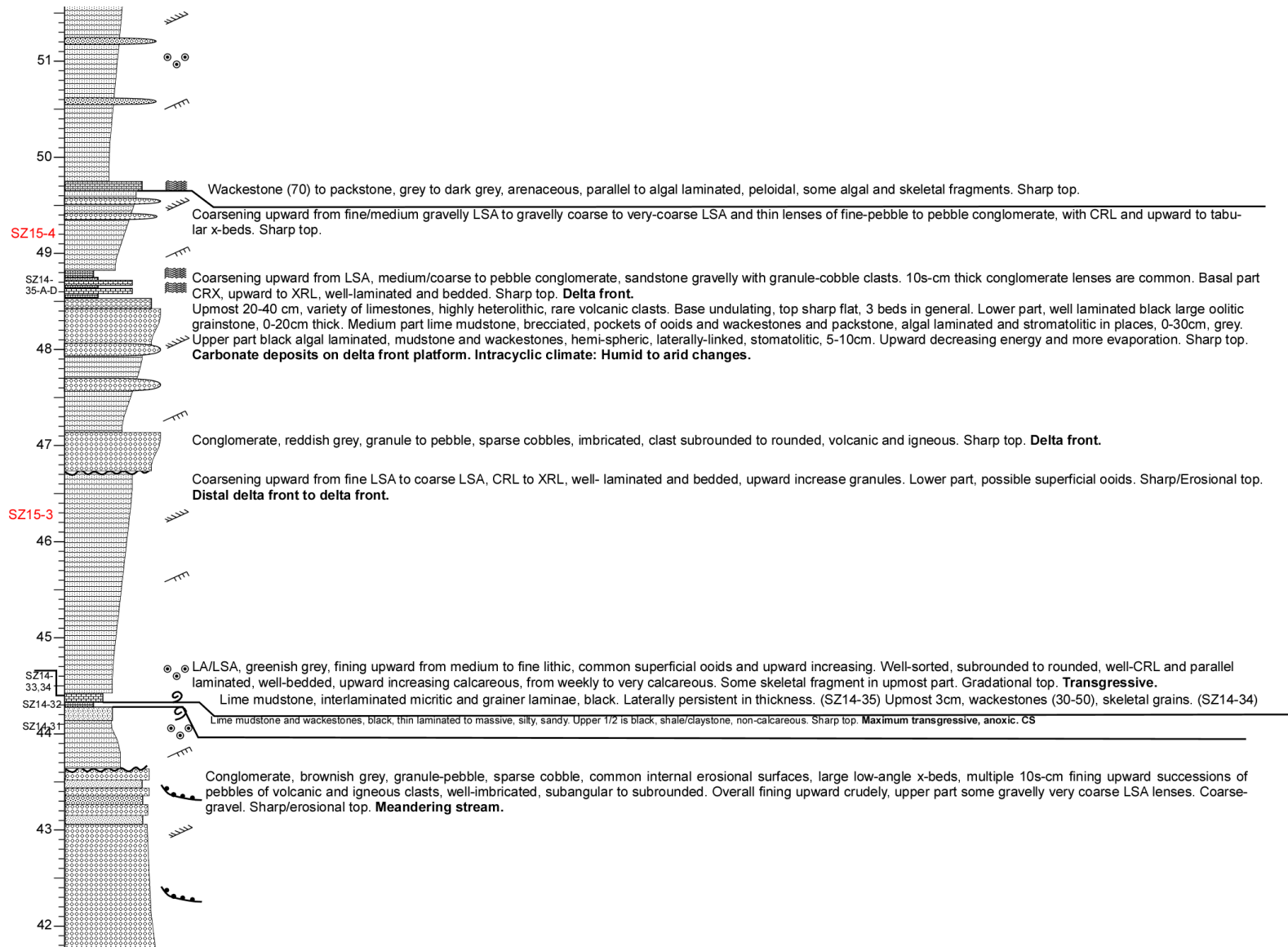


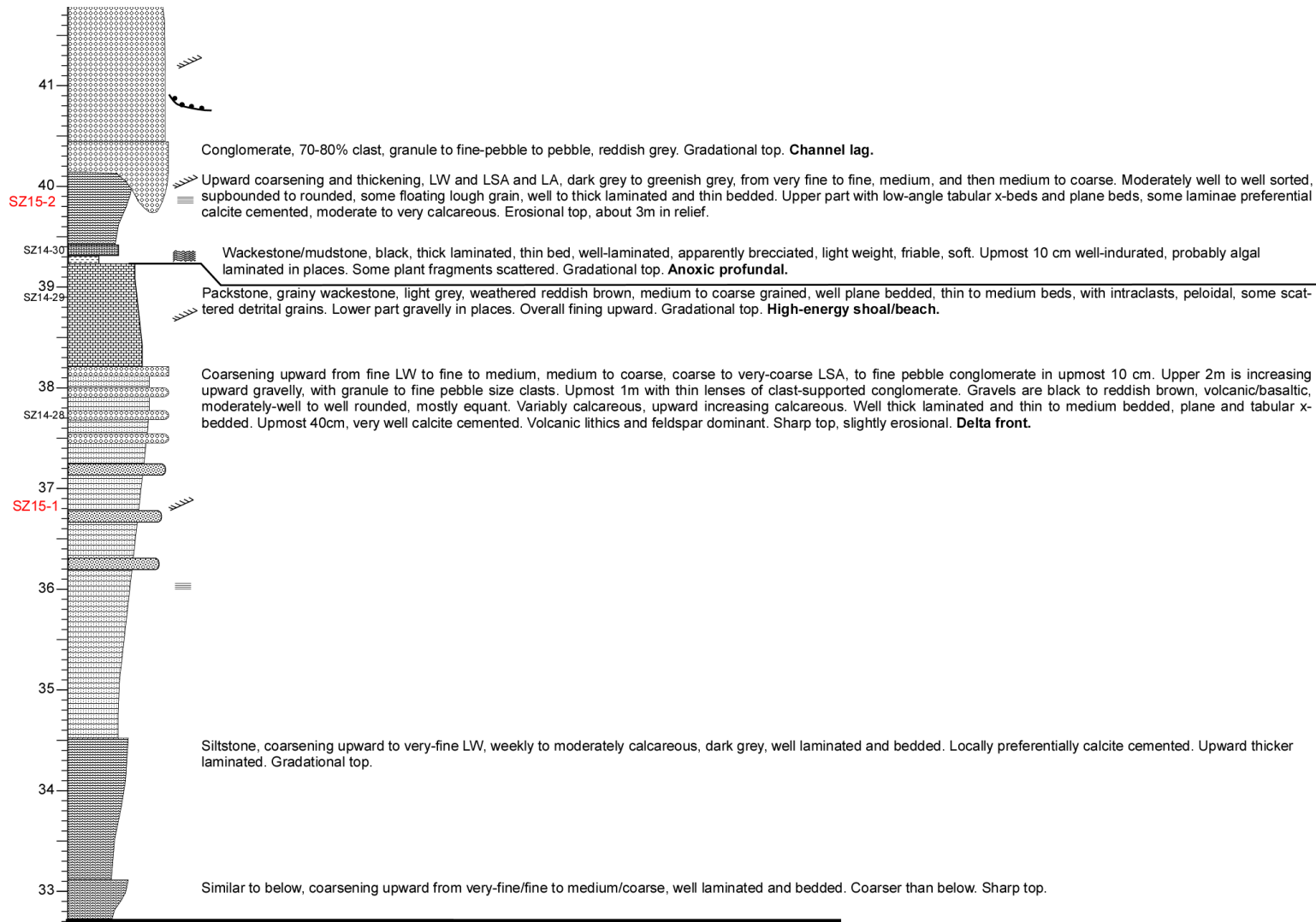
↑
A thick cycle, partially
clue to reverse fault-
ing.





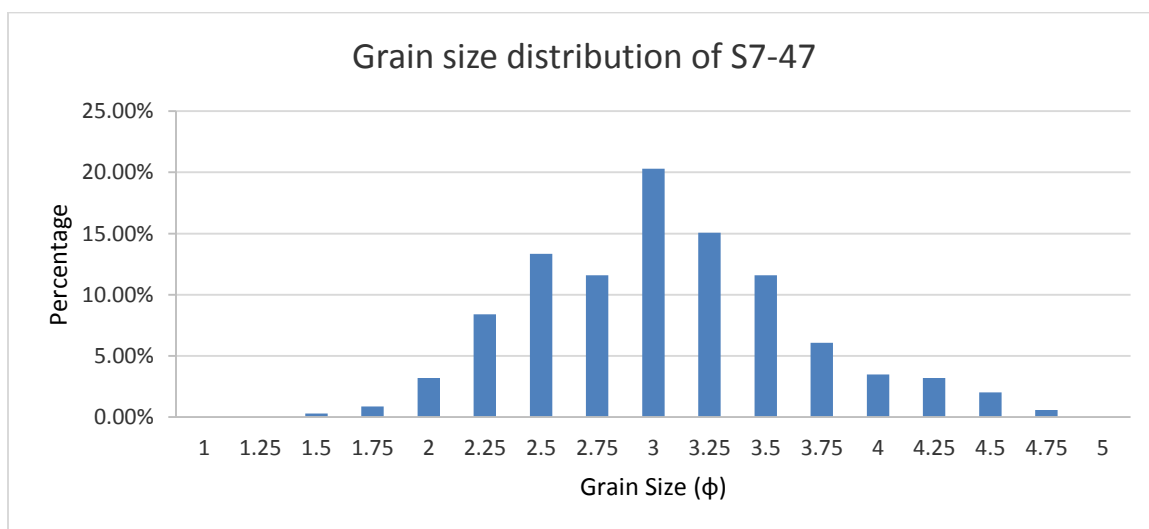
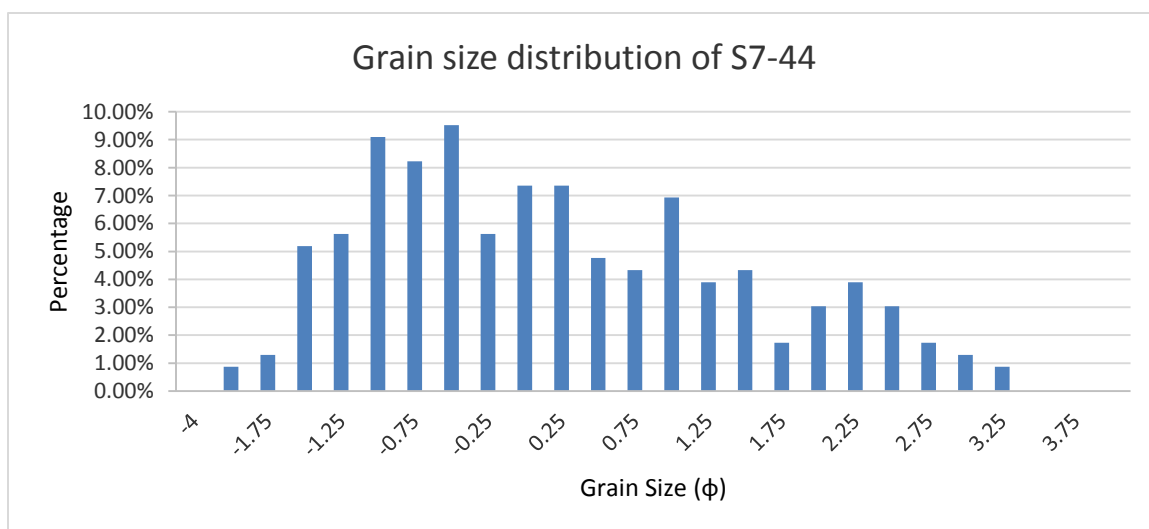
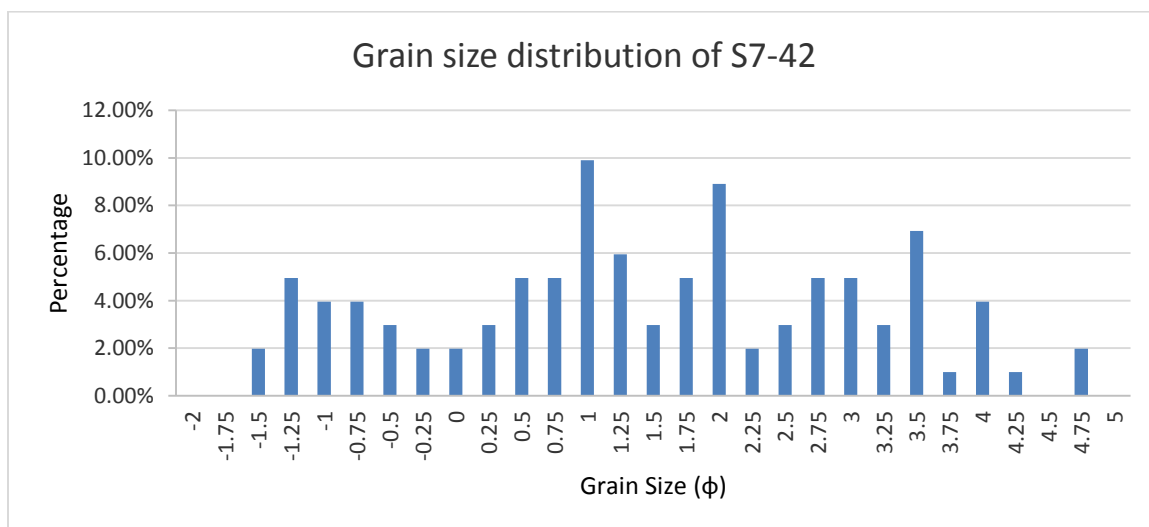


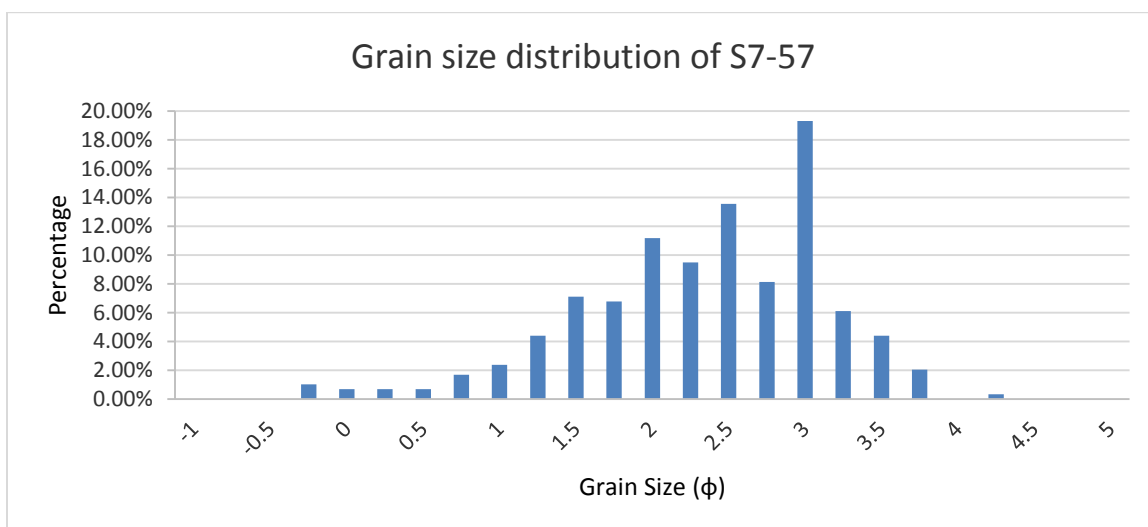
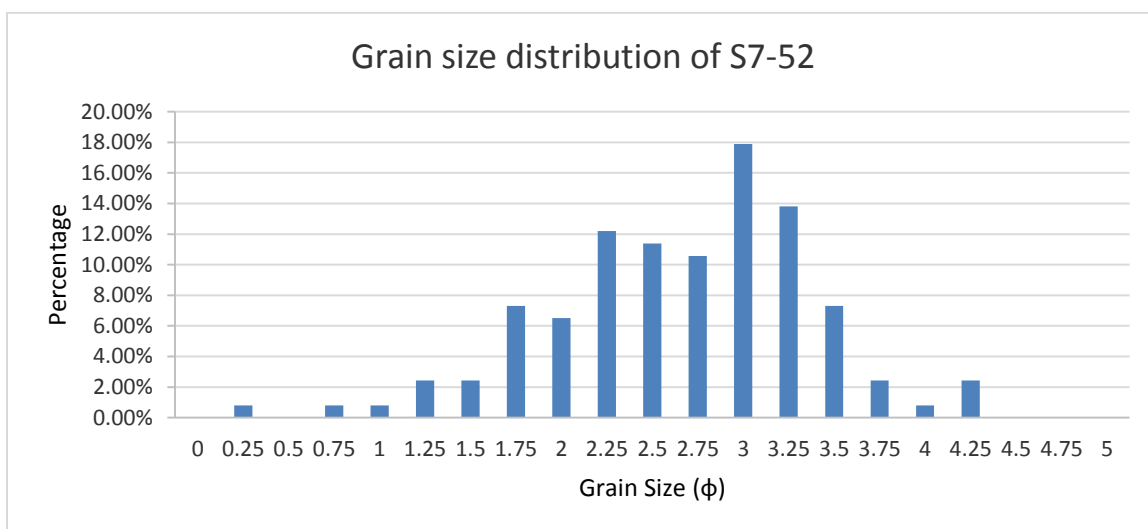
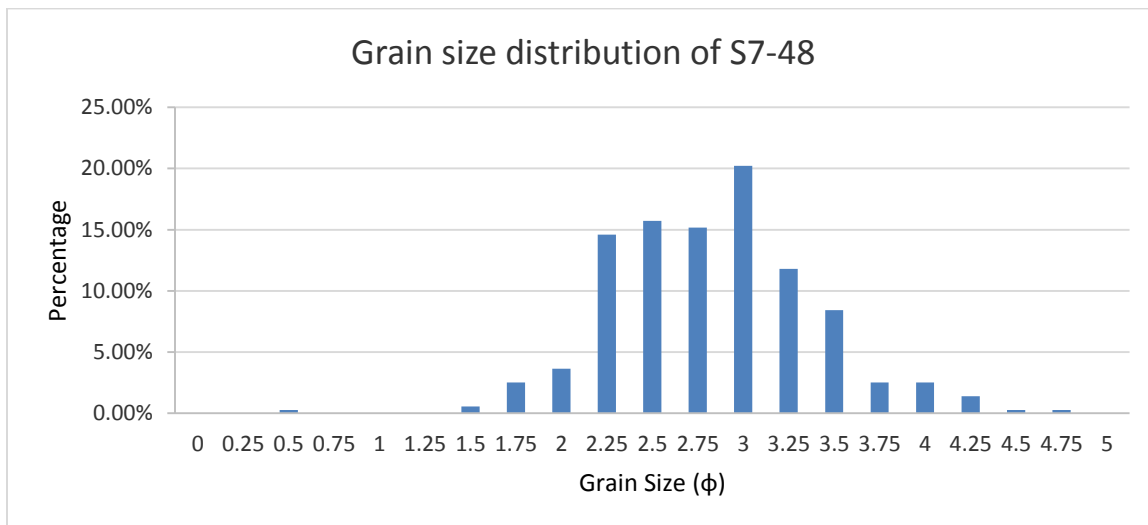


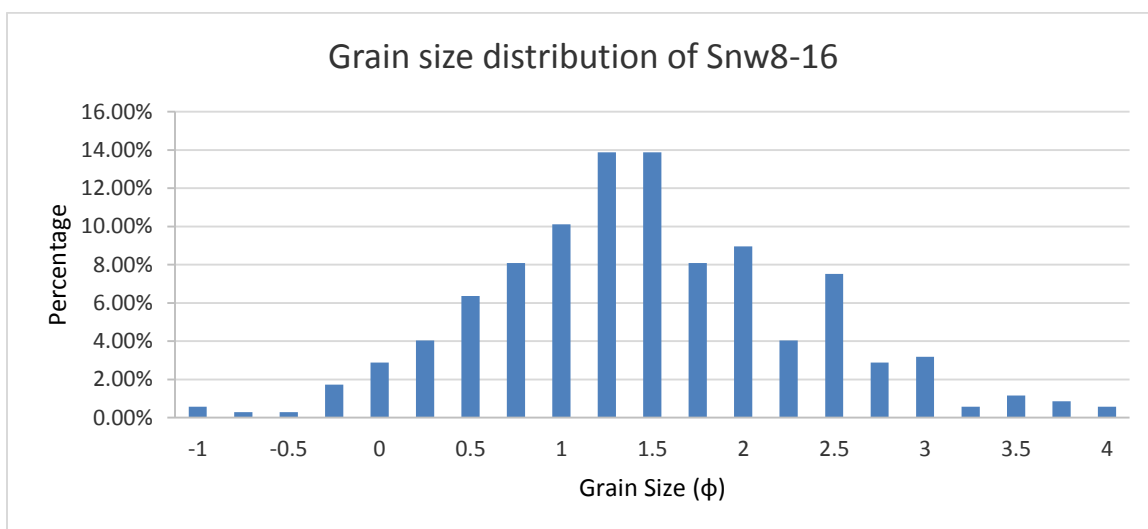
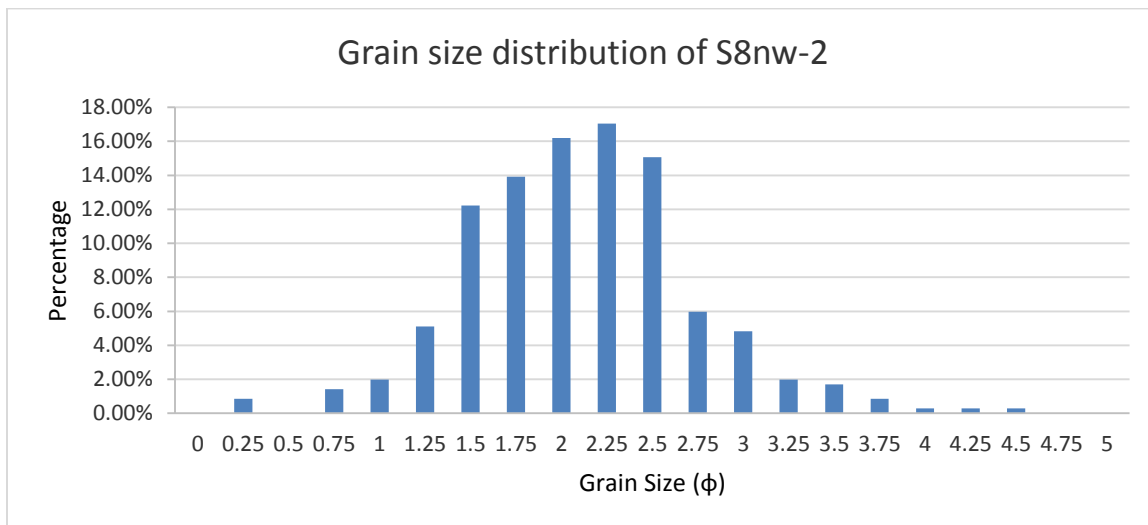


APPENDIX G
GRAIN SIZE DISTRIBUTION OF ALL SANDSTONES

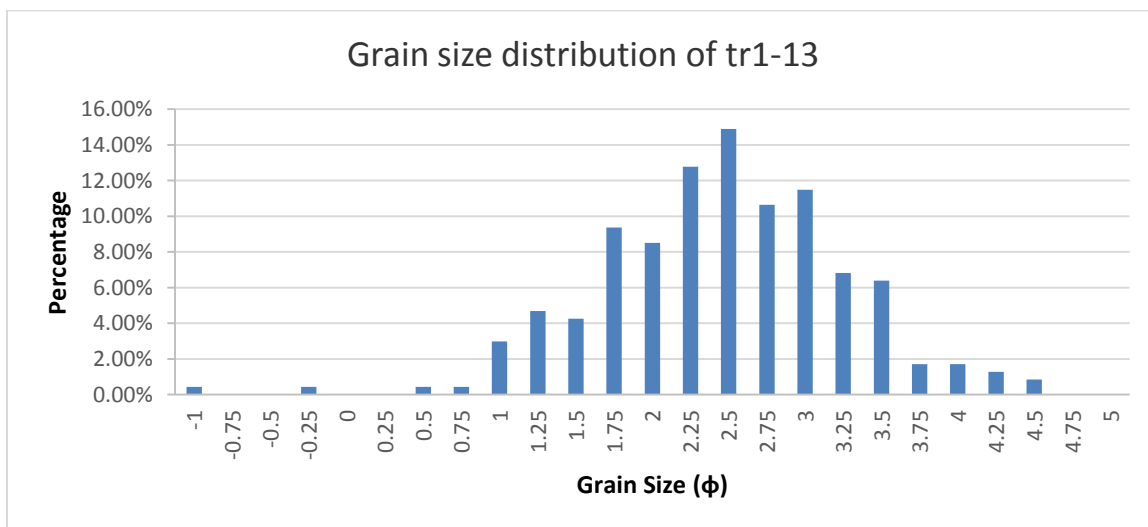
NW Tarlong

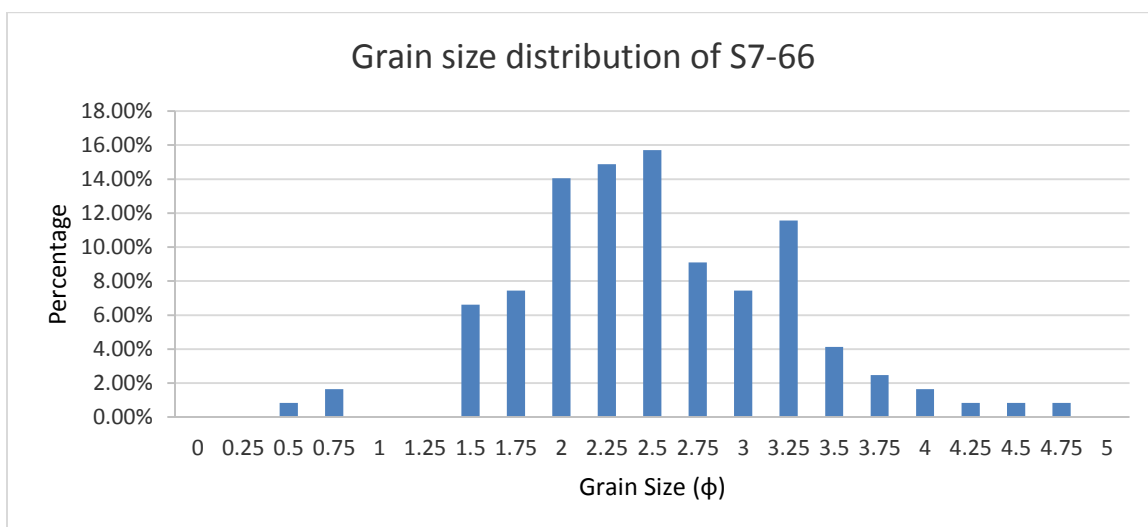
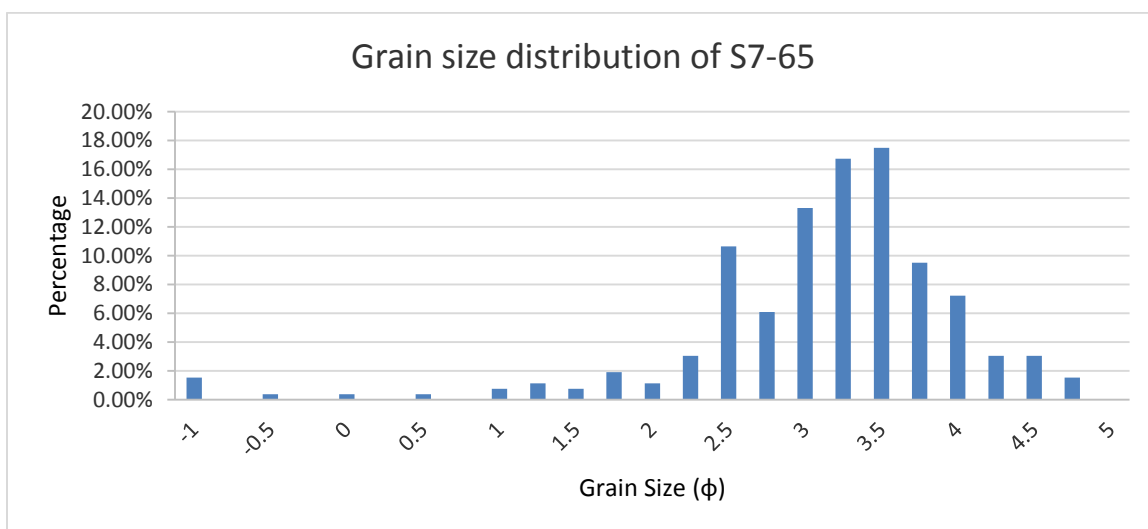
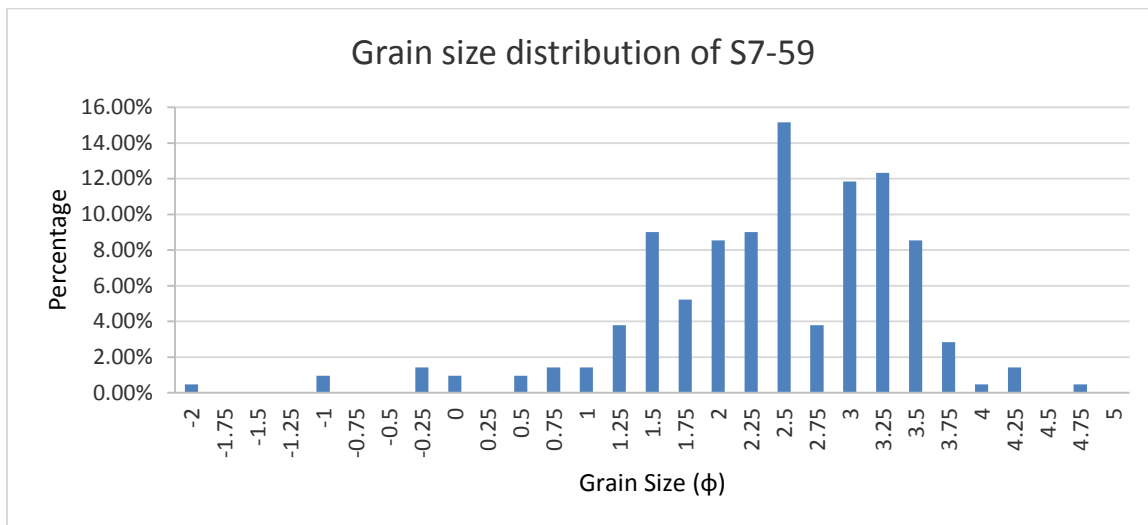


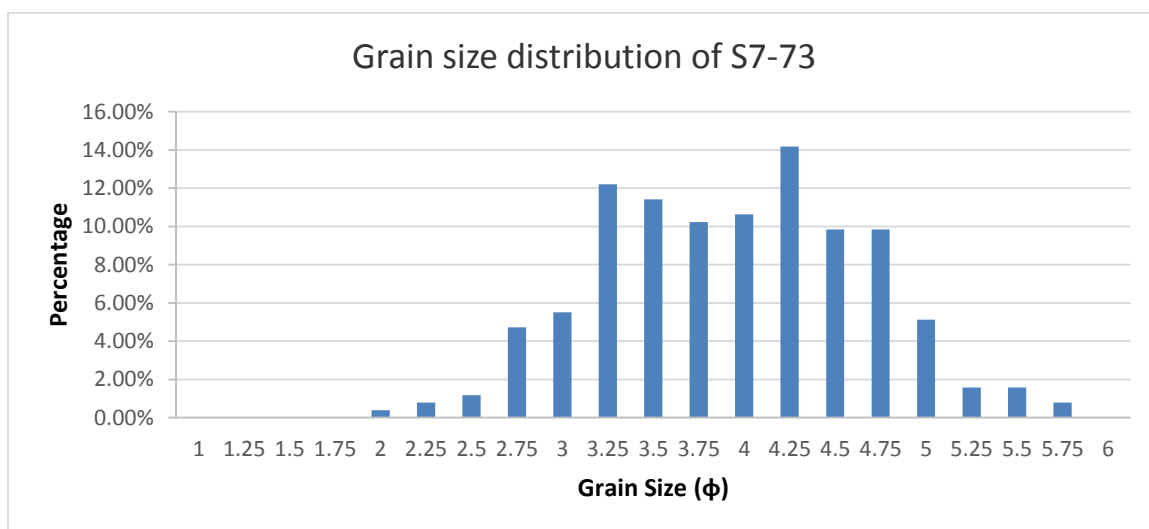
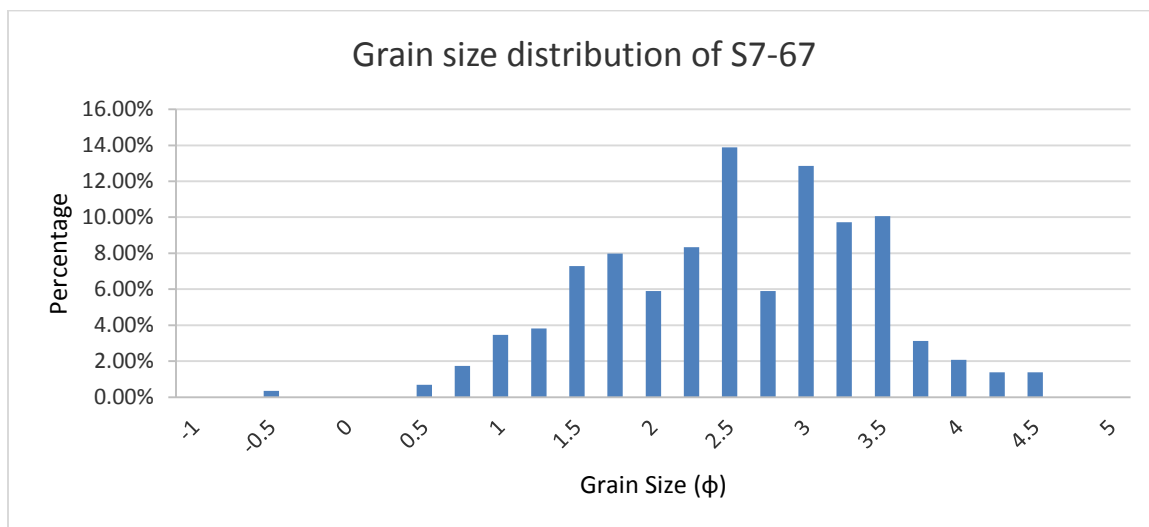




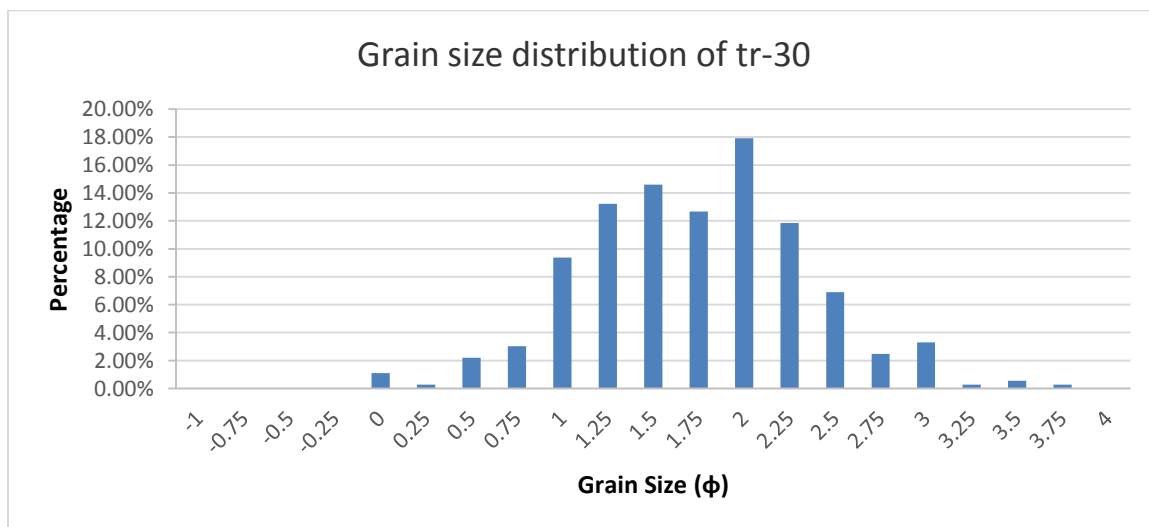
S Tarlong

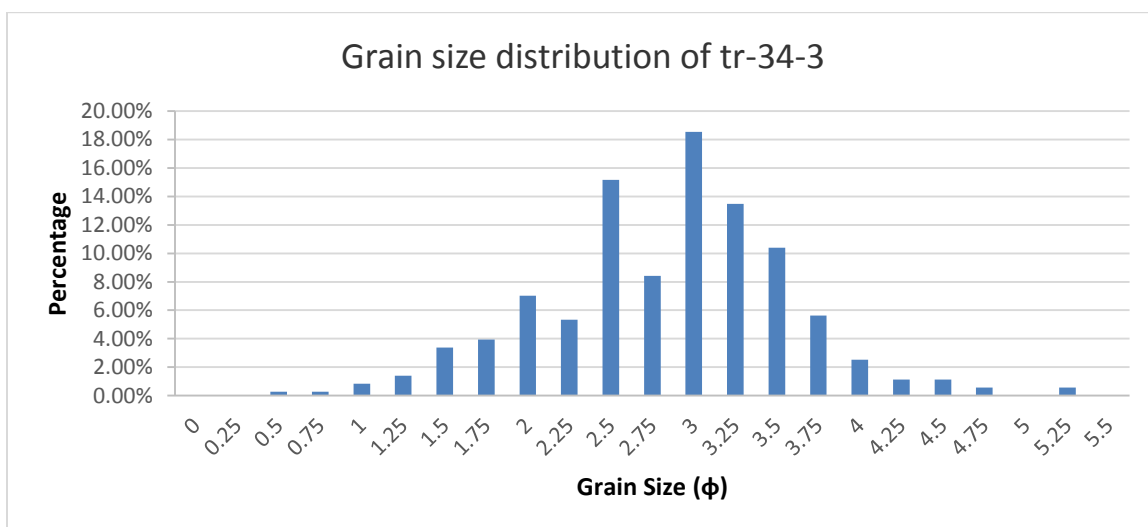
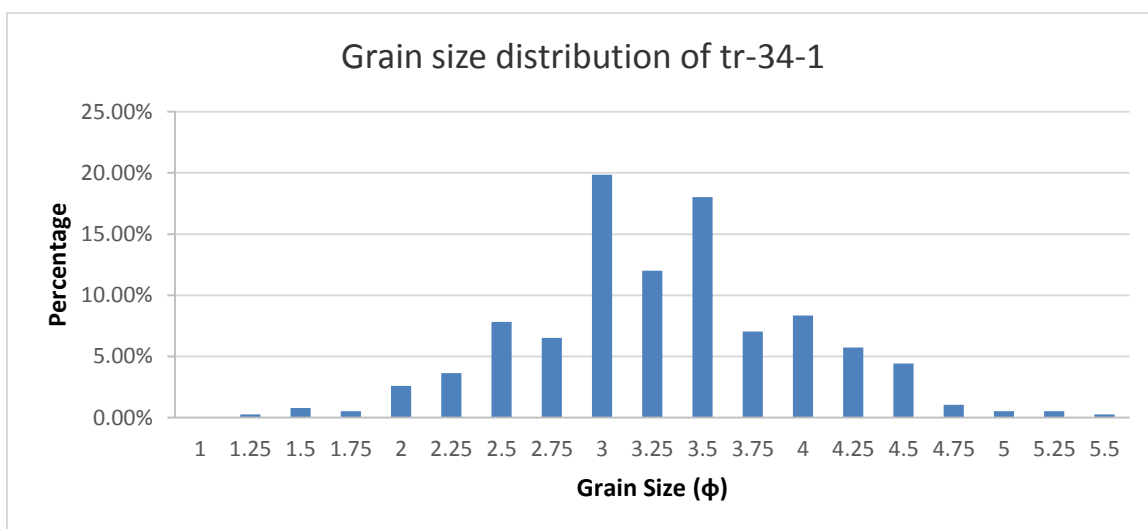
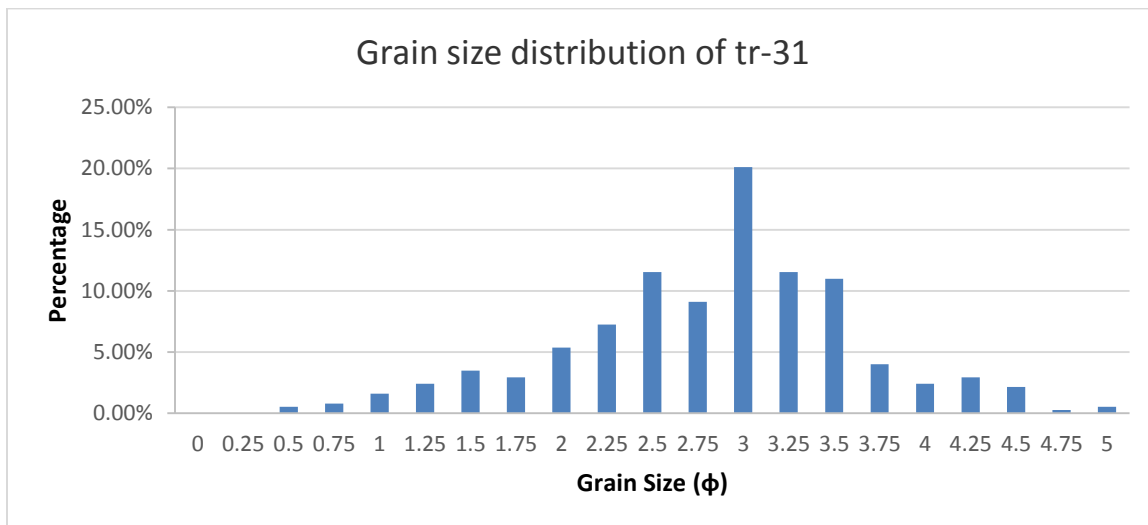


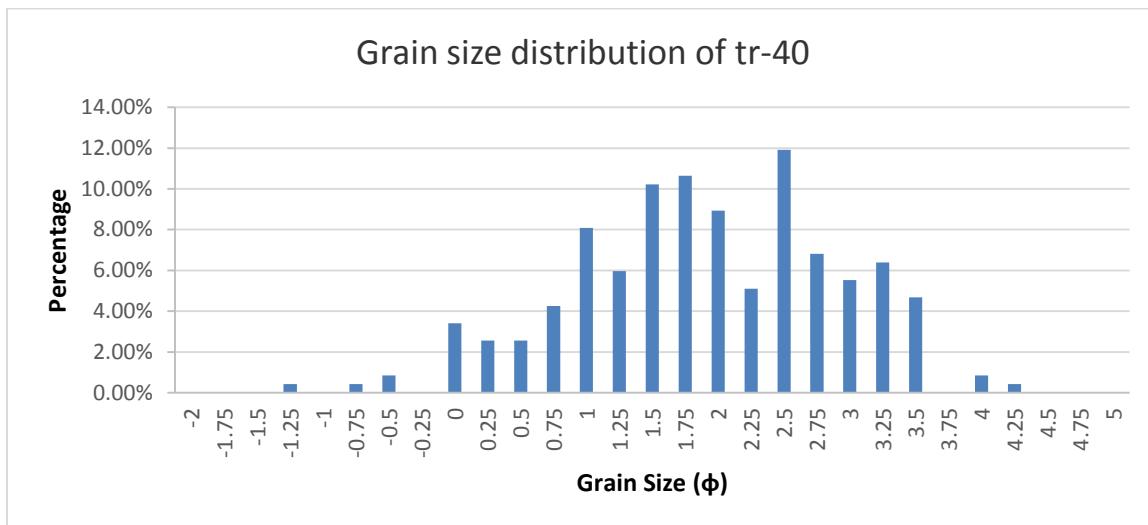




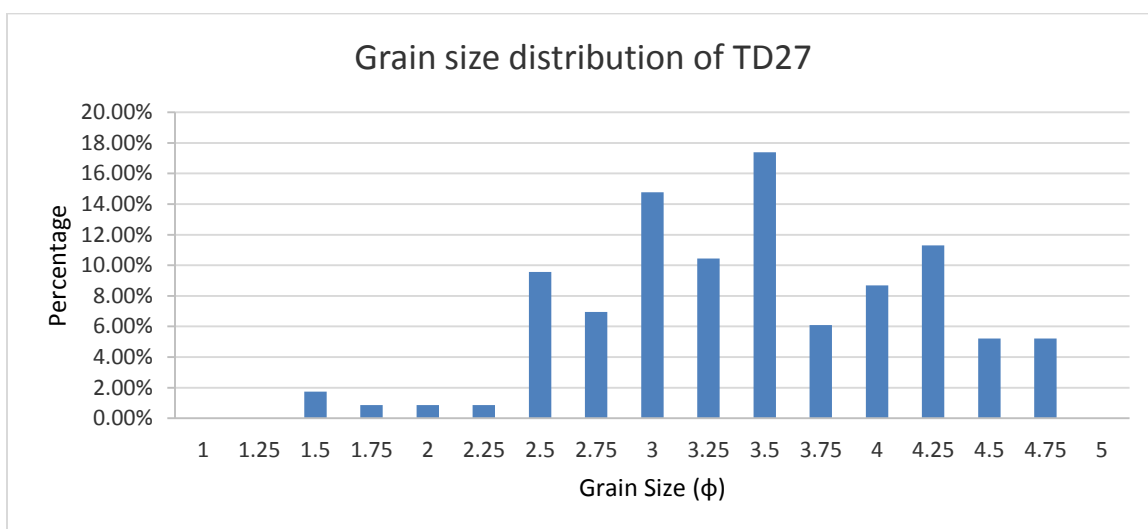
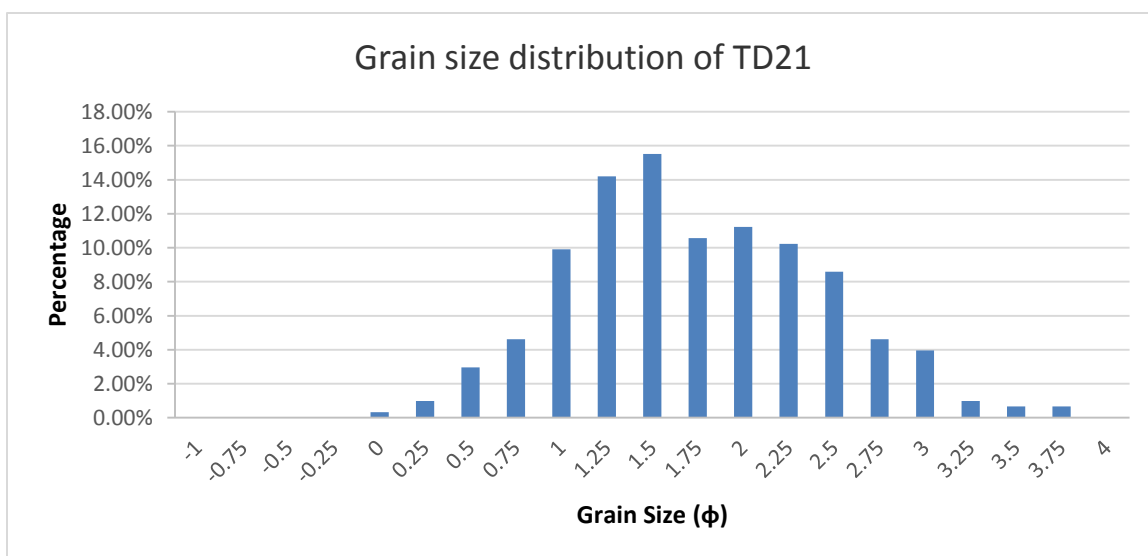
N Tarlong

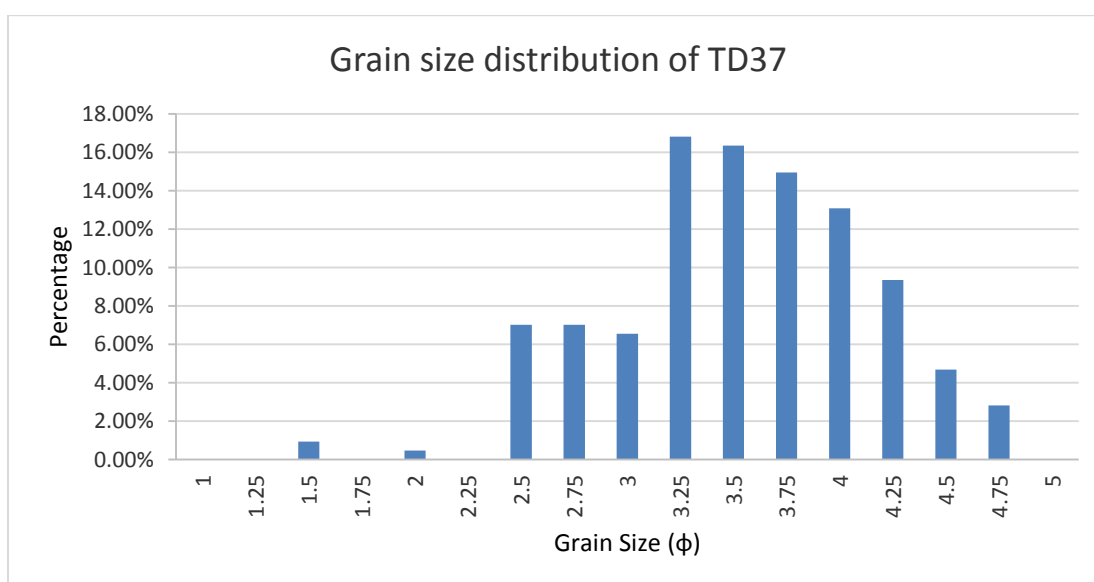
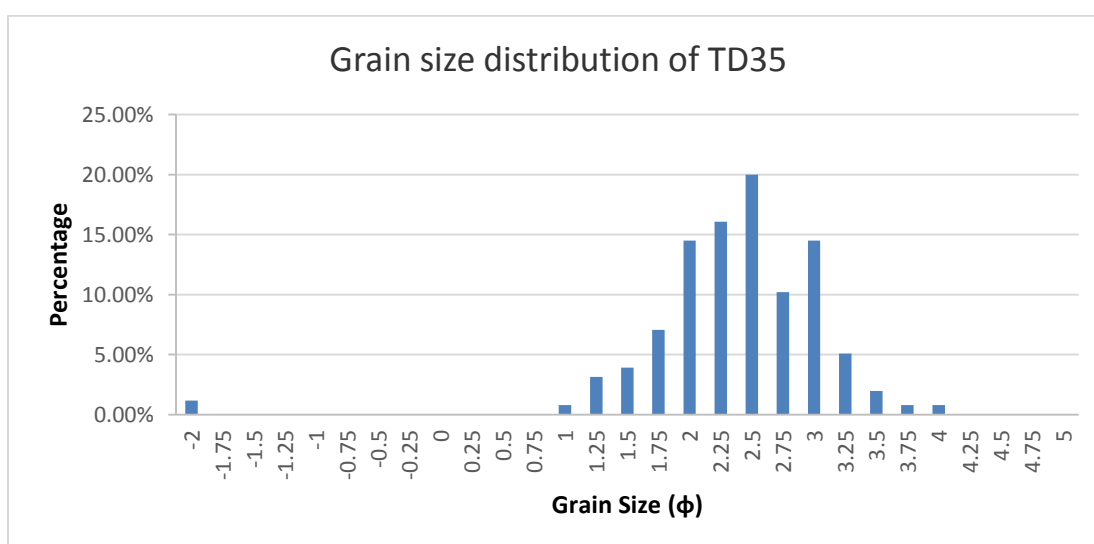
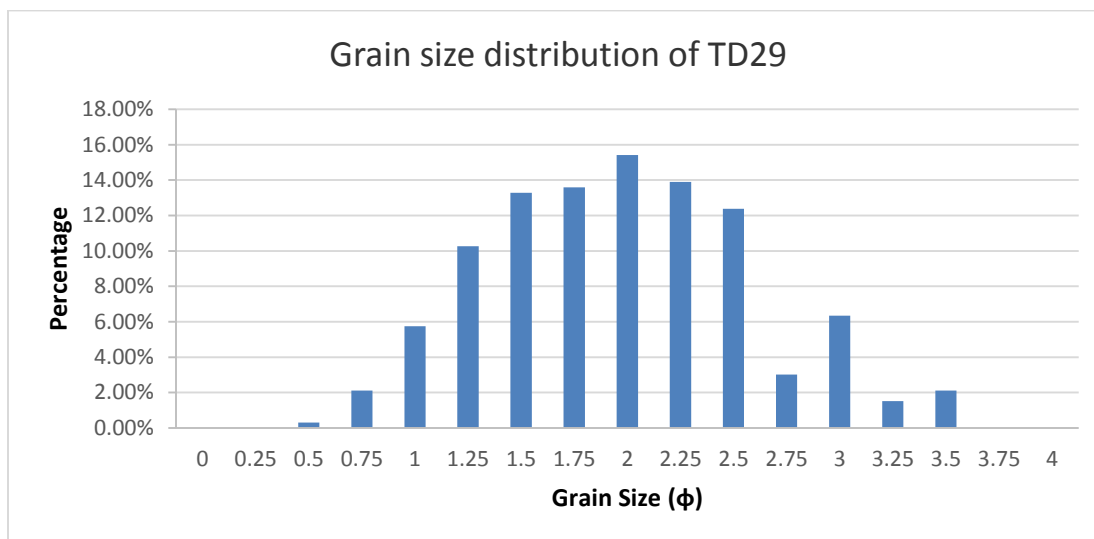




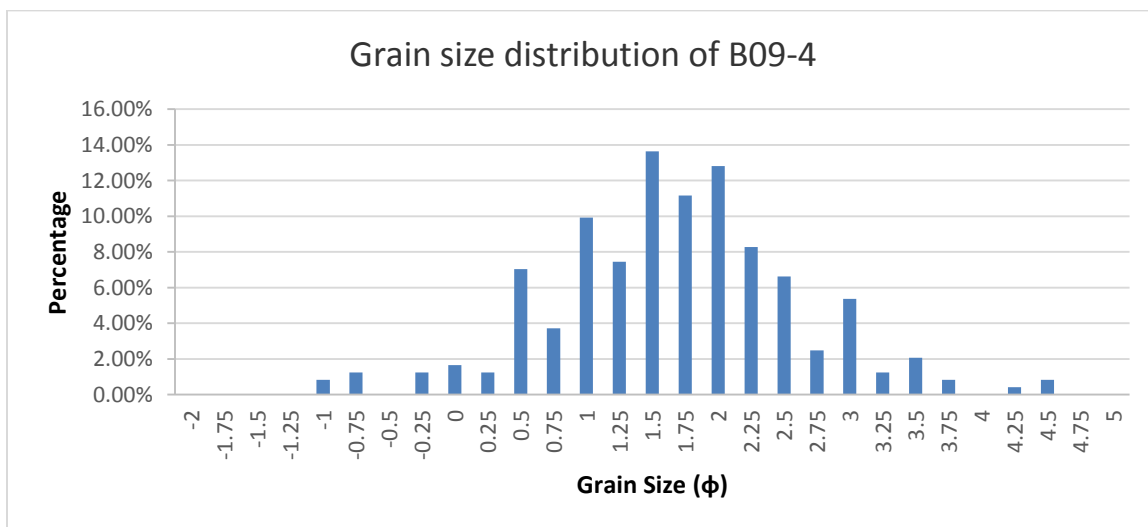
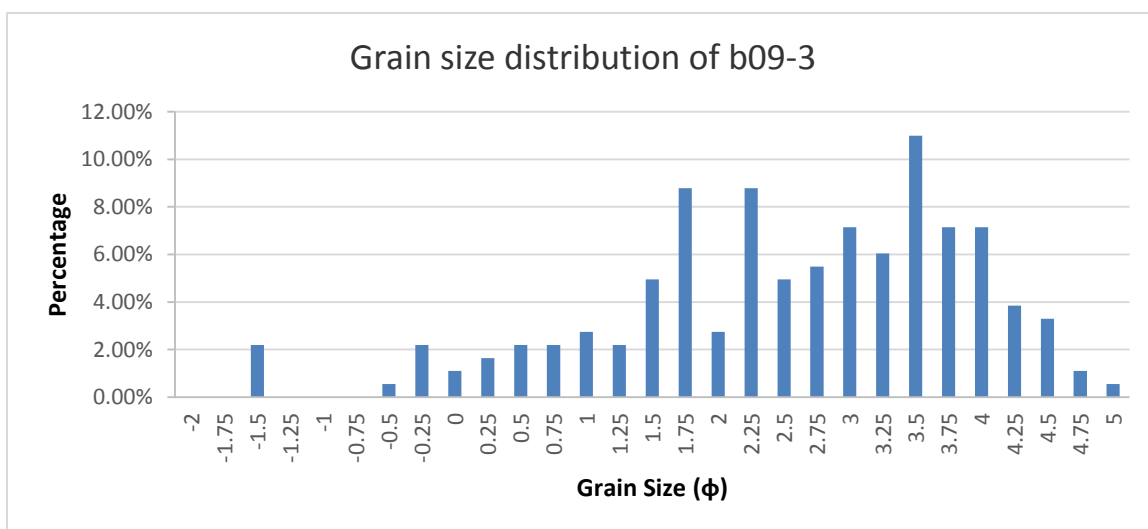
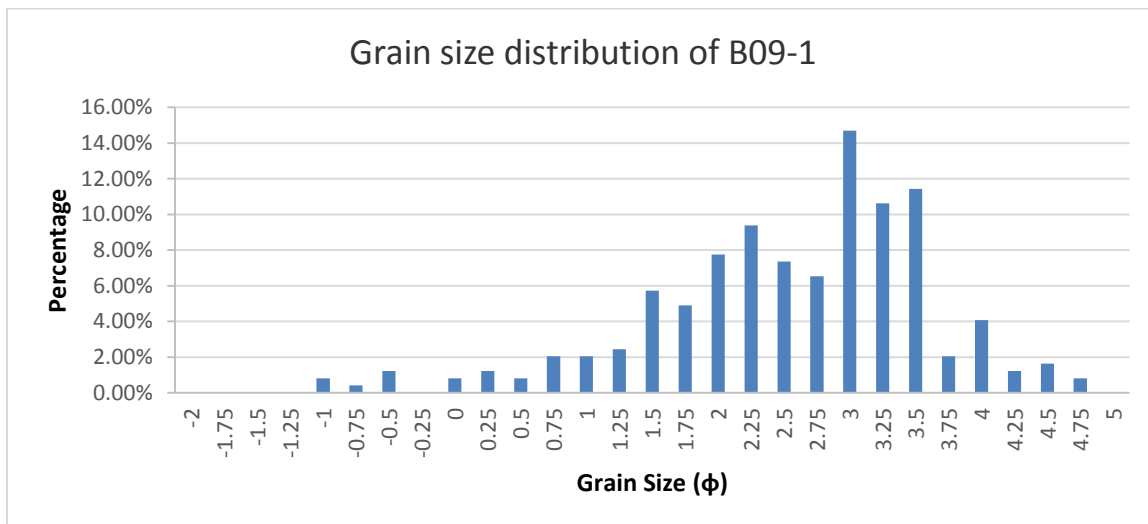


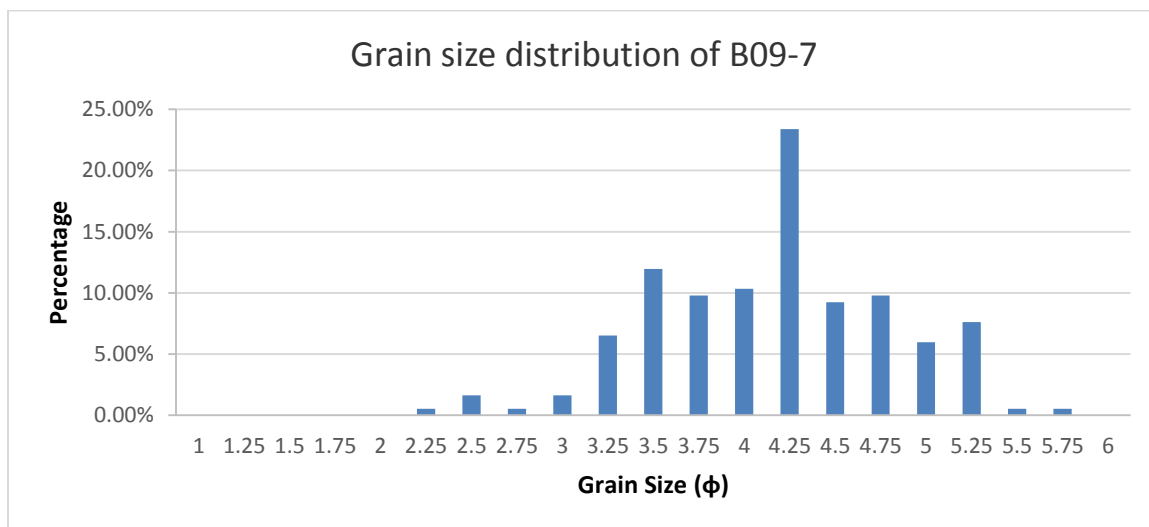
Taodonggou



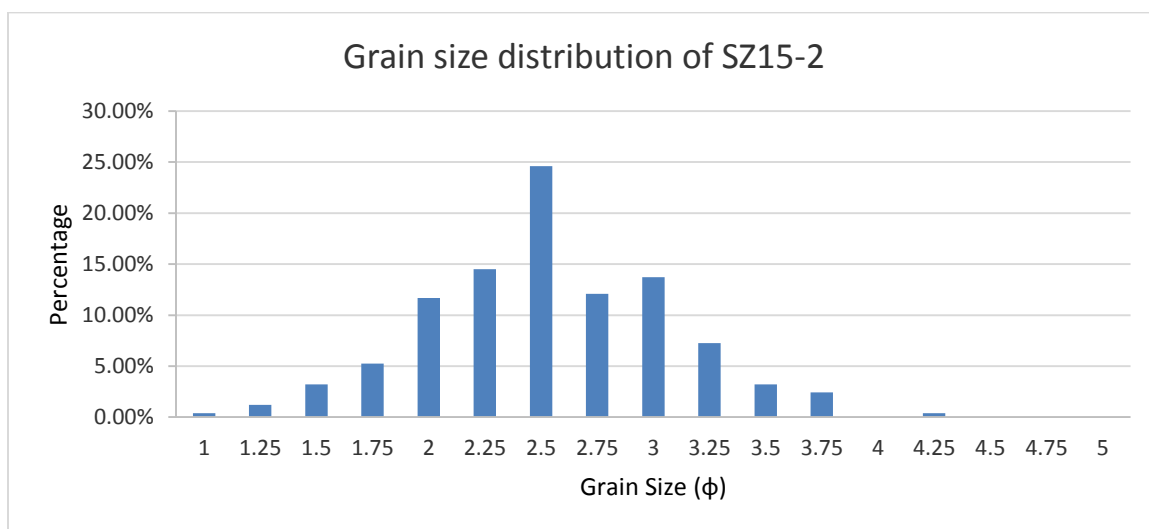
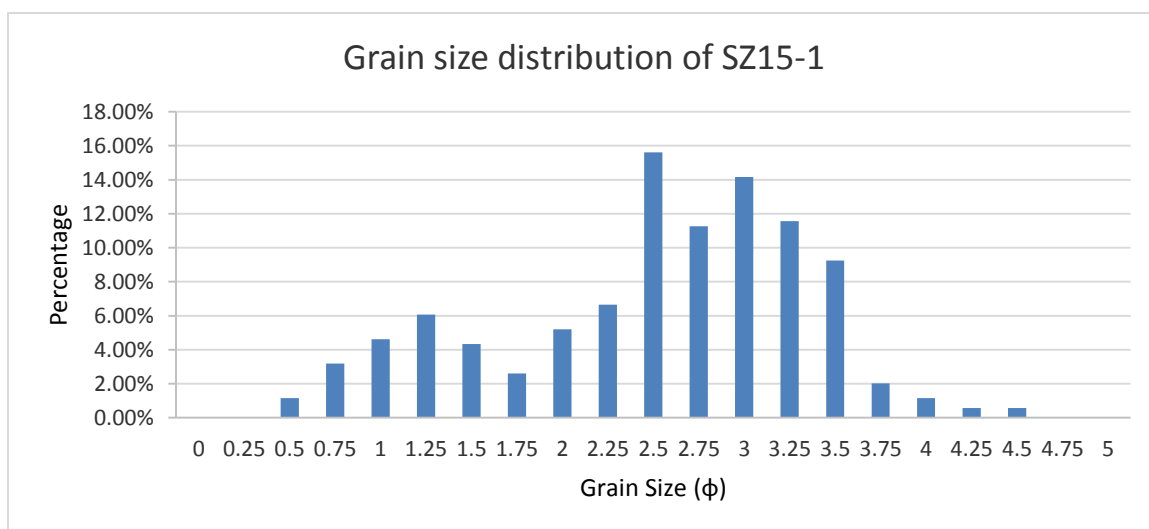


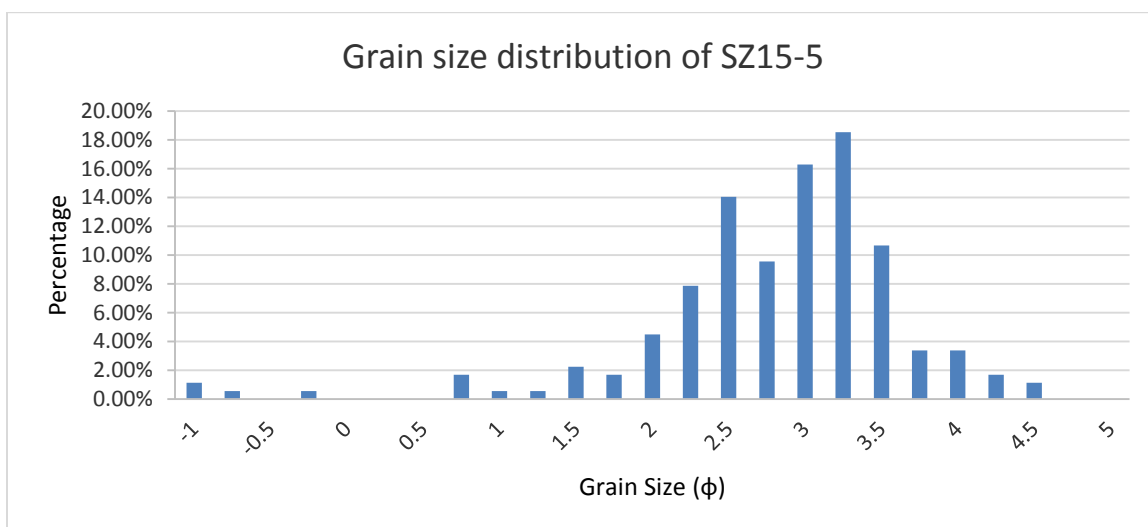
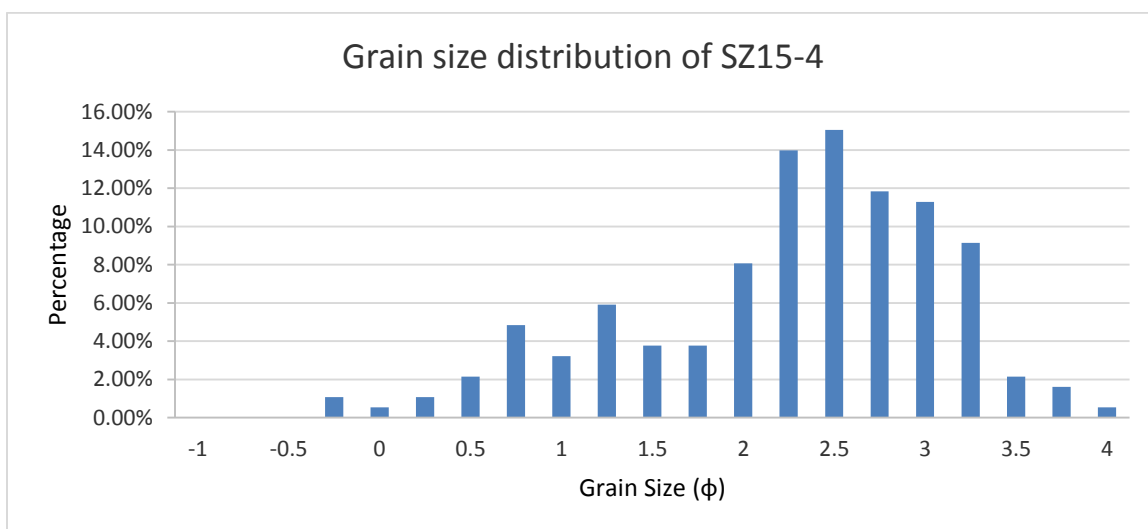
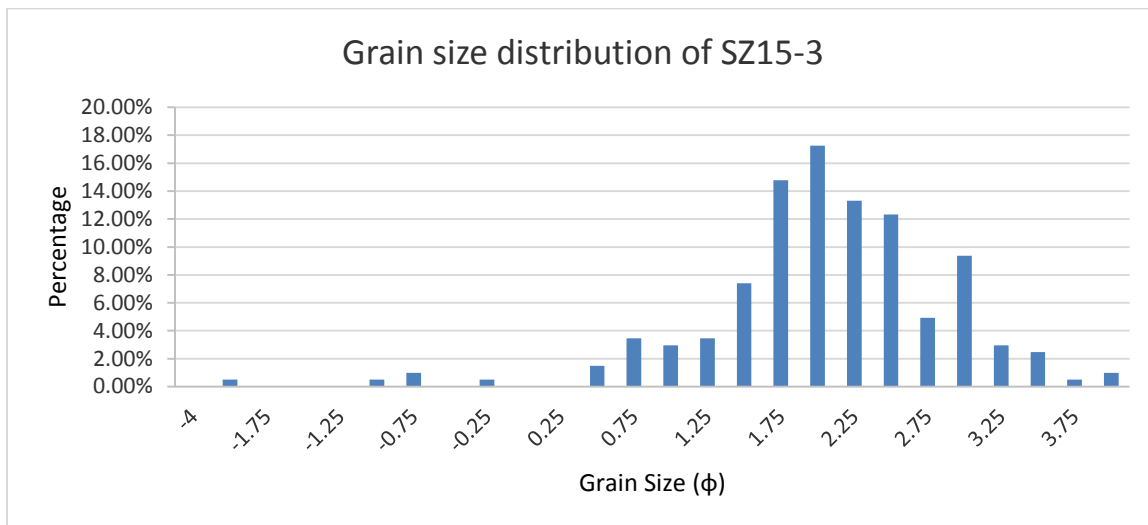
SW Tarlong

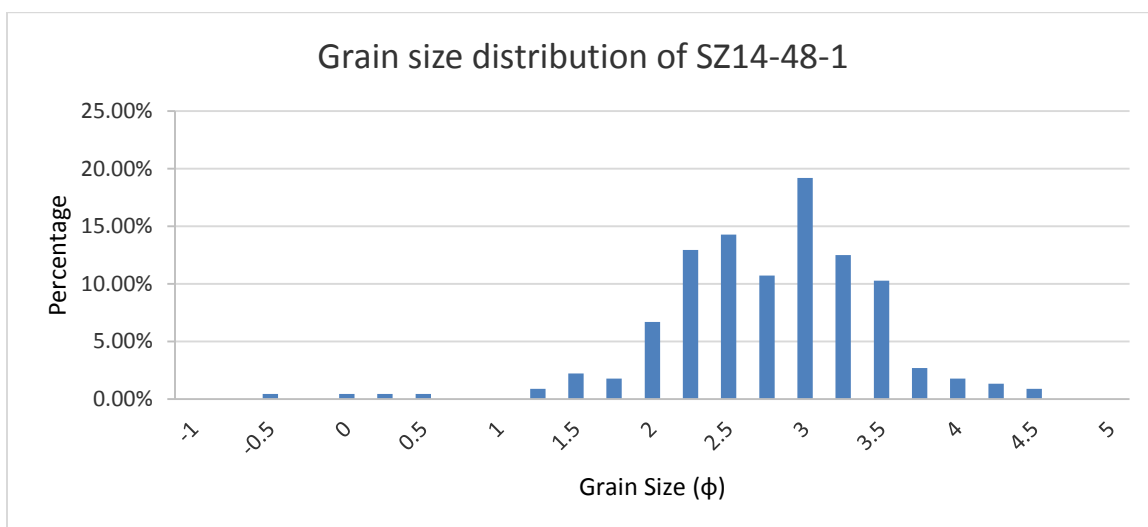
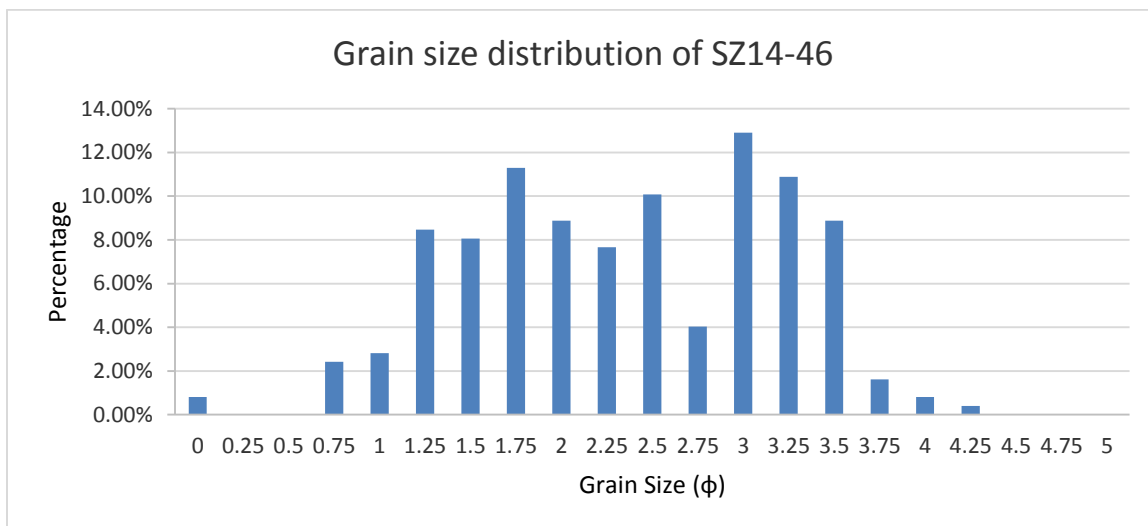
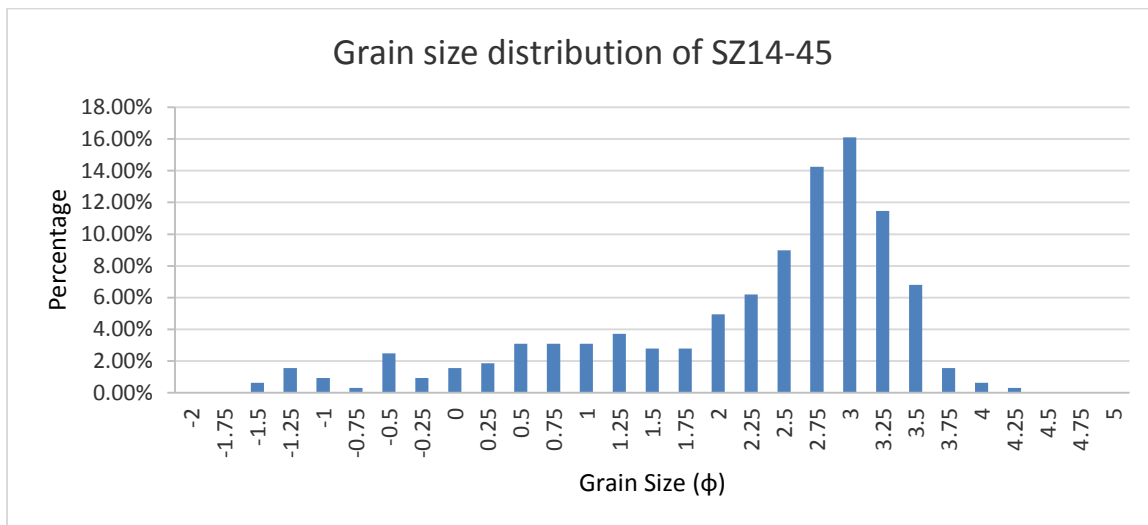


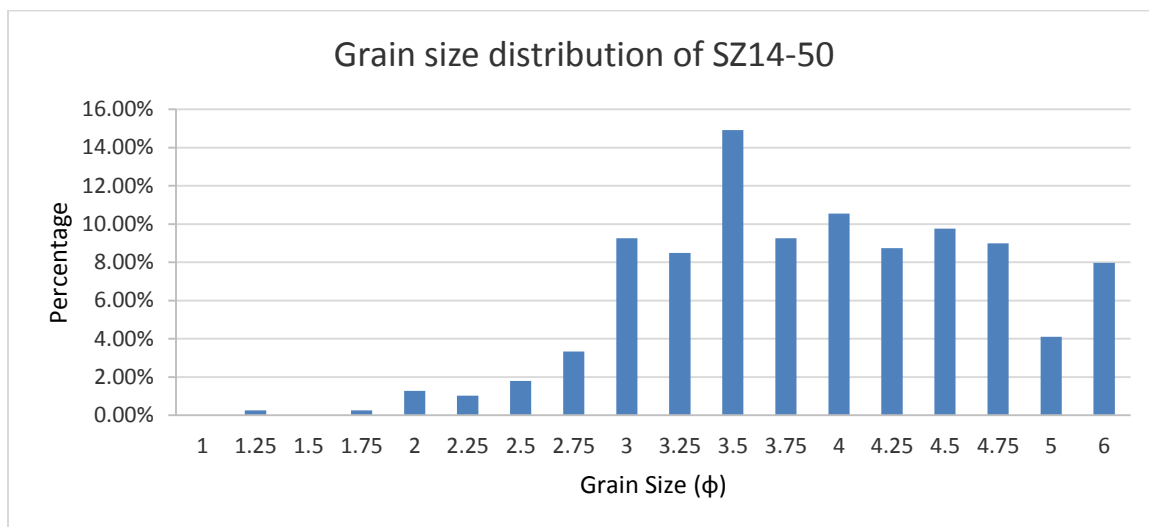


Zhaobishan









BIBLIOGRAPHY

- Allen, M.B. and Natal'in, B.A., 1995. Junggar, Turfan and Alakol basins as Late Permian to? Early Triassic extensional structures in a sinistral shear zone in the Altaid orogenic collage, Central Asia. *Journal of the Geological Society*, 152(2), pp. 327-338.
- Allen, M.B., Windley, B.F., Chi, Z., ZHONG-YAN, Z.H.A.O. and GUANG-REI, W.A.N.G., 1991. Basin evolution within and adjacent to the Tien Shan Range, NW China. *Journal of the Geological Society*, 148(2), pp. 369-378.
- Basu, A., 1976. Petrology of Holocene fluvial sand derived from plutonic source rocks: implications to paleoclimatic interpretation. *Journal of Sedimentary Research*, 46(3). pp. 694-709.
- Bates, R.L. and Jackson, J.A. eds., 1984. *Dictionary of geological terms* (Vol. 584). Anchor Books.
- Blair, T.C., 1987. Tectonic and hydrologic controls on cyclic alluvial fan, fluvial, and lacustrine rift-basin sedimentation, Jurassic-Lowermost Cretaceous Todos Santos Formation, Chiapas, Mexico. *Journal of Sedimentary Research*, 57(5). pp. 845-862
- Blatt, H., 1967. Provenance determinations and recycling of sediments. *Journal of Sedimentary Research*, 37(4). pp. 1031-1041.
- Boggs, S. and Boggs, S., 2014. *Principles of sedimentology and stratigraphy* (No. 551.3. 051 BOG).
- Burrett, C.F., 1974. Plate tectonics and the fusion of Asia. *Earth and Planetary Science Letters*, 21(2), pp. 181-189.
- Carroll, A.R., Brassell, S.C. and Graham, S.A., 1992. Upper Permian Lacustrine Oil Shales, Southern Junggar Basin, Northwest China (1). *AAPG Bulletin*, 76(12), pp. 1874-1902.
- Carroll, A.R., Graham, S.A., Hendrix, M.S., Ying, D. and Zhou, D., 1995. Late Paleozoic tectonic amalgamation of northwestern China: sedimentary record of the northern Tarim, northwestern Turpan, and southern Junggar basins. *Geological Society of America Bulletin*, 107(5), pp. 571-594.
- Carroll, A.R., Yunhai, L., Graham, S.A., Xuchang, X., Hendrix, M.S., Jinchi, C. and McKnight, C.L., 1990. Junggar basin, northwest China: trapped Late Paleozoic ocean. *Tectonophysics*, 181(1-4), pp. 1-14.

- Dickinson, W.R., 1970. Interpreting detrital modes of graywacke and arkose. *Journal of Sedimentary Research*, 40(2). pp. 695-707.
- Dickinson, W.R., 1985. Interpreting provenance relations from detrital modes of sandstones. In *Provenance of arenites* (pp. 333-361). Springer Netherlands.
- Dott Jr, R.H., 1964. Wacke, Graywacke and Matrix--What Approach to Immature Sandstone Classification?. *Journal of Sedimentary Research*, 34(3). pp. 625-632.
- Folk, R.L., 1951. Stages of textural maturity in sedimentary rocks. *Journal of Sedimentary Research*, 21(3).
- Folk, R.L., 1959. Practical petrographic classification of limestones. *AAPG Bulletin*, 43(1), pp. 1-38.
- Folk, R.L., 1974. The natural history of crystalline calcium carbonate: effect of magnesium content and salinity. *Journal of Sedimentary Research*, 44(1). pp. 40-53.
- Folk, R.L., 1980, *Petrology of sedimentary rocks*: Hemphill Publishing Company, Austin, Texas, 184 pp.
- Folk, R.L. and Ward, W.C., 1957. Brazos River bar: a study in the significance of grain size parameters. *Journal of Sedimentary Research*, 27(1). pp. 3-26
- Garzanti, E., Padoan, M., Andò, S., Resentini, A., Vezzoli, G. and Lustrino, M., 2013. Weathering and relative durability of detrital minerals in equatorial climate: sand petrology and geochemistry in the East African Rift. *The Journal of Geology*, 121(6), pp. 547-580.
- Graham, S.A., Hendrix, M.S., Wang, L.B. and Carroll, A.R., 1993. Collisional successor basins of western China: Impact of tectonic inheritance on sand composition. *Geological Society of America Bulletin*, 105(3), pp.323-344.
- Greene, T.J., Carroll, A.R., Hendrix, M.S., Graham, S.A., Wartes, M.A. and Abbink, O.A., 2001. Sedimentary record of Mesozoic deformation and inception of the Turpan-Hami basin, northwest China. *Paleozoic and Mesozoic tectonic evolution of central and eastern Asia*, 194, p. 317.
- Greene, T.J., Carroll, A.R., Wartes, M., Graham, S.A. and Wooden, J.L., 2005. Integrated provenance analysis of a complex orogenic terrane: Mesozoic uplift of the Bogda Shan and inception of the Turpan-Hami Basin, NW China. *Journal of Sedimentary Research*, 75(2), pp. 251-267.
- Hsü, K.J., 1988. Relict back-arc basins: principles of recognition and possible new examples from China. In *New perspectives in basin analysis*(pp. 245-263). Springer New York.

- Ingersoll, R.V. and Eastmond, D.J., 2007. Composition of modern sand from the Sierra Nevada, California, USA: Implications for actualistic petrofacies of continental-margin magmatic arcs. *Journal of Sedimentary Research*, 77(9), pp. 784-796.
- Ingersoll, R.V., 1990. Actualistic sandstone petrofacies: discriminating modern and ancient source rocks. *Geology*, 18(8), pp. 733-736.
- Ingersoll, R.V., Bullard, T.F., Ford, R.L., Grimm, J.P., Pickle, J.D. and Sares, S.W., 1984. The effect of grain size on detrital modes: a test of the Gazzi-Dickinson point-counting method. *Journal of Sedimentary Research*, 54(1), pp.103-116.
- Mack, G.H. and Suttner, L.J., 1977. Paleoclimate interpretation from a petrographic comparison of Holocene sands and the Fountain Formation (Pennsylvanian) in the Colorado Front Range. *Journal of Sedimentary Research*, 47(1).
- Mack, G.H., 1981. Composition of modern stream sand in a humid climate derived from a low-grade metamorphic and sedimentary foreland fold-thrust belt of north Georgia. *Journal of Sedimentary Research*, 51(4).
- Obrist-Farner, J., 2015. Origin and stratigraphic architecture of the Middle Permian lower and upper Quanzijie low-order cycles, Bogda Mountains, NW China. *Doctoral Dissertations*. 2381 pp.
- Obrist-Farner, J., Yang, W. 2015. Nonmarine time-stratigraphy in a rift setting: An example from the Mid-Permian lower Quanzijie low-order cycle Bogda Mountains, NW China. *Journal of Palaeogeography*, 4(1), pp. 27-51.
- Peng, X. and Zhang, G., 1989. Tectonic features of the Junggar basin and their relationship with oil and gas distribution. *Chinese sedimentary basins: Amsterdam, Elsevier*, pp. 17-31.
- Pettijohn, F.J., Potter, P.E. and Siever, R., 1972. *Sand and sandstone*. Springer Science & Business Media.
- Powers, M.C., 1953. A new roundness scale for sedimentary particles. *Journal of Sedimentary Research*, 23(2). pp. 117-119.
- Shao, L., Stattegger, K. and Garbe-Schoenberg, C.D., 2001. Sandstone petrology and geochemistry of the Turpan basin (NW China): implications for the tectonic evolution of a continental basin. *Journal of Sedimentary Research*, 71(1), pp.37-49.
- Todd Thompson, 2007, <http://mypage.iu.edu/~tthomps/programs/html/tnttriplot.htm>.
- Wartes, M.A., Carroll, A.R. and Greene, T.J., 2002. Permian sedimentary record of the Turpan-Hami basin and adjacent regions, northwest China: Constraints on postamalgamation tectonic evolution. *Geological Society of America Bulletin*, 114(2), pp. 131-152.

- Wernicke, B. and Burchfiel, B.C., 1982. Modes of extensional tectonics. *Journal of Structural Geology*, 4(2), pp. 105-115.
- Xinjiang, B.G.M.R., 1993. Regional geology of the Xinjiang Uygur autonomous region.
- Yang, W., 2008. Depositional Systems Analysis within a Seismic Sequence Stratigraphic Framework, Turpan-Hami Basin, NW China. Tu-Ha Oil Company Internal Report, PetroChina.
- Yang, W., Crowley, J.L., Obrist-Farner, J., Tabor, N.J., Feng, Q. and Liu, Y.Q., 2013, October. A marine back-arc origin for the Upper Carboniferous basement of intracontinental greater Turpan-Junggar basin-Volcanic, sedimentary, and geochronologic evidence from southern Bogda Mountains. In NW China: Geological Society of America Annual Meeting, GSA Abstract with Programs (Vol. 45, No. 1).
- Yang, W., Feng, Q., Liu, Y., Tabor, N., Miggins, D., Crowley, J.L., Lin, J. and Thomas, S., 2010. Depositional environments and cyclo- and chronostratigraphy of uppermost Carboniferous–Lower Triassic fluvial–lacustrine deposits, southern Bogda Mountains, NW China—A terrestrial paleoclimatic record of mid-latitude NE Pangea. *Global and Planetary Change*, 73(1), pp. 15-113.
- Yang, W., Liu, Y., Feng, Q., Lin, J., Zhou, D. and Wang, D., 2007. Sedimentary evidence of Early–Late Permian mid-latitude continental climate variability, southern Bogda Mountains, NW China. *Palaeogeography, Palaeoclimatology, Palaeoecology*, 252(1), pp. 239-258.

VITA

Xiaowei Peng was in Panjin, Liaoning, China. In July 2010, he received his B.S. in Petroleum Geology and B.A. in English from China University of Petroleum (Beijing), China. In December 2016, he received his M.S. degree in Geology and Geophysics from Missouri University of Science and Technology, Rolla, Missouri, USA.

He has published one conference paper: Peng, X.W. and Yang, W., 2016. Provenance of Fluvial-Lacustrine Sandstones of Lower Permian Lucaogou Low-Order Cycle, Bogda Mountains, NW China. Geological Society of America Abstracts with Programs. Vol. 48, No. 7.

Xiaowei Peng has been a member of the American Association of Petroleum Geologists (AAPG), the Geological Society of America (GSA), and the Society of Petroleum Engineers (SPE) since 2015. He has been a member of Association of Environmental & Engineering Geologists (AEG) since 2016.